Investigating Sex Differences in Astrocytes and the Adaptive Immune System in the APP/PS1 AD mouse model and in Alzheimer's Disease Patients



Thesis submitted for the degree of

Doctor of Philosophy, Physiology

2026

Jessica Beth Lambe

Supervisor: Prof. Maeve Caldwell

Co-Supervisor: Dr. Marie-Victoire Guillot-Sestier

Department of Physiology, School of Medicine,

Trinity College Dublin, Ireland

Declaration and statement of plagiarism

I declare that this thesis has not been submitted as an exercise for a degree at this or any other university and it is entirely my own work. The unpublished and/or published work of others, has been duly acknowledged in the text wherever included.

Prof. Maeve Caldwell and Dr. Marie Victoire Guillot Sestier were involved in study design, analysis and interpretation of data. Prof. Jean Fletcher and Dr. Barry Moran assisted in the design of the flow cytometry panel and aided in initial analysis (Chapter 3 and 4). In collaboration with Prof. Seán Kennelly in Tallaght University Hospital (TUH) Institute of Memory and Cognition, blood samples and cerebrospinal fluid (CSF) were collected by Dr. Adam Dyer, Dr. Helena Dolphin and Dr. Sarah Fullam from patients.

I agree to deposit this thesis in the University's open access institutional repository or allow the Library to do so on my behalf, subject to Irish Copyright Legislation and Trinity College Library conditions of use and acknowledgement.

I consent to the examiner retaining a copy of the thesis beyond the examining period, should they so wish (EU GDPR May 2018).

Signed: 

Date:

Abstract

Alzheimer's disease (AD) is the most common neurodegenerative disease. The prevalence of this disease amongst the sexes is heterogenous with females making up 2/3 of AD patients. The pathohistological hallmarks of the disease are the build-up of extracellular Aβ plaque, intracellular neurofibrillary tau tangles and neuroinflammation in the brain. In more recent years, it has been reported that microglia from females and males present differences in their morphology, metabolism, phagocytic ability and iron retention. It has been shown that the release of pro-inflammatory cytokines TNF-α, IL-1α, and complement component 1q (C1q) by microglia (TIC factors) are required for astrocytes to become reactive, indicating an important interplay between the glial cells.

The role of the adaptive immune system in AD has become an area of research more recently as T lymphocytes from the adaptive immune system have been shown to be implicated in AD pathogenesis. Although their role in the disease and potential sexual dimorphisms in T cell subsets is not fully understood.

The general hypothesis of my PhD project is that alterations in abundance and/or phenotype of T cells and/or astrocytes differ in males and females in response to AD pathology.

The aim of my project is to investigate potential sex differences in astrocytes and in $CD4^+$ and $CD8^+$ T cells. To do so, flow cytometry was performed on secondary lymphoid organs in $APP_{swe}/PSEN1_{dE9}$ mice (model of Alzheimer's disease (AD) and cerebral amyloidoisis) once pathology was well established (16-17 months). The secondary lymphoid organs (lymph nodes and spleen) contain mature T and B cells and become activated by encountering antigens and initiate an adaptive immune response. Immunofluorescence on brain sections was used for the evaluation of astrogliosis. In this study, significant changes in $CD8^+$ T cell populations were observed in lymph nodes (IFN-γ, TNF-α and IL-17) which did not occur in T cells isolated from spleens. There was also a significant decrease in regulatory T cells located in the brain but not in the lymph nodes or spleen. In relation to astrocyte response, GFAP expression is significantly increased in the CA3 of the hippocampus in female APP/PS1 mice compared to male APP/PS1 mice. This indicates that the

adaptive immune system, specifically T cells and astrocytes are altered in AD pathology in the APP/PS1 model.

Additionally, peripheral blood mononuclear cells (PBMCs) and cerebrospinal fluid (CSF) were collected from AD and non-AD patients to investigate alterations in T cell phenotypes and cytokine response. Meso-scale discovery analysis revealed significant alterations in proteins secreted in the CSF but not PBMCs of AD patients (MIP1β and IFN-γ). The effect of sex was also observed in the CSF with specific protein secretions altered in only male or female AD patients alone (IL-1Rα in males and IL-6 in females). Furthermore, induced pluripotent stem cells (iPSC) were utilised to generate cortical astrocytes. Astrocytes were treated with male and female non-AD and AD patients' CSF and conditioned media from PBMCs to elucidate the potential sex differences and interplay between the immune system and astrocytes. Interestingly, treatment with AD CSF but not PBMCs resulted in significant decrease in astrocyte protein secretion confirmed by ELISA (CXCL10). In conclusion, CSF is key to further elucidating the pathogenesis of AD along with the inclusion of both male and females as the response to pathology is not uniform between the sexes.

Future studies could utilise this approach in identifying sex specific differences in both the adaptive immune system as well as astrocytes to prevent the characteristic neuroinflammation and neurodegeneration in AD with pharmaceutical interventions.

Acknowledgements

First and foremost I would like to say a massive go raibh míle maith agaibh to my two supervisors Prof. Maeve Caldwell and Dr. Marie Victoire Guillot Sestier.

To Maeve, thank you so much for taking me under your wing and allowing me to join your wonderful lab. I am so grateful for the support, guidance and patience you have offered me from the very beginning. Thank you for reading all of my drafts and always being available for words of advice whenever I needed it.

To Marie, thank you for giving me the opportunity to carry out this research I am extremely grateful. Thank you for the support and patience you have offered to me in this PhD. I appreciate all the drafts you have read and the advice you have given me throughout.

I am extremely grateful for the time and effort you have both shown me throughout this PhD. I would not be the scientist I am today without your help!

To Prof. Jean Fletcher and Dr. Barry Moran, thank you both so much for all of the time you put into this project and helping with any immunology challenges I had. I am so grateful for all the patience and expertise you offered throughout this project I truly appreciate it!

To the Physiology Dept. in TCD, especially Dr. Eva Jimenez-Mateos who provided so much of her time and energy to help me with anything I needed. I am so grateful for all that you did for me.

Thank you so much as well to Dr. Adam Dyer, Dr. Helena Dolphin, Dr. Sarah Fulham, Prof. Sean Kennelly and Dr. Nollaig Bourke in Tallaght University Hospital and Trinity Translational Medicine Institute, St. James. Thank you to all the patients who so kindly donated samples to allow me to carry out this research. This work would not have been possible without each one of you. I especially want to thank Dr. Adam Dyer for offering any help I needed and answering any questions I had.

To my wonderful lab friends in the Caldwell lab and beyond. Julia thank you so much for always listening to me and being there to help and advise when I needed it! To Maddie, thank you for being so patient, kind and generous with your time and showing me how to look after iPSCs and make astrocytes successfully! To Adina, thank you for always listening to me and understanding my worries and knowing everything

would be ok! To Lei, thank you for always offering to help. I feel so grateful that our paths have crossed and I have learned so much from you. To Rebecca, thank you for always being there when I was having my good days and my bad days. I know I have made a friend for life and so lucky to have met you!

To my extended work friends in TCIN, thank you all so much for making the PhD so enjoyable and fun. I feel so lucky to have met you all and gained all these friendships.

I want to especially say thank you so much to my Mam and Dad, Barbara and Johnny Lambe. You have always supported me in anything I have wanted to achieve and have always been there. Thank you for all the cups of tea, the lifts and listening to me. I hope I have done you both proud. To my brother Oliver and sister Allyson, thank you for always making me laugh, for all the chats, cheering me up and believing in me. To my nanny Helena thank you for always being there for me I love you very much! I especially want to thank my nanny Veronica, who I love and miss. You have left an indelible mark on me and others. Thank you for always seeing my potential, all of this work is a dedication to you!

To my best friends, Rachel, Noor and Isabelle I am so lucky to have met you and experienced this PhD at the same time as you all. You have always been so supportive and kept me going! Love you all.

Table of Contents

1 Chapter 1: Introduction 1

1.1 Alzheimer's Disease 2

1.2 Genes associated with familial versus sporadic AD 2

1.2.1 The APOE4 allele and Alzheimer's disease 3

1.2.2 TREM2 Arg-to-His variants and Alzheimer's Disease 6

1.3 What role do astrocytes play in Alzheimer's Disease? 8

1.3.1 The genotype of reactive astrocytes in Alzheimer's disease 9

1.3.2 Astrocyte phenotypes identified in Alzheimer's Disease 11

1.3.3 Suppressing astrocyte reactivity in neurodegenerative diseases 14

1.4 Sex differences in Alzheimer's Disease 15

1.4.1 Genetic heterogeneity in males and females 15

1.4.2 Glial phenotypes in males and females 19

1.4.3 Impairment of metabolic and mitochondrial function in microglia in AD 20

1.4.4 The effect of endocrine aging and the role of HRT in menopause to combat AD risk in females 21

1.5 Does the adaptive immune system help or hinder in Alzheimer's disease? . 24

1.5.1 Dysfunction of blood brain barrier integrity in Alzheimer's disease 25

1.5.2 $CD4^+$ T cell subsets and the unclear role of Regulatory T cells in Alzheimer's Disease 27

1.5.3 The role of Th1, Th2 and Th17 in AD pathology 31

1.5.4 $CD8^+$ T cell profile in Alzheimer's patients and mouse models 32

1.5.5 Glia-T cell crosstalk 35

1.6 Hypothesis and aims of the project 38

2 Chapter 2: Materials and methods 39

2.1 Animals 40

2.1.1 Genotyping 40

2.1.2 Preparation of Animal Tissue 42

2.2 Immunohistochemistry 42

2.3 Immunocytochemistry for IPSC derived neurons and astrocytes 43

2.4 Image Analysis and Acquisition 44

2.4.1 Tissue sections of APP/PS1 mice 44

2.4.2 Imaging of iPSC derived cortical astrocytes 46

2.5 RNA Isolation, cDNA manufacture and RT-qPCR 46

2.5.1 RNA Isolation 46

2.5.2 Use of Reverse Transcriptase to generate cDNA 47

2.5.3 Real Time quantitative polymerase chain reaction (RT-qPCR) 48

2.6 Patient Samples 48

2.6.1 Diagnosis Criteria 48

2.7 Peripheral blood mononuclear cell isolation from whole blood 49

2.8 Thawing and counting iPSCs derived neurons and astrocytes and PBMCs ...50

2.9 Statistical methods.....50

3 Chapter 3: Investigating sex differences in astrocytes and T cells in the APP/PS1 AD mouse model..... 51

3.1 Introduction.....52

3.2 Methods 56

3.2.1 Overview of methods.....56

3.2.2 Flow Cytometry 57

3.2.3 ASCA2$^+$ Astrocyte and CD11b$^+$ Microglia Isolation from Adult Mouse Brains 60

3.2.4 RT-qPCR 62

3.3 Results 64

3.3.1 Sex affects T cell phenotype in secondary lymphoid organs and the brain in APP/PS1 and wild-type littermates 64

3.3.2 The effect of sex and APP/PS1 transgene on ASCA-2$^+$ astrocytes and CD11b$^+$ microglial genotype 78

3.3.3 Influence of sex and the APP/PS1 transgene on astrocyte abundance and GFAP expression in 13-15 month old APP/PS1 males and females and wild-type littermates 86

3.4 Discussion.....98

4 Chapter 4 Investigating sex differences in T cells and cytokine concentration in the cerebrospinal fluid of Alzheimer's disease patients..... 106

4.1 Introduction.....107

4.2 Methods 110

4.2.1 Patient Overview 110

4.2.2 PBMCs conditioned media 110

4.2.3 PBMCs Flow Cytometry.....110

4.2.4 Meso-Scale Discovery (MSD) assays for the detection of cytokines.....113

4.3 Results 116

4.3.1 Investigation of T cell populations in peripheral blood mononuclear cells of Non Alzheimer's Disease/MCI and Alzheimer's Disease patients using flow cytometry.....116

4.3.2 Investigation of cytokines released by stimulated peripheral blood mononuclear cells and cerebrospinal fluid in non-Alzheimer's/MCI and Alzheimer's disease patients using meso-scale discovery.....129

4.4 Discussion.....137

Chapter 5: Investigating the effect of sex specific differences in Alzheimer's disease patients' cerebrospinal fluid and PBMCs on iPSC derived cortical astrocytes 144

5 144

5.1 Introduction.....145

5.2 Methods 148

5.2.1 Cell Line 148

5.2.2 iPSC Cell Culture 148
5.2.3 Neural Progenitor Cell (NPC) Culture 148
5.2.4 Astrocyte Progenitor Cell (APC) Culture 149
5.2.5 Treatment of mature cortical astrocytes with microglial factors (TIC) 151
5.2.6 Treatment of mature cortical astrocytes with CSF and PBMCs conditioned media 151
5.2.7 Enzyme linked immunosorbent assay (ELISA) 152
5.2.8 Immunocytochemistry 152
5.2.9 RT-qPCR 153
5.2.10 Statistical Methods 155
5.3 Results 156
5.3.1 iPSC derived cortical astrocytes develop a reactive phenotype when treated with TIC factors 156
5.3.2 The effect of PBMCs conditioned media and CSF on cortical astrocytes' protein secretion and gene expression 161
5.4 Discussion 173
6 Final Discussion 178
6.1 Introduction 179
6.2 Findings and future directions 179
6.3 Is sex a risk factor? 182
6.4 The prospect of immunotherapies 185
6.5 Conclusions 187
7 Bibliography 188

List of Figures

Figure 1.1 The effect of sex on microglial and astrocyte phenotype in human cases and mouse models of AD 24
Figure 1.2 Influence of peripheral and brain microenvironment on disease progression 37
Figure 2.1 Schematic diagram of cell profiler analysis of AD mouse brain sections 45
Figure 3.1 Experimental design of tissue retrieved from APP/PS1 and wild-type mice with downstream applications 56
Figure 3.2 Gating Strategy for flow cytometry analysis of cytokine response in cervical lymph node, inguinal/auxiliary lymph node (pooled) and spleen of male and female APP/PS1 mice and wild-type littermates. 65
Figure 3.3 Proportion of $CD4^+$ and $CD8^+$ T cells in Cervical Lymph Nodes, Inguinal and Axillary Lymph Nodes and Spleens of APP/PS1 male and female mice and wild-type littermates by flow cytometry 66
Figure 3.4 Analysis of T cell cytokine populations in Cervical Lymph Nodes of APP/PS1 males and females and wild-type littermates by flow cytometry 68
Figure 3.5 Analysis of T cell populations in Inguinal and Axillary Lymph Nodes of APP/PS1 males and females and wild-type littermates by flow cytometry 71
Figure 3.6 Analysis of T cell populations in Spleens of APP/PS1 males and females and wild-type littermates by flow cytometry 73
Figure 3.7 Gating Strategy for flow cytometry analysis of inguinal/auxiliary lymph node (pooled), spleen and brain in male and female APP/PS1 mice and wild-type littermates. 75
Figure 3.8 Analysis of Regulatory T cell populations in APP/PS1 males and females and wild-type littermates by flow cytometry 76
Figure 3.9 Abstract summary of flow cytometry results of T cell cytokine response and regulatory T cells in male and female APP/PS1 and wild-type littermates 78
Figure 3.10 Gating Strategy for flow cytometry analysis of ASCA-2^+ astrocytes and $CD11b^+$ microglia isolated from brains of male and female APP/PS1 mice and wild-type littermates 79
Figure 3.11 Confirmation of ASCA-2^+ astrocyte and $CD11b^+$ microglia populations present after magnetic separation by flow cytometry from brains of APP/PS1 males and females and wild type littermates 80
Figure 3.12 GFAP gene expression from ASCA-2^+ astrocytes and $CD11b^+$ microglia populations by RT-qPCR from brains of APP/PS1 males and females and wild type littermates 81
Figure 3.13 Gene expression of MHC-II and CD86 was significantly higher in astrocytes from female APP/PS1 mice compared to male APP/PS1 mice 82

Figure 3.14 ***Gene expression of MHC-II, CD86 and TNF-αwas significantly higher in astrocytes from APP/PS1 mice compared to wild-type mice*** 83
Figure 3.15 Investigation of sex on gene expression in CD11b microglia in APP/PS1 males and females and wild type littermates 84
Figure 3.16 The APP/PS1 transgene alters gene expression of antigen presenting genes in CD11b microglia in males 85
Figure 3.17 Abstract summary of RT-qPCR results of ASCA-2$^+$ astrocyte antigen presentation genes in male and female APP/PS1 and wild-type littermates 86
Figure 3.18 Investigation of astrocyte abundance and reactivity in the hippocampus of APP/PS1 males and females and wild type littermates using immunofluorescence 88
Figure 3.19 Investigation of plaque abundance and profile in the CA1 of the hippocampus of APP/PS1 males and females using immunofluorescence 90
Figure 3.20 Investigation of astrocyte abundance and reactivity in the CA1 of the hippocampus of APP/PS1 males and females using immunofluorescence 91
Figure 3.21 Investigation of plaque abundance and profile in the CA3 of the hippocampus of APP/PS1 males and females using immunofluorescence 92
Figure 3.22 Investigation of astrocyte abundance and reactivity in the CA3 of the hippocampus of APP/PS1 males and females using immunofluorescence 93
Figure 3.23 Investigation of plaque abundance and profile in the dentate gyrus of the hippocampus of APP/PS1 males and females using immunofluorescence 94
Figure 3.24 Investigation of astrocyte abundance and reactivity in the dentate gyrus of the hippocampus of APP/PS1 males and females using immunofluorescence 95
Figure 3.25 Representative images of APP/PS1 40µm sections of the CA1, CA3 and the dentate gyrus of the hippocampus 96
Figure 3.26 Abstract summary of GFAP immunohistochemistry analysis in male and female APP/PS1 and wild-type littermates 97
Figure 4.1 Schematic diagram of the methods carried out on PBMCs isolated from non-AD/MCI and AD patients 115
Figure 4.2 Outline of flow cytometry gating strategy for cytokine response in CD4$^+$ and CD8$^+$ T cells 116
Figure 4.3 Analysis of T cell populations in non-Alzheimer's Disease/MCI and Alzheimer's Disease patients 117
Figure 4.4 Analysis of T cell populations in male and female non-Alzheimer's Disease/MCI and Alzheimer's Disease patients 118
Figure 4.5 Analysis of Cytokine Expression in T cell populations of non-Alzheimer's Disease/MCI and Alzheimer's Disease patients 119
Figure 4.6 Analysis of Cytokine Expression in CD4$^+$ T cell populations of male and female non-Alzheimer's Disease/MCI and Alzheimer's Disease patients 120

Figure 4.7 Analysis of Cytokine Expression in CD8⁺ T cell populations of male and female non-Alzheimer's Disease/MCI and Alzheimer's Disease patients 121
Figure 4.8 Outline of flow cytometry gating strategy for activation and senescent markers and regulatory T cells in peripheral blood mononuclear cells..... 122
Figure 4.9 Analysis of activation, senescence and regulatory CD4⁺ T cells in non-Alzheimer's Disease/MCI and Alzheimer's Disease patients..... 123
Figure 4.10 ***Analysis of activation and senescence in CD8⁺ T cells in non-Alzheimer's Disease/MCI and Alzheimer's Disease patients***..... 124
Figure 4.11 Analysis of activation, senescence and regulatory CD4⁺ T cells in male and female non-Alzheimer's Disease/MCI and Alzheimer's Disease patients..... 126
Figure 4.12 Analysis of activation and senescence CD8⁺ T cells in male and female non-Alzheimer's Disease/MCI and Alzheimer's Disease patients..... 127
Figure 4.13 Abstract summary of flow cytometry results investigating sex differences in cytokine and T cell subsets in male and female non-AD and AD patients' PBMCs..... 128
Figure 4.14 MSD Analysis of cytokines released by stimulated peripheral blood mononuclear cells in non-Alzheimer's Disease/MCI and Alzheimer's Disease patients..... 130
Figure 4.15 MSD Analysis of cytokines released by stimulated peripheral blood mononuclear cells in male and female Non-Alzheimer's Disease/MCI and Alzheimer's Disease patients 131
Figure 4.16 MSD Analysis of cytokines in cerebrospinal fluid of non-Alzheimer's Disease/MCI and Alzheimer's Disease patients 133
Figure 4.17 MSD Analysis of cytokines in cerebrospinal fluid of male and female non-Alzheimer's Disease/MCI and Alzheimer's Disease patients 134
Figure 4.18 Abstract summary of sex differences reported in the cytokines present in the CSF of AD patients 136
Figure 5.1 Differentiated NAS2 cortical astrocytes respond to TIC factors to adopt a reactive phenotype using GFAP expression to assess morphology.... 157
Figure 5.2 Differentiated NAS2 cortical astrocytes respond to TIC factors to adopt a reactive phenotype using S100β expression to assess morphology... 158
Figure 5.3 NAS2 cortical astrocytes increase cytokine protein secretion in response to TIC factors..... 159
Figure 5.4 NAS2 cortical astrocytes undergo altered gene expression in response to TIC factors..... 160
Figure 5.5 NAS2 cortical astrocytes increase cytokine protein expression in response to stimulated PBMCs conditioned media from non-Alzheimer's disease/MCI and Alzheimer's disease patients 162

Figure 5.6 NAS2 cortical astrocytes cytokine protein expression in response to stimulated PBMCs conditioned media from male and female non-Alzheimer's disease/MCI and Alzheimer's disease patients 163
Figure 5.7 CSF-induced increased expression of CXCL10, IL-6, RANTES and GMCSF in NAS2 cortical astrocytes from non-Alzheimer's disease/MCI and Alzheimer's disease patients 165
Figure 5.8 CSF-induced increased expression of CXCL10, IL-6, RANTES and GMCSF in NAS2 cortical astrocytes from male and female non-Alzheimer's disease/MCI and Alzheimer's disease patients 166
Figure 5.9 NAS2 cortical astrocytes gene expression in response to stimulated PBMCs conditioned media from non-Alzheimer's disease /MCI and Alzheimer's disease patients 167
Figure 5.10 NAS2 cortical astrocytes mRNA gene expression in response to stimulated PBMCs conditioned media from male and female non-Alzheimer's disease/MCI and Alzheimer's disease patients 168
Figure 5.11 NAS2 cortical astrocytes mRNA gene expression in response to cerebrospinal fluid from non-Alzheimer's disease/MCI and Alzheimer's disease patients 170
Figure 5.12 NAS2 cortical astrocytes mRNA gene expression in response to cerebrospinal fluid from male and female non-Alzheimer's disease/MCI and Alzheimer's disease patients 171

List of Tables

Table 1.1 Helper T Cell Subsets.....24
Table 2.1 Thermocycler cycle conditions for amplification of PSEN1 and prion primers 41
Table 3.1 Flow cytometry antibodies used to investigate regulatory T cell populations.....59
Table 3.2 Flow cytometry antibodies used to investigate T cell cytokine responses 60
Table 3.3 Flow cytometry antibodies used to confirm astrocyte and microglia populations.....62
Table 3.4 ***Primers used for RT-qPCR analysis on magnetically separated astrocytes and microglia*** 63
Table 4.1 Mean age +/- standard deviation of non-AD/MCI and AD patients samples including PBMCs isolated from blood, conditioned media from stimulated PBMCS and cerebrospinal fluid. 110
Table 4.2 Flow cytometry antibodies used to investigate cytokine expression112
Table 4.3 Flow cytometry antibodies used to investigate activation, senescence and regulatory T cells.....113
Table 4.4 List of V-Plex plates used for meso-scale discovery analysis 114
Table 5.1 Primary antibodies for immunocytochemistry.....153
Table 5.2 Secondary antibodies for immunocytochemistry 153
Table 5.3 TaqMan primers used for RT-qPCR.....154
Table 5.4 Summary of ELISA results of iPSC derived astrocytes treated with PBMCs conditioned media or CSF from non-AD/MCI or AD patients.....172

Abbreviations

Aβ-	amyloid beta
AD-	Alzheimer's disease
ADAM-	A disintegrin and metalloproteinase
ALDH1L1-	Aldehyde dehydrogenase 1 family, member L1
ALS-	Amyotrophic lateral sclerosis
APCs-	Astrocyte progenitor cells
APOE-	Apolipoprotein E
APP-	Amyloid precursor protein
AQP-	Aquaporin
AREG-	Amphiregulin
ARM-	Activated response microglia
ASCA-2 –	Astrocyte cell surface antigen 2
AU-	Arbitrary units
β2Mα -	Beta 2 microglobullin alpha
BAC-	Bacterial artificial chromosome
BACE1-	β-APP cleaving enzyme
BBB-	Blood brain barrier
BCL6-	B cell lymphoma 6 protein
BMP4-	Bone morphogenic protein 4
Bp-	Base pairs
C1q-	Complement component 1q
C3-	Complement component 3
C4b-	Complement component 4B
CA-	Cornu ammonis
CAR-	Chimeric antigen receptor
CCL-	Chemokine ligand
CCR-	C- C chemokine receptor
CCT5-	Chaperonin containing TCP1 subunit 5
CHI3L1-	Chitinase 3 like 1

Clec7a-	C type lectin domain family 7, member A
CLU-	Clusterin
CD-	Cluster of differentiation
CM-	Conditioned media
c-Myc-	Cellular myelocytomatosis oncogene
CNS-	Central nervous system
CP-	Choroid plexus
CSF-	Cerebrospinal fluid
CSF2-	Colony stimulating factor 2
CTLA4-	Cytotoxic T lymphocyte associated antigen 4
CTS-	Cathepsin
CXCL10-	Chemokine ligand 10
CXCR-	CXC chemokine receptor
DAA-	Disease associated astrocytes
DAM-	Disease associated microglia
DEGs-	Differentially expressed genes
DG-	Dentate gyrus
DNA-	Deoxyribonucleic acid
EAAT1-	Excitatory amino acid transporter 1
EAE-	Experimental autoimmune encephalomyelitis
EBV-	Epstein Barr Virus
EC-	Entorhinal cortex
EDTA-	Ethylenediaminetetraacetic
EGF-	Epidermal growth factor
EGR1-	Early growth response 1
EIF1-	Eukaryotic translation initiation factor 1
ELISA-	Enzyme linked immunosorbent assay
ERT-	Estrogen replacement therapy
ESC-	Embryonic stem cells
FAD-	Familial Alzheimer's Disease
FBS-	Foetal bovine serum
FGF2-	Fibroblast growth factor 2

FoxP3-	Forkhead Box P3
FSC-	Front scatter
GAPDH-	Glyceraldehyde 3 phosphate dehydrogenase
GATA3-	GATA binding protein 3
G-CSF-	Granulocyte colony stimulating factor
GFAP-	Glial fibrillary acidic protein
GJA1-	Gap junction protein alpha 1
GLUT1-	Glucose transporter type 1
GM-CSF-	Granulocyte macrophage colony stimulating factor
GPCR-	G protein coupled receptor
GRIA-	Dense granule protein
GWAS-	Genome wide association study
HCl-	Hydrochloric acid
Hes-	Hairy and enhancer of split
HLA-DR-	Human leukocyte antigen DR
hLIF-	Human leukaemia inhibitory factor
HSP-	Heat shock protein
HRT-	Hormone replacement therapy
Iba1-	Ionised calcium binding adaptor molecule 1
ICAM-	Intercellular adhesion molecule
IFN -	Interferon
IgG-	Immunoglobulin G
IL-	Interleukin
IP10-	Interferon gamma induced protein 10
iPSC-	Induced pluripotent stem cells
ITGAX-	Integrin alpha X
IVF-	in-vitro fertilisation
IVW-	Inverse variance weighted
JAK-STAT-	Janus kinase and signal transducer and activator of transcription proteins
JunB-	JunB proto-oncogene
KCl-	Potassium chloride

KLF4- Krüppel like factor 4

KLRG1- Killer cell lectin-like receptor G1

KO- Knock out

LAG3- Lymphocyte activation gene 3

LAP- Latent associated peptide

LCN2- Lipocalin 2

LMP7- Lower molecular mass peptide 7

LOAD– Late onset Alzheimer's disease

LPS- Lipopolysaccharide

LRP1- Low density lipoprotein receptor 1

LYZ- Lysozyme

MAOB- Monoamine oxidase B

MAP2- Microtubule associated protein 2

MAPK3- Mitogen activated protein kinase 3

MAST- Microtubule associated serine/threonine kinases

MCI- Mild cognitive impairment

MCP1- Monocyte chemoattractant protein 1

MEF2a- Myocyte enhancer factor 2a

MEGF10- Multiple epidermal growth factor like domains 10

MERTK- MER proto-oncogene tyrosone kinase

MHC i- Major histocompatibility complex I

MHC ii- Major histocompatibility complex II

MIP1β- Macrophage inflammatory protein 1-beta

MMP3- Matrix metallopeptidase 3

MRI- Magnetic resonance imaging

mRNA- Messenger RNA

MS- Multiple sclerosis

MS4A4A- Membrane spanning 4 domains A4A

MSD- Meso scale discovery

mTOR- Mammalian target of rapamycin

NAS2- Non-affecting sibling 2

NEAA- Non essential amino acids

NF-kB – Nuclear factor kappa-light-chain-enhancer of activated B cells

NFL- Neurofilament light chain

NGS- Natural goat serum

NKG- Natural killer group

NMDA- N-methyl-D-aspartate

NMM- Neural maintenance media

NOD- Non obese diabetic

NOG- Noggin

NOS- Nitric oxide synthase

NPCs- Neural progenitor cells

NRG1- Neuregulin 1

Oct 3/4- Octamer binding transcription factor ¾

P2RY12- P2Y purinoceptor 12

PBMCs- Peripheral blood mononuclear cells

PBS- Phosphate buffered saline

PCR- Polymerase chain reaction

PD1- Programmed cell death protein 1

PFA- Paraformaldehyde

PGAM- Phosphoglycerate mutase

PGK1- Phosphoglycerate kinase 1

PLP1- Proteolipid protein 1

PMA- Phorbol 12-myristate 13-acetate

PSD- Pleckstrin and sec 7 domain

PSEN- Presenilin

P tau- Phosphorylated tau

PU- Pixel units

RA- Rheumatoid arthritis

RANTES- Regulated on activation, normal T cell expressed and secreted

R-BANS- Repeatable Battery Assessment of Neuropsychological Status

RNA- Ribonucleic acid

ROCK- Rho associated coiled-coil containing protein kinase inhibitor

RORγT- Retinoid related orphan receptor γT

RPTOR-	Regulator protein of mTOR pathway
RT-	Room temperature
RT-qPCR-	Reverse transcription quantitative polymerase chain reaction
S100β-	S100 calcium binding protein beta subunit
SerioBL-	Serio with bone morphogenic factor 4 and human leukaemia inhibitory factor
SerioEL-	Serio with epidermal growth factor and human leukaemia inhibitory factor
SEM-	Standard error of the mean
SLC1A-	Solute carrier family 1
SLE-	Systemic lupus erythematosus
ShRNA-	Short hairpin RNA
SnRNA seq-	Single nucleus RNA sequencing analysis
SOCS-	Suppressor of cytokine signalling
SOX2-	SRY-box 2
SPARCL1-	Secreted protein, acidic and rich cysteine like 1
sPDGRFRß-	Soluble platelet derived growth factor receptor ß
SSC-	Side scatter
TBE-	Tris borate EDTA buffer
Tbet-	T-box expressed in T cells
TBI-	Traumatic brain injury
TBR1-	T box transcription factor 1
Tcm-	Central memory T cells
TCR-	T cell receptor
Teff-	Effector T cells
TEM-	Effector memory T cells
TEMRA-	Terminally differentiated effector memory cells re-expressing CD45RA
Tfh-	T follicular helper cells
Tg-	Transgene
TGF-β -	Transforming growth factor beta
TGFBR1-	Transforming growth factor beta receptor 1
Th-	T helper cells

TIC- Transcriptional induction cocktail

TLR- Toll like receptor

TMB- 3,3',5,5'- Tetramethylbenzidine

TNFα- Tumour necrosis factor alpha

Treg- Regulatory T cells

TREM- Trigger receptor expressed on myeloid cells

TRPA- Transient receptor potential ankyrin

TYROBP- TYRO protein tyrosine kinase binding protein

UV- Ultraviolet

VCAM- Vascular cell adhesion molecule

VEGFA- Vascular endothelial growth factor A

VTN- Vitronectin

WT- Wild type

ZO-1 – Zonula occludens 1

1 Chapter 1: Introduction

1.1 Alzheimer's Disease

AD is the most common form of dementia with progressive neurodegeneration overtime in the individual. First observed by Alois Alzheimer at the beginning of the 20th century, postmortem reports published in 1907 on his patient Auguste D in Frankfurt hospital stated the presence of neurofibrillary tangles, amyloid beta (Aβ) plaques and gliosis.

The pathophysiology of AD can be defined as a build-up of Aβ plaques, neurofibrillary tau tangles and neuroinflammation. Consequences of these malformations lead to loss of cognitive function, memory loss, changes to mood and loss of independence for the individual. According to the European Brain Council seven million people in Europe live with AD with projections of up to fourteen million cases being diagnosed by 2030. Furthermore, the incidence rates are not homogenous between the sexes with females making up two thirds of AD patients in Europe and North America (Gustavsson et al., 2022). Yet, there is no cure for AD, and treatment lies within symptom management with pharmacological agents such as acetylcholine esterase inhibitors (donepezil and rivastigmine), memantine (NMDA receptor antagonist) and newer immunomodulatory agents such as Lecanemab being used.

1.2 Genes associated with familial versus sporadic AD

Genetic causes of AD were first identified in familial forms of AD in the early nineties. The chromosome location of the gene encoding amyloid precursor protein (*APP*) was first identified on chromosome 21 in 1987 (St George-Hyslop et al., 1987). Subsequently, specific point mutations carried by *APP* (Goate et al., 1991), presenilin-1 (*PSEN1*) (Rogaev et al., 1995) and presenilin-2 (*PSEN2*) genes (Rogaev et al., 1995, Levy-Lahad et al., 1995) have all been associated with an increased production of aggregating forms of Aβ (Wisniewski et al., 1991, Selkoe, 1991, Hardy and Higgins, 1992). However, genetic variation is also present in sporadic late onset AD mostly associated with a deficit in clearance of Aβ rather than an overproduction and depends on the presence of the Apolipoprotein E4 (*APOE4*) allele (Corder et al., 1993) and *TREM2* variants (Jonsson et al., 2012, Guerreiro et al., 2013). Additional

GWAS studies in recent years have identified several other genes associated with an increased risk of AD such as *CLU, PICALM* (Harold et al., 2009), *BIN1* and *MS4A4A* (Naj et al., 2011).

1.2.1 The APOE4 allele and Alzheimer's disease

In the CNS, *APOE* expression is mostly associated with astrocytes (Boyles et al., 1985), to a lesser extent with microglia (Xu et al., 2006) and is expressed in neurons in response to injury (Xu et al., 2006). The main function of *APOE* is related to cholesterol redistribution via lipid metabolism (Mahley, 1988). *APOE* is located on the 19q.13.22 chromosome with three introns and four exons (Das et al., 1985) and alterations in the amino acid sequence of the receptor region account for different *APOE* isoforms with variable binding affinities (Weisgraber et al., 1982). The amino acid variants that distinguish the three *APOE* isoforms are located at the positions 112 and 158, E2: Cysteine 112, Cysteine 158, E3: Cysteine 112, Arginine 158 and E4: Arginine 112, Arginine 158 (Weisgraber et al., 1981). In the global population, the frequency of the three different *APOE* alleles is distributed with 6.4% of the population having the E2 allele, 78.3% with the E3 allele and 14.5% with the E4 allele (Eisenberg et al., 2010).

Having at least one copy of the *APOE4* allele has been reported to increase the risk of developing AD by disrupting homeostatic function of astrocytes and microglia (Corder et al., 1993). This is supported by evidence that selective modification of *APOE* gene expression impacts the pathophysiology of AD including Aβ accumulation as well as microglial and astrocyte phenotype and function as detailed below.

An initial study carried out in the $APP_{Swe}PSEN1_{L166P}$ mouse model of cerebral amyloidosis indicated that deletion of the *APOE* gene led to an increase in Aβ plaques present in the parenchymal area by 6 months of age (Ulrich et al., 2018) whereas in $APP_{Swe}PS1_{\Delta E9}$ mice, deletion of *APOE* led to a decrease in the number of Aβ plaques present at 10 months (Ulrich et al., 2018). However, in both cohorts plaque size increased (Ulrich et al., 2018). These conflicting results reflect an important role of *APOE* in Aβ deposition as both AD mouse models had a significant decrease in the percentage area of plaque in cortical and hippocampal tissue (Ulrich et al., 2018). While the specific role of *APOE4* was not investigated in the study aforementioned

(Ulrich et al., 2018), other studies confirmed that depletion of the E4 isoform reduced overall Aβ load. Evidence from $APP_{swe}/PS1_{\Delta E9}$ mice in which expression of the E4 isoform is induced during the seeding stage of Aβ (before 6 months of age) showed an increased Aβ load overall compared to E3 isoform carriers (Liu et al., 2017). Interestingly, induction of *APOE4* during the growth stage of amyloidosis (6-9 months) did not impact Aβ deposition (Liu et al., 2017), thereby confirming the impact of *APOE* alleles on the seeding stage of amyloidosis. Furthermore, tamoxifen-induced selective depletion of *APOE3* or *APOE4* in astrocytes in $APP_{swe}PSEN1_{L166P}$ mice reduced Aβ plaque deposits and associated microgliosis (Mahan et al., 2022). Altogether, the current literature highlights that the presence of specific *APOE* alleles modifies amyloidosis progression. It is interesting to note that knocking out *APOE3* or *APOE4* genes has a significantly stronger effect in females compared to their male counterparts (Mahan et al., 2022). Importantly, neutralisation of *APOE4* in tau transgenic P301S mice led to reduction of Aβ deposition and Aβ-led tau seeding (Gratuze et al., 2022), indicating that *APOE4* involvement in AD pathoetiology goes beyond β-amyloid seeding.

First described in 5xFAD mice, disease associated microglia (DAM) unique to AD presented an upregulation of *APOE, TREM2* and *CTSD* genes, while genes related to homeostasis were downregulated (Keren-Shaul et al., 2017). Corroborating data showed a positive correlation between *APOE4* and disease progression in $APP_{Swe}PSEN1_{L166P}$ mice and was associated with a decrease in expression of *TGFBR1* and *MEF2A* homeostasis-related genes in microglia (Krasemann et al., 2017). Further studies in P301S *TREM2*$^{-/-}$ mice showed that in presence of tauopathy, *APOE4* alone can induce microglial reactivity along with expression of lysosome-associated genes *CTSB*, *CTSD* and *LYZ* (Gratuze et al., 2022).

In subsequent studies, deletion of *APOE4* in $APP_{Swe}PSEN1_{L166P}$ mice caused an increase in the microglial homeostasis marker *P2RY12* along with reduction of markers associated with immune activation such as *MHC-II* and *CLEC7A* (Mahan et al., 2022). This was not the case with *APOE3* depletion, indicating that the E4 isoform specifically skews microglial activation (Wang et al., 2021a). In microglia cultures from neonatal *APOE* transgenic mice (TR-*APOE3* or *APOE4*), basal levels of pro-

inflammatory cytokines IL-1β and TNF-α and anti-inflammatory cytokine IL-10 were significantly increased in microglia from both sexes (Mhatre-Winters et al., 2022). Interestingly, secondary to an inflammatory insult (LPS treatment or LPS + IFN-γ), microglia isolated from female *APOE4* carriers had the greatest increase in cytokine secretion compared to any other group following the order of "E4 female > E4 male > E3 female > E3 male" (Mhatre-Winters et al., 2022). In previous studies, knock-in *APOE4* or *APOE3* in 5xFAD mice resulted in a greater Aβ load in *APOE4* females versus *APOE4* males and *APOE3* female mice (Stephen et al., 2019).

Transcriptomic analysis of human samples confirmed that the gene set associated with microglia in healthy donors has a strong association with *APOE2* allele, which reduces expression of genes linked to a senescent microglia phenotype including genes associated with LOAD (late onset AD) such as *CD33, TREM2* and *MS4A4A* (Olah et al., 2018). Here again sex differences were reported in cerebrospinal fluid (CSF) samples from *APOE4* carriers, where higher concentrations of IL-16 and IL-18, shown to increase in AD (Di Rosa et al., 2006), were measured in females compared to males (Duarte-Guterman et al., 2020). Interestingly, this sex-difference was not seen in non-*APOE4* carriers patients, once more indicating that it is imperative to consider sex as a significant variable to further elucidate neuroinflammatory responses in AD. *APOE4* also impacts astrogliosis, as reported by Mahan and colleagues, showing that selective *APOE4* depletion led to reduced astrocyte reactivity (Mahan et al., 2022). Moreover, studies investigating plasma levels of cytokines and chemokines in AD patients, reported patients with at least one APOE4 allele had increased GFAP plasma levels compared to AD patients without the E4 allele (Bettcher et al., 2021).

Interestingly, the impact of the *APOE* allele has also been revealed in the adaptive immune response of AD patients (van Olst et al., 2024). It was reported PBMCs isolated from the blood of homozygous *APOE4 APOE4* carriers with AD had a significant increase in $CD4^+$ T cells, naïve $CD4^+$, memory $CD4^+$, $CD49d_{lo}$ $CD161_{lo}$ $CD57^-$ $KLRG1^-$ memory $CD4^+$, $CD161_{hi}$ $CD57^-$ $KLRG1^+$ $CD8^+$ T cells compared to *APOE3 APOE3* carriers with AD. Additionally, in the *APOE3 APOE4* subset of AD patients a positive correlation was reported between $PD1^-$ $CD57^+$ $CD8^+$ TEMRA and CSF $A\beta_{42}$

(indicating a lower amyloid burden). Additionally, an intricate interplay between *APOE* and *TREM2* has been reported, with *TREM2* suppression preventing *APOE* expression (Krasemann et al., 2017).

1.2.2 TREM2 Arg-to-His variants and Alzheimer's Disease

TREM2 is a transmembrane receptor expressed on microglia that can interact with different ligands such as lipoproteins, DNA and bacteria and activate intracellular signal transduction with transmembrane adaptor proteins including DAP10 and DAP12, which in turn leads to the phagocytosis of apoptotic cells and debris by microglia (Tagliatti et al., 2024). Ligands including ApoE, LPS and Aβ are all capable of binding to TREM2 (Lin et al., 2024). TREM2 is also reported to maintain microglia cell survival and decrease microglial apoptosis (McQuade et al., 2023). TREM2 is also key to modulating the inflammatory response and the switch to disease associated microglia first characterised by Keren-Shaul et al., (2017).

It is now well defined that variations in *TREM2* genetic sequence increases the risk of developing AD, this includes Arg-to-His variants at position 47 or 62 that impacts microglial function (Jonsson et al., 2012, Guerreiro et al., 2013), while other *TREM2* variants linked to increased *TREM2* and *TREML1* expression are associated with a decreased AD risk (Carrasquillo et al., 2017).

The capability of microglia to surround Aβ is mediated by TREM2 signalling (Wang et al., 2016). In TREM2 KO iPSC derived microglia 5xFAD AD mouse model, microglia failed to surround Aβ plaques and alterations in morphology characteristic of activated microglia were lost (McQuade et al., 2023). In *TREM2* deficient $APP_{Swe}PSEN1_{L166P}$ mice, a significant decrease in cortical amyloid plaque area at the early stage of disease progression (2 months) has been reported (Jay et al., 2017). However, at a later stage (8 months) *TREM2* deficient mice showed increased cortical $Aβ_{42}$ deposition accompanied by reduced microglial proliferation and recruitment around Aβ plaques (Jay et al., 2017). Astrocytic reactivity assessed by GFAP expression was also reduced along with inflammatory markers IL-1β and TNF-α (Jay et al., 2017). *TREM2*'s influence on microglial phenotype has also been investigated in the 5xFAD mouse model where BAC (bacterial artificial chromosome) *TREM2* forced expression resulted in reduced $Aβ_{42}$ load in 4 month-old mice whereas this

effect was lost by 7 months (Lee et al., 2018), confirming aforementioned data showing that *TREM2* influence on amyloidosis depends on the stage of the disease, similarly to *APOE4* impact.

Furthermore, forced expression of *TREM2* in 5xFAD mice resulted in downregulation of genes related to DAM phenotype, reduction in number of plaque associated microglia and modification of morphology, with cells showing further processes (Lee et al., 2018). Autophagy and metabolic fitness are other aspects of microglial functions dependent on *TREM2* expression, as shown by abnormal metabolism and increased abundance of autophagic vesicles in *TREM2* deficient microglia and AD patients carrying *TREM2* risk variants (Ulland et al., 2017).

Another component to consider when discussing *TREM2* is its soluble form (sTREM2), derived from the cell surface receptor proteolytic cleavage by ADAM proteases (Wunderlich et al., 2013). Indeed, elevated concentrations of sTREM2 in the CSF of AD patients has been reported and was positively correlated with tau and p-tau abundance but not with $A\beta_{42}$ (Piccio et al., 2016). Additionally, patients carrying AD-risk-related R47H *TREM2* mutation presented a significant rise in CSF levels of sTREM2 compared to non-carriers (Piccio et al., 2016). Conversely, for patients with mild cognitive impairment (MCI), the risk of developing AD was inversely proportional to sTREM2 CSF levels (Zhao et al., 2022). However, in a separate cohort, increased sTREM2 plasma levels positively correlated with the likelihood of developing AD (Zhao et al., 2022). In this study however, patient status with regards to *TREM2* variants was not reported although it would undeniably be useful to reconcile conflicting reports. Therefore, the contribution of sTREM2 as a biomarker for AD development remains unclear. What is noteworthy in this study, women were more likely to progress from MCI to AD compared to men, indicating that sex is an important factor impacting on the risk related to CSF sTREM2 levels (Zhao et al., 2022).

In vitro investigation of the role of sTREM2 was done in microglial cultures from *TREM2* KO mice. When incubated with recombinant sTREM2, *TREM2* KO microglia adopt an NF-kB-dependent pro-inflammatory phenotype characterised by the dose dependent release of cytokines including IL-1β, IL-6, TNF-α and the anti-inflammatory cytokine IL-10 and hypertrophic morphology denoted by a greater

surface area and diameter (Zhong et al., 2017). This was accompanied by stimulation of the Akt-GSK3b-b-catenin survival pathway and reduction of apoptosis in response to removal of GM-CSF (Zhong et al., 2017). Reconciling this work with their previous studies the authors propose that non-soluble TREM2 classically associated with anti-inflammatory phenotype and sTREM2 may work antagonistically (Zhong et al., 2015).

1.3 What role do astrocytes play in Alzheimer's Disease?

Astrocytes are a highly abundant glial cell which are estimated to make up 20-40% of total cells in the CNS (Herculano-Houzel, 2014). They are crucial for synaptic formation and maturation (Allen et al., 2012) as well as homeostasis maintenance (Xu et al., 2010, Diniz et al., 2012). Astrogliosis is the term used to describe astrocytic responses to neuronal injury which is seen both acutely and chronically (Gao et al., 2013) (Hostenbach et al., 2014). It has been shown that the cross talk between microglia and astrocytes happens through the release of mediators such as cytokines like IL-6 in acute CNS injuries (Gao et al., 2013), and microglial-induced astrogliosis (Liddelow et al., 2017). Emerging evidence supports the hypothesis that astrocytes develop a continuum of reactive phenotypes in response to insults and present region-specific homeostatic identities (Makarava et al., 2023) just like microglia (Paolicelli et al., 2022). Recent data supports a novel function for astrocytes as phagocytes of microglial debris, further highlighting the importance of the microglial-astrocytic interplay regarding brain homeostasis and neurodegeneration (Zhou et al., 2022). Astrocyte reactivity is dependent on the release of proinflammatory cytokines such as TNF-α, IL-1α and the complement component 1q (C1q) by microglia (Liddelow et al., 2017). This can be experimentally reversed by anti-inflammatory TGF-β or fibroblast growth factors (FGFs) (Liddelow et al., 2017), indicating that microglial influence is vital to induce astrocytic reactivity in neuroinflammatory states. Furthermore, Liddelow and colleagues have gathered evidence that reactive astrocytes lose their capacity to phagocytose myelin debris as well as their supportive function leading to weakened synapses (Liddelow et al., 2017).

1.3.1 The genotype of reactive astrocytes in Alzheimer's disease

Disease associated astrocytes (DAA), similar to disease associated microglia (Keren-Shaul et al., 2017), have been an area of recent research and are formally postulated to increase with disease progression (Habib et al., 2020). Using single nucleus RNA sequencing (snRNAseq) a specific astrocyte subtype was identified in hippocampal and cortical tissue in 5xFAD mice (Habib et al., 2020). This cluster was associated with the decline of homeostatic astrocyte genes, involved in complement cascade and increased expression of inflammatory genes and resulted in enhanced pathology (Habib et al., 2020). They are also reported to be present as early as 4 months of age prior to cognitive decline in 5xFAD model (Habib et al., 2020). It is interesting to note that DAA are also increased with age in wild type mice in this study, which highlights the contribution of astrocytic phenotypical changes to age-related neurodegeneration. More recently, a core signature of astrocytic genes in response to tau and Aβ has been identified in other murine models of tauopathy and amyloidosis (Jiwaji et al., 2022). Additionally, a disease specific astrocyte cluster was identified with increased expression of vimentin, Serpina3n and genes related to interferon response in single cell RNA seq (scRNAseq) carried out on TauPS2APP model (Lee et al., 2021). In $APP_{swe}PS1_{\Delta E9}$ mice, astrocyte expression of genes associated with reactivity such as *CLEC7A, CST7* and *CCL4* were upregulated while genes associated with astrocytic function such as *HES5* and *FAML23A* were downregulated suggesting that pathways associated with synaptic transmission and neurogenesis are impaired in the context of cerebral amyloidosis (Orre et al., 2014). These findings were recently corroborated with genes associated with cholesterol homeostasis, potassium homeostasis and synaptic function downregulated in astrocytes in the $APP_{swe}PS1_{\Delta E9}$ mouse model (Endo et al., 2022).

In human studies, snRNAseq analysis of astrocytes in different brain regions in AD versus healthy controls have also been reported (Smith et al., 2022, Belonwu et al., 2022, Sadick et al., 2022, Mathys et al., 2024, Serrano-Pozo et al., 2024, Soudy et al., 2025). Pathways related to oxidative stress, cell death, lipid storage and protein unfolding are enriched, whereas genes related to axonal guidance, angiogenesis and blood brain barrier (BBB) maintenance were downregulated in astrocytes isolated

from *APOE2* and *APOE3* prefrontal cortex AD patients (Sadick et al., 2022). Astrocytes from the entorhinal cortex (EC) and somatosensory region were investigated for transcriptional changes in AD and the potential correlation with Aβ and tau (Smith et al., 2022). Astrocyte clusters enriched for immune response pathways and GFAP were positively correlated with Aβ and tau (Smith et al., 2022). Conversely, clusters enriched for glutamine synthase and homeostatic function were negatively correlated with Aβ and tau (Smith et al., 2022). Furthermore, the heterogeneity of astrocyte expression with age, pathology and regionality was investigated in recent transcriptome analysis of astrocytes from human brains (Serrano-Pozo et al., 2024, Mathys et al., 2024). With age, astrocyte expression of genes such as *APOE, GJA1* and *AQP4* were upregulated and genes such as *ALDH1L1* and *SLC1A2* were down regulated in the EC (Serrano-Pozo et al., 2024). Conversely, in the primary visual cortex *AQP4* and *GJA1* were downregulated and *GFAP, CLU* and *MAOB* were upregulated highlighting a heterogenous population of astrocytes in the brain with age without disease (Serrano-Pozo et al., 2024). In relation to AD pathology, a positive correlation between p-tau and gene sets related to cytoskeleton, cell proliferation such as *AQP4* and *MAP2* and oxidative stress were reported (Serrano-Pozo et al., 2024, Mathys et al., 2024). However, genes associated with cellular movement, glycosaminoglycan and carbohydrate metabolism (*SLC1A2, ADAM12* and *PSD3*) negatively correlated with p-tau (Serrano-Pozo et al., 2024, Mathys et al., 2024). In relation to Aβ, a positive correlation with gene sets related to biological adhesion, GPCR signalling and lymphocyte activation (*MEF2A, SLC1A3* and *GRIA4*) were reported (Serrano-Pozo et al., 2024). As observed with p-tau, gene sets related to metabolism were negatively correlated with Aβ (Serrano-Pozo et al., 2024). Reactive astrocytes defined in the Mathys et al., 2024 study, increased with Aβ plaques but not tau, and were enriched for genes related to oxidative stress, cholesterol biosynthesis and protein folding. The relationship between cognitive resilience and astrocytes was further elucidated and highlighted that patients with a better cognitive score were more likely to have enriched pathways in astrocytes for antioxidant and choline metabolism (Mathys et al., 2024).

1.3.2 Astrocyte phenotypes identified in Alzheimer's Disease

Although until now astrocytes had been associated with AD to a lesser extent than microglia, astrogliosis has been reported in specific hippocampal regions in human samples, specifically in the Cornu Ammonis (CA) (Gonzalez-Rodriguez et al., 2021). In the $APP_{swe}PS1_{\Delta E9}$ mouse model, astrocyte size was significantly decreased in the cortex compared to wild-type mice (Endo et al., 2022). Furthermore, differences in astrocytic distribution were identified in AD donors, with astrogliosis (determined by GFAP staining) significantly higher in the CA1 and CA3 regions compared to non-AD donors (Gonzalez-Rodriguez et al., 2021). In AD brain samples, astrocytes were mainly clustered around plaques located in the pyramidal cell layer and in the striatum radiatum whereas in non-AD samples, astrocytes were located mainly in stratum oriens (Gonzalez-Rodriguez et al., 2021). Additionally, astrocytes in post mortem tissue from AD patients were characterised by a loss of expression of the chaperone protein HSP90AB1, involved in destruction of abnormal proteins (Gonzalez-Rodriguez et al., 2021).

The role of GFAP in AD pathology has been highlighted in several studies. In human postmortem tissue, GFAP positively correlated with each Braak stage and amyloid load of AD patients (Kamphuis et al., 2014). In relation to GFAP plasma levels, GFAP negatively correlated with cognition (Sánchez-Juan et al., 2024, Bettcher et al., 2021), white matter integrity in the temporal lobe (Bettcher et al., 2021) and brain weight (Sánchez-Juan et al., 2024) of AD patients. Patients with $A\beta^+$ tau^+ plasma had a significant increase in GFAP plasma levels compared to $A\beta^-$ tau^- patients (Guo et al., 2024, Dyer et al., 2024). In the EC, $CD68^+$ microglia negatively correlated with GFAP plasma levels in AD highlighting the important interplay between microglia and astrocytes (Sánchez-Juan et al., 2024). Further analyses also shows elevated GFAP levels in plasma and CSF from AD patients at various stages of the disease, including in pre-symptomatic phases and in cognitively unimpaired (CU) older individuals at risk of AD (Chatterjee et al., 2021, Benedet et al., 2021, Hirata et al., 2024). This is further supported by a study in a cohort of CU individuals classified based on plasma GFAP levels as positive (Ast^+) or negative (Ast^-) for astrocyte reactivity. In this study, only CU Ast^+ individuals' Aβ load correlated with plasma p-tau, suggesting a key role

for reactive astrocytes in Aβ-tau phosphorylation which seemed independent of the individual's *APOE4* status (Bellaver et al., 2023). However this hypothesis is disputed by Ferrari-Souza and colleagues, presenting the analysis of *APOE4* status together with positron emission tomography for Aβ, tau and microglial activation (Ferrari-Souza et al., 2022). The study reports that the presence of *APOE4* activates microglia in brain regions associated with early tau deposition independently of cerebral amyloidosis (Ferrari-Souza et al., 2022). Intriguingly, Bellaver and colleagues also present data indicating that the impact of astrocyte reactivity on the association of Aβ with tau was greater in men than women, which may contribute to the higher efficiency of anti-Aβ Lacanemab therapy in men compared to women recently reported (van Dyck et al., 2022).

A subset of reactive astrocytes expressing the complement component 3 (C3) were upregulated in the prefrontal cortex of post-mortem AD samples (Liddelow et al., 2017). Moreover, C1q and C3 expression was significantly increased in astrocytes in the Thy1-APP$^{KM670/671NL}$; Thy1-PS1^{L166P} and Tau P301S mouse model (Wu et al., 2019). In this study, C3 KO APP or Tau P301S mice had a significant increase in spine density, brain volume and improvement in cognitive scoring however this did not translate to significant changes in Aβ plaque number or size or changes in GFAP expression (Wu et al., 2019).

The JAK2-STAT3 pathway has been suggested as a key pathway for reactivity in astrocytes. JAK-STAT pathways involve cytokines binding to cytokine specific receptor at the cell surface activating Janus Kinases (JAK) leading to the phosphorylation of signal transducers and activators of transcription (STATs) which move to the nucleus and directs transcription within the cell (Darnell et al., 1994). To regulate this response Suppressor of Cytokine Signalling (SOCs) are key to preventing aberrant signalling via the JAK-STAT pathway by preventing cytokine receptor phosphorylation and STAT activation (Endo et al., 1997, Starr et al., 1997).

By injecting APP$_{swe}$PS1$_{\Delta E9}$ mice with adeno-associated vector containing SOCS3, an inhibitor of the JAK2-STAT3 pathway, there was a significant decrease in GFAP expression and vimentin^{+} astrocytes (Ceyzériat et al., 2018). RNA seq analysis reported that JAK2-STAT3 inhibition by SOCS3 led to downregulation in pathways

related to cytokine induction (*IL-1B, CCL2, CCL4* and *CCL6*), the complement cascade (*C1QA, C1QB, C1QC* and *C4B*) and reactivity (*GFAP*, Vimentin, Serping1) indicating SOCS3 as a "master inhibitor" of astrocyte reactivity (Ceyzériat et al., 2018). In relation to plaques, SOCS3 treatment led to a decrease in plaques and improvements in learning indicating the consequences of JAK-STAT3 activation in relation to astrocyte reactivity (Ceyzériat et al., 2018).

In humans, IL-6 expression on astrocytes are co-localised with Aβ plaques in post mortem tissue (Lyra e Silva et al., 2021). ELISA carried out on human brain homogenates revealed significant increases in IL-6 and SOCS3B versus healthy controls (Lyra e Silva et al., 2021). Furthermore, IL-6 plasma levels which are significantly increased in AD patients, negatively correlated with MMSE scores, hypothalamic and hippocampal grey matter densities (Lyra e Silva et al., 2021). Additionally, the use of IL-6 antibodies on $APP_{swe}PS1_{\Delta E9}$ mice led to a significant decrease in IL-6 expression which is reported to be increased in APP/PS1 brains and led to improvements in cognition (Lyra e Silva et al., 2021).

Dysregulated calcium signalling in astrocytes has also been identified in reactive iPSC derived astrocytes (McComish et al., 2024) and in AD (Paumier et al., 2021) with astrocytes adopting a "hyperactive" calcium signalling when incubated with Aβ oligomers (Paumier et al., 2021). Furthermore, by blocking the specific calcium channel in astrocytes, TRPA1, a significant decrease in glutamate release was reported and resulted in cognitive improvements in the Thy1-$APP^{KM670/671NL}$;Thy1-$PS1^{L166P}$ mouse model (Paumier et al., 2021). The improvement in cognition was not directly related to plaque accumulation however as TRPA1 blocking did not alter plaque load (Paumier et al., 2021).

Astrocytic ability to phagocytose and degrade synaptosomes in the Thy1-$APP^{KM670/671NL}$;Thy1-$PS1^{L166P}$ mouse model is also significantly inefficient compared to wild type or tau models (Sanchez-Mico et al., 2021). Furthermore, genes related to phagocytosis *MEFG10* and *MERTK* were significantly decreased whereas genes related to reactivity were upregulated (Sanchez-Mico et al., 2021). In a recent preprint, chronic exposure of iPSC derived astrocytes to cytokines led to induced MHC-II expression on astrocytes (Hill et al., 2025).

Alteration of metabolic pathways in microglia and astrocytes in the CSF and brains of AD patients has now gathered the attention of the scientific community, with a study highlighting that alterations in inflammatory mediators and metabolic markers in the CSF preceded cognitive manifestations of AD in the patients, opening the way to potential new early diagnostic tools (Johnson et al., 2020). Of most interest, altered lipid metabolism in astrocytes and microglia is linked to *APOE4* expression (Tcw et al., 2022). In microglia and astrocytes derived from *APOE4*$^{+}$ human iPSCs, genes associated with cholesterol biosynthesis were enriched while genes related to actin cytoskeleton, focal adhesion and endocytosis linked to impaired lipid uptake were decreased (Tcw et al., 2022). The authors suggest that *APOE4*$^{+}$ cells may be incorrectly detecting cholesterol levels thereby triggering aberrant de novo intracellular cholesterol synthesis (Tcw et al., 2022).

Astrocytes are also important in maintaining BBB integrity which has an essential role in controlling the CNS microenvironment in health and disease. In 5xFAD mice, links between astrocyte activation/reactivity and BBB decline have been revealed by a drastic reduction of markers of vascular integrity (GLUT1 expressed by vascular endothelial cells and the tight junction marker ZO-1) accompanied by an increased in GFAP expression (Ahn et al., 2018).

1.3.3 Suppressing astrocyte reactivity in neurodegenerative diseases

Attempts to prevent astrocytic reactivity have been beneficial in other neurodegenerative diseases. In Parkinson's disease, blocking microglial mediated astrocytic activation using the peptide 1 receptor agonist, NLY01, showed neuroprotective capacity (Yun et al., 2018). Similarly, in the SOD1^{G938} mouse model of amyotrophic lateral sclerosis (ALS), knock out of microglial mediators TNF-α, IL-1a and C1q reduced astrocytic reactivity, preventing neuromuscular junction denervation and slowing down the progression of ALS (Guttenplan et al., 2020). Although, this ultimately had no effect on pathology end point this indicated that reactive astrocytes are tightly involved in ALS progression (Guttenplan et al., 2020).
An interesting study linked microglia, astrocytes and T cells in the context of multiple sclerosis: in the experimental autoimmune encephalomyelitis (EAE) induced NOD (non-obese diabetic) knock-in IL10 mouse model (Mayo et al., 2016). The nasal

delivery of $CD3^+$ T cells induced generation of IL-10^+ LAP^+ (latent associated peptide) Tr-1 like T cells and led to a systemic increase in IL-10 levels and a decrease in IL-17^+ T cells (Mayo et al., 2016). This treatment prevented astrocytic activation in association with a down regulation of the expression of *CCL2, CCL5* and *IL-6* and upregulation of *AQP4, VEGFA* and *MMP3* genes that prevent blood brain barrier degradation (Mayo et al., 2016). Furthermore, following nasal delivery of $CD3^+$ T cells, genes associated with inflammation such as *IL-1B* and *IL-6* were downregulated in microglia (Mayo et al., 2016). All together this showed that regulation of astrocytic and microglial activation can improve neuroinflammation seen in the EAE mouse model. Similar interactions have been reported in a rodent model of stroke with brain Tregs successfully suppressing astrogliosis by producing the epidermal growth factor, amphiregulin (Ito et al., 2019). This study highlights that without Treg infiltration, astrogliosis associated with a neurotoxic and reactive phenotype increases. Furthermore, the authors discovered that the neuroprotective function of Tregs depended on the release of the key regulatory component amphiregulin which is associated with tissue repair (Zaiss et al., 2015). Specific genes required for astrogliosis were identified as *IL-6, STAT3* and *SOCS2* (Okada et al., 2006) and their expression was downregulated by Tregs (Ito et al., 2019). Interestingly, a recent study from the Dorothée lab showed that the balance of reactive astrocyte subtypes, including amyloid-associated C3-positive A1 astrocytes is modulated by Tregs in Thy1-$APP^{KM670/671NL}$;Thy1-$PS1^{L166P}$ mice (Stym-Popper et al., 2023). These works not only highlight that along with microglia, astrocytes are also key players, that have a crucial impact on disease progression.

1.4 Sex differences in Alzheimer's Disease

1.4.1 Genetic heterogeneity in males and females

The interface between genetic variation and sex is an area more recently explored in several AD studies. Evidence gathered by a few research groups in human samples and mouse models suggest a heterogeneity between microglia and more recently astrocytes from males and females that becomes more apparent with age (Stephen et al., 2019, Sanfilippo et al., 2022, Mhatre-Winters et al., 2022, Duarte-

Guterman et al., 2020, Coales et al., 2022, Mathys et al., 2019, Belonwu et al., 2022, Soudy et al., 2025).

Transcriptional analysis carried out on postmortem microglial nuclei of the somatosensory and entorhinal cortex from non-AD and AD male and female donors indicated that genes associated with AD pathology have a greater association with female donors compared to male donors (Coales et al., 2022). Using snRNA seq an upregulation in inflammatory pathway genes such as interferon type I, antigen processing and presentation via MHC-I was observed in microglial nuclei isolated from females, whereas pathways associated with protein localisation and phosphorylation were upregulated in microglia nuclei from males (Coales et al., 2022). Furthermore gene set variation analysis confirmed that microglial nuclei from female donors were enriched for genes associated with the inflammatory response in AD such as *IFN* (interferon) response genes which were not enriched in microglial nuclei from male donors (Coales et al., 2022). However, sex specific differences in microglia were less apparent in AD male and female patients compared to aged matched non AD patients (Coales et al., 2022). The authors suggest this predisposition towards pro-inflammatory gene expression may play a part in female susceptibility to AD (Coales et al., 2022). Sex differences in other cell types other than microglia were reported in snRNAseq analysis of the prefrontal cortex of male and female AD patients with females having a stronger correlation between AD pathology and downregulation of excitatory and inhibitory neurons whereas males had a stronger correlation with AD pathology and global activation of oligodendrocytes (Mathys et al., 2019). Sexual dimorphism of microglia in response to pathology also seem to be impacted by astrocyte phenotype. Investigation into the chitinase-like protein, CHI3L1, expressed mainly by astrocytes (Bonneh-Barkay et al., 2012) highlights an upregulation in AD brains compared to healthy controls with sex being a modulating factor of expression (Sanfilippo et al., 2016). Reuse of publicly available microarray data sets from AD and non-AD brain donors facilitated the identification of sex-differential expression of CHI3L1, significantly higher in brains from female LOAD and non-AD donors compared to males (Sanfilippo et al., 2016). In a follow-on study, using publicly available transcriptome data sets from AD and non-AD brain donors, the authors investigated cellular distribution profiles and gene expression

related to CHI3L1 (Sanfilippo et al., 2022). Deconvolution analysis showed that CHI3L1 expression was positively correlated to astrocytes in non-AD donors whereas in AD donors CHI3L1 expression was positively correlated to microglia (Sanfilippo et al., 2022). However, the impact of increased CHI3L1 expression on microglial function and phenotype in female AD patients requires further elucidation (Sanfilippo et al., 2022) .

The effect of sex on astrocyte gene expression in AD, has been investigated using snRNA-seq studies. Astrocytes isolated from the prefrontal cortex in AD females had a significant decrease in pathways related to transport and vascular transport across the BBB which was not observed in males (Belonwu et al., 2022). In astrocytes isolated from AD males, there was a downregulation in pathways related to pre-synaptic filopodia which was not observed in females (Belonwu et al., 2022). This highlights that astrocytes are both affected by AD, but the pathways differ between the sexes (Belonwu et al., 2022). Another study investigating transcriptional changes between AD and healthy control astrocytes in the prefrontal cortex revealed sex specific alterations with pathology (Soudy et al., 2025). Astrocytes from male AD brains had a significant decrease in *ERBB4* which has been linked to synaptic dysfunction in AD previously (Zhang et al., 2017) and *RPTOR* (a regulator protein of mTOR pathway) compared to healthy male controls (Soudy et al., 2025). Astrocytes from female AD patients had a significant increase in *CCL2* a regulator in neuroinflammation (Posillico et al., 2021) compared to healthy female controls (Soudy et al., 2025). In gene set enrichment analysis, male astrocytes had enriched pathways for programmed cell death and apoptosis (Soudy et al., 2025). However, females had enrichment in pathways related to Wnt signalling (important in synaptic maintenance) (Palomer et al., 2019), cell cycle, motility and migration (Soudy et al., 2025). Key upstream regulators for the DEGs identified in this study were also investigated with genes related to protein folding, and mTOR signalling (*NRG1, CCT5* and *RPTOR*) identified as regulators in male astrocytes. In female astrocytes, the key regulatory gene was reported to be low density lipoprotein receptor 1 (*LRP1*) which is a key regulator of Aβ metabolism (Soudy et al., 2025).

Comparative medicine studies corroborate human data. Whole genome gene expression in hippocampal tissue of healthy mice confirms the presence of a more

inflammatory phenotype linked to microglia specific genes in old females compared to males (Mangold et al., 2017). ScRNAseq profiling in the neocortex of Tg2576 AD mice highlighted disease associated sex-dependent alteration in gene expression in cell types involved in neuroinflammation (Ali et al., 2022). Expression of microglial *APOE, CX3CR1* and *CTSD* were downregulated in Tg2576 males compared to CT littermates, while another set of genes (*JUNB, CD83* and *HSPA5*) was downregulated in microglia from Tg2576 females (Ali et al., 2022). A compelling aspect of this analysis also highlighted that genes specific for angiogenesis, vascular development and reactive oxygen species metabolism were upregulated in males but not in females indicating perhaps a more neuroprotective role being adopted in males (Ali et al., 2022). In astrocytes, expression of *JUNB* was increased in Tg2576 females compared to wild-type controls, whereas males had a different group of genes upregulated (*PLP, APOD* and *SPARCL1*) (Ali et al., 2022). Additionally, sexual dimorphism in *EGR1* expression in astrocytes was also observed which has been previously related to exacerbating AD pathology (Qin et al., 2017). It is interesting to note that sex was not a modulating factor for genes associated with the adaptive immune system. Sex differences have also been observed in astrocytes of tau models from males and females. In the THY-Tau 22 mouse model, astrocytes from the female cohort had increased expression of *GJA1* and *EIF1* compared to wild-type females whereas male mice astrocytes increased expression of *HSPA5* compared to wild-type cohorts (Ali et al., 2024). Taken together this suggests that both the presence of Aβ and tau can generate a sex specific response in glial cells.

In $APP_{NL\text{-}G\text{-}F}$ mice, microglia from females progressed into activated response microglia (ARMs) earlier than their male counterparts at 6 months of age (Sala Frigerio et al., 2019). Additionally at 16–18 month in the $APP_{swe}PSEN1_{\Delta E9}$ model, microglia from female mice had a significant increase in expression of genes associated with DAMs and ARMs such as *TYROBP, CTSD* and *CCL6* compared to male $APP_{swe}PSEN1_{\Delta E9}$ mice (Guillot-Sestier et al., 2021).

In 7-9 months $APP_{sw695}/PSEN1_{dE9}$ mice, sex also impacted the quality of adult neurogenesis with spine density decreased in females versus males (Richetin et al., 2017). Furthermore, hippocampal cell proliferation was swayed toward glial

production and away from neuronal proliferation in female mice whereas glial and neuronal proliferation was balanced in males (Richetin et al., 2017).

1.4.2 Glial phenotypes in males and females

Along with differences in gene expression, amyloidosis, astrogliosis and microgliosis are increased in females compared to males in AD mouse models (Guillot-Sestier et al., 2021, Gallagher et al., 2013, Stephen et al., 2019, Melnikova et al., 2016, Stephen et al., 2022). Morphological differences in microglia have been reported between the sexes with females presenting a higher abundance of rod-like shaped microglia with more complex processes than the amoeboid shape classically associated with a phagocytic phenotype more commonly found in brains from males in the $APP_{swe}PSEN1_{\Delta E9}$ mouse model (Guillot-Sestier et al., 2021). This was also observed in post-mortem brain samples from female AD patients which present more dystrophic microglia accompanied by a characteristic increase in iron accumulation compared to samples from male AD patients (Guillot-Sestier et al., 2021, O'Neill et al., 2022). Additionally, expression of markers of senescence assessed by immunostaining of P16 and lipofuscin in post mortem parietal cortex tissue of female and male AD and non-AD donors reported increased senescence in AD females compared to non-AD females which was not observed in male patients (O'Neill et al., 2022).

Astrocytic reactivity in relation to possessing the *APOE3* or *APOE4* allele in 5XFAD model is further modulated by sex (Stephen et al., 2022). Astrocytes in *APOE3* males possessed a less hypertrophic phenotype with a reduced soma compared to females with a significant increase in soma size (Stephen et al., 2022). Astrocyte coverage and interaction with plaques was also significantly reduced in *APOE4* females compared to *APOE3* females or *APOE4* males indicating that sex and genotype have an effect on astrocytic phenotype (Stephen et al., 2022).

CSF studies from human cohorts have also identified sex differences in relation to CSF biomarkers and the pathogenesis of AD. Female patients at increased risk for developing AD (one parent with AD diagnosis or the *APOE4* genotype) had a stronger correlation between CSF GFAP levels and p-tau compared to males (Vila-Castelar et al., 2025). However, another study investigating prodromal alterations reported male patients with higher expression of plasma GFAP levels had a stronger

correlation with p-tau and Aβ compared to women with high GFAP plasma levels (Bellaver et al., 2023).

In several AD studies, plasma GFAP levels have been reported to be significantly increased in female compared to male patients (Boccalini et al., 2025, Labonte et al., 2025, Sánchez-Juan et al., 2024). Furthermore, plasma GFAP levels in females had a negative correlation with hippocampal volume which was not observed in male AD patients (Abbas et al., 2023). Once again this highlights that the presence of these primary AD features (Aβ and tau) do not elicit a uniform response in males and females.

1.4.3 Impairment of metabolic and mitochondrial function in microglia in AD

In relation to metabolic alterations in AD, microglia are reported to undergo metabolic reprogramming and trigger acute inflammation responses (Baik et al., 2019). The authors propose that Aβ exposure triggers defective metabolism by shifting microglia from oxidative phosphorylation to glycolysis which can be reversed by activation of the mTOR pathway associated with recombinant IFN-γ (Baik et al., 2019; (Kroczynska et al., 2016). Furthermore, heterogeneity in metabolic pathways has also been observed in microglia from male and female $APP_{swe}PSEN1_{\Delta E9}$ mice (Guillot-Sestier et al., 2021, O'Neill et al., 2022) and non-transgenic mice (Baik et al., 2019). Microglia in female $APP_{swe}PSEN1_{\Delta E9}$ mice shifted toward a more glycolytic metabolism compared to their male littermates and genes encoding key enzymes involved in the glycolytic pathway such as *GAPDH, PGK1* and *PGAM* were upregulated in female microglial samples (Guillot-Sestier et al., 2021). Iron accumulation was more marked in $APP_{swe}PSEN1_{\Delta E9}$ microglia from female mice compared to males which is suggestive of enhanced mitochondrial dysfunction (O'Neill et al., 2022). Furthermore, greater accumulation of reactive oxygen species, ROS, was specifically increased in $APP_{swe}PSEN1_{\Delta E9}$ versus WT female littermates, while no difference was recorded in the males regardless of the presence of the $APP_{swe}PSEN1_{\Delta E9}$ transgene (O'Neill et al., 2022). On the other hand, basal and maximal respiration were significantly decreased in microglia isolated from female $APP_{swe}PSEN1_{\Delta E9}$ mice compared to males (Guillot-Sestier et al., 2021). Taken together, these studies highlight the sexual dimorphism in relation to microglial metabolic responses in AD.

1.4.4 The effect of endocrine aging and the role of HRT in menopause to combat AD risk in females

With age, the endocrine system functioning shifts for all individuals, including the sexual reproductive hormones in both males and females. In females a key timeframe marking endocrinological aging is perimenopause, when menstrual cycles become irregular until menopause is reached 12 months after the final menstrual period, occurring on average at 51 years of age (Broekmans et al., 2009). Based on the remarkable prevalence of AD in women compared to men, perimenopausal and menopausal states have been investigated with regards to AD in several human and animal studies.

Initial investigation in brains of perimenopausal Sprague-Dawley rats, 9-10 months old with an irregular cycle, identified a decline in expression of genes associated with mitochondrial bioenergetics, glucose uptake and synaptic plasticity (Yin et al., 2015). However, once the animals reached menopause (acyclic group), expression of genes associated with mitochondrial function, fatty acid uptake and inflammation increased (Yin et al., 2015). Further investigation of the impact of menopause on hippocampal gene expression by bulk-RNA sequencing in 9 month old perimenopausal rats compared to 6 month old regular cycle rats, showed an age-dependant increase in DAM associated genes, complement and microglial reactivity genes as well as *MHC-I* and *MHC-II* genes prior to the onset of perimenopause (Mishra et al., 2020). Gene expression analyses showed a decrease in TGF-β signalling associated genes such as *MAPK3* and *NOG* along with decrease in expression of *APOE, TREM2, TYROBP* and complement signalling in perimenopausal 9 month-old rats compared to regular cycle 6 month-old rats (Mishra et al., 2020). Genes associated with the interferon I and II pathways and lipid metabolism were upregulated as well in perimenopausal rats compared to regular cycle rats (Mishra et al., 2020). Besides, while in post-menopausal rats upregulation of interferon I and II was lost, a marked upregulation of lysosomal marker *CD68* and *MHC-II* genes was also observed (Mishra et al., 2020). Additionally, microglia isolated from post-menopausal rats presented an increase in non-mitochondrial oxygen consumption compared to microglia isolated from pre-menopausal rats (Mishra et al., 2020).

Interestingly, reproductive senescence in acyclic 9 months old animals was also accompanied by an upregulation in genes involved in inflammation such as TNF signalling and *ICAM1*, as well as *CD4* and *CD69* characteristic of T helper cell activation (Mishra et al., 2020).

Interestingly, in 6 month-old rats oestradiol depletion by ovariectomy induced the same expression pattern as endocrine ageing in perimenopausal 9mo rats: the upregulation of *IFN I* and *IFN II, TREM2* and complement pathways (Mishra et al., 2020). This was partially mitigated by oestradiol treatment which decreased interferon pathway, but had no effect on *TREM2* and *C1S* (Mishra et al., 2020). Translational validity of these findings was also investigated in datasets of human hippocampal tissue from women at 20-34, 35-59 and 60-75 years of age with age matched men. Expression level of *MHC-I*, *MHC-II*, *TREM2* and *TYROBP* all increased with age in both sexes however a greater increase was seen in females compared to age matched males (Mishra et al., 2020). This suggests that hormonal fluctuations brought on by menopause lead to alterations in cellular immune and metabolic function and highlights that menopause is a key timepoint at which hormone-dependant cellular changes may participate to the enhanced vulnerability of females vis-à-vis AD. It is important to note that the studies by Yin and colleagues and Mishra and colleagues were carried out in non-transgenic rats and therefore future studies would need to apply these methods to an AD rodent model to further understand the implications of these findings with regards to AD pathology. It does however suggest that oestrogen supplementation via hormone replacement therapy may reduce the risk of developing AD by preventing an increase in expression of genes relate to inflammation.

Human studies have indeed shown that the presence of oestrogen does decrease the risk of AD in females. Analysis of F-fluoro-2-deoxyglucose (FDG) highlighted glucose hypometabolism in the frontal cortex of perimenopausal and postmenopausal women compared to premenopausal women (Mosconi et al., 2017). In this study, the use of Pittsburgh compound B PET scan allowed the identification of a significant decrease in grey and white matter volume found in menopausal women associated with an increase in Aβ deposits, which was further exacerbated in *APOE4* carriers (Mosconi et al., 2017). Additionally, both

perimenopausal and menopausal females had decreased mitochondrial activity in brain regions associated with AD (Mosconi et al., 2017). Furthermore, the risk of developing AD was reduced in patients who had received oestrogen replacement therapy (ERT) compared to controls with duration of treatment overall not impacting the effectiveness of ERT as confirmed by meta regression analysis (Song et al., 2020). Another study carried out by Imtiaz and colleagues reported that administration of oestrogen to a cohort of Finnish women for less than 10 years was not beneficial and increased the risk of AD, while extending the administration for over 10 years was protective (Imtiaz et al., 2017). It was reported in *APOE4* carriers that HRT improved cognition compared to non-users of HRT with the *APOE4* allele (Saleh et al., 2023). The entorhinal cortex and amygdala were also larger in the HRT *APOE4* carriers compared to non-users of HRT with the *APOE4* allele. Within the *APOE4* carrier group hippocampal volume was larger in the HRT users compared to non-users indicating a protective role for HRT in AD (Saleh et al., 2023).

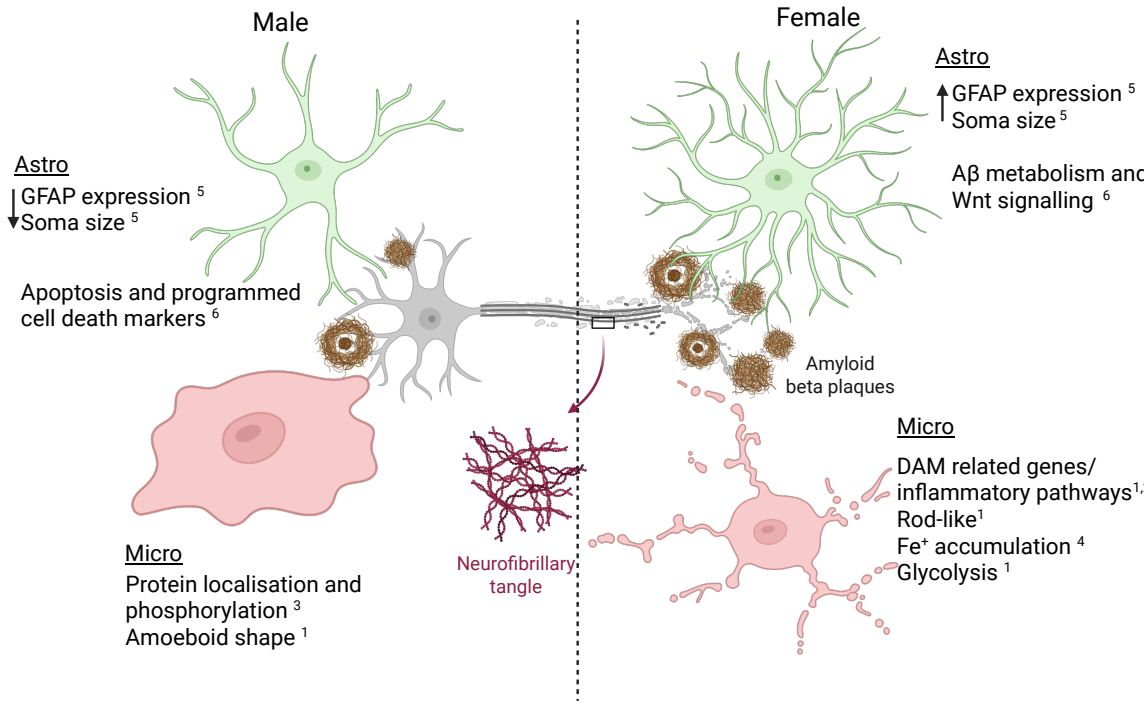


Figure 1.1 The effect of sex on microglial and astrocyte phenotype in human cases and mouse models of AD

***Microglia**: $APP_{swe}PSEN1_{\Delta E9}$ females had a shift toward glycolysis, a higher proportion DAM related gene expression (Guillot-Sestier et al., 2021[1]) (Keren-Shaul et al., 2017[2]). In human post-mortem microglial nuclei gene expression differed between sexes, with females having increased expression in inflammatory pathways and males increased expression in protein localisation and phosphorylation (Coales et al., 2022[3]). Microglia from $APP_{swe}PSEN1_{\Delta E9}$ females had increased Fe^{+} accumulation and mitochondrial increased production of ROS compared to microglia isolated from males (O'Neill et al., 2022[4]).*

***Astrocytes**: 5XFAD APOE4 Females had a significant increase in GFAP expression and soma size compared to APOE3 5XFAD male who had a decrease in GFAP and cell soma size (Stephen et al., 2022)[5]. Female astrocytes isolated from pre-frontal cortex female brains had enriched gene pathways related to Aβ catabolism and Wnt signalling (Soudy et al., 2025)[6]. Astrocytes from prefrontal cortex male brains had enriched gene pathways for apoptosis and programmed cell death (Soudy et al., 2025)[6]. Figure was generated with the use of BioRender.*

1.5 Does the adaptive immune system help or hinder in Alzheimer's disease?

The adaptive immune system is an arm of the body's defence against pathogens and self-antigens including conformationally abnormal self-proteins, deemed harmful to the host. Within adaptive immunity, lymphocytes, consists of B cells, natural killer (NK) cells and T cells. T cells express the surface marker CD3 and are distinguished further into subsets including Cytotoxic ($CD8^{+}$), Helper ($CD4^{+}$), and more recently described γδ T cells. Furthermore, helper T cells can be distinguished based on surface marker, transcription factors and cytokines expressed by the cell (Fang and Zhu, 2017). Regulatory T cells (Treg) are identified by FoxP3 and IL-10 expression; Th17 cells express RORγT and IL-17; Th1 cells express T-bet and IFN-γ; Th2 cells express GATA3 and IL4, IL-5 and IL-13 and Tfh (follicular) cells which express Bcl6 and IL-21 (Fang and Zhu, 2017) (See **Table 1.1** below). These immune subsets are required for appropriate responses to insults and injuries throughout our lifetime.

Table 1.1 Helper T Cell Subsets

Cell Type	Surface Markers	Transcription Factors	Signature cytokines released
Th1	CD3, CD4	Tbet	IFN-γ, TNF-α
Th2	CD3, CD4	GATA3	IL-4, IL-5 and IL13
Tregs	CD3, CD4, CD25	FoxP3	IL-10
Th17	CD3, CD4	RoRγT	IL-17 and IL-22

It is also important to note T cell differentiation from naïve to senescent T cell can be identified by certain surface marker combinations (Xu and Larbi, 2017). CD45RA, CCR7, CD27 and CD28 are identified on naïve T cells (Förster et al., 2008, Dolfi and Katsikis, 2007). Central Memory T cells (T_{CM}) will develop by removing CD45RA and expressing CD45RO (Mahnke et al., 2013). Effector memory T cells (T_{EM}) will only express CD45RO and Terminal Effector T cells (T_{EMRA}) will express CD45RA with both cell types no longer expressing CD27, CD28 and CCR7 (Mahnke et al., 2013). Senescence can be identified by KLRG1 and CD57 expression (Larbi and Fulop, 2014, Stubbe et al., 2006)

T cells are paramount for protection against disease and infection, however, they are also shown to play a role in autoimmune disease such as arthritis (Banerjee et al., 1992) (Breedveld et al., 1989) and multiple sclerosis (MS) (Giunti et al., 2003). Initial reports of T cells present in brain parenchyma and grey matter of AD patients were first published in the late 1980s (Itagaki et al., 1988, Rogers et al., 1988). Additionally, significant increases in T cell subsets have been reported in several animal models of AD. In the ArcAβ AD mouse model, $CD3^+$ T cells were significantly increased in the brain parenchyma (Ferretti et al., 2016) and in more recent studies increases in $CD8^+$ and $CD4^+$ T cells in the parenchyma in TE4 tau model of AD (Chen et al., 2023), 5XFAD (Wang et al., 2024a, Su et al., 2023) and APP/PS1 Thy1-APP $^{KM670/671NL}$; Thy1-PS1 ^{L166P} model (Su et al., 2023) have been reported. More recent human studies have reported a larger proportion of T cells in PBMCs of AD patients (Wang et al., 2024b), as well as $CD4^+$ (Wang et al., 2024b) and cytotoxic $CD8^+$ T cells circulating in the CSF of AD patients (Gate et al., 2020, Wang et al., 2024b).

1.5.1 Dysfunction of blood brain barrier integrity in Alzheimer's disease

A highly specialised vasculature provides the brain with the nutrients required to meet its energy demands. The BBB allows for strict regulation of what enters and

exits the CNS. The key structural mechanism that regulates influx and efflux of substrates and products is the neurovascular unit comprised of many different cell types, these include pericytes, astrocytes, endothelial cells and neurons (Gong et al., 2025, Nehra et al., 2022). BBB leakage was initially observed in AD patients over 40 years ago (Glenner, 1979) however the implications of the impaired BBB in AD patients has been more widely investigated in recent years. The pericyte injury marker soluble platelet derived growth factor receptor ß (sPDGFRß), was reported to be significantly increased in the CSF of individuals with cognitive impairment compared to cognitively normal individuals (Nation et al., 2019). In a subsequent study using dynamic contrast enhanced MRI, cognitively normal individuals with at least one copy of the APOE4 gene had increased BBB breakdown in the hippocampus and parahippocampal gyrus compared to cognitively normal APOE3 homozygous individuals (Montagne et al., 2020). Furthermore, in cognitively impaired individuals, carriers of the APOE4 allele had significant increase in BBB disruption compared to cognitively impaired APOE3 homozygous individuals (Montagne et al., 2020). Additionally, sPDGFRß correlated with BBB breakdown in APOE4 but not APOE3 individuals (Montagne et al., 2020).

The lymphatic system, CSF and choroid plexus (CP) are important avenues for infiltration of peripheral lymphocytes into the brain (Kipnis et al., 2004). Given that T cells are directed to the CP under the influence of IFN-γ for repair and surveillance (Kunis et al., 2013), any alterations in expression of CP proteins may understandably impact on T cell response to CNS injury and AD pathology. Indeed, CP dysfunction is indicated by the decrease in key endothelial proteins such as ICAM-1, VCAM-1 along with chemokines/cytokines CXCL1, CCL2 and IFN-γ in 5xFAD mice and is a likely promoter of leucocyte trafficking (Baruch et al., 2015). Additionally immunoassays carried out on CSF from AD patients showed a significant increase in cytokines/chemokines such as IL-1Rα, IL-4, IL-7, IL-8, IL-9, IL-10, IL-15, Eotaxin, G-CSF, PDGF-BB and TNF-α (Taipa et al., 2019). Consequently, AD-linked alterations in the blood brain barrier (BBB) integrity characterised by loss of tight junction proteins such as ZO-1, Claudin-5 and Occludin (Wan et al., 2015) likely contribute to an

accrued permeability to T cells, further impacting the neuroinflammatory status of AD patients.

1.5.2 $CD4^+$ T cell subsets and the unclear role of Regulatory T cells in Alzheimer's Disease

Implication of $CD4^+$ T cell subsets in the pathoetiology of AD, including Th1 cells, Th17 cells and Tregs is also an important field of research (Machhi et al., 2021, Dansokho et al., 2016, Baek et al., 2016, Faridar et al., 2020, Faridar et al., 2022, Yeapuri et al., 2023).

Tregs isolated from peripheral blood have been reported to be decreased in AD compared to healthy age match controls (Larbi et al., 2009, Ciccocioppo et al., 2019, Fu et al., 2020) with one study reporting a correlation between Tregs and MMSE scores (Fu et al., 2020). GWAS analysis using two sample Mendelian randomisation reported a Treg association with AD with subsequent IVW (inverse variance weighted) analysis revealing a protective function in AD (Zhang et al., 2025). Using MAST differential expression in T cells isolated from MCI and healthy controls, significant transcriptional dysregulation was reported in Tregs (Piehl et al., 2022). However, other studies have reported no difference in Treg proportions in AD compared to age match controls with an increase in their suppressive activity with age (Rosenkranz et al., 2007). Conversely, TGF-β secretion in PBMCs was significantly decreased in severe AD patients versus MCI patients (Fu et al., 2020). Tg2576 mice Treg suppression was significantly decreased at 12 months however increased at 20 months indicating a modulatory effect of pathology on Treg response (Abdelmoaty et al., 2023).

Furthermore, there are conflicting arguments whether Tregs are beneficial or detrimental in AD. There is research to suggest that increasing Treg populations in AD mouse models leads to an improvement in AD pathology (Faridar et al., 2020, Dansokho et al., 2016, Baek et al., 2016, Faridar et al., 2022, Yeapuri et al., 2023). However, there are also contradictory findings that report increasing Tregs negatively impacts AD pathology (Baruch et al., 2015, Di Benedetto et al., 2019). In human studies, there is evidence that indicates Treg suppression of effector T cells (Teff) proliferation is compromised in AD patients compared to patients with MCI or age-

matched controls (Faridar et al., 2020). This is consistent with two studies investigating potential therapeutic benefit of Tregs in AD mouse models by administering low-dose IL-2 (Dansokho et al., 2016, Alves et al., 2017, Yuan et al., 2023). Treg amplification via peripheral administration of low dose IL-2 improved cognition and lead to recruitment of microglia toward plaques in transgenic APP/PS1 mice (Thy1-APP $^{KM670/671NL}$; Thy1-PS1 ^{L166P}) (Dansokho et al., 2016, Yuan et al., 2023). Administration of low dose IL-2 peripherally prompted Treg expansion and activation in the brain of $APP_{swe}PSEN1_{\Delta E9}$ mice and led to an increase in IL-2 concentration in the hippocampus of the treated group and rescued memory impairment (Alves et al., 2017). Interestingly, in the same study, hippocampal biopsies from AD patients showed a significant decrease in IL-2 expression indicating the link between IL-2 and Treg expansion as a potential avenue of investigation in treating AD (Alves et al., 2017). In recent years, IL-2 therapy has been examined in human clinical trials (Faridar et al., 2025). Subcutaneous IL-2 administration (5 days every 4 weeks) in patients with mild to moderate AD, led to a significant increase in Tregs versus placebo (Faridar et al., 2025). Moreover, decreases in IL-15, CCL2 and CCL11 and increases in IL-4 and CCL13 were observed in the plasma of treatment versus placebo patients (Faridar et al., 2025). $A\beta_{42}$ levels in the CSF of treated patients significantly increased and an improvement in cognitive scores was observed (Faridar et al., 2025).

In other CNS disorders, it was suggested enhancing CNS resident Tregs via astrocytic delivery of IL-2 would be more efficient than peripheral administration of IL-2 as astrocytes are the most abundant glial cell in the CNS (Yshii et al., 2022). This treatment had preventative effects in models of stroke, traumatic brain injury (TBI) and the EAE model of Multiple Sclerosis and curative effects in TBI and EAE (Yshii et al., 2022). This method applied to an AD rodent model would undoubtably help elucidate the potential therapeutic effect of resident Tregs of the CNS compared to peripheral Tregs and how they impact the inflammatory and phagocytic capacity of microglia and astrocytes.

Furthermore, adoptive transfer of $CD4^+CD25^+$ Treg or $CD4^+CD25^-$ Teff cells was investigated in 3xTgAD mice in which Treg transfer led to slowing down of cognitive decline in memory deficiencies and learning impairments suggesting a

neuroprotective function in AD (Baek et al., 2016). Cytokine release in the splenocytes of 3xTgAD mice with Treg or Teff transfer was also investigated in this study. IFN-γ release was decreased in 3xTgAD mice receiving Teff and Treg transfer, while IL-6 was significantly reduced by Treg transfer compared to control 3xTgAD mice (Baek et al., 2016). This is consistent with the requirement of IL-6 and transforming growth factor-β (TGF-β) for differentiation of naïve T cells into Th17 cells and not Tregs, previously reported (Veldhoen et al., 2006, Bettelli et al., 2006). In more recent years, *ex vivo* expansion of Treg from healthy participants have been transferred in an immunodeficient AD mouse model (5xFAD-Rag2KO) and led to a decrease in Aβ burden and reactivity of glial cells in the frontal cortex and dentate gyrus (Faridar et al., 2022). The generation of Aβ specific Tregs reported a beneficial response to pathogenesis of AD (Yeapuri et al., 2023). Intravenous adoptive transfer of Aβ Tregs led to an improvement in cognition in Tg2576 mouse model with a significant increase in Tregs located in the brain (Yeapuri et al., 2023). Plaque load, $IBA1^{+}$ amoeboid shape microglia and GFAP expression in astrocytes were all significantly decreased (Yeapuri et al., 2023). This is consistent with findings in subsequent Aβ Treg adoptive transfer studies in other AD mouse models such as 3xTg AD and 5xFAD with improvements in cognition, decrease in genes associated with inflammation (*CD86, NOS, IL-1β* and *TNF-α*) and a decrease in Aβ and tau consistently reported (Park et al., 2024b, Park et al., 2024a, Yang et al., 2024). Suppressive abilities of Aβ-specific human Tregs on microglia have also been assessed with TNF-α and IFN-γ release and *NOS2, CD86, CXCR1, ITGAX* and *TREM2* gene expression all significantly decreased in microglia (Yang et al., 2024). However, introduction of Aβ specific Tregs into patients with AD, enrolled into a phase I clinical study, revealed no improvement in cognitive scores (Yang et al., 2024).

More novel therapies to enhance Treg populations in AD models have also been investigated. A rapamycin-incorporated lipid nanoparticle containing Aβ "nanovaccine" injected intradermally into 5xFAD mice revealed an increase in Aβ antibodies in brain lysates, Tfh in the spleen (indicating antibody production) and an increase in Aβ Tregs in the brain which led to a decrease in plaques (Jung et al., 2023). Tregs isolated from the spleens had increased expression of FoxP3, IL10 and TGFβ

(Jung et al., 2023). Additionally, an Aβ chimeric antigen receptor (CAR)-Treg was successfully designed and proven to have suppressive functions against $CD8^+$ T cells (Saetzler et al., 2023). Phenotypically the CAR-Tregs did not differ from normal Tregs confirmed by expression of Treg markers such as CD25, CTLA4, FoxP3 and $CD127_{lo}$ (Saetzler et al., 2023).

It is important to note that several studies present contradictory findings in relation to beneficial upregulation of Tregs in AD. Depletion of $FoxP3^+$ T cells have been shown to lead to an increase in leucocyte trafficking across the choroid plexus (CP) which had been previously shown to be impaired in the AD mouse model (5xFAD) (Baruch et al., 2015). Interestingly, the previously mentioned decrease of ICAM-1 signalling and IFN-γ expression at the CP of 5xFAD mice was accompanied by elevated levels of $FoxP3^+$ Treg along disease progression (Baruch et al., 2015). Weekly injections of GA (glatiramer acetate-immunomodulatory compound) in 5xFAD mice reduced plaque build-up, enhanced leukocyte trafficking and decreased neuroinflammation (Baruch et al., 2015). Moreover, Aβ burden decreased in mice treated with P300i (impairing Treg suppressive activity), although the possible influence on microglial phagocytic capacity was not determined (Baruch et al., 2015). Treatment of mice with retinoic acid (RA), a key trigger of Treg proliferation, led to an increase in Aβ plaques and a decline in spatial learning (Baruch et al., 2015). These findings were corroborated by a subsequent study in which decreasing Treg suppressive function improved cognition in the AD mouse model 3xTgAD (Di Benedetto et al., 2019). Anti-CD25 antibodies injected into $APP/PS1_{NL\text{-}G\text{-}F}$ mice led to a significant increase in gene expression in the pre-frontal cortex of *CD3* and a decrease in *IL-1B* and *IL-6* (Casares et al., 2023). These mice also had an improved fear conditioning responses (Casares et al., 2023). This response was replicated in the same study treating $APP_{swe}PS1_{\Delta E9}$ mice with menthol inhalation with the authors suggesting a potential relationship between olfactory stimulation and immune response (Casares et al., 2023). No change in Aβ load indicated that the improvements were independent of Aβ clearance (Casares et al., 2023). A partial resolution of amyloidosis and cognitive deficits linked to depletion of IL-10 in $APP_{Swe}PS1_{\Delta E9}$ mice has also been reported (Guillot-Sestier et al., 2015) with

confirmation of increased Iba1$^+$ microglia population and phagocytic function. Along the same lines, forced expression of IL-10 in TgCRND8 mice worsened Aβ load and cognitive deficits (Chakrabarty et al., 2015). Thus, supporting the argument that tipping the balance in favour of Teff vs. Treg leads to a decrease in Aβ load.

Taken together, these studies indicate that the role of the adaptive immune system specifically the dynamic of Tregs vs Teff is not fully understood and requires further elucidation with regards to AD.

1.5.3 The role of Th1, Th2 and Th17 in AD pathology

Consequently, it is imperative to note Treg suppression likely leads to Teff proliferation. Recently, single cell analysis from publicly available datasets reported significant increases in CD4$^+$ effector memory T cells (TEM) and CD4$^+$ terminal differentiated effector memory CD45RA$^+$ cells (TEMRA) in PBMCs of AD patients (Wang et al., 2024b). Serum levels in AD patients have reported increased levels of IL-17, IL-18 and IL-23 compared to controls (Chen et al., 2014, Dubenko et al., 2021). Studies investigating Th subsets, revealed a significant increase in Th17 cells in PBMCs isolated from MCI- AD patients compared to healthy controls (Oberstein et al., 2018, Zeng et al., 2022, Li et al., 2023, Cao et al., 2023). Additionally, increases in Th1 and decreases in Th2 Teff subsets have been reported in PBMCs isolated from AD patients compared to healthy controls (Zhang and Niu, 2022, Li et al., 2023). The expression of lower molecular mass peptide 7 (LMP7) was positively correlated to Th1 and Th17 in AD patients (Li et al., 2023). PR-597 a LMP7 inhibitor led to a downregulation of Th1 and Th17 cells from CD4$^+$ T cells isolated from AD patients along with their cytokine response (Li et al., 2023).

In animal studies, changes in CD4$^+$ T cell subsets have reported a negative effect on AD pathogenesis. In the brain of 9 month APP/PS1 mice, a significant increase in gene expression of *IL-17* and *TNF-*α was observed (Cao et al., 2023). Additionally, IL-17A serum levels correlated with cognitive decline and intraperitoneal injection of IL-17A in 8 month old APP/PS1 mice led to a significant decrease in cognition (Cao et al., 2023).

Intracerebroventricular injection with Aβ specific CD4$^+$ Th1 cells in the 5XFAD model, induced microglia characterised by a high expression of MHC-II with

enhanced phagocytic capacity and a reduction in Aβ plaques (Mittal et al., 2019). Conversely, in another study, Tg2576 mice reported cognitive impairment upon transfer of Aβ specific Th1 and Th17 cells (Machhi et al., 2021). The transfer was accompanied by an increase in systemic TNF-α, IFN-γ and IL-17 in both Th1 and Th17 Aβ treated groups (Machhi et al., 2021). Additionally, Iba1$^+$ microglia in cortex and hippocampus were significantly increased while Tregs decreased in the periphery and CNS (Machhi et al., 2021). Furthermore, inhibiting Th1 and Th17 T cells via PR-957, a selective ß5i subunit (LMP7) of the immunoproteasome (Muchamuel et al., 2009), in $APP_{swe}PS1_{\Delta E9}$ showed a marked increase in cognition and a decrease in Th17 present in the brain (Li et al., 2023). The impact of IL-17 on AD-like pathology has also been investigated in the 3xTgAD mouse model (Brigas et al., 2021). IL-17 accumulation at 5 months was associated with memory deficits in a sex specific manner, as only female but not male mice presented cognitive decline (Brigas et al., 2021). Additionally, treatment with an IL-17 antibody led to prevention of short-term memory decline (Brigas et al., 2021). It was confirmed that the cells responsible for IL-17 production were another subset of T cells known as γδT cells and not Th17, it is however interesting to see the impact that this shared cytokine can have in AD (Brigas et al., 2021). Treatment of AD PBMCs with all-trans retinoic acid led to a significant decrease in IL-17 secretion indicating an immunomodulatory effect of all-trans retinoic acid on cytokine signalling (Behairi et al., 2015).

1.5.4 CD8$^+$ T cell profile in Alzheimer's patients and mouse models

CD8$^+$ T cells have been identified in both WT and $APP_{swe}PS1_{\Delta E9}$ mice using transcriptomic analysis (Altendorfer et al., 2022) and in human AD post-mortem tissue of the hippocampus (Gate et al., 2020) and the middle temporal gyrus using immunofluorescence (van Olst et al., 2024). Recently, a significant increase in subsets of CD8$^+$ T_{EM} and T_{EMRA} has been reported in both PBMCs (Gate et al., 2020, van Olst et al., 2024, Wang et al., 2024b) and CSF (Gate et al., 2020, Wang et al., 2024b) from AD patients. Furthermore, the stages of AD have been shown to influence the population of T cell subsets present. CD8$^+$ T cells present in the brain parenchyma of human postmortem tissue significantly increases at the AD dementia stage which is not reported at the AD MCI stage (Wang et al., 2024b). Two studies employing mass

cytometry analysis of PBMCs, revealed significant increases in $CD8^+$ $CD27^-$ T_{EMRA} (Gate et al., 2020) and $PD1^+$ $CD57^+$ $CD8^+$ T_{EMRA} (van Olst et al., 2024) in MCI and AD patients compared to controls. Additionally, $PD1^-$ $CD57^+$ $CD8^+$ T cells significantly increased in AD dementia patients only compared to age match healthy controls (van Olst et al., 2024). Additionally, cytokine response following PMA stimulation revealed MCI and AD patients released significantly more IFN-γ from $CD8^+$ T cells compared to healthy controls (Gate et al., 2020).

Correlation between CSF markers and $CD8^+$ T cells confirmed a negative correlation between $CD161_{lo}$ $KLRG1^+$ $CD57^-$ $CD8^+$ effector cells and CSF $A\beta_{42}$ levels in MCI AD patients. Interestingly, once the disease progressed to AD dementia $CD57^-$ $CD8^+$ T_{EMRA} cells had a negative correlation with p-tau levels (van Olst et al., 2024). Relationships between $CD8^+T_{EMRA}$ cells and other immune cells revealed that AD MCI and AD dementia patients' $CD8^+$ T_{EMRA} population positively correlated with $KLRG1^+$ $CD57^+$ $CD4^+$ by van Olst et al., (2024). $CD8^+$ T_{EMRA} correlated negatively with naïve $CD4^+$ T cells at the MCI AD stage and correlated with Tregs at the AD dementia stage (van Olst et al., 2024). It is also postulated that the strength of "cellular control" $CD4^+$ and $CD8^+$ T_{EM} have on $CD8^+$ T_{EMRA} is weakened in AD patients compare to controls indicating a potential risk for dysfunction in $CD8^+$ T_{EMRA} cells in AD pathology (Wang et al., 2024b). Another $CD8^+$ subset expressing HLA-DR has also been implicated in AD with T cells from both PBMCs and CSF samples having a significant increase in HLA-DR expression in AD patients compared to age matched or other dementia patients (Lueg et al., 2015). In relation to cognition, activated $HLA\text{-}DR^+$ $CD8^+$ T cells in the CSF and $CD8^+$ T_{EMRA} cells in PBMCs were negatively correlated with cognition in AD patients (Lueg et al., 2015, Gate et al., 2020).

T cells in the CSF were further investigated in order to understand if clonal expansion was increased in AD. The number of T cells with different TCR$\alpha\beta$ receptors was increased in AD patients compared to healthy controls (Gate et al., 2020). Additionally, T cells that were highly expanded had increased expression of cytotoxic genes *NKG7* and *GRZA, H* and *K* and antigen presenting genes *HLA-C* and *B2MA* (Gate et al., 2020). It was interesting to note that the only antigen that had specificity for the TCR in AD was Epstein Barr Virus (EBV) trans-activator protein BZLF1 although the

authors are cautious to state that this does not imply EBV is the causative agent of AD (Gate et al., 2020). These studies highlight the transient nature of the adaptive immune system in Alzheimer's disease thus highlighting the importance of timing potential pharmaceutical interventions to ensure efficacious response to specific immune targets.

Whether the $CD8^+$ T cells present in AD play a beneficial (Su et al., 2023) or detrimental role (Wang et al., 2024a) is still debated. In the 12 month old 5XFAD mouse model, $CD8^+$ T cells exacerbated AD pathology by significantly increasing cytokine release (TNF-α, IFN-γ , IL1-α and Granzyme B) compared to wild-type controls post stimulation (Wang et al., 2024a). Treatment with anti-$CD8^+$ in 8-12 month 5XFAD mice led to a decrease in tissue resident $CD8^+$ T cells, Aβ plaques, $Iba1^+$ microglia, neuronal loss and restored cognition compared to vehicle (Wang et al., 2024a). Conversely, Aβ mRNA vaccination of 2-3 month old 5XFAD mice led to a significant increase in $CD8^+$ T cells present in dentate gyrus and subiculum, $CD8^+$ T cells expressing exhaustion markers (PD-1 and Lag3) and an increase in $CD8^+$ cytokine release (TNF-α, IFN-γ, IL-10, TGF-β and Granzyme B) (Wang et al., 2024a). However, the beneficial role of $CD8^+$ in AD pathology has also been argued in the 5XFAD model by Su et al., (2023). TCRα-deficient 5XFAD mice targeting $CD8^+$ T cells not $CD4^+$ led a significant increase in Aβ plaques and a decline in cognition (Su et al., 2023).

Considering the reports of sex differences in prevalence of autoimmune diseases and in adaptive immune responses in the general population careful evaluation of sex differences in the efficacy of these T cell modulatory interventions would also be primordial. In the general population sex differences in the frequency of T cell subsets have been reported (Lee et al., 1996, Sankaran-Walters et al., 2013, Afshan et al., 2012) and this effect is influenced by age (Huang et al., 2021). In gut biopsies, baseline inflammatory pathways gene expression was increased in healthy females versus males under 40 years of age and included genes involved in antigen presenting function (Sankaran-Walters et al., 2013). Furthermore, in PBMCs and the lamina propria of females a higher abundance of proliferating $CD4^+$ and $CD8^+$ T cells compared to males was reported (Sankaran-Walters et al., 2013). In another study,

PBMC samples presented significantly lower Treg population in young females compared to males (Afshan et al., 2012). Microarray analysis of T cells isolated from PBMCs of 25-35 year old healthy male and female participants reported sex differences in response to restimulation, with cytotoxic gene expression higher in males compared to females except for IL-17A (Hewagama et al., 2009). Altogether, these reports indicate that over-regulation of inflammatory genes in females may contribute to the higher prevalence of autoimmunity in females. Indeed, females are more prone to autoimmune diseases including MS with a female: male patient ratio reported at 3:1 (Ortona et al., 2016) and rheumatoid arthritis before the age of 50 with a ratio of 4:1 (Alpízar-Rodríguez et al., 2017). In the study previously mentioned above by (van Olst et al., 2024) groups were also separated by sex to further elucidate the adaptive immune response in AD. In females, $CD8^+$ T cells and $CD57^+$ $CD8^+$ TEMRA T cells were significantly increased in MCI-AD compared to AD dementia or healthy controls (van Olst et al., 2024). Whereas male patients had a significant increase in $CD57^+$ $CD8^+$ TEMRA T cells in the AD dementia cohort compared to healthy male controls (van Olst et al., 2024). Males and females possessed a similar proportion of $PD1^+$ $CD57^+$ $CD8^+$ TEMRA with an increase at the MCI AD stage versus control indicating sex does not modulate this T cell subset (van Olst et al., 2024). $PD1^-$ $CD57^+$ $CD8^+$ TEMRA was significantly increased in MCI AD and AD dementia female cohorts compared to healthy controls whereas this significant increase did not appear in males until the AD dementia stage (van Olst et al., 2024). Recently, a specific signature for tissue resident $CD45^+CD8^+$ T cells was identified in AD patients' blood and CSF samples and negatively correlated with cognition (Gate et al., 2020). Hence treatments targeting the adaptive immune system in neurodegenerative disease like AD requires systematic assessment of T cell abundance and response in both females and males.

1.5.5 Glia-T cell crosstalk

The signalling pathway adopted by T cells and microglia has been an area of study in more recent years. In humans, scRNAseq revealed CXCL16 – CXCR6 as a unique signalling pathway in MCI with CXCR6 being strongly associated with T_{EM} cells (Piehl et al., 2022). Additionally, CXCL16 correlated significantly with neurofilament

light chain (NfL) in MCI-AD but not in AD patients CSF (Piehl et al., 2022). This seems to be conserved across species as scRNAseq analysis determined CXCL16 – CXCR6 as a key signalling pathway between $CD8^+$, not $CD4^+$ T cells and microglia in the 5XFAD mouse model (Su et al., 2023). Additionally, $CXCR6^+$ $CD8^+$ T cells revealed to be a tissue specific subset as $CD8^+$ T cells from spleens of 5XFAD mice had significantly lower CXCR6 expression (Su et al., 2023). In both 5XFAD and human tissue, $CD8^+$ $CXCR6^+$ and $Iba1^+$ microglia colocalised with Aβ plaques (Piehl et al., 2022, Su et al., 2023). Furthermore, CXCR6 5XFAD KO mice had a significant decrease in $CD8^+$ T cells specifically in the brain indicating this pathway is key to $CD8^+$ T cells role in AD pathology (Su et al., 2023). Functionally, $CD8^+$ T cells have been suggested to act as a "cellular brake" as they have been shown in co-culture to cause a significant decrease in TNF-α and IL-1β in microglia when cultured with $PD\text{-}1^+$ $CD8^+$ T cells (Su et al., 2023). Furthermore, microglial-T cell communication investigated with TE4 mice reported an increased expression of genes associated with antigen presentation, complement and cytokine release compared to $APP/PS1_{21E4}$ (Chen et al., 2023). The authors also report that depleting microglia had the ability to decrease brain T cell infiltration and reduced atrophy in 7.5-9.5 months TE4 male mice compared to E4 controls. This seem to indicate the functionality of microglia in the adaptive immune response to tauopathies (Chen et al., 2023). Immunostaining further revealed an increase of $CD3^+$ T cells in the hippocampus and piriform-entorhinal cortex in tau models at 9.5 months of age, along with a positive correlation with microglial abundance and a negative correlation with T cell number and thickness of the granule cell layer (Chen et al., 2023). Not surprisingly, from single cell analysis the dominant signalling pathways utilised by $CD8^+$ TEMRA cells in AD patients were MHC-I, CCL and proteins associated with brain injury and repair, including amyloid β protein precursor (Wang et al., 2024b).

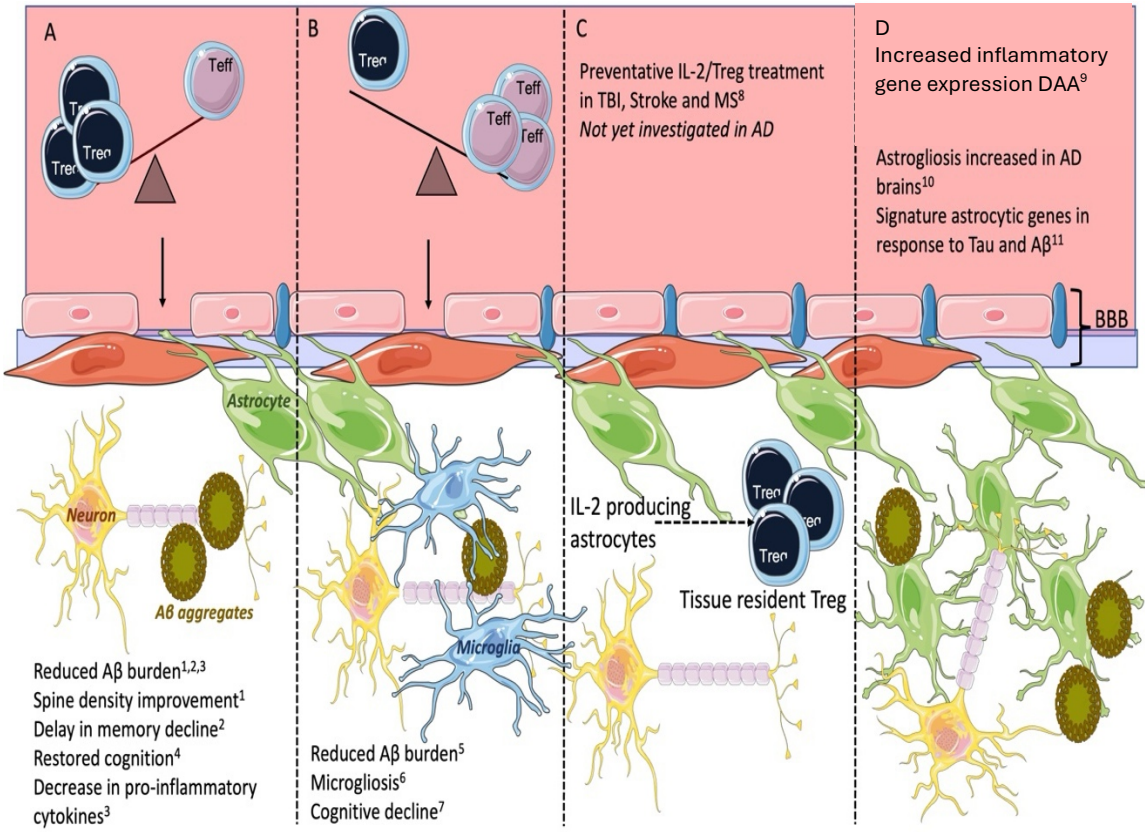


Figure 1.2 Influence of peripheral and brain microenvironment on disease progression

***A**: Peripheral increase of Treg population in AD mouse models decreased Aβ load (Alves et al., 2017[1], Baek et al., 2016[2], Faridar et al., 2022[3]), improved spine density (Alves et al., 2017[1]), delays learning decline (Baek et al., 2016[2]), restored cognition (Dansohko et al., 2016[4]) and decreased the release of pro-inflammatory cytokines (Faridar et al., 2022[3]). **B**: Parenchymal Aβ burden is decreased in mice treated with P300 inhibitors (impairing Treg suppression), although the possible influence on microglial phagocytic capacity was not determined (Baruch et al., 2015)[5]. An increase in Teff populations triggered increased Iba1⁺ microglia (Machhi et al., 2021[6]) and cognitive decline in 3xTgAD females but not in males (Brigas et al., 2021[7]). **C**: The increase of tissue resident Tregs in MS, stroke and TBI mouse models was preventative for all three groups and this treatment was also curative in TBI and MS (Yshii et al., 2022[8]). However, it has not yet been investigated in an AD model. **D**: Disease associated astrocytes (DAA) have been identified in 5xFAD mice, characterised by increased expression of genes related to the complement cascade and inflammatory pathways (Habib et al., 2020). In post mortem AD brain tissue, GFAP⁺ astrocytes are more abundant than in non-AD brains (Gonzalez-Rodriguez et al., 2021[10]). In murine models of tauopathy and amyloidosis, core signature of astrocytic genes in response to Tau and Aß has been identified (Jiwaji et al., 2022[11]). This figure was generated with the use of BioRender.*

1.6 Hypothesis and aims of the project

There is limited understanding of the role sex plays in modulating the response of astrocytes and T cells in AD. Therefore the aims of this project are to further understand the heterogeneity of astrocytic and T cell phenotypes in males and females. This will be carried out by investigating T cell subsets isolated from secondary lymphoid organs and GFAP expression in astrocytes from the APP_{swe},$PSEN1_{dE9}$ mouse model (Jankowsky et al., 2004). Additionally, human samples of cerebrospinal fluid and peripheral blood mononuclear cells and astrocytes derived from induced pluripotent stem cells will also be employed to further analyse the role sex plays in AD pathogenesis.

2 Chapter 2: Materials and methods

2.1 Animals

The animal colony examined in this study overexpressed chimeric mouse/human amyloid precursor protein (Mo/HuAPP695swe) and a mutant human presenilin 1(PS1-dE9), (034832 from Jackson's laboratory; (Jankowsky et al., 2004) referred to as APP/PS1 mice in this study. It included both male and female mice and wild-type littermates. Housing environment for the mice were maintained at controlled conditions (temperature 20-22°C, food and water ad libitum). Veterinary supervision was maintained throughout the study until euthanising at different time points (13-15 and 16-17 months). The project was approved by the Trinity College Animal Welfare Body, certified by, and adhering strictly to the guidelines and recommendations from the Irish Health Products Regulatory Authority (HPRA), enforced under the European Union Regulations 2012 (S.I. No. 543 of 2012 and Directive 2010/63/EU of the European Parliament on the protection of animals used for scientific purposes).

2.1.1 Genotyping

Genotyping of the mouse cohort was carried out to confirm expression of the PSEN1 transgene using ear punches collected from pups at the time of weaning and verified using tail snips collected at the time of humane killing of the animals. This was carried out initially as stated below but genotyping for later generations were outsourced to the vendor Transnetyx, UK.

Ear or tail tissue was digested in a solution made up of proteinase K (MP Biomedicals LLC, USA; Cat Code: 02193981-CF) at a concentration of 0.15mg/mL in digestion buffer (0.1% (v/v) Triton X 100 (ThermoFisher Scientific, USA; HFH100), 50mM KCl (Sigma Aldrich; 529552) and 10mM Tris-HCl (Sigma Aldrick; 320331) (pH=9)) and incubated in a thermoblock (3 hours at 60°C then at 94°C for 15 minutes). The digested tissue was genotyped for *PSEN1* and prion protein (PrP) (to confirm the presence of the endogenous mouse PrP gene) for the following primers:

PSEN forward:	5'-AATAGAGAACGGCAGGAGCA-3'	
PSEN reverse:	5'-GCCATGAGGGCACTAATCAT-3'	608bp product

Prion forward: 5'-CTAGGCCACAGAATTGAAAGATCT-3'

Prion reverse: 5'-GTAGGTGGAAATTCTAGCATCATCC-3' 324bp product

Per sample the following assay mix was made:

Forward primer (Prion or *PSEN1*)	1µl
Reverse primer (Prion or *PSEN1*)	1µl
Go Taq Green)	12.5µl
RNAse Free H_2O	5.5µl
DNA sample	5µl
Total Volume	25 µl

A negative and a positive control were also included. The negative control included the primers, GoTag Green (Invitrogen; K1082) and H_2O and the positive used a known PSEN1 positive animal sample. The samples were run on the thermocycler (PTC-200 Peltier Thermal Cycler) under the following cycle conditions.

Step	Temperature °C	Time	Note
1	94	3 minutes	
2	94	30 seconds	
3	52	1 minute	
4	72	1 minute	Repeat step 2-4 for 35 cycles
5	72	2 minute	
6	10	-	Hold

Table 2.1 Thermocycler cycle conditions for amplification of PSEN1 and prion primers

2.1.1.1 PCR product electrophoresis and visualisation

5 µL of cDNA samples were loaded into wells of 1.5% (w/v) agarose gel with GelRed® Nucleic Acid Gel Stain (Biotium Inc., USA; Cat Code; 41001) immersed in 1X TBE (5X Stock: 54g Tris Base, 27.5g Boric Acid, 20 mL of 0.5M EDTA at pH 8, 1L of dH_20) along with DNA ladder (10 µL; VWR Life Sciences; Cat code: 733-2062) and underwent electrophoresis at 200V for 40 minutes. Migration of PCR products was visualised under the lumination iBright 1500 (ThermoFisher Scientific). Quality of

DNA was assessed by amplification using prion primers, with a band expected at 300bp. PSEN1 positive samples were confirmed by comparison with the positive control and DNA ladder (10 µL), band expected at 600bp.

2.1.2 Preparation of Animal Tissue

Animals were humanely killed using CO_2 inhalation and death was confirmed by neck dislocation. The animals were perfused with ice cold PBS (1X; ThermoFisher Scientific, Gibco™, Cat Code: 18912014) the cervical (C), axillary (A) and inguinal (I) lymph nodes and spleen were removed and stored in RPMI (ThermoFisher Scientific, Gibco™, Cat Code: 11875093) on ice before processing. The brain was removed and either stored in PBS (1X) for glia isolation or quartered and fixed in paraformaldehyde (PFA; 4%; Biotium Inc., USA; Cat Code; 22023). Posterior quarters of the cortex were incubated in PFA (4% (w/v) ; 4°C) overnight and washed in PBS (1X; 5mins; repeat 3 times). Posterior right quarters were then stored in 70% ethanol and dehydrated (removing water by submerging tissue in increasing concentration of alcohol) to be subsequently embedded in paraffin (tissue is then placed in xylene before being submerged in paraffin (60 °C) and left to solidify).

2.2 Immunohistochemistry

Quarter brains embedded in paraffin were sectioned (10µm) by Mr. Fergus Woods (UCD, Ireland) and stored at RT. Tissue was then deparaffinised before immunostaining. Tissue sections were submerged in a series of baths as follows to rehydrate sections:

1) Xylene (100%; 15 minutes)
2) Xylene (100%; 15 minutes)
3) Ethanol (100%; 5 minutes)
4) Ethanol (90%; 5 minutes)
5) Ethanol (70%; 5 minutes)
6) Deionised water (30 minutes)

Sections were washed in PBS (1X; 5mins; repeat 3 times) followed by antigen retrieval step using citrate buffer (2.1g citric acid in 1L of deionised water). Sections were submerged in citrate buffer and placed in the microwave (high heat; 5 minutes)

then removed to cool for 5 minutes before being placed back into the microwave (high heat; 5 minutes) and then left to cool at RT. The use of heat and low pH with citrate buffer breaks formaldehyde-induced protein cross-links which occurs when tissue is preserved and increases epitope antibody binding and enhances specificity. Sections were washed in PBS (1X; 5mins; repeat 3 times) and the perimeter of the brain tissue was marked using a DAKO/PAP pen (Agilent Technologies, Denmark; Cat Code: S2002). The tissue was incubated with a blocking and permeabilization buffer (10% (v/v) natural goat serum (NGS), 0.3% (v/v) Triton 100-X in PBS (1X); 1hr; RT) followed by an incubation with the primary antibody GFAP (1:500 in blocking buffer, Invitrogen, RRID: AB_2532994, overnight 4ºC humidity chamber). The primary antibody was washed with PBS (1X; 5mins; repeat 3 times) and the tissue was incubated with the secondary antibody Alexa Flour 594 donkey anti-rat (1:500 in blocking buffer, 1h, RT in the dark,). Sections were washed in PBS (1X; 5mins; repeat 3 times). Thioflavin S staining (0.0005% v/v in PBS; 20 minutes; RT in the dark; Sigma Aldrich, UK) was carried out to stain Aβ plaques. Sections were washed with ethanol (100% and 80%; 10 minutes each). Tissue was then immunolabelled with Hoechst to identify nuclei (stock concentration: 10mg/mL; 1:1000 in PBS (1X) 20 minutes; RT in the dark; Cell Signalling Technology; Cat code: H33342) followed by two PBS (1X) washes and one final ddH2O wash before mounting using ProLong™ (ThermoFisher Scientific; Cat Code: P36930) antifade mounting medium and stored overnight at room temperature in the dark. Between imaging, microscope slides were stored at 4°C.

2.3 Immunocytochemistry for IPSC derived neurons and astrocytes

Neurons or astrocytes on coverslips were fixed with PFA (4% (v/v) ; 30 minutes; RT). PFA was removed and coverslips were washed with PBS-Triton (0.02% (v/v) ; repeat 3 times). Coverslips were blocked for 2 hours (10% NGS (v/v), 0.3% PBS-Triton (v/v); RT). Blocking buffer was removed and coverslips were incubated with primary antibody (2% NGS in 0.06% PBS-Triton (v/v); overnight; 4°C). The next day, the primary antibody was removed and the coverslips were washed with PBS-Triton (0.02% (v/v); repeat 3 times). The secondary antibody was added to the cells in a PBS-Triton mix (0.02% (v/v) ; 2 hours; in the dark at RT). Secondary antibody was removed and the

coverslips were washed with PBS-Triton (0.02% (v/v); repeat 3 times). To identify nuclei, Hoechst was added (stock concentration: 10mg/mL; 1:1000 in PBS; 30 minutes; in the dark at RT). Hoechst was removed and the coverslips were washed with PBS (1X; repeat 3 times). Coverslips were then mounted onto glass slides using ProLong™ (ThermoFisher Scientific; Cat Code: P36930) and stored overnight at RT protected from light. Between imaging, microscope slides were stored at 4°C.

2.4 Image Analysis and Acquisition

2.4.1 Tissue sections of APP/PS1 mice

Brain sections from 13-15 month male and female APP/PS1 and wild-type littermates were imaged using a fluorescent microscope at 40X (Carl Zeiss Axio Imager Z1 microscope) at the same florescence exposure times. Analysis of images generated was carried out on Cell Profiler software. Cell profiler is a free, open source software designed by researchers in the Cimini lab at the Broad Institute of MIT and Harvard to carry out quantitative analysis of microscopy images (https://cellprofiler.org). Each mouse brain had two-three sections imaged per hippocampus sub region (CA1, CA3 and dentate gyrus). Cell Profiler analysis was carried out as outlined; Plaques positively immunolabelled for Thioflavin S were visually verified to be accurately identified. Nuclei were identified and visually confirmed ensuring false positives (plaques or clumps of nuclei) were excluded. To investigate cells proximally and distally located to plaques a circle crop was generated. To note if one plaque was present in the image the circle would be a diameter of 800 pixel units (PU) or if more than one plaque was identified per section a circle with a diameter of 1000PU was generated. $GFAP^+$ $DAPI^+$ cells within this crop were considered proximal and $GFAP^+$ $DAPI^+$ cells outside of the crop were considered distal. Outputs from this analysis were: total number of $GFAP^+$ cells, number of proximal $GFAP^+$ cells, number of distal $GFAP^+$ cells, total GFAP integrated intensity and GFAP integrated intensity surrounding the plaque. Integrated intensity is defined as the sum of pixel intensities within an object. Additionally, plaque number and profile (area, perimeter and Thioflavin S integrated intensity) was collected. See **Figure 2.1** a schematic diagram of analysis carried out.

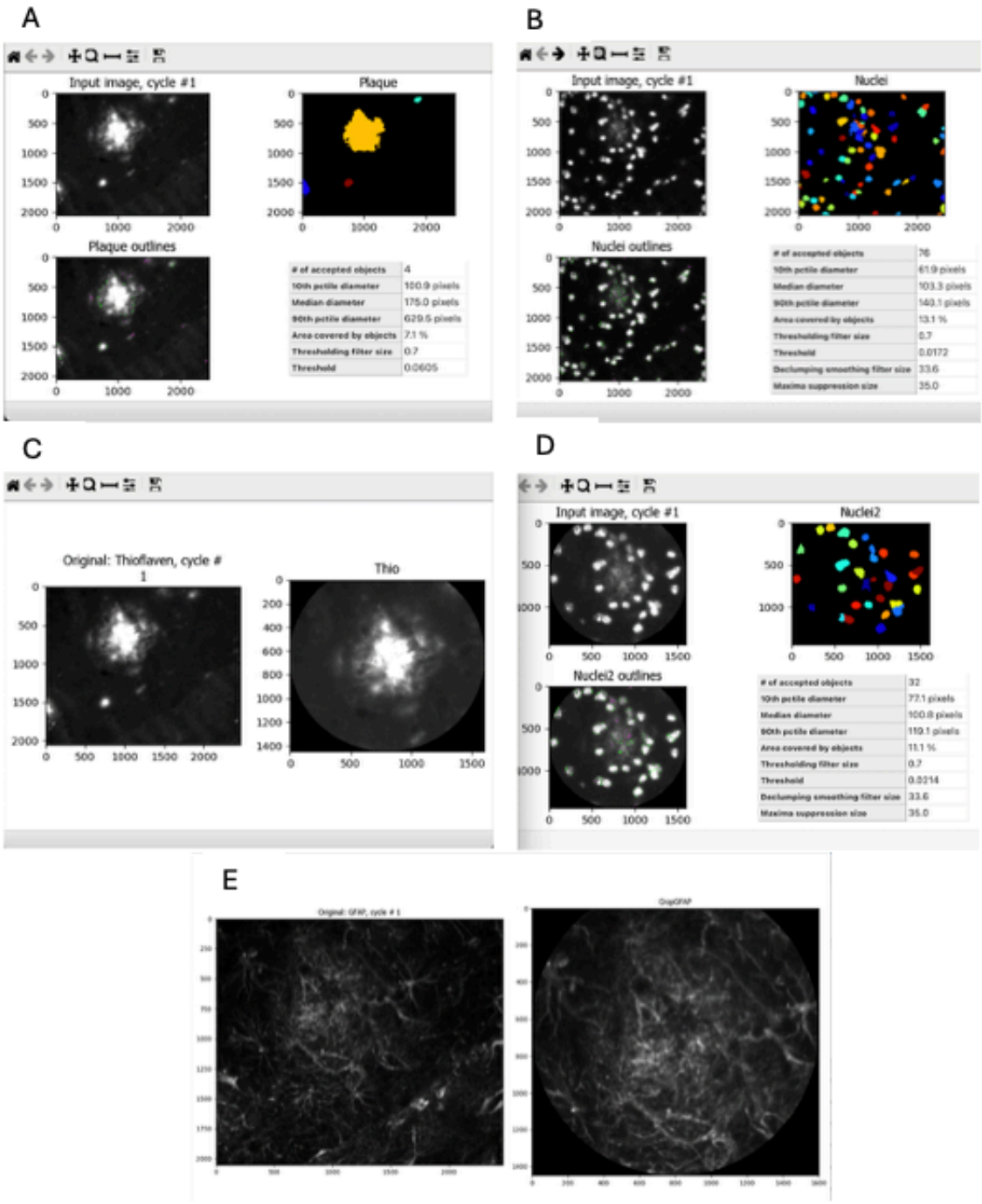


Figure 2.1 Schematic diagram of cell profiler analysis of AD mouse brain sections

*Plaques present in the image were first identified **(A)**, nuclei were then identified using Hoechst staining **(B)**, the image was cropped 800 pixel units surrounding a plaque to identify cells proximally and distally located **(C)**, the nuclei proximal to the plaque were identified **(D)** and the GFAP⁺ cells proximal to the plaque were identified **(E)**.*

2.4.2 Imaging of iPSC derived cortical astrocytes

Slides were imaged using a fluorescent microscope at 20X (Carl Zeiss Axio Imager Z1 microscope) at the same florescence exposure times. 20 images were taken per coverslip. Analysis of images generated was carried out on Cell Profiler software. Nuclei were identified and visually confirmed ensuring false positives (clumps of nuclei) were excluded. Secondary staining was then identified to ensure correct outlines of cells were generated. Features such as circularity, maximum feret diameter, minimum feret diameter, perimeter and area were reported in pixel units and intensities of protein expression were reported in arbitrary units (AU).

2.5 RNA Isolation, cDNA manufacture and RT-qPCR

2.5.1 RNA Isolation

Astrocyte and microglia magnetically separated from APP/PS1 and wild-type brains (outlined in 3.2.3) frozen in Trizol (350 µL; Invitrogen; Cat Code: 15596026) were thawed and chloroform added (1:5; Sigma Aldrich; Cat Code: C2432). Samples were vortexed and incubated for 2-3 minutes and centrifuged (12,000 × *g*; 15 minutes). The aqueous phase (containing RNA) was removed from the top of the supernatant and added to isopropanol (175 µL) and vortexed briefly. Samples were stored for 2-3 nights at -80°C to enhance the purity in each sample. Once thawed, samples were centrifuged (13,000 x *g*; 15 minutes) and the supernatant removed. The pellet was resuspended in ethanol (350 µL; 70%; ThermoFisher Scientific; Cat Code: 16606002) and centrifuged (12,000 x *g*; 5 minutes). The supernatant was removed and the pellet left to air dry for 5-10 minutes before resuspending in 10 µL of RNAse free water (ThermoFisher; Cat Code: 15657708). Samples were heated on a heat block at 65°C for 10 minutes to denature DNA present. Samples were stored at -20°C before cDNA manufacture.

RNA iPSC derived astrocytes were isolated using the NucleoSpin RNA isolation kit (Machery Nagel Bioanalysis, Fisher Scientific Ltd; Cat Code:740955.5). Cells were initially lysed using RNA lysis buffer (3.5µl β-mercaptaethonol (Sigma Aldrich, UK; Cat Code: M6250) and 350µl RA1 buffer) and stored until later processing (-80°C). To begin RNA isolation, samples were thawed on ice and pipetted into filter

tube to filter cell homogenate and capture RNA present in the sample, centrifuged (11,000 x *g*; 1 minute). The filtrate was collected and diluted with 70% ethanol (1:1; ThermoFisher Scientific; Cat Code: 16606002). The solution was added to the blue filter tube (silica membrane filter binds the RNA), centrifuged (11,000 x *g*; 30 seconds) and the filtrate was discarded. To desalt the silica membrane, membrane desalting buffer was added (350µl) and centrifuged (11,000 x *g*; 1 minute). rDNAse (95µl) was added to remove DNA present and the sample was incubated (15 minutes; RT). To stop the reaction, the sample was washed with RAW2 buffer (Guanidine hydrochloride (36%, v/v) and ethanol (34%, v/v) diluted in water) (200µl; 11,000 x *g*; 30 seconds). Guanidine hydrochloride inactivates RNases to prevent the breakdown of RNA present on the sample and ethanol assists with RNA precipitation. The sample was then washed with RA3 buffer (ethanol (100% v/v) and guanidine hydrochloride (600µl; 11,000 x *g*; 30 seconds). The filtrate was discarded and a second RA3 wash was carried out (250µl; 11,000 x *g*; 1 minute). The filter was then transfer into RNAse-free Eppendorf tube with RNAse free water added (40ul) and centrifuged (11,000 x *g*; 1 minute) to collect the RNA sample. Samples were stored at -80°C until cDNA manufacture.

2.5.2 Use of Reverse Transcriptase to generate cDNA

RNA concentration and purity (260/280 nm acceptable ratio =1.8-2.1) were assessed using the Nanodrop 2000 spectrophotometer (ThermoFisher Scientific). RNA samples were equalised to 40ng/µl concentration using RNase free water. Each master mix for cDNA manufacture (Applied Biosystems, ThermoFisher Scientific; Cat Code: 4368814) contained the following components: MultiScribe Reverse Transcriptase (1 µL), 10X RT Random Primers (2 µL), 25X dNTP mix (0.8 µL), 10X RT Buffer (2 µL) and 4.2 µL of RNAse free water. 10 µL of RNA was added to 10 µL reverse transcriptase master mix and placed in the thermocycler (PTC- Peltier Thermal Cycler, MJ Research) under the following cycle conditions: 25°C 10 minutes, 37°C 120 minutes. The generation of cDNA begins with single stranded mRNA and random primers (contain random base pairs) that anneal to the strand of mRNA with complimentary base pairs. Reverse transcriptase is the enzyme used with dNTPs

(Deoxynucleotide Triphosphates) to extend the primer adding complimentary nucleotides in 5' to 3' direction to synthesise cDNA and DNA polymerisation.

2.5.3 Real Time quantitative polymerase chain reaction (RT-qPCR)

RT-qPCR was carried out on all samples using TaqMan mix (5 µL; Applied Biosystems, ThermoFisher Scientific; Cat Code: 15344674) with the endogenous gene GAPDH (0.5 µL) and the gene of interest (0.5 µL). cDNA (4 µL) and the TaqMan master mix (6 µL) were loaded into MicroAmp® Fast Optical 96-Well Reaction Plate (Applied Biosystems, ThermoFisher Scientific; Cat Code:4346906). Plates were sealed, centrifuged (200 x g; 1 minute; SORVALL ST40R, ThermoFisher Scientific) and ran in the StepOne Real-Time PCR System (Applied Biosystems; ThermoFisher Scientific) for the following program; Holding stage 1: 50°C, 2 min, Holding stage 2: 95°C, 20 s, cycling stage 1: 95°C, 1 s, cycling stage 2: 60°C, 20 s. Results were analysed using the Design and Analysis software (version 2.7.0; Applied Biosystems, ThermoFisher Scientific). Values for target gene expression were reported as relative quantity (RQ) using the Livak $\Delta\Delta Ct$ method.

$$\Delta Ct = Ct \text{ Target} - Ct\ Endogenous$$
$$\Delta\Delta Ct = \Delta Ct\ Sample - \Delta Ct\ Control\ Sample$$
$$RQ = 2^{-\Delta\Delta Ct}$$

2.6 Patient Samples

In collaboration with Prof. Seán Kennelly in Tallaght University Hospital (TUH) Institute of Memory and Cognition, blood samples and CSF were collected by Dr. Adam Dyer, Dr. Helena Dolphin and Dr. Sarah Fullam from Alzheimer's and non-Alzheimer's disease patients. Blood samples were collected in heparinised tubes and remained at RT with patients giving informed consent. Ethical approval was achieved by the St. James's Hospital/Tallaght University Hospital Joint Research Ethics Committee.

2.6.1 Diagnosis Criteria

Clinical and neuropsychological assessments were carried out according to (Dyer et al., 2023). Briefly, a Repeatable Battery Assessment of Neuropsychological

Status (R-BANS) (Randolph et al., 1998) and clinical assessments such as routine blood tests were carried out by an advanced nurse practitioner. R-BANS can be broken into 5 indexes. Index I; Immediate memory, Index II; Visuospatial/Constructional, Index III; Language, Index IV; Attention and Index V; Delayed Memory (Randolph et al., 1998). MRI brain scans were also carried out to assess atrophy. Each patient's case was discussed at the multidisciplinary team meeting where decisions on diagnosis or further assessments for the patient were determined. Once initial assessments were determined, appropriate patients were sent for a biomarker analysis of the cerebrospinal fluid (CSF) usually to rule out or confirm Alzheimer's diagnosis by assessing concentrations of $A\beta_{1-42}$, t-tau (total) and p-tau (phosphorylated) in the CSF. A concentration of $A\beta_{1-42}$ < 1030pg/mL was considered positive for Aβ pathology (indicates Aβ is sequestered in the brain and therefore not present in high concentrations in the CSF) and a concentration of p-tau > 27pg/mL was considered positive for tau pathology (Doecke et al., 2020). Patients presenting with MCI but $A\beta_{1-42}$ and p-tau outside of the stated ranges were considered non-AD/MCI controls for this study.

2.7 Peripheral blood mononuclear cell isolation from whole blood

Approximately 20mL of blood was collected per patient and diluted 1:1 with PBS (1X) and slowly layered on top of LymphoPrep (20mL) (Stem Cell Technologies, Cat Code: 18060). Samples were then centrifuged (800 x *g;* 10 minutes; deceleration=0, acceleration=1; SORVALL ST40R, ThermoFisher Scientific). The plasma layer was removed and the buffy coat (containing white blood cells) was collected. This solution was then diluted with Dulbecco's PBS (1X; D-PBS; Sigma Aldrich, UK; Cat Code: D8537) and centrifuged (600 x *g*; 10 minutes; deceleration=9, acceleration=9). The supernatant was removed and the pellet was resuspended in D-PBS (1X; 50mL) and centrifuged (400 x *g*; 10 minutes; deceleration=9, acceleration=9). The supernatant was removed and the pellet was resuspended in 1 mL completed RPMI (cRPMI media with 10% FBS (Sigma Aldrich, UK; Cat Code: F9665), 1% penicillin streptomycin (ThermoFisher Scientific; Cat Code: 15140122), 1% GlutaMAX (ThermoFisher Scientific; Cat Code: 35050061)) and counted. 5-10 million cells were cryopreserved per vial in 10% DMSO (v/v) (Sigma Aldrich, UK; Cat Code: D4540) with

FBS and stored overnight in Mr. Frosty (ThermoFisher Scientific) to slow freeze the samples before being transferred into the liquid nitrogen dewar for long term storage.

2.8 Thawing and counting iPSCs derived neurons and astrocytes and PBMCs

PBMCs or iPSC derived astrocytes and neurons were thawed in a water bath (37°C) until a small ice pellet remained. PBMCs or iPSC derived astrocytes and neurons were diluted in desired cell culture media (1:10). Cells were centrifuged (500 x g; 10 minutes for PBMCs) (200 x g; 3 minutes for astrocytes and neurons). Cells were resuspended in 1 mL of appropriate media. An aliquot of the cell suspension was diluted (1:10) in Trypan Blue (stock concentration: 0.4%; ThermoFisher Scientific; Gibco™; Cat Code: 15250061) and loaded into a haemocytometer for counting. Trypan blue stain will dye dead cells blue due to the increased permeability of dead cells whereas live cells will not absorb trypan blue as live cells are impermeable. Trypan blue negative cells (colourless) were counted, in four large squares (1 mm^2 each) and averaged to calculate the number of cells in 1 mL (see equation below).

$$cell\ count \div 4 = x \times 10\ (dilution\ factor)$$
$$= 10x \times 10^4 (height\ under\ coverslip)$$
$$= cells/ml$$

2.9 Statistical methods

Statistical analysis was carried out using Prism (Version 10.5) and Microsoft Excel. Two-way ANOVA was used when two independent variables were investigated (male versus female, non-AD/MCI vs AD). Main effects of AD pathology, sex or the interaction of sex and AD pathology are initially reported prior to post-hoc analysis. Šidák's post-hoc multiple comparison tests was carried out when a significant main effect was determined. For parametric data, Unpaired t-tests were used when comparing two groups. For non-parametric data, Mann-Whitney T test was used when comparing two groups. Values that did reach significance are identified by the following symbols e.g * <0.05, **<0.01, ***<0.0001. Trends discussed throughout this thesis were identified as p values with a range of 0.1-0.05 that did not reach significance. Data was presented as mean +/- standard error of the mean (SEM).

3 Chapter 3: Investigating sex differences in astrocytes and T cells in the APP/PS1 AD mouse model

3.1 Introduction

Animal models are an important component of understanding the pathoetiology of AD and investigating the use of potential therapeutics in a preventative or curative capacity. In the case of AD research, pathologies are centred around Aβ plaques, tau pathology and neuroinflammation. In transgenic lines, there is significant control over genetic background to prevent confounding results caused by possible population variation. However, this cannot be avoided in human studies and must be overcome with very large study cohorts. Additionally, AD does not present itself in humans until later in life and the prominent sporadic form of AD means identifying the appropriate cohort cannot occur until post-diagnosis when pathology has set in and manifested itself in cognitive impairments. Thus, longitudinal studies are required to elucidate the prodromal molecular changes in AD human studies. In contrast, animal models can establish pathology as early as 2 months (Oakley et al., 2006) allowing the prodromal, early and late AD disease stage to be elucidated.

Limitations however have been observed in animal model use such as inefficacious therapeutics in humans that have originally worked in animal studies (Cummings et al., 2014, Banik et al., 2015). Moreover, the generation of AD models mainly relate to mutations observed in familial AD which may reduce their translational capacity in sporadic AD studies. However, fresh tissue experiments such as the ones presented in this study would not be logistically possible in human participants and hence the requirement for AD models is imperative.

The objective of animals models is to mirror particular pathological hallmarks present in the disease of interest. In AD, these features are established by generating transgenic lines with human genes known to cause familial Alzheimer's Disease such as APP (St George-Hyslop et al., 1987, Goate et al., 1991) and PSEN1 (Rogaev et al., 1995) which are introduced in section **Error! Reference source not found.**. APP is a large transmembrane glycoprotein that can be cleaved at several sites to generate smaller amyloid proteins using the enzymes β-APP cleaving enzyme (BACE1) and γ secretase. In familial AD, several mutations in amino acids adjacent to the cleavage sites at the N and C terminus have been identified in kindred studies (Mullan et al.,

1992, Murrell et al., 1991, Goate et al., 1991, Eckman et al., 1997, Guerreiro et al., 2010). The consequence of these mutations is increased insoluble Aβ aggregate formation (Jankowsky and Zheng, 2017). Additionally, mutations in PSEN1 gene have also been identified in familial AD studies (Rogaev et al., 1995, Sherrington et al., 1995, Perez-Tur et al., 1995, Moehlmann et al., 2002). Both of these reported mutations provide the foundation for the design of AD animal models. The first successful transgenic mouse model was first reported by Games et al., 1995. A platelet derived growth factor (PDGF- β) promoter was utilised to drive expression of mutant human APP (valine mutated to phenylalanine on residue 717) V717F in mice (Games et al., 1995). This transgenic model possessed hallmark pathology features such as extracellular Aβ plaques, neurite plaques, gliosis in astrocytes and microglia and a decrease in synaptic and dendrite density in the dentate gyrus of the hippocampus (Games et al., 1995). Currently, the Swedish mutation, methionine to leucine on exon 16 of APP (Mullan et al., 1992, Citron et al., 1992) is the most common APP mutation adopted in transgenic lines (Jankowsky and Zheng, 2017).

The use of double transgenic lines refers to models that possess mutations related to both the APP and the PSEN1 gene (Zhong et al., 2024). The argument for the use of double transgenic lines was supported by evidence reporting earlier amyloid aggregation compared to the APP_{swe} transgene alone where amyloid deposits are not established until 20 months (Borchelt et al., 1997). Commonly used double transgenic models include 5xFAD and APP_{swe}/PS1. 10% of studies related to AD pathoetiology have been assessed using the 5xFAD model (Zhong et al., 2024). The transgenes present in this model are 3 familial APP mutations London V717I (Goate et al., 1991), Swedish K670N and M671L (Mullan et al., 1992) and Florida I716V (Eckman et al., 1997) with 2 familial PSEN1 mutations M146L (Clark et al., 1995) and L286V (Sherrington et al., 1995). Features of this model include producing $Aβ_{42}$ from a very young age between 1.5 -4 months old, amyloid plaques by 2-6 months and gliosis in astrocytes and microglia (Oakley et al., 2006). Synaptic loss and spatial memory deficits are also present in the 5xFAD model (Oakley et al., 2006).

Another model used is the triple transgenic first established by Oddo et al., (2003) which includes both plaque and tau pathology. The familial mutations introduced are APP Swedish K670N and M671L (Mullan et al., 1992) , PSEN1 M146V

(Sherrington et al., 1995) and Tau MAPT P301L (Dumanchin et al., 1998, Bird et al., 1999). Intraneuronal Aβ present in the hippocampus and the amygdala correlates with behavioural deficits in memory retention at 4 months (Billings et al., 2005). Plaque deposition becomes prominent in the hippocampus of this model by 12 months of age (Belfiore et al., 2019). However, there is no neuronal loss reported in this model (Zhong et al., 2024) and the risk of genetic drift has also been reported (Jankowsky and Zheng, 2017).

The model used in this study is APP_{swe},$PSEN1_{dE9}$ was first established by (Jankowsky et al., 2004). In this model, the Swedish APP mutation (Mullan et al., 1992) and the PSEN1 exon 9 deletion mutation (Perez-Tur et al., 1995) are co-injected into the pronuclei and are located on the single locus of chromosome 9 (Jankowsky et al., 2004). In this model, amyloid deposits are present by 6 months and the $Aβ_{40}$: $Aβ_{42}$ ratio is 0.75:1 (Jankowsky et al., 2004). It is also important to note that familial exon 9 deletion individuals feature atypical diffuse plaques however the plaques characterised in this model are dense and compact, characteristic of AD pathology (Jankowsky et al., 2004). Other pathological features have been identified in this model such as synaptic dysfunction at 9-11 months (Meyer-Luehmann et al., 2009) and behavioural deficits including impaired fear conditioning at 6 months (Kilgore et al., 2010) and impaired navigation and spatial learning at 12 months (Lalonde et al., 2005).

Studies related to astrocyte reactivity and the adaptive immune system have been carried out in the APP_{swe},$PSEN1_{dE9}$ model (see section 1.3 and 1.5). Thus, the use of this model to further elucidate the role of astrocytes and T cells in AD is appropriate. The use of this model to investigate potential sex differences in astrocytes and the adaptive immune system is also advantageous as sex differences in microglia have already been characterised in this model (Guillot-Sestier et al., 2021, Mela et al., 2023). As this model does not establish neurofibrillary tau tangles (Jankowsky et al., 2004) it would not be an appropriate model to investigate the effect of sex on tau pathology.

Therefore the two aims of this study are to investigate the effect of sex on:

1) T cell cytokine response in the peripheral lymphoid organs (cervical lymph nodes, inguinal and auxiliary lymph nodes and the spleen).

2) Astrocyte GFAP expression and antigen presenting capacity

3.2 Methods

3.2.1 Overview of methods

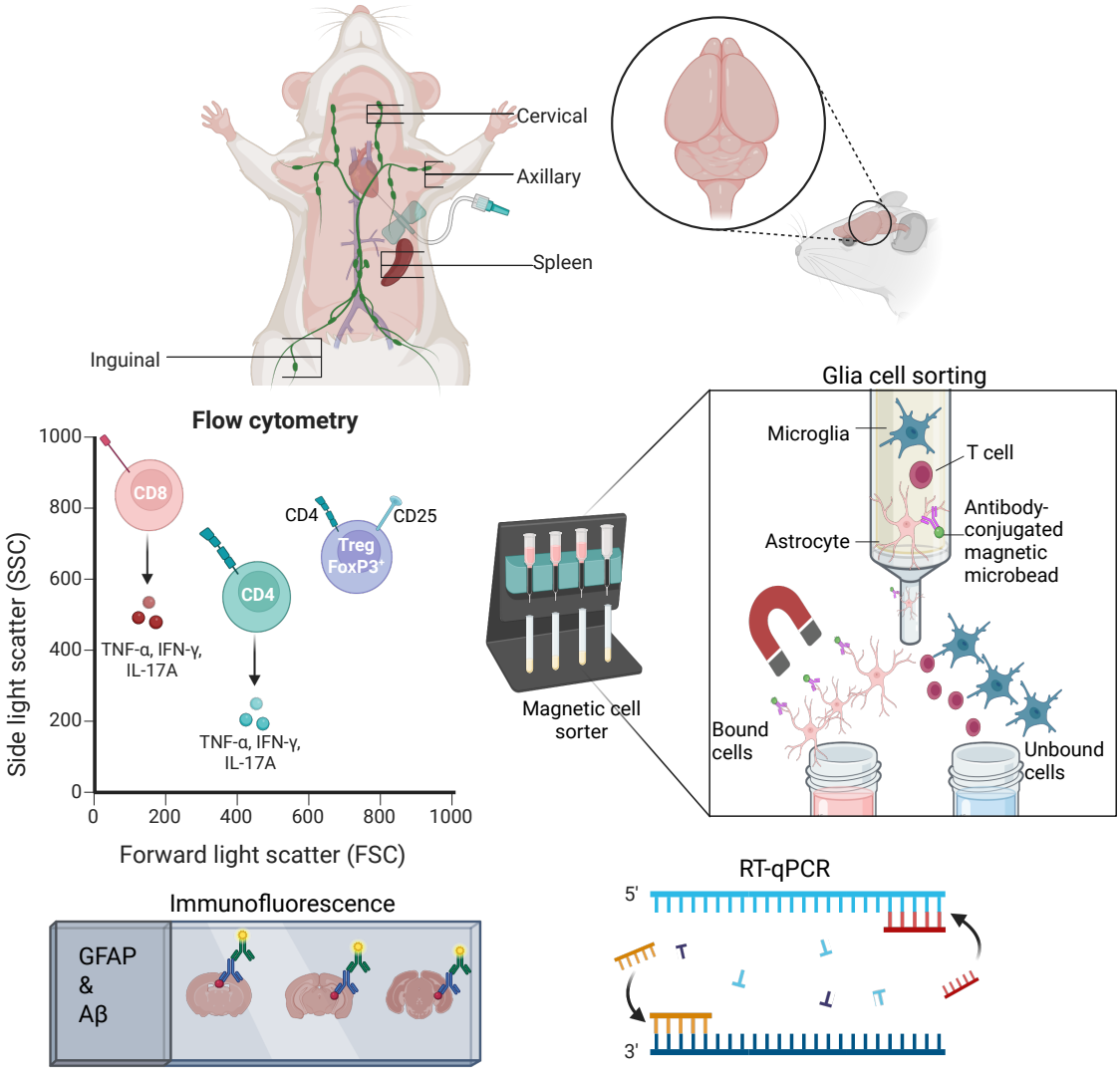


Figure 3.1 Experimental design of tissue retrieved from APP/PS1 and wild-type mice with downstream applications

Male and female APP/PS1 and wild-type littermates were humanely killed using CO_2 inhalation. Cervical, inguinal, axillary lymph nodes and spleen were dissected to carry out flow cytometry and investigate the proportion of regulatory T cells and cytokine response in $CD4^+$ and $CD8^+$ T cells. The whole brain was isolated and astrocytes and microglia were magnetically separated to carry out RT-qPCR on both cell types. T cells from the brain were identified using flow cytometry. In a different cohort brains were dissected, preserved and immunolabelled for the astrocyte marker GFAP and Aß plaques. This figure was generated with the use of BioRender.

3.2.2 Flow Cytometry

3.2.2.1 Cell suspension preparation (Lymph Nodes and Spleen)

All lymphoid tissue was collected in RPMI media (ThermoFisher Scientific) and stored on ice. Spleen tissue was homogenised through 70μm nylon mesh strainer and resuspended in RPMI (5 mL). Axillary and inguinal lymph nodes were pooled together and incubated in trypsin (0.25% in PBS; 5 minutes; on ice) before being homogenised through 40μm nylon mesh strainer and resuspended in RPMI (5 mL). As cervical lymph nodes have been reported to be the location of drainage for the CNS (Louveau et al., 2015), cervical lymph nodes were prepared and analysed independently of other lymph nodes. Samples were centrifuged (340 x *g*; 5 minutes; 4°C; SORVALL ST40R, ThermoFisher Scientific) and the supernatant was decanted. For spleen samples a red blood cell removal step was included: 1X red blood cell lysis buffer (1 mL; RBC Lysis Buffer 10X; BioLegend; Cat Code: 420301) incubated (10 minutes; 4°C), washed with PBS (1X), centrifuged (340 x *g*; 5 minutes; 4°C;) and the supernatant was decanted. All lymphoid samples were resuspended in PBS (1 mL; 1X) and divided over two staining panels 1) Regulatory T cell panel (500μl) 2) Stimulated Cytokine Panel (500μl). The single cell suspension immunolabelled for the cytokine panel were stimulated with phorbol 12-myristate 13-acetate (PMA; 50ng/mL; Sigma Aldrich, UK; Cat Code: P8139), ionomycin (0.5μg/mL; Sigma Aldrich, UK; Cat Code: I0634) and brefeldin A (5μg/mL; Sigma Aldrich, UK; Cat Code: B7651) with each sample also having an unstimulated control using just brefeldin A (5μg /mL). PMA and ionomycin have been reported as optimal stimulants for T cell cytokine response and Brefeldin A is used to accumulate cytokines inside cells working as Golgi blocker (Mandala et al., 2021). To identify the stimulated cytokine response the unstimulated sample paired with the corresponding stimulated sample were analysed side by side to ensure baseline stimulation was not included and strictly PMA and Ionomycin induced stimulation was accounted for. All samples for the cytokine panel were incubated for 4 hours (37°C; 5% CO_2).

3.2.2.2 Staining and immunolabelling T cells

All samples were immunolabelled with Live Dead Aqua stain (LIVE/DEAD™ Fixable Aqua Dead Cell Stain Kit, for 405 nm excitation; ThermoFisher Scientific; Cat

Code: L34957) in PBS (1X; 1:500; 100µl; 15 minutes; RT; in the dark). Extracellular and intracellular staining was carried out to detect the presence of T cell subsets (**Table 3.1** and **Table 3.2**). Extracellular antibodies were diluted in Brilliant Buffer Stain (Cat Code: 563794; BD Pharmingen) and FcBlock (1:50; Cat Code: 553142; BD Pharmingen) (see tables for dilution factors) and added to the samples (100µl; 20 minutes; RT; in the dark). After incubation, cells were washed with FACs Buffer (200µl; D-PBS (1X), 0.4% EDTA (0.5M), 2.5% FBS) centrifuged (340 x *g*; 5 minutes; 4°C) and the supernatant was decanted. Cells were fixed and permeabilized using the FoxP3 staining kit (eBioscience™ Foxp3 / Transcription Factor Staining Buffer Set; Invitrogen; Cat Code: 00-5523-00). Fixation concentrate solution was diluted in the perm dilute solution (1:4) and added to each sample (100µl; 20 minutes; RT; in the dark). Cells were centrifuged (340 x *g*; 5 minutes; 4°C) and supernatant decanted. The intracellular antibodies were diluted in permeabilisation buffer (1:10 H_2O) and added to the samples (50µl; 40 minutes; RT; in the dark). Samples were washed with diluted permeabilisation buffer (200µl; 1:10 H_2O) and centrifuged (340 x *g*; 5 minutes; 4°C). The supernatant was decanted and samples were washed with FACs buffer (1000µl; 340 x *g*; 5 minutes; 4°C). Samples were resuspended in FACs buffer (200µl; 4°C). Compensation beads (40µl; OneComp eBeads™ Compensation Beads; Invitrogen; Cat Code: 01-1111-41 and 160µl FACs Buffer) and single stain samples (a mixture of cells from different tissue groups) were immunolabelled with one specific antibody from the antibody panel to account for wavelength overlap between antibodies. Negative controls consisted of samples with a mixture of cells from different tissues immunolabelled with all fluorescent antibodies minus one (FMO). Samples were processed on the Aurora Cytometer (Cytek Biosciences) in TCD Flow cytometry core facility.

Emission Peak (approx.)	Channel	Fluorophore	Target	Species	Manufacturer and Catalogue No.	Dilution Factor
428	V1	BV421	CD127	Rat	BD Horizon 566300	1:200
720	V13	BV711	CD4	Rat	BD Horizon 563726	1:200
780	V15	BV786	CD25	Rat	BD Horizon 564023	1:200
692	B9	PerCP-Cy5.5	CD8	Rat	BioLegend 140418	1:200
615	YG3	PE-CF594	CD3	Hamster	BD Horizon 562286	1:200
780	YG9	PE-Cy7	CD19	Rat	BD Pharmingen 552854	1:200
679	R2	AF647	FoxP3	Mouse	BD Pharmingen 567462	1:100

Table 3.1 Flow cytometry antibodies used to investigate regulatory T cell populations

Emission Peak (approx.)	Channel	Fluorophore	Target	Species	Manufacturer and Catalogue No.	Dilution Factor
615	V10	BV605	IFN-γ	Rat	BioLegend 560221	1:200
720	V13	BV711	CD4	Rat	BD Horizon 563726	1:200
780	V15	BV785	TNF-α	Rat	BioLegend 506341	1:200
525	B2	AF488	IL-17A	Rat	BD Horizon 560221	1:100
692	B9	PerCP-Cy5.5	CD8	Rat	BioLegend 140418	1:200
615	YG3	PE-CF594	CD3	Hamster	BD Horizon 562286	1:200
780	YG9	PE-Cy7	CD19	Rat	BD Pharmingen 552854	1:200
780	R7	APC-Cy7	CD45	Rat	BD Horizon 557659	1:1000

Table 3.2 Flow cytometry antibodies used to investigate T cell cytokine responses

3.2.3 ASCA2$^+$ Astrocyte and CD11b$^+$ Microglia Isolation from Adult Mouse Brains

Each brain was cut into several sections and placed into a gentleMACS C tube (Miltenyi Biotec, UK; Cat Code: 130-093-237) to be dissociated as per the manufacturer's recommendations (Adult Brain Dissociation Kit, Miltenyi Biotec, UK; Cat Code: 130-107-677) containing 1950 µL of Enzyme mix 1 (Enzyme P (50 µL) and buffer z (1900 µL)) and 30 µL of enzyme mix 2 (Enzyme A (10 µL) and buffer y (20 µL)). The C tubes were placed upside down in the holder of the GentleMACS Octo Dissociator with heaters (Miltenyi Biotec, UK). Homogenates were strained through a 70µm nylon mesh strainer into a 50 mL tube. Each sample was centrifugated (300 x *g*; 10 minutes; 4°C; SORVALL ST40R) and the supernatant was discarded.

3.2.3.1 Debris Removal

The pellet was resuspended in Dulbecco's PBS (D-PBS; 3100 µL) and debris removal solution (900 µL). Very gently, 4 mL of D-PBS was overlayed on top to

distinguish a separate phase in the mixture. This was centrifuged at 3000 x *g* for 10 minutes at 4°C (deceleration=0). Three phases formed; the first two phases were removed. More D-PBS was added until the final volume was 15 mL. The mixture was centrifuged again at 1000 x *g* for 10 minutes at 4°C (deceleration=0) and the supernatant discarded.

3.2.3.2 Red blood cell removal

The red blood cell removal solution prepared in distilled water (1:10 dilution) was used to resuspend the cell pellet and incubated for 10 mins at 4°C. Cold PB Buffer (PBS, 0.5% FBS and 2mM EDTA) was added (10 mL) and the mixture was centrifuged at 300 x *g* for 10 minutes at 4°C. The supernatant was removed and the pellet was resuspended in PB buffer.

3.2.3.3 Magnetic labelling of ASCA-2$^+$ cells

Cell suspension was centrifuged at 300 x *g* for 10 minutes and the supernatant discarded. The pellet was resuspended in PB buffer (80 µL) (PBS, 0.5% FBS and 2mM EDTA) and Fc Block (10 µL) was added and incubated at 4°C for 10 minutes. ASCA2$^+$ beads were then added (10 µL) and incubated at 4°C for 15 minutes. The mixture was centrifuged at 300 x *g* for 10 minutes and the supernatant was removed. The magnetic separator Quadro Macs (Miltenyi Biotec, UK) was used to separate ASCA2$^+$ astrocytes and were resuspended in PB Buffer with 10ul of the cell suspension taken for flow cytometry staining. The remaining volume was centrifuged (300 x *g*; 10 minutes), with the supernatant discarded and the pellet resuspended in Trizol and snap frozen (80°C) for RNA isolation.

3.2.3.4 Magnetic labelling of CD11b$^+$ cells

The elute collected from the magnetic separation of ASCA2$^+$ astrocytes was centrifuged at 300g for 10 minutes and the supernatant discarded. The pellet was resuspended in buffer (90 µL) (PBS, 0.5% BSA and 2mM EDTA) and CD11b Microbeads (10 µL) was added and incubated at 4°C for 30 minutes. The mixture was centrifuged at 300 x *g* for 10 minutes and the supernatant was removed. The magnetic separator Quadro Macs (Miltenyi Biotec, UK) was used to separate CD11b$^+$ microglia and were resuspended in PB Buffer. Samples were centrifuged (300 x *g*; 10 minutes), with the supernatant discarded and the pellet resuspended in PB Buffer with 10ul of

the cell suspension taken for flow cytometry staining. The remaining volume was centrifuged (300 x *g*; 10 minutes), with the supernatant discarded and the pellet resuspended in Trizol and snap frozen (80°C) for RNA isolation.

3.2.3.5 Flow Cytometry

10 uL of each cell suspension was collection for flow cytometry analysis. Samples were resuspended in FACs buffer and centrifuged (*340 x g*; 5 minutes; 4C). Extracellular staining was carried out to detect microglia (CD11b) and intracellular staining was carried out to detect the presence of astrocytes (GFAP). The cell suspension that was not positive for ASCA-2 astrocytes and CD11b microglia was collected and centrifuged (340 *x g*; 5 minutes; 4C) and immunolabelled with antibodies from the regulatory T cell panel as outlined above to investigate the presence of T cells in the brain.

Emission Peak (approx.)	Channel	Fluorophore	Target	Species	Manufacturer and Catalogue No.	Dilution Factor
679	R2	eF660	GFAP	Rat	eBioscience 50-9892-80	1:100
780	YG9	PE-Cy7	CD11b	Rat	eBioscience 25-0112-82	1:100

Table 3.3 Flow cytometry antibodies used to confirm astrocyte and microglia populations

3.2.4 RT-qPCR

As outlined in section 2.5, RT-qPCR was carried out on ASCA-2$^+$ astrocytes and CD11b$^+$ microglia for the genes listed below (**Table 3.4**; ThermoFisher Scientific, USA). RQ was calculated using the average Ct value of the target and endogenous gene from the wild-type male group. As we were comparing differences in gene expression in males and females from two cohorts wild-type and APP/PS1 the use of an average Ct instead of an individual sample from a male or female is more appropriate for this experiment.

$$\Delta Ct = Ct \text{ Target} - Ct\ Endogenous$$

$$\Delta\Delta Ct = \Delta Ct\ Sample - \Delta Ct\ Control\ Sample$$

$$RQ = 2^{-\Delta\Delta Ct}$$

Primer	Gene Name	Gene Code
Gapdh	Endogenous Primer: Glyceraldehyde-3-phosphate dehydrogenase	Mm99999915_g1
GFAP	Glial fibrillary acidic protein	Mm01253033_m1
MHC-II	Major histocompatibility complex II	Mm00439216_m1
CD40	Cluster of differentiation 40	Mm00441891_m1
CD80	Cluster of differentiation 80	Mm00711660_m1
CD86	Cluster of differentiation 86	Mm00444540_m1
LCN2	Lipocalin 2	Mm01324470_m1
TNF-α	Tumour necrosis factor alpha	Mm00443258_m1
IL-6	Interleukin 6	Mm00446190_m1

Table 3.4 ***Primers used for RT-qPCR analysis on magnetically separated astrocytes and microglia***

3.3 Results

3.3.1 Sex affects T cell phenotype in secondary lymphoid organs and the brain in APP/PS1 and wild-type littermates

3.3.1.1 Cytokine Response

Initially, the effect of sex and the APP/PS1 transgene on proportions of $CD4^+$ and $CD8^+$ T cells were investigated in all three lymphoid organs. The gating strategy applied to investigate $CD4^+$ and $CD8^+$ cytokine responses is outlined in Figure 3.2. Two-way ANOVA revealed a significant main effect of the APP/PS1 transgene on $CD4^+$ T cell populations in the cervical lymph node **(Figure 3.3 A**, p=0.0005). Šidák's post-hoc multiple comparison tests revealed that APP/PS1 female had a significant decrease in the proportion of $CD4^+$ T cell population isolated from cervical lymph nodes compared to wild-type females **(Figure 3.3 A**, p=0.0043). There was no difference reported in $CD4^+$ populations isolated from cervical lymph nodes in the wild-type male cohorts compared to APP/PS1 males.

Two-way ANOVA revealed a significant main effect of the APP/PS1 transgene on $CD4^+$ T cell population in the inguinal and axillary lymph nodes compared to the wild-type cohort (**Figure 3.3 B**, p=0.0058). Šidák's post-hoc multiple comparison tests however did not reach statistical significance for any of the groups (**Figure 3.3 B**).

In the spleen the main effect of the APP/PS1 transgene on the $CD4^+$ T cell population did not reach statistical significance (**Figure 3.3 C**, p=0.0587). Furthermore, neither sex nor APP/PS1 transgene expression impacted the proportion of $CD8^+$ T cells in any of the secondary lymphoid organs (**Figure 3.3 D-F**).

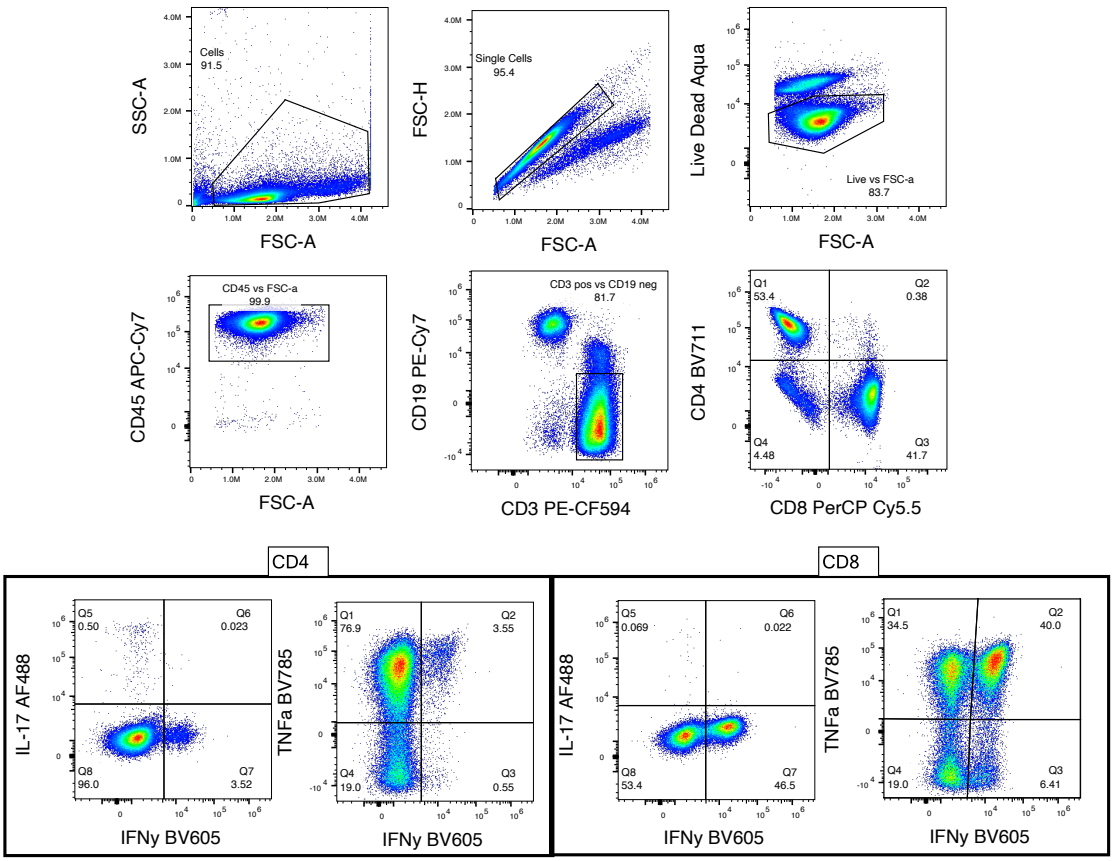


Figure 3.2 Gating Strategy for flow cytometry analysis of cytokine response in cervical lymph node, inguinal/auxiliary lymph node (pooled) and spleen of male and female APP/PS1 mice and wild-type littermates.

Single cell suspension immunolabelled for the cytokine panel was stimulated with phorbol 12-myristate 13-acetate (PMA; 50ng/mL), ionomycin (0.5μg/mL) and brefeldin A (5μg/mL) with each sample also having an unstimulated control using just brefeldin A (5μg/mL). All samples for the cytokine panel were incubated for 4 hours (37°C). Lymphocytes were gated side scatter area (SSC-A) vs front scatter area (FSC-A), live cells were gated on live dead stain vs FSC-A. Live cells were gated on CD45⁺ vs FSC-A, this population was gated on CD19⁻ vs CD3 and cells were gated on CD4 vs CD8. CD4⁺ and CD8⁺ cytokine expression was gated for IL-17a, TNFα and IFNγ. Gating was established using single stain and fluorescent minus one (FMO) controls.

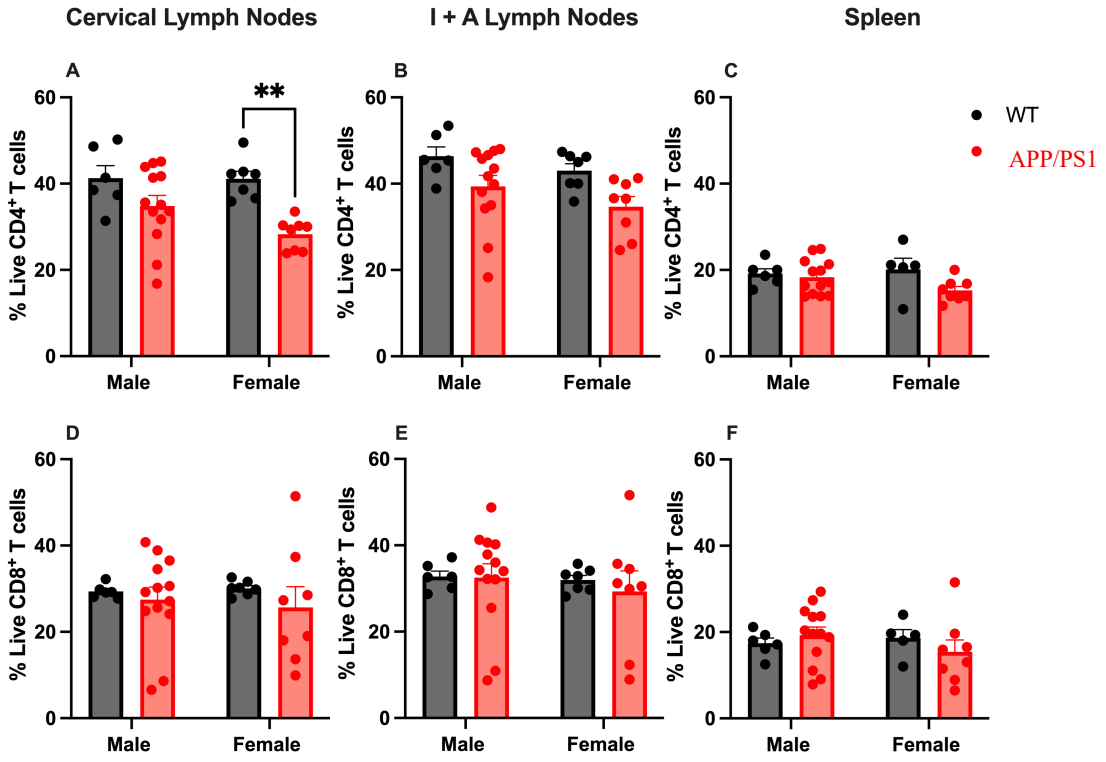


Figure 3.3 Proportion of CD4⁺ and CD8⁺ T cells in Cervical Lymph Nodes, Inguinal and Axillary Lymph Nodes and Spleens of APP/PS1 male and female mice and wild-type littermates by flow cytometry

*The percentage of CD4⁺ and CD8⁺ T cells isolated from cervical lymph nodes (**A and D**), inguinal and axillary lymph nodes pooled together (**B and E**) and spleen (**C and F**). Cells were stimulated with 50ng/mL PMA, 0.5µg/mL Ionomycin and 5µg/mL Brefeldin A in 16-17 month old WT (n= 6) and APP/PS1 (n=13) males and WT (n=7) and APP/PS1 (n=8) females in all lymph node groups and spleens from WT (n= 6) and APP/PS1 (n=13) males and WT (n=5) and APP/PS1 (n=8) females. Data is presented as mean +/- SEM, two-way ANOVA statistical test reported a significant main effect of the APP/PS1 transgene on CD4⁺ T cell population in the cervical lymph node (**A**, p=0.0005) and the inguinal and axillary lymph nodes (**B**, p=0.0058).* Šidák's post-hoc multiple comparison tests showed *a significant decrease in the proportion of live CD4⁺ T cells in APP/PS1 females compared to WT females (**p=0.0043). See Figure 3.2 for the gating strategy applied.*

In the cervical lymph nodes, cytokine response in CD4⁺ T cells following stimulation differed in APP/PS1 and wild-type males and females (**Figure 3.4**). Two-way ANOVA reported a main effect of the APP/PS1 transgene on CD4⁺ TNF-α^+ IFN-γ^- expression (**Figure 3.4 A**, p=0.0222). The male APP/PS1 group trended towards an increase in CD4⁺ TNF-α^+ IFN-γ^- expression compared to wild-type males (**Figure 3.4**

A, p=0.0812), however Šidák's post-hoc multiple comparison tests did not reach statistical significance for any of the groups. Two-way ANOVA reported a main effect of the APP/PS1 transgene on $CD4^+$ TNF-α^+ IFN-γ^+ abundance (**Figure 3.4 B**, p=0.0111). An increase in the proportion of $CD4^+$ TNF-α^+ IFN-γ^+ cells in APP/PS1 compared to wild-type males trended towards significance **(Figure 3.4 B**, p=0.0792), however Šidák's post-hoc multiple comparison tests did not reach statistical significance for any of the groups. Neither sex nor APP/PS1 transgene impacted the proportion of $CD4^+$ IFN-γ^+ TNF-α^- or $CD4^+$ IL-17^+ IFN-γ^- (**Figure 3.4 C and D**). Two-way ANOVA reported a main effect of the APP/PS1 transgene on the proportion of $CD4^+$ IFN-γ^+ IL-17^- cells **(Figure 3.4 E**, p=0.0358). Šidák's post-hoc multiple comparison tests however did not reach statistical significance for any of the groups.

In relation to cytokine response in $CD8^+$ T cells in the cervical lymph nodes, there was no effect of sex in both wild-type and the APP/PS1 cohort on the proportion of $CD8^+$ TNF-α^+ IFN-γ^- cells (**Figure 3.4 F**). A slight increase in $CD8^+$ TNF-α^+ IFN-γ^- proportion was observed in APP/PS1 mice compared to their wild-type counterparts which trended towards significance (**Figure 3.4 F**, p=0.0856). There was no effect of sex in both wild-type and the APP/PS1 cohort on $CD8^+$ TNF-α^+ IFN-γ^+ abundance (**Figure 3.4 G**). There was a trend towards significance for the main effect of the APP/PS1 transgene on the number of $CD8^+$ TNF-α^+ IFN-γ^+ cells **(Figure 3.4 G**, p=0.0693). Two-way ANOVA reported a main effect of sex on the proportion of $CD8^+$ IFN-γ^+ TNF-α^- cells (**Figure 3.4 H**, p<0.0001). Šidák's post-hoc multiple comparison tests revealed a significant decrease in $CD8^+$ IFN-γ^+ TNF-α^- abundance in wild-type females compared to wild-type males (**Figure 3.4 H**, p=0.0003) and in APP/PS1 females compared to APP/PS1 males (**Figure 3.4 H**, p=0.0496). Two-way ANOVA reported a main effect of sex (p=0.0066), the APP/PS1 transgene (p<0.0001) and the interaction of sex *x* APP/PS1 transgene (p=0.0022) in the proportion of $CD8^+$ IL-17^+ IFN-γ^- cells in the cervical lymph nodes (**Figure 3.4 I**). Šidák's post-hoc multiple comparison tests revealed a significant decrease in the number of $CD8^+$ IL-17^+ IFN-γ^- cells in APP/PS1 males compared to wild-type males (**Figure 3.4 I**, p<0.0001) and a significant decrease in $CD8^+$ IL-17^+ IFN-γ^- abundance in wild-type females compared

to wild-type males (**Figure 3.4 I**, p=0.0014). Neither sex not the APP/PS1 impacted on the proportion of $CD8^+$ $IFN\gamma^+$ $IL\text{-}17^-$ cells (**Figure 3.4 J**).

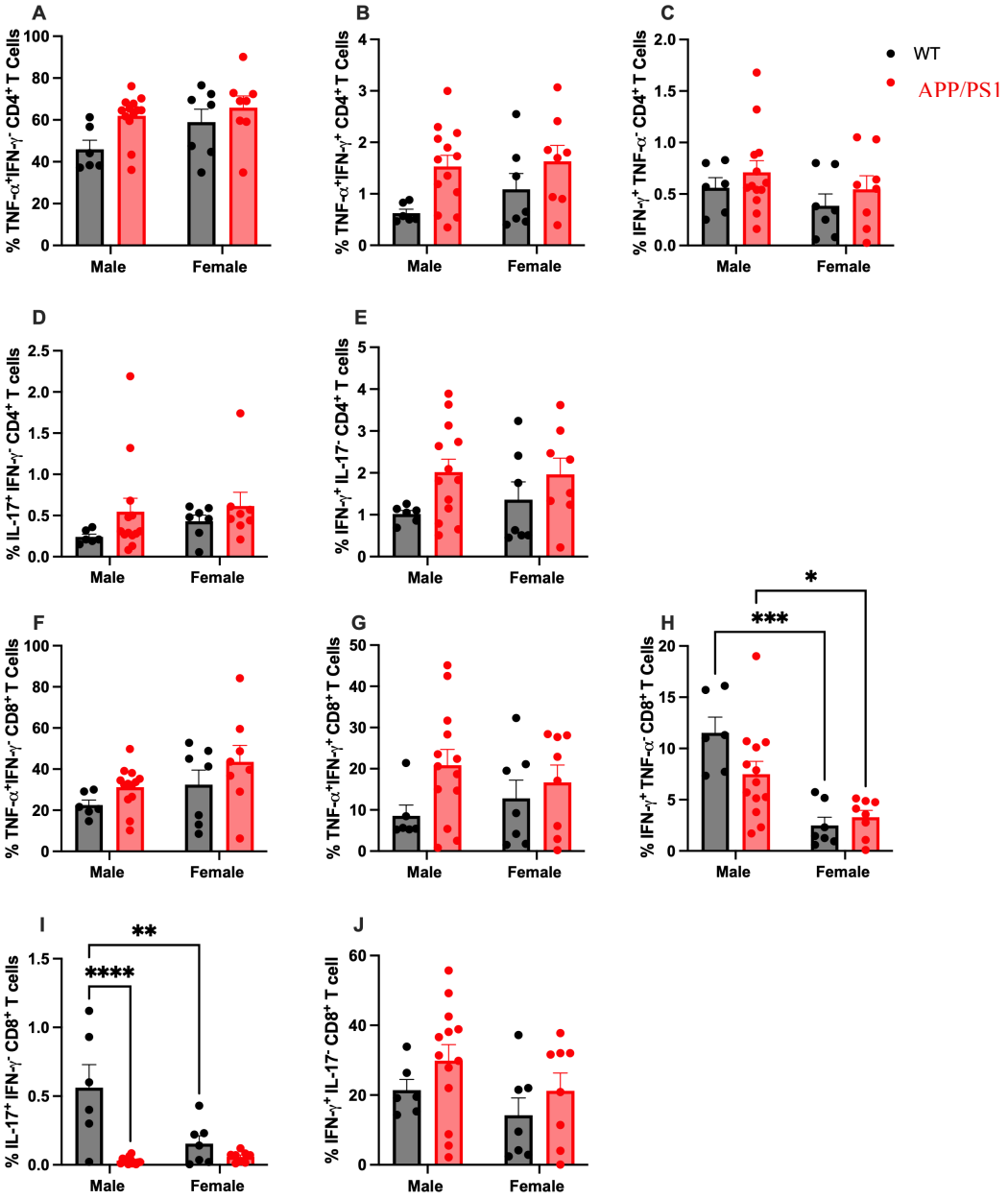


Figure 3.4 Analysis of T cell cytokine populations in Cervical Lymph Nodes of APP/PS1 males and females and wild-type littermates by flow cytometry

*The percentage of intracellular TNF-α, TNF-α and IFN_γ, IFN_γ and IL-17 in $CD4^+$ (**A-E**) and $CD8^+$ (**F-J**) T cells. Cells isolated from cervical lymph nodes were stimulated with 50ng/mL PMA, 0.5µg/mL Ionomycin and 5µg/mL Brefeldin A in 16-17 month old WT (n= 6) and APP/PS1 (n=13) males and WT (n=7) and APP/PS1 (n=8) females. Data is presented as mean +/- SEM, two-way ANOVA statistical test reported a significant main effect of the APP/PS1 transgene on the proportion of $CD4^+$ TNF-α^+*

*IFN-γ^- cells (**A**, p=0.0222), CD4$^+$ TNF-α^+ IFN-γ^+ cells (**B**, p=0.0111) and CD4$^+$ IFN-γ^+ IL-17$^-$ cells (**E**, p=0.0358) was reported. Šidák's post-hoc multiple comparison tests however did not reach statistical significance for any of the groups. A main effect of sex on the proportion of CD8$^+$ IFN-γ^+ TNF-α^- cells was reported (**H**, p<0.0001). There was a significant decrease in IFN$_\gamma^+$ CD8$^+$ T cells in WT females compared to WT males (**H**, ***p=0.0003). There was a significant decrease in CD8$^+$ IFN$_\gamma^+$ abundance in APP/PS1 females compared to APP/PS1 males (**H**,*p=0.0496). A main effect of sex (**I**, p=0.0066), the APP/PS1 transgene (**I**, p<0.0001) and the interaction of sex x APP/PS1 transgene (**I**, p=0.0022) on the proportion of CD8$^+$ IL-17$^+$ IFN-γ^- cells was observed. There was a significant decrease in IL-17$^+$ CD8$^+$ T cells in WT females compared to WT males (**I**, **p=0.0014). There was a significant decrease in CD8$^+$ IL-17$^+$ cells in APP/PS1 males compared to WT males (**I**, ****p<0.0001). See Figure 3.2 for the gating strategy applied.*

Similarly, cytokine response in CD4$^+$ and CD8$^+$ T cells following stimulation differed in APP/PS1 and wild-type males and females in the inguinal and axillary lymph nodes (pooled together) (**Figure 3.5**). Two-way ANOVA reported a main effect of sex (p=0.0185) and the APP/PS1 transgene (p=0.0356) on the abundance of CD4$^+$TNF-α^+IFN-γ^- cells (**Figure 3.5 A**). However, Šidák's post-hoc multiple comparison tests reported no significant differences between male and female wild-type and APP/PS1 cohorts. Two-way ANOVA reported a significant main effect of the APP/PS1 transgene on CD4$^+$ TNF-α^+IFN-γ^+ expression (**Figure 3.5 B**, p=0.0297). However, Šidák's post-hoc multiple comparison tests did not reach statistical significance for any of the groups. Neither sex nor the APP/PS1 transgene impacted the proportion of CD4$^+$ IFN-γ^+ TNF-α^- cells (**Figure 3.5 C**). The main effect of sex trended towards significance in the proportion of CD4$^+$ IFN-γ^+TNF-α^- cells (**Figure 3.5 C**, p=0.0648). Both sex (p=0.0409) and the APP/PS1 transgene (p=0.0402) impacted on the proportion of CD4$^+$ IL-17$^+$ IFN-γ^- cells (**Figure 3.5 D**). There was a slight increase in the proportion of CD4$^+$ IL-17$^+$ IFN-γ^- cells in APP/PS1 females compared to males however, Šidák's post-hoc multiple comparison tests revealed no significant change (**Figure 3.5 D**, p=0.0932). Neither sex nor the APP/PS1 transgene had an effect on the abundance of CD4$^+$ IFN-γ^+IL-17$^-$ cells (**Figure 3.5 E**). Two-way ANOVA reported a main effect of sex (p=0.0032) and the APP/PS1 transgene (p=0.0473) on the proportion of CD8$^+$TNF-α^+IFN-γ^- cells (**Figure 3.5 F**). There was a significant increase in the proportion of CD8$^+$TNF-α^+IFN-γ^- cells in APP/PS1 females compared to APP/PS1

males (**Figure 3.5 F**, p=0.0143). There was effect of sex on the proportion of $CD8^+$ TNF-α^+IFN-γ^+ cells (**Figure 3.5 G**). A slight increase in the number of $CD8^+$ TNF-α^+IFN-γ^+ cells was observed in APP/PS1 mice compared to their wild-type counterparts (**Figure 3.5 G**, p=0.0760) however this did not reach significance. Two-way ANOVA reported a main effect of sex (p=0.0002) and the interaction of sex *x* the APP/PS1 transgene (p=0.0045) on the proportion of $CD8^+$ IFN-γ^+ TNF-α^- cells (**Figure 3.5 H**). Šidák's post-hoc multiple comparison tests revealed a significant decrease in the abundance of $CD8^+$ IFN-γ^+ TNF-α^- cells in wild-type females compared to wild-type males (**Figure 3.5 H**, p=0.0002). Additionally, there was a significant decrease in the proportion of $CD8^+$ IFN-γ^+ TNF-α^- cells observed in APP/PS1 males compared to wild-type males (**Figure 3.5 H**, p=0.004). The APP/PS1 transgene impacted on the proportion of $CD8^+$ IL-17^+ IFN-γ^- cells (**Figure 3.5 I**, p<0.0001). Šidák's post-hoc multiple comparison tests revealed a significant decrease in $CD8^+$ IL-17^+ IFN-γ^- expression in male APP/PS1 mice compared to wild-type males (**Figure 3.5 I**, p=0.0014) and female APP/PS1 mice compared to wild-type females (**Figure 3.5 I**, p=0.0432). Neither sex nor the APP/PS1 transgene impacted on the abundance of $CD8^+$ IFN-γ^+ IL-17^- cells (**Figure 3.5 J**).

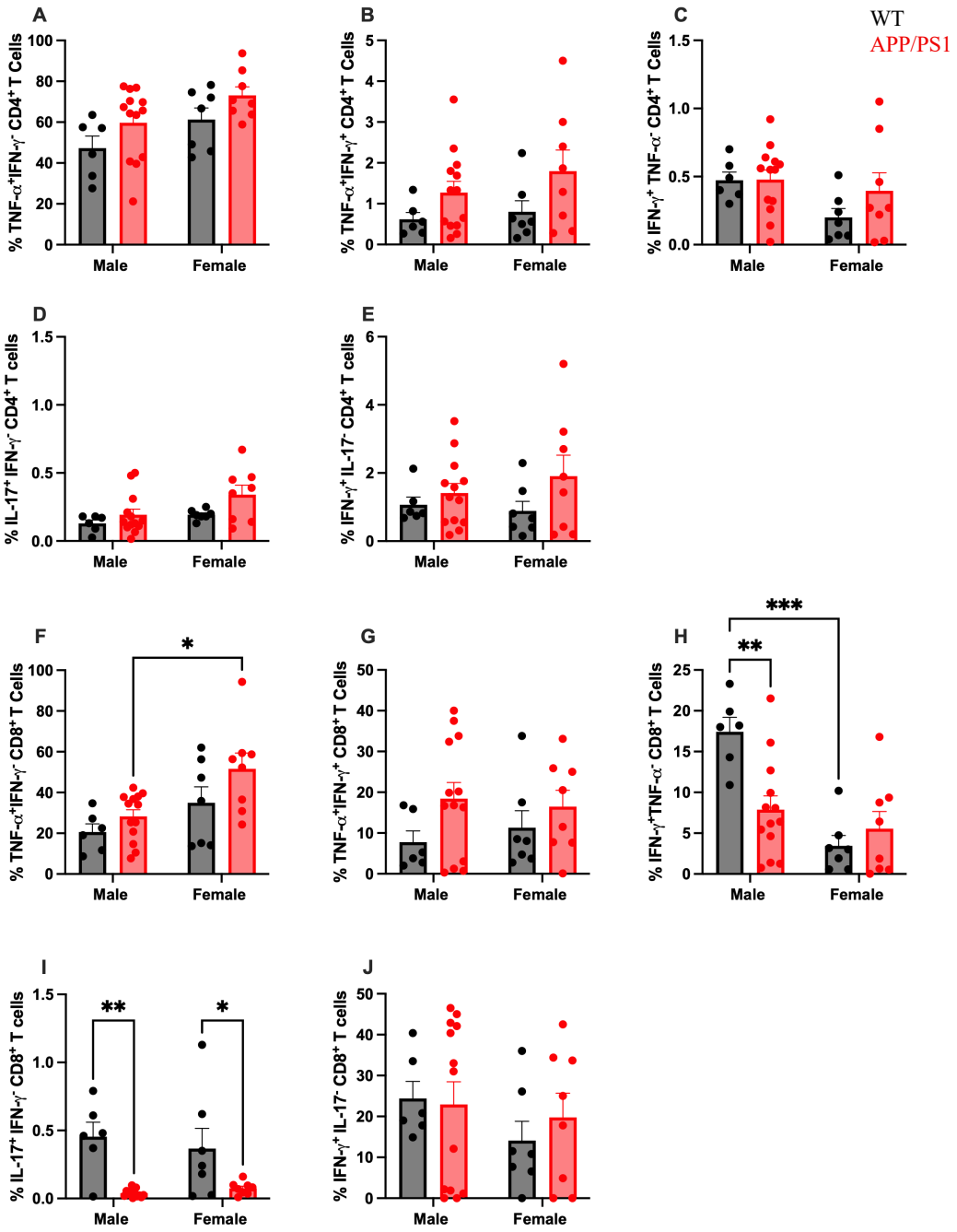


Figure 3.5 Analysis of T cell populations in Inguinal and Axillary Lymph Nodes of APP/PS1 males and females and wild-type littermates by flow cytometry

*The percentage of intracellular TNF-α, TNF-α and IFN$_\gamma$, IFN$_\gamma$ and IL-17 expression in CD4$^+$ (**A-E**) and CD8$^+$ (**F-J**) cells. Cells isolated from inguinal and axillary lymph nodes were stimulated with 50ng/mL PMA, 0.5µg/mL Ionomycin and 5µg/mL Brefeldin A in 16-17 month old WT (n= 6) and APP/PS1 (n=13) males and WT (n=7) and APP/PS1 (n=8) females. Data is presented as mean +/- SEM, two-way ANOVA statistical test reported a main effect of sex (**A**, p=0.0185) and the APP/PS1 transgene (**A**, p=0.0356) on the proportion of CD4$^+$TNF-α$^+$IFN-γ$^-$ cells. A main effect of the APP/PS1 transgene on CD4$^+$ TNF-α$^+$IFN-γ$^+$ abundance was reported (**B**,*

*p=0.0297). A main effect of sex (**D**, p=0.0409) and the APP/PS1 transgene (**D**, p=0.0402) on the proportion of CD4$^+$ IL-17$^+$ IFN-γ^- cells was reported (**D**). However, Šidák's post-hoc multiple comparison tests reported no significant differences between male and female wild-type and APP/PS1 cohorts. A main effect of sex (**F**, p=0.0032) and the APP/PS1 transgene (**F**, p=0.0473) on the proportion of CD8$^+$ TNF-α^+IFN-γ^- cells was reported. There was a significant increase in CD8$^+$ TNF-α abundance in APP/PS1 females compared to APP/PS1 males (**F**, *p=0.0143). A main effect of sex (**H**, p=0.0002) and the interaction of sex x the APP/PS1 transgene (**H**, p=0.0045) on the proportion of CD8$^+$ IFN-γ^+ TNF-α^- cells was reported. There was a significant decrease in IFN$_\gamma^+$ CD8$^+$ T cells in WT females compared to WT males (**H**, ***p=0.0002) and in APP/PS1 males compared to WT males (**H**, **p=0.004). A main effect of the APP/PS1 transgene on the proportion of CD8$^+$ IL-17$^+$ IFN-γ^- cells was reported (**I**, p<0.0001). There was a significant decrease in CD8$^+$ IL-17$^+$ in APP/PS1 males compared to WT males (**I**, **p=0.0014) and APP/PS1 females compared to WT females (**I**, *p=0.0432). See Figure 3.2 for the gating strategy applied.*

Cytokine response in CD4$^+$ and CD8$^+$ T cells were also investigated in the spleen on male and female wild-type and APP/PS1 mice. Neither APP/PS1 transgene nor sex effected the proportion of CD4$^+$ TNF-α^+ IFN-γ^- cells (**Figure 3.6 A**). The effect of sex on the proportion of CD4$^+$ TNF-α^+ IFN-γ^- cells trended towards significance (**Figure 3.6 A**, p=0.085). The effect of sex or the APP/PS1 transgene did not impact the proportion of CD4$^+$ TNF-α^+ IFN-γ^+ cells in the spleen (**Figure 3.6 B**). Sex did not impact the abundance of CD4$^+$ IFN-γ^+ TNF-α^- cells (**Figure 3.6 C**). The APP/PS1 transgene as a main effect on CD4$^+$ IFN-γ^+ TNF-α^- expression trended towards significance (**Figure 3.6 C**, p=0.0691). An effect of the APP/PS1 transgene was observed on the abundance of CD4$^+$ IL-17$^+$ IFN-γ^- cells in the spleen (**Figure 3.6 D**, p=0.024). However, Šidák's post-hoc multiple comparison tests reported no significant difference between male and female APP/PS1 and wild-type cohorts (**Figure 3.6 D**). Two-way ANOVA reported no main effect of sex on CD4$^+$ IFN-γ^+ IL-17$^-$ expression (**Figure 3.6 E**). The APP/PS1 transgene as a main effect on CD4$^+$ IFN-γ^+ IL-17$^-$ expression trended towards significance (**Figure 3.6 E**, p=0.0712). Neither the APP/PS1 transgene nor sex impacted the proportion of CD8$^+$ TNF-α^+ IFN-γ^- or CD8$^+$ TNF-α^+ IFN-γ^+ cells in the spleen (**Figure 3.6 F and G**). There was no effect of sex observed on the proportion of CD8$^+$ IFN-γ^+ TNF-α^- cells present in the spleen (**Figure 3.6 H**). The APP/PS1 transgene as a main effect on CD8$^+$ IFN-γ^+ TNF-α^- expression trended towards significance

(**Figure 3.6 H**, p=0.0763). There was no effect of sex or the APP/PS1 transgene reported on the proportion of CD8$^+$ IL-17$^+$ IFN-γ^- or CD8$^+$ IFN-γ^+ IL-17$^-$ cells in the spleen (**Figure 3.6 I and J**).

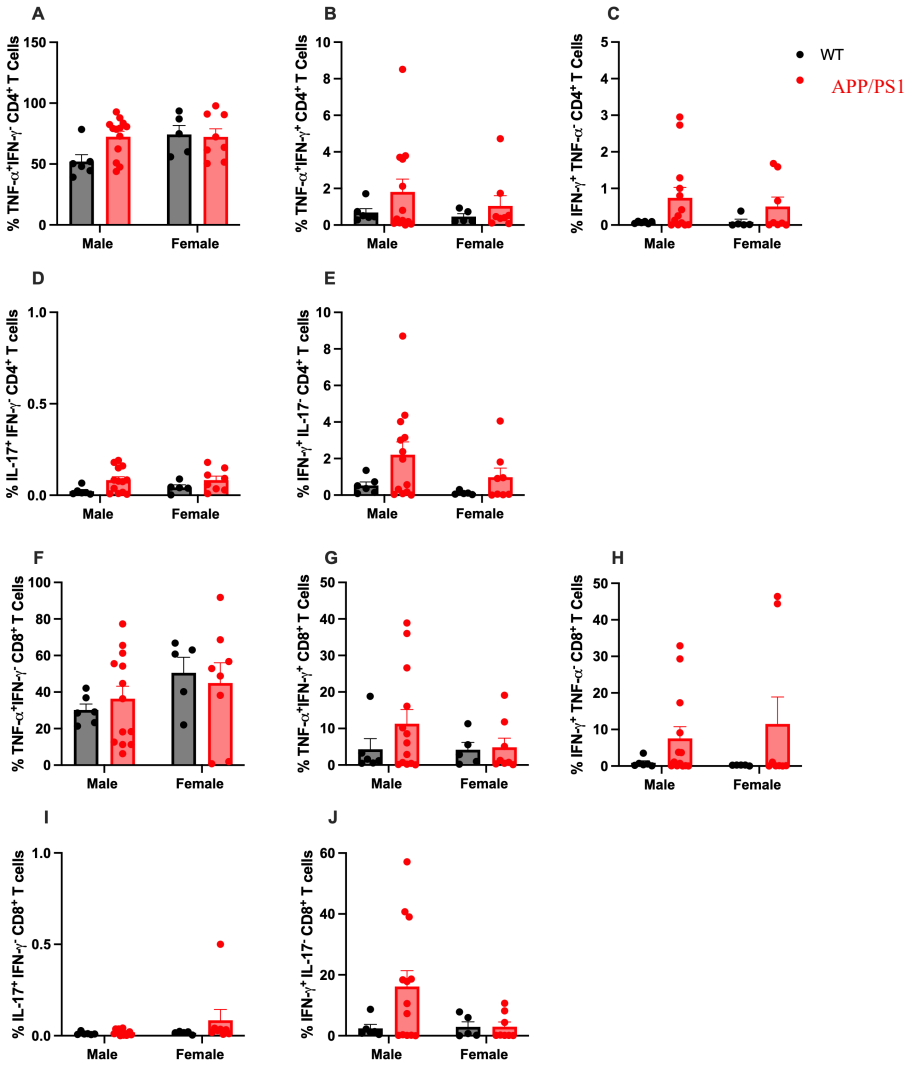


Figure 3.6 Analysis of T cell populations in Spleens of APP/PS1 males and females and wild-type littermates by flow cytometry

*The percentage of intracellular TNF-α, TNF-α and IFN$_\gamma$, IFN$_\gamma$ and IL-17 expression in CD4$^+$ (**A-D**) and CD8$^+$ (**E-H**) cells. Cells isolated from spleens were stimulated with 50ng/mL PMA, 0.5µg/mL Ionomycin and 5µg/mL Brefeldin A in 16-17 month old WT (n= 6) and APP/PS1 (n=13) males and WT (n=5) and APP/PS1 (n=8) females. Data is presented as mean +/- SEM, 2-way ANOVA statistical test reported a main effect of the APP/PS1 transgene on the proportion of CD4$^+$ IL-17$^+$ IFN-γ cells in the spleen (**D**, p=0.024). Šidák's post-hoc multiple comparison tests reported no significant difference between male and female APP/PS1 and wild-type cohorts. See Figure 3.2 for the gating strategy applied.*

3.3.1.2 Regulatory T cells (Tregs)

$CD4^+$ T cells can be further subdivided into regulatory T cells (Tregs) identified by the expression of CD25 and low expression of CD127 as well as the transcription factor FoxP3. Treg populations were investigated in the inguinal and axillary lymph nodes (pooled) and the spleen. The gating strategy applied to this analysis is outlined in **Figure 3.7**. In addition, the negative elute of brain homogenates that underwent magnetic separation of ASCA-2^+ astrocytes and $CD11b^+$ microglia (3.2.3) was used to assess Treg populations (will be referred to as brain Treg throughout). Neither sex nor the APP/PS1 transgene had an effect on the proportion of $CD8^+$ T cells present in the inguinal and axillary lymph nodes (**Figure 3.8 A**). Two-way ANOVA reported a main effect of sex proportion of $CD4^+$ T cells present in the inguinal and axillary lymph nodes (**Figure 3.8 B**, $p<0.0001$). Šidák's post-hoc multiple comparison tests revealed a significant decrease in $CD4^+$ T cells in wild-type females compared to males (**Figure 3.8 B**, $p=0.0192$) and in APP/PS1 females compared to APP/PS1 males (**Figure 3.8 B**, $p=0.0002$). Two-way ANOVA reported a significant interaction of sex *x* APP/PS1 transgene in relation to proportion of Tregs in inguinal and axillary lymph nodes (**Figure 3.8 C**, $p=0.0139$). There was a trend towards significance between wild-type females and wild-type males (**Figure 3.8 C**, $p=0.0879$) however, Šidák's post-hoc multiple comparison tests reported no significant difference in the groups.

There was no effect of sex observed in relation to the proportion of $CD8^+$ T cells present in the spleen (**Figure 3.8 D**). The main effect of the APP/PS1 transgene did trend towards significance (**Figure 3.8 D**, $p=0.079$). Two-way ANOVA reported a main effect of sex on $CD4^+$ proportions in the spleen (**Figure 3.8 E**, $p=0.0065$). Šidák's post-hoc multiple comparison tests revealed a significant decrease in $CD4^+$ T cells in APP/PS1 females compared to APP/PS1 males in the spleen (**Figure 3.8 E**, $p=0.0022$). There was no effect of sex observed in relation to the proportion of Tregs present in the spleen (**Figure 3.8 F**). The main effect of the APP/PS1 transgene did trend towards significance (**Figure 3.8 F**, $p=0.0997$).

Neither the APP/PS1 transgene nor sex impacted on $CD8^+$ or $CD4^+$ populations present in the brain (**Figure 3.8 G and H**). Two-way ANOVA reported a main effect of sex (**Figure 3.8 I**, $p=0.0467$), the APP/PS1 transgene (**Figure 3.8 I**, $p=0.0011$), and an interaction (sex *x* APP/PS1 transgene) (**Figure 3.8 I**, $p=0.0295$) in relation to Tregs

present in the brain (**Figure 3.8 I**). Šidák's post-hoc multiple comparison tests revealed a significant decrease in Tregs in the brains of wild-type females compared to wild-type males (**Figure 3.8 I**, p=0.0239). Additionally a significant decrease in Tregs in the brains of APP/PS1 males compared to wild-type males was observed (**Figure 3.8 I**, p=0.0015).

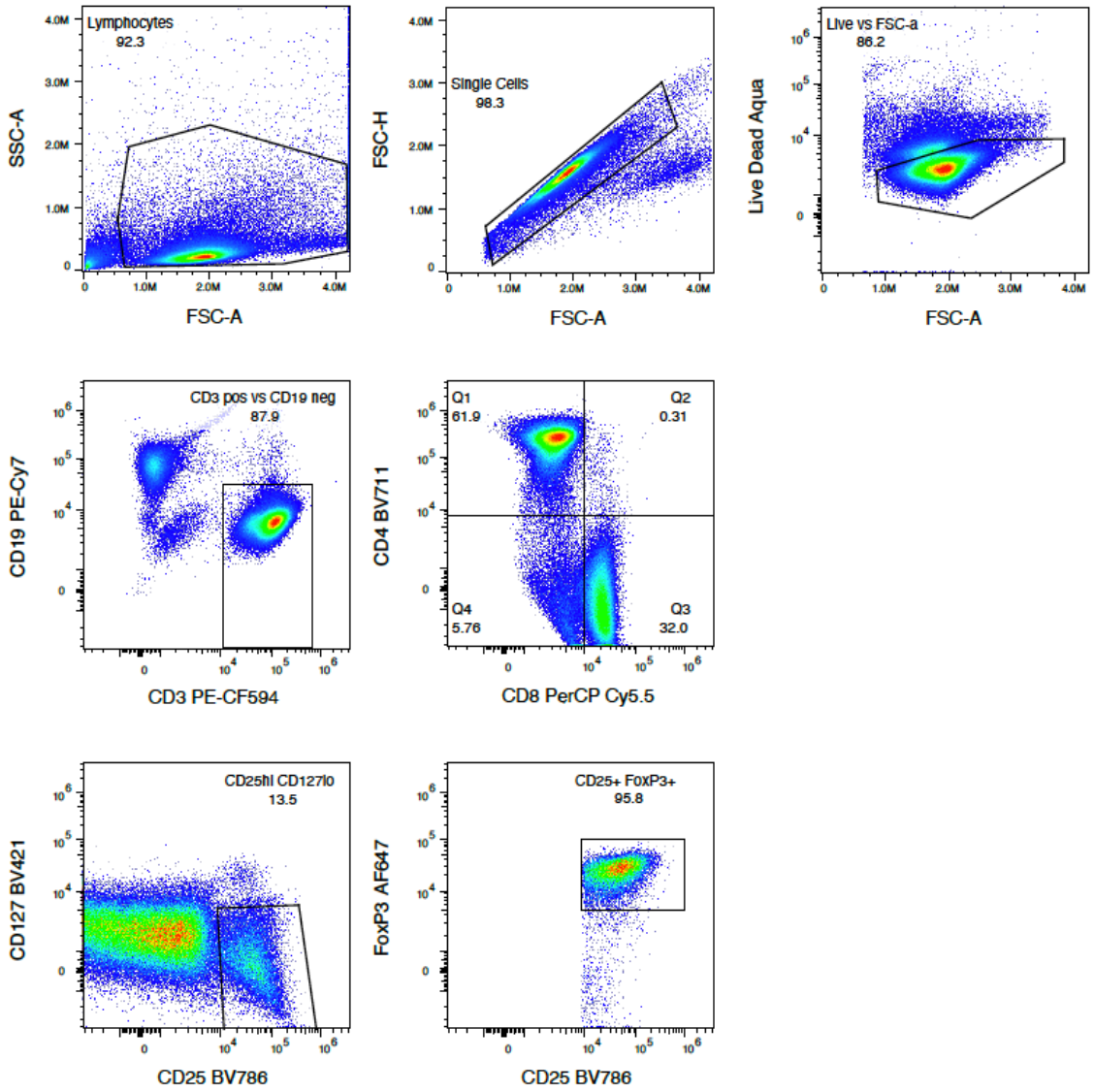


Figure 3.7 Gating Strategy for flow cytometry analysis of inguinal/auxiliary lymph node (pooled), spleen and brain in male and female APP/PS1 mice and wild-type littermates.

Lymphocytes were gated side scatter area (SSC-A) vs front scatter area (FSC-A), live cells were gated on live dead stain vs FSC-A. Live cells were gated on CD19⁻ vs CD3 and cells were gated on CD4 vs CD8 to identify T helper cell population (CD4⁺). Tregs were identified by gating on $CD25^+CD127_{lo}$ and $CD25^+FoxP3^+$ cells. Gating was established using single stain and fluorescent minus one (FMO) controls.

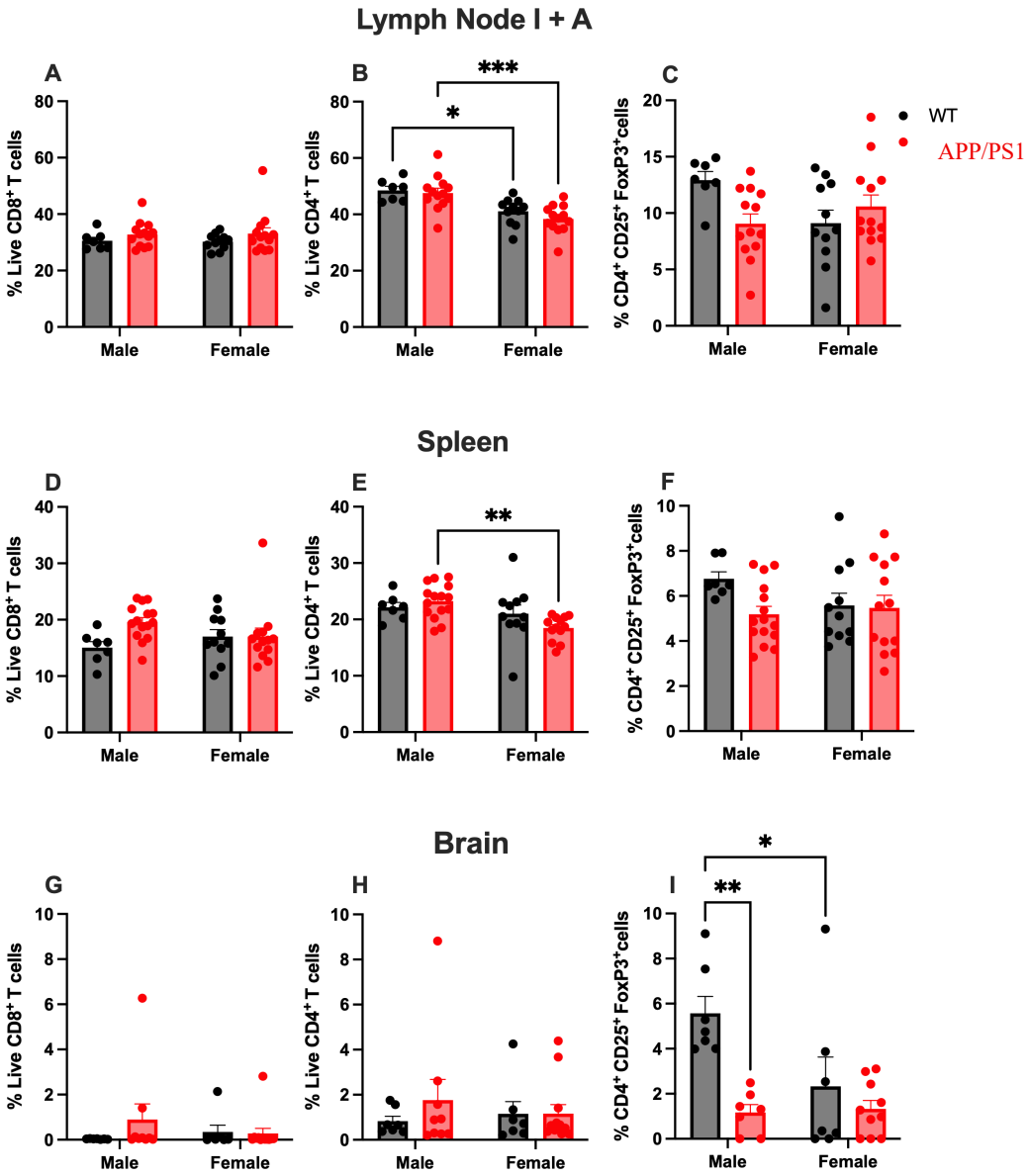


Figure 3.8 Analysis of Regulatory T cell populations in APP/PS1 males and females and wild-type littermates by flow cytometry

*The percentage of CD4⁺, CD8⁺ and FoxP3⁺CD25⁺CD4⁺ T cells in live cells isolated from inguinal and axillary lymph nodes (**A-C**) in 16-17 month old WT (n= 7) and APP/PS1 (n=13) males and WT (n=11) and APP/PS1 (n=13) females. (**D-F**) CD4⁺, CD8⁺ and FoxP3⁺CD25⁺CD4⁺ T cells in live cells isolated from spleen in WT (n= 7) and APP/PS1 (n=13) males and WT (n=11) and APP/PS1 (n=15) females. CD4⁺, CD8⁺ and FoxP3⁺CD25⁺CD4⁺ T cells in live cells isolated from the brain after magnetic separation of ASCA-2⁺ astrocytes and CD11b⁺ microglia (**G-I**) in WT (n= 7) and APP/PS1 (n=9) males and WT (n=7) and APP/PS1 (n=12) females. Data is presented as mean +/- SEM, two-way ANOVA statistical test reported a main effect of sex on the proportion of CD4⁺ T cells present in the lymph nodes (**B**, p<0.0001). There was a significant decrease in CD4⁺ T cells in APP/PS1 females compared to APP/PS1 males (***p=0.0002) and in WT females compared to WT males (*p=0.0192). Two-way*

*ANOVA reported a significant interaction of sex x APP/PS1 transgene in relation to proportion of Tregs in inguinal and axillary lymph nodes (**C**, p=0.0139). In the spleen, two-way ANOVA reported a main effect of sex on CD4⁺ proportions in the spleen (**E**, p=0.0065). There was a significant decrease in CD4⁺ T cells in APP/PS1 females compared to APP/PS1 males (**E**, **p=0.0022). In the brain, two-way ANOVA reported a main effect of sex (**I**, p=0.0467), the APP/PS1 transgene (**I**, p=0.0011), and an interaction (sex x APP/PS1 transgene) (**I**, p=0.0295) in relation to Tregs present in the brain (I). There was a significant decrease in FoxP3⁺CD25⁺CD4⁺ T cells in APP/PS1 males compared to WT males (**p=0.0015). There was also a significant decrease in FoxP3⁺CD25⁺CD4⁺ T cells in WT females compared to WT males in the brain (*p=0.0239). See Figure 3.7 for the gating strategy applied.*

Summary of results obtained while assessing the impact of sex and APP/PS1 transgene on T cell abundance and phenotype:

- Despite a significant decrease in the proportion of CD4⁺ T cells in APP/PS1 females this did not translate to an increase or decrease in the proportion of CD4⁺ cytokines or Tregs in secondary lymphoid tissue in wild-type or APP/PS1 mice.
- Sex and the expression of APP/PS1 transgene altered CD8⁺ T cell cytokine responses in the lymph nodes but not in the spleen
- There is a sexual dimorphism in the Treg population present in the brain with wild-type males possessing a larger proportion of Tregs compared to wild-type females. This is not observed in the APP/PS1 cohort.

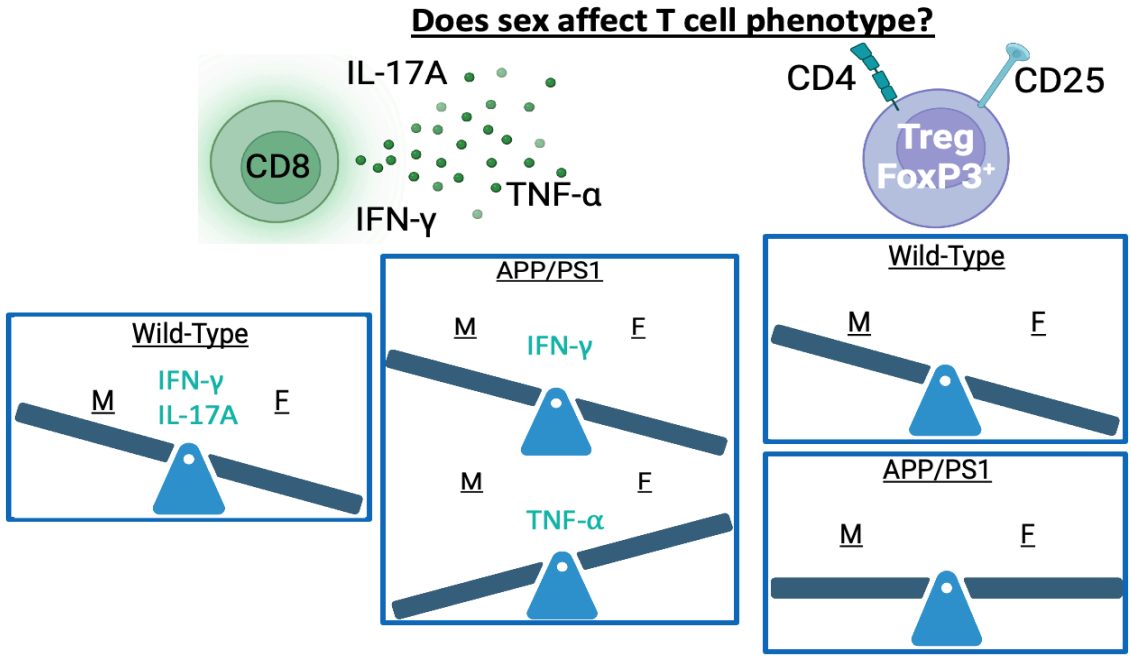


Figure 3.9 Abstract summary of flow cytometry results of T cell cytokine response and regulatory T cells in male and female APP/PS1 and wild-type littermates

***Cytokines**: In the cervical lymph nodes, there was a significant decrease in $CD8^+$ IFN-γ T cells in both wild-type females and APP/PS1 females compared to their male counterparts. There was a significant decrease in $CD8^+$ IL-17A T cells in wild-type females compared to wild-type males. In the inguinal and axillary lymph nodes, there was a significant decrease in $CD8^+$ IFN-γ T cells in wild-type females compared to wild-type males. There was a significant increase in $CD8^+$ TNF-α T cells in APP/PS1 females compared to males.*

***Regulatory T cells**: In the brain, there was a significant decrease in the proportion of $CD4^+$ $CD25^+$ $Foxp3^+$ Tregs in wild-type females compared to wild-type males. This reported sex difference was not observed in the APP/PS1 cohort.*

3.3.2 The effect of sex and APP/PS1 transgene on ASCA-2^+ astrocytes and $CD11b^+$ microglial genotype

To further elucidate the potential implications of sex and the APP/PS1 transgene on pathogenesis in AD, gene expression was explored in astrocytes and microglia from the brains of APP/PS1 and wild-type animals.

As previously outlined, astrocytes and microglia were positively separated using ASCA-2^+ and $CD11b^+$ magnetic antibodies respectively (3.2.3). The gating strategy applied is outlined below in **Figure 3.10.** Initially, we confirmed that ASCA-2^+ and

CD11b$^+$ isolations contained astrocytes expressing GFAP and microglia expressing CD11b by flow cytometry in both APP/PS1 and wild-type males and females (**Figure 3.11**).

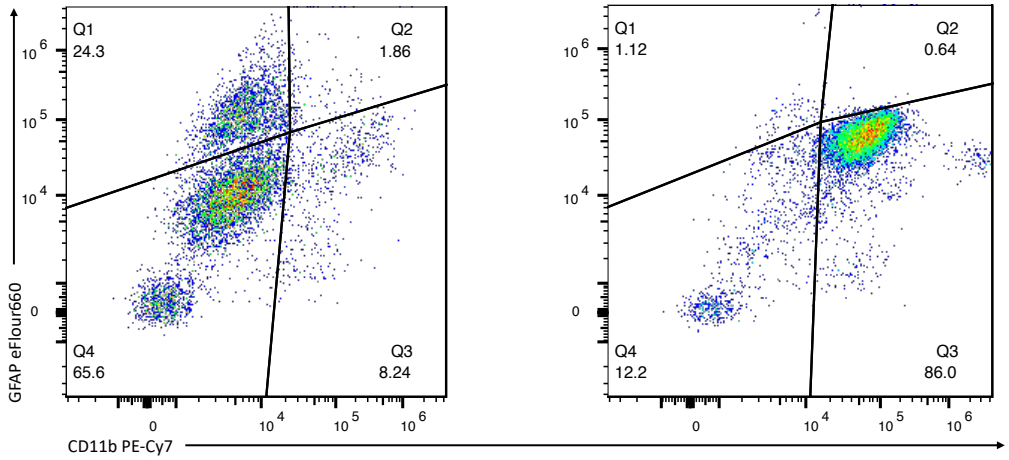


Figure 3.10 Gating Strategy for flow cytometry analysis of ASCA-2$^+$ astrocytes and CD11b$^+$ microglia isolated from brains of male and female APP/PS1 mice and wild-type littermates

Single cell suspensions were gated for GFAP vs CD11b to ensure desired populations of astrocytes and microglia were present. Gating was established using single stain and fluorescent minus one (FMO) controls.

.

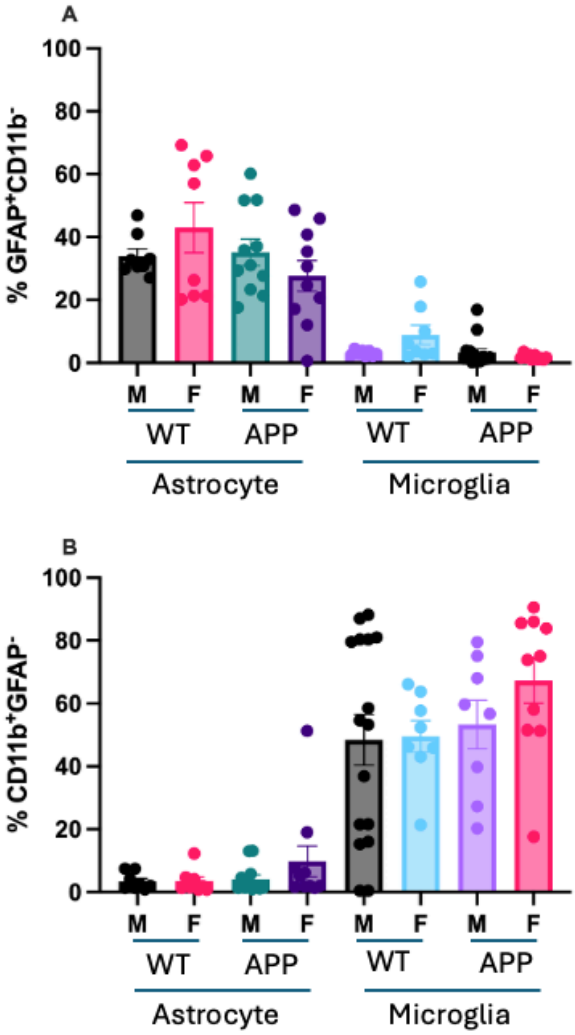


Figure 3.11 Confirmation of ASCA-2⁺ astrocyte and CD11b⁺ microglia populations present after magnetic separation by flow cytometry from brains of APP/PS1 males and females and wild type littermates

*The population percentage of GFAP⁺CD11b⁻ cells in magnetically isolated ASCA-2 astrocytes and CD11b microglia (**A**) and CD11b⁺ GFAP⁻ cells in magnetically isolated ASCA-2 astrocytes and CD11b microglia (**B**) from brains of 16-17 month old APP/PS1 males and females and wild type littermates (Astrocyte WT M=8, F=8, APP M=11, F=10, Microglia WT M=8, F=8, M=16 and F=10). Data, presented as mean +/- SEM.*

Furthermore, we confirmed using RT-qPCR GFAP gene expression of ASCA-2⁺ astrocytes and the lack of GFAP expression in the microglia isolates (**Figure 3.12**). Two-way ANOVA reported a main effect of the APP/PS1 transgene on ASCA-2⁺ astrocyte expression (**Figure 3.12 A**, p=0.0143). Šidák's post-hoc multiple

comparison tests reported no significant difference in GFAP expression in the ASCA-2$^+$ astrocytes isolated from any of the four groups (**Figure 3.12 A**).

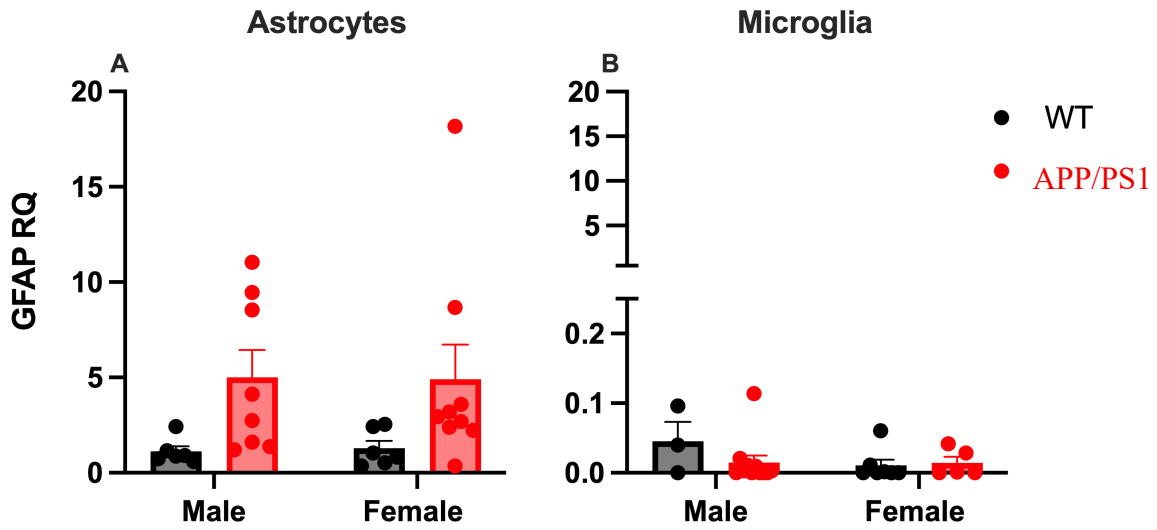


Figure 3.12 GFAP gene expression from ASCA-2$^+$ astrocytes and CD11b$^+$ microglia populations by RT-qPCR from brains of APP/PS1 males and females and wild type littermates

*GFAP expression in magnetically isolated ASCA-2$^+$ astrocytes (**A**) and magnetically isolated CD11b$^+$ microglia (**B**) from brains of 16-17 month old APP/PS1 males and females and wild type littermates (Astrocyte WT M=6, F=6, APP M=8, F=9, Microglia WT M=3, F=7, M=12 and F=5). Two-way ANOVA reported a main effect of the APP/PS1 transgene on ASCA-2$^+$ astrocyte expression (A, p=0.0143). Data, presented as mean +/- SEM.*

Once the cell isolates were confirmed to be astrocytes and microglia as expected, the effect of sex and the APP/PS1 transgene on the cell's capacity for antigen presentation (as reflected by the expression of MHC-II, CD40, CD80, CD86) and expression of pro-inflammatory biomarkers (LCN2, TNF-α and IL-6) was explored using RT-qPCR.

A significant increase was observed in MHC-II expression in astrocytes from APP/PS1 females compared to APP/PS1 males which was not apparent in wild-type mice (**Figure 3.13 A**, p=0.0222). Similarly, CD86 expression was increased in astrocytes from APP/PS1 females compared to APP/PS1 males (**Figure 3.13 D**, p=0.0089) but not in wild-type mice. There was no significant sex difference reported in the expression of LCN2, CD40, TNF-α or IL-6 in ASCA-2$^+$ astrocytes from wild-type or APP/PS1 mice (**Figure 3.13 B-C, E and F**).

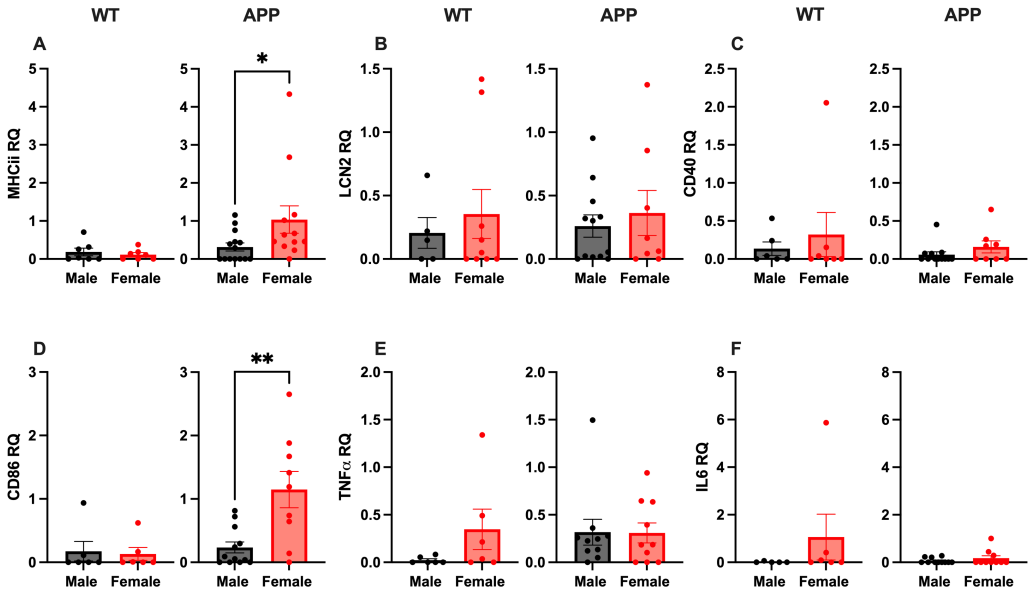


Figure 3.13 Gene expression of MHC-II and CD86 was significantly higher in astrocytes from female APP/PS1 mice compared to male APP/PS1 mice

*Gene expression by RT-qPCR of MHC-II (**A**), LCN2 (**B**), CD40 (**C**), CD86 (**D**), TNF-α (**E**) and IL-6 (**F**) in ASCA-2 astrocytes in 16-17 month old APP/PS1 and wild type males and females (WT M=7, F=7, APP M=12, F=14). There was a significant increase in gene expression of MHC-II and CD86 in APP/PS1 females compared to APP/PS1 males (*p=0.0222) and (**p=0.0089) respectively. Data, presented as mean +/- SEM, were analysed by unpaired t-tests or Mann Whitney when appropriate for non-parametric data.*

The effect of APP/PS1 transgene on ASCA-2$^+$ gene expression was then investigated (**Figure 3.14**). There was a significant increase in MHC-II expression in ASCA-2$^+$ astrocytes isolated from APP/PS1 females compared to wild-type females **(Figure 3.14 A**, p=0.0018) which was not observed in APP/PS1 and wild-type male ASCA-2$^+$ astrocytes. There was no significant difference reported in LCN2, CD40 or IL-6 (**Figure 3.14 B, C and F**) expression in ASCA-2$^+$ astrocytes from male or female APP/PS1 and wild-type mice. There was a significant increase in CD86 expression in APP/PS1 female ASCA-2$^+$ astrocytes compared to the wild-type female cohort (**Figure 3.14 D** p=0.0122). This was not observed ASCA-2$^+$ astrocytes from male APP/PS1 and wild-type ASCA-2$^+$ mice. There was a significant increase observed in TNF-α expression in APP/PS1 male ASCA-2$^+$ astrocytes compared to wild-type males

(**Figure 3.14 E**, p=0.007). This was not observed in the ASCA-2^{+} astrocytes isolated from female APP/PS1 and wild-type mice.

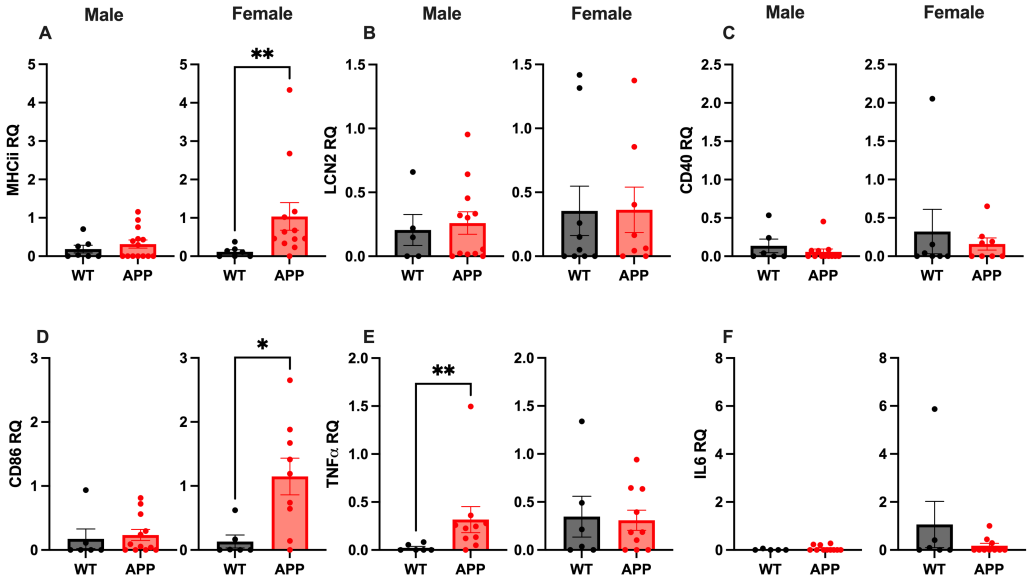


Figure 3.14 ***Gene expression of MHC-II, CD86 and TNF-α was significantly higher in astrocytes from APP/PS1 mice compared to wild-type mice***

*Gene expression by RT-qPCR of MHC-II (**A**), LCN2 (**B**), CD40 (**C**), CD86 (**D**), TNF-α (**E**) and IL-6 (**F**) in ASCA-2 astrocytes in 16-17 month old APP/PS1 and wild type males and females (WT M=7, F=7, APP M=12, F=14). There was a significant increase in gene expression of MHC-II and CD86 in APP/PS1 females compared to WT females (**p=0.0018) and (*p=0.0122) respectively. There was a significant increase in TNF-α expression in APP/PS1 males compared to WT males (**p=0.007). Data, presented as mean +/- SEM, were analysed by unpaired t-tests or Mann Whitney when appropriate for non-parametric data.*

The effect of sex and the APP/PS1 transgene on genes linked to antigen presentation and inflammation in CD11b^{+} microglia was also investigated (**Figure 3.15** and **Figure 3.16**). Firstly, we investigated the effect of sex in CD11b^{+} microglia isolated from APP/PS1 and wild-type mice (**Figure 3.15**). MHC-II expression decreased in microglia from wild-type females compared to wild-type males, trended towards significance (**Figure 3.15 A**, p=0.0667). Sex had no effect on CD40 or CD80 gene expression of in either wild-type or APP/PS1 cohorts (**Figure 3.15 B and C**). There was a significant decrease in CD86 expression in wild-type females compared to wild-type males (**Figure 3.15 D**, p=0.046). This was not observed in APP/PS1 mice

(**Figure 3.15 D**). Sex had no effect on TNF-α or IL-6 gene expression in CD11b$^+$ microglia isolated from APP/PS1 or wild-type mice (**Figure 3.15 E and F**).

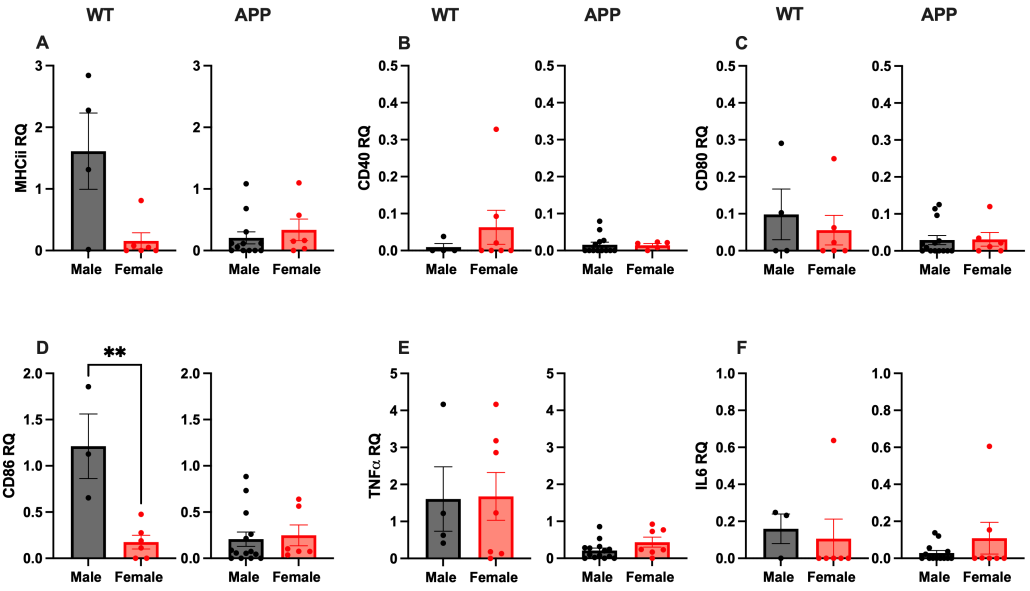


Figure 3.15 Investigation of sex on gene expression in CD11b microglia in APP/PS1 males and females and wild type littermates

*Gene expression by RT-qPCR of MHC-II (**A**), LCN2 (**B**), CD40 (**C**), CD86 (**D**), TNF-α (**E**) and IL-6 (**F**) in CD11b microglia in 16-17 month old APP/PS1 and wild type males and females (WT M=4, F=6, M=12-14 and F=5-6). There was a significant reduction in gene expression of CD86 in WT females compared to WT males (**p=0.0046). Data, presented as mean +/- SEM, were analysed by unpaired t-tests or Mann Whitney when appropriate for non-parametric data.*

The effect of the APP/PS1 transgene on gene expression in CD11b$^+$ microglia was then investigated (**Figure 3.16**). There was a significant decrease in MHC-II expression in APP/PS1 male microglia compared to wild-type males (**Figure 3.16 A**, p=0.0401). However, APP/PS1 transgene had no effect on CD40 or CD80 gene expression (**Figure 3.16 B and C**). There was a significant decrease in CD86 and TNF-α gene expression in microglia from APP/PS1 compared to wild-type males (**Figure 3.16 D and E**, p=0.0118 and p=0.0046 respectively). However, the effect of the APP/PS1 transgene was not observed on IL-6 microglial gene expression (**Figure 3.16 F**).

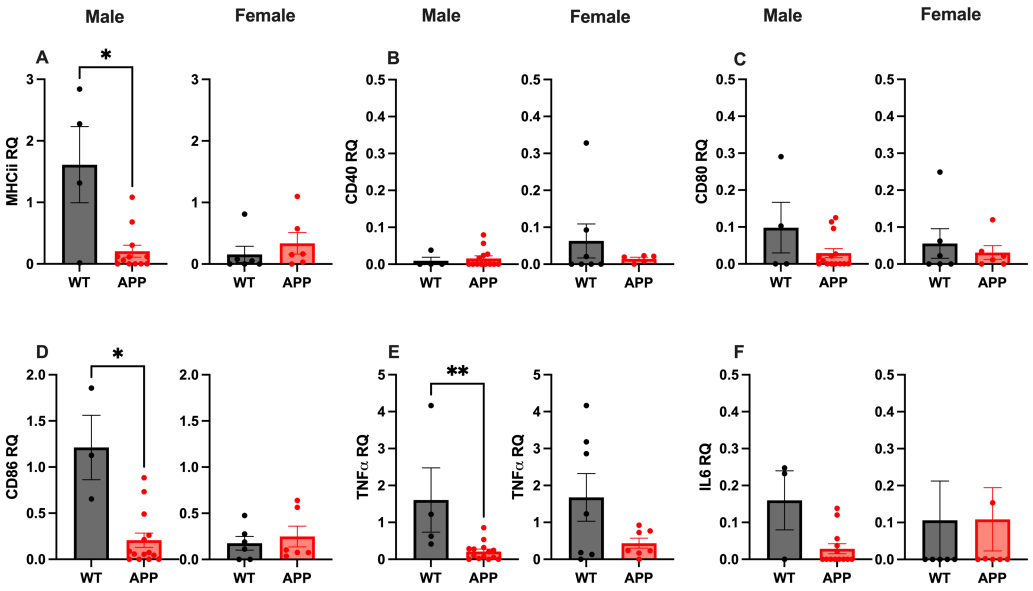


Figure 3.16 The APP/PS1 transgene alters gene expression of antigen presenting genes in CD11b microglia in males

*Gene expression by RT-qPCR of MHC-II (**A**), LCN2 (**B**), CD40 (**C**), CD86 (**D**), TNF-α (**E**) and IL-6 (**F**) in CD11b microglia in 16-17 month old APP/PS1 and wild type males and females (WT M=4, F=6, M=12-14 and F=5-6). There was a significant decrease in gene expression of MHC-II and CD86 in APP/PS1 males compared to WT males (*p=0.0401) and (*p=0.0118). There was a significant decrease in TNF-α expression in APP/PS1 males compared to WT males (**p=0.0046). Data, presented as mean +/- SEM, were analysed by unpaired t-tests or Mann Whitney when appropriate for non-parametric data.*

Summary of results obtained while assessing the effect of sex and APP/PS1 transgene on the genes associated with antigen presentation and inflammation in astrocytes and microglia

- Astrocytes from APP/PS1 females show an increase in expression of genes associated with antigen presentation (MHC-II and CD86) compared to both APP/PS1 males and wild-type females.
- Microglia from APP/PS1 males show a decrease in expression genes associated with antigen presentation (MHC-II and CD86) and gene expression of TNF-α compared to wild-type males.

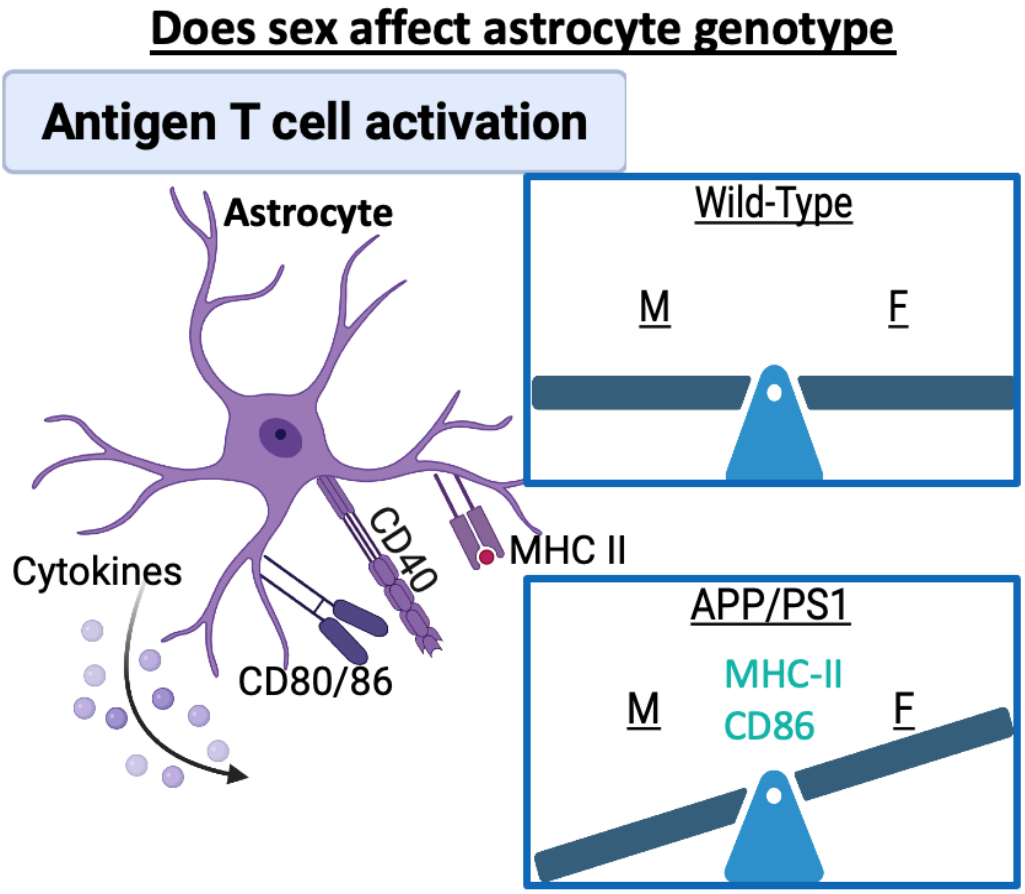


Figure 3.17 Abstract summary of RT-qPCR results of ASCA-2⁺ astrocyte antigen presentation genes in male and female APP/PS1 and wild-type littermates

The effect of sex on antigen presentation genes was only reported in the APP/PS1 cohort and was not observed in the wild-type cohort. In APP/PS1 female ASCA-2⁺ astrocytes, there was a significant increase in MHC-II and CD86 gene expression compared to APP/PS1 male ASCA-2⁺ astrocytes.

3.3.3 Influence of sex and the APP/PS1 transgene on astrocyte abundance and GFAP expression in 13-15 month old APP/PS1 males and females and wild-type littermates

To further elucidate the effect of sex and the APP/PS1 transgene on astrocytic response, brain sections from APP/PS1 and wild type males and females were immunolabelled for GFAP using immunofluorescence. Abundance was determined by numbers of GFAP⁺ cells and alterations in GFAP intensity was assessed to determine potential sex differences. Due to its integral role in memory and learning we investigated the hippocampus. To ensure regional differences were captured, three subregions of the hippocampus were investigated: CA1, CA3 and dentate gyrus.

The rationale behind this decision is based on reported modulatory role astrocytes located in the CA1 region of the hippocampus play on memory function (Wang et al., 2022). Additionally, previous work has also reported differences in astrocyte distribution in AD donors (determined by GFAP staining) in the CA1 and CA3 regions of the hippocampus compared to non-AD donors (Gonzalez-Rodriguez et al., 2021).
We first investigated the effect of the APP/PS1 transgene and sex on GFAP expression and total numbers of $GFAP^+$ astrocytes (**Figure 3.18**). In the CA1 and the CA3, neither sex nor the APP/PS1 transgene impacted on the number of $GFAP^+$ astrocytes (**Figure 3.18 A and C**). Additionally, there was no effect of sex or the APP/PS1 transgene observed in GFAP intensity in the CA1 region (**Figure 3.18 B**). Two-way ANOVA did report a main effect of sex *x* APP/PS1 transgene interaction in GFAP intensity in the CA3 (**Figure 3.18 D**, p=0.0009). Šidák's post-hoc multiple comparison tests revealed a significant decrease in GFAP intensity in APP/PS1 males compared to wild-type males (**Figure 3.18 D**, p=0.0193) and a significant increase in GFAP intensity in APP/PS1 females compared to APP/PS1 males (**Figure 3.18 D**, p=0.0045). In the dentate gyrus, two-way ANOVA reported a main effect of sex (**Figure 3.18 E**, p=0.037), the APP/PS1 transgene (**Figure 3.18 E**, p=0.0043) and the interaction of sex *x* APP/PS1 transgene **(Figure 3.18 E**, p=0.0311) in relation to the number $GFAP^+$ astrocytes. Šidák's post-hoc multiple comparison tests revealed a significant decrease in the number of $GFAP^+$ astrocytes in wild-type females compared to wild-type males (**Figure 3.18 E**, p=0.031) and a significant increase in $GFAP^+$ astrocytes in APP/PS1 females compared to wild-type females (**Figure 3.18 E**, p=0.005)

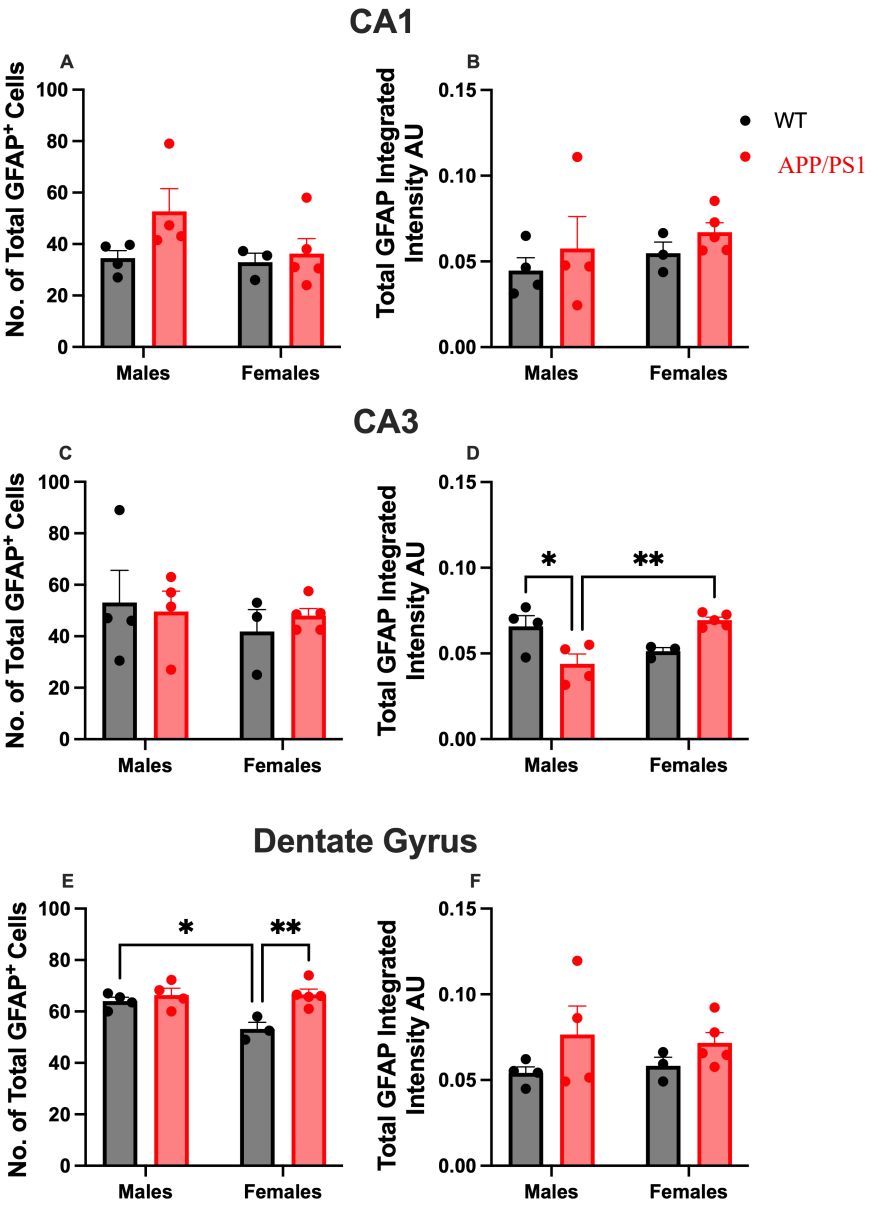


Figure 3.18 Investigation of astrocyte abundance and reactivity in the hippocampus of APP/PS1 males and females and wild type littermates using immunofluorescence

*The total number of astrocytes and GFAP intensity in 13-15 month old APP/PS1 males (n=4) and females (n=5) and wildtype males (n=4) and females (n=3) in the CA1 (**A and B**), CA3 (**C and D**) and dentate gyrus (**E and F**) of the hippocampus. In the CA3, two-way ANOVA reported a main effect of sex x APP/PS1 transgene interaction in GFAP intensity in the CA3 (***Figure 3.18D**, p=0.0009). There was a significant decrease in total GFAP integrated intensity in APP/PS1 males compared to WT males (**D**, *p=0.0193). Additionally, in the CA3 there was a significant increase in GFAP integrated intensity in APP/PS1 females compared to APP/PS1 males (**D**, **p=0.0045). In the dentate gyrus, two-way ANOVA reported a main effect of sex (**E**, p=0.037), the APP/PS1 transgene (**E**, p=0.0043) and the interaction of sex x APP/PS1 transgene (**E**, p=0.0311) in relation to the number GFAP+ astrocytes. There was a significant*

*decrease in the total numbers of GFAP⁺ nuclei in WT females compared to WT males (**E**, *p=0.0310) and a significant increase in GFAP⁺ nuclei in APP/PS1 females compared to WT females (**E**, **p=0.0055). Data, presented as mean +/- SEM, were analysed by 2-way ANOVA and Šidák's post-hoc multiple comparison tests.*

Potential sex differences within the APP/PS1 cohort regarding ThioflavinS⁺ amyloid plaque load and GFAP⁺ astrocytes were further investigated in the CA1, CA3 and dentate gyrus of the hippocampus. The abundance of astrocytes located proximally or distally to plaques were also investigated to understand any potential sex differences in astrocyte response to plaques.

In the CA1, there was a significant decrease in the numbers of ThioflavinS⁺ amyloid plaques in APP/PS1 females compared to males trending towards significance (**Figure 3.19 A** p=0.0184). There was an increase in ThioflavinS⁺ amyloid plaque area in APP/PS1 females that did not reach significance (**Figure 3.19 B**, p=0.0691). There was a significant increase in ThioflavinS⁺ amyloid plaque perimeter in APP/PS1 females compared to males (**Figure 3.19 C**, p=0.0159). Thioflavin S staining intensity did not differ between sexes (**Figure 3.19 D**).

In the CA1, the total number of GFAP⁺ astrocytes was similar between male and female APP/PS1 mice, furthermore sex did not impact the number of GFAP⁺ astrocytes proximal to plaques (**Figure 3.20 A and B**). Interestingly, APP/PS1 females presented with less GFAP⁺ astrocyte located distally to the plaques compared to males (**Figure 3.20 C**, p=0.0362). GFAP staining intensity (for total or proximal astrocytes) was unchanged between the sexes. (**Figure 3.19 D and F**).

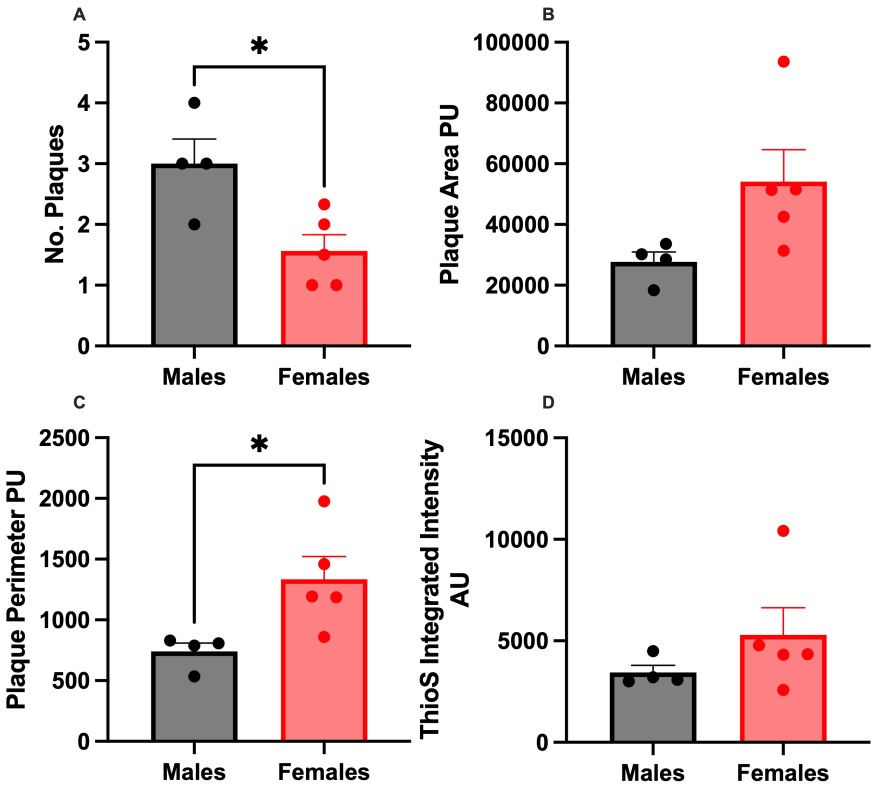


Figure 3.19 Investigation of plaque abundance and profile in the CA1 of the hippocampus of APP/PS1 males and females using immunofluorescence

*The total number of plaques (**A**), plaque area (**B**), plaque perimeter (**C**) and Thioflavin S intensity (**D**) in the CA1 of the hippocampus in 13-15 month old APP/PS1 males (n=4) and females (n=5). There was significant decrease in number of plaques in APP/PS1 females compared to males (A, *p=0.0184). There was a significant increase in plaque perimeter in APP/PS1 females compared to males (C, *p=0.0159). Data, presented as mean +/- SEM, were analysed by unpaired t-tests or Mann Whitney when appropriate for non-parametric data.*

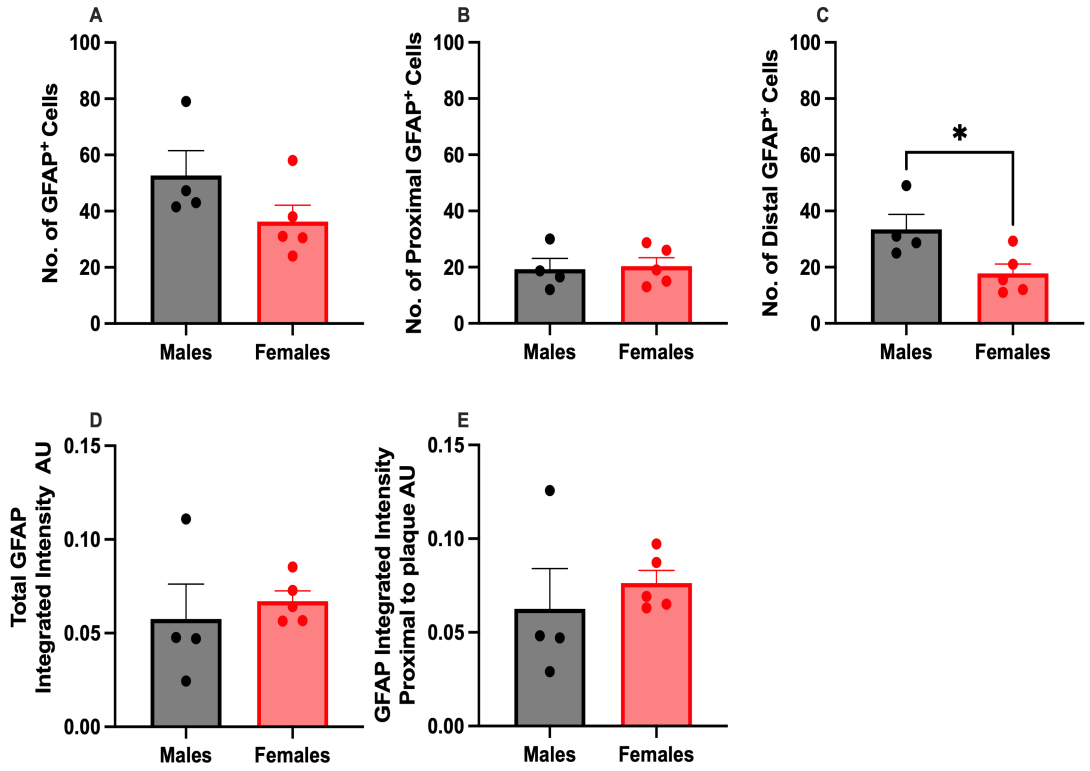


Figure 3.20 Investigation of astrocyte abundance and reactivity in the CA1 of the hippocampus of APP/PS1 males and females using immunofluorescence

*The total number of astrocytes and GFAP intensity (**A and D**), numbers of astrocytes and GFAP intensity proximal to plaques (**B and E**) and number of astrocytes distal to plaques (**C**) in the CA1 of the hippocampus in 13-15 month old APP/PS1 males (n=4) and females (n=5). There was a significant decrease in number of astrocytes located distally to plaques in the CA1 (**C**, *p=0.0362). Data, presented as mean +/- SEM, were analysed by unpaired t-tests or Mann Whitney when appropriate for non-parametric data.*

In the CA3, the total number of ThioflavinS$^+$ amyloid plaques, plaque area, plaque perimeter and ThioflavinS staining intensity did not differ between the sexes **(Figure 3.21 A-D**).

In the CA3, the total number of GFAP$^+$ astrocytes and the number of GFAP$^+$ astrocytes located proximally or distally to plaques did not differ between the sexes (**Figure 3.22 A-C**). Interestingly, APP/PS1 females had greater GFAP staining intensity (for total and proximal astrocytes) compared to males (**Figure 3.22 D and E**, p=0.0022 and p=0.0028 respectively).

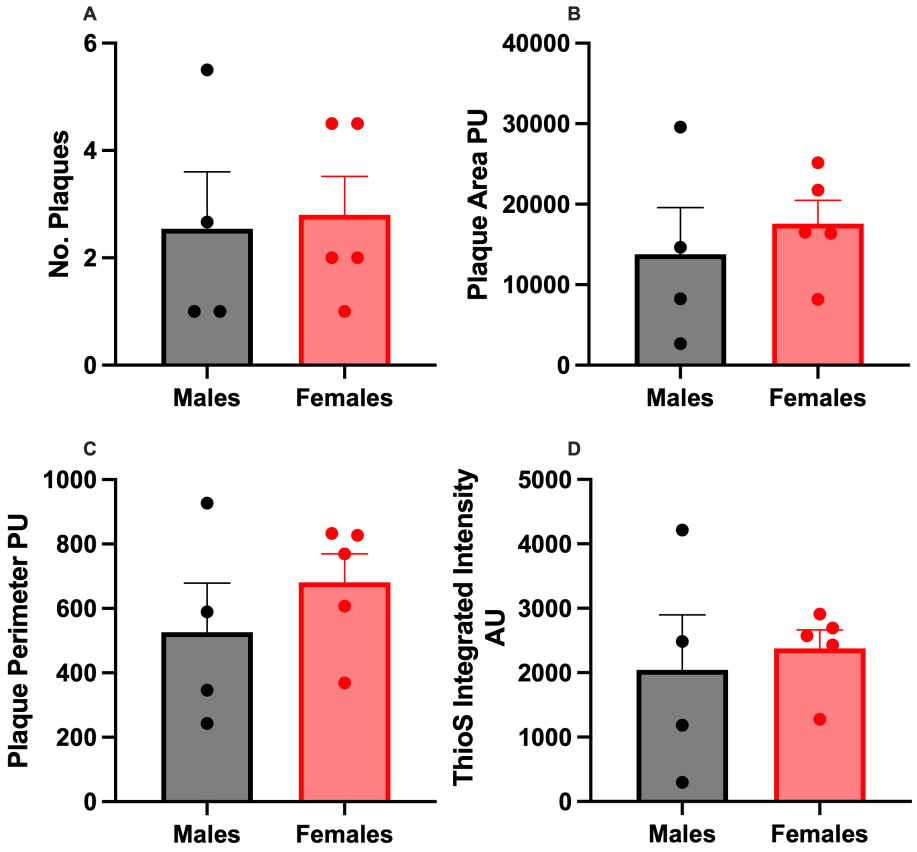


Figure 3.21 Investigation of plaque abundance and profile in the CA3 of the hippocampus of APP/PS1 males and females using immunofluorescence

*The total number of plaques (**A**), plaque area (**B**), plaque perimeter (**C**) and Thioflavin S intensity (**D**) in the CA3 of the hippocampus in 13-15 month old APP/PS1 males (n=4) and females (n=5). Data, presented as mean +/- SEM, were analysed by unpaired t-tests or Mann Whitney when appropriate for non-parametric data*

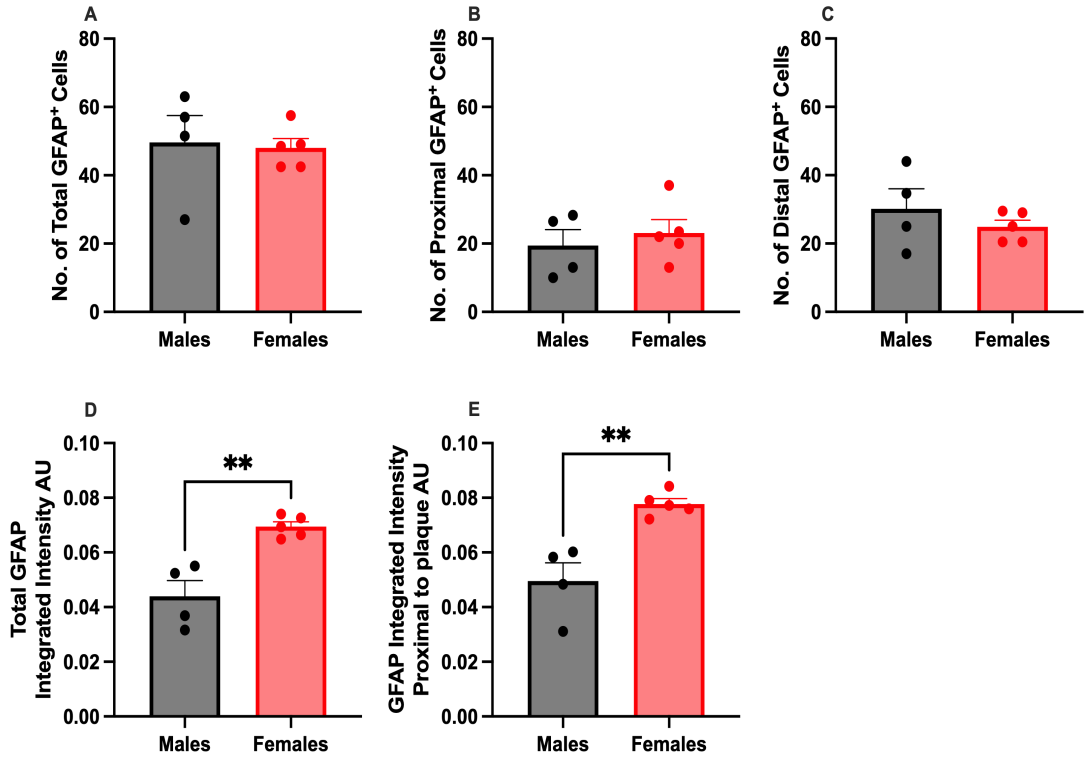


Figure 3.22 Investigation of astrocyte abundance and reactivity in the CA3 of the hippocampus of APP/PS1 males and females using immunofluorescence

*The total number of astrocytes and GFAP intensity (**A and D**), numbers of astrocytes and GFAP intensity proximal to plaques (**B and E**) and number of astrocytes distal to plaques (**C**) in the CA3 of the hippocampus in 13-15 month old APP/PS1 males (n=4) and females (n=5). There was a significant increase in total GFAP intensity (**D**, **p=0.0022) and GFAP intensity surrounding plaques (**E**, **p=0.0028) in APP/PS1 females compared to males. Data, presented as mean +/- SEM, were analysed by unpaired t-tests or Mann Whitney when appropriate for non-parametric data.*

In the DG, the total number of ThioflavinS$^+$ amyloid plaques, plaque area, plaque perimeter and ThioflavinS staining intensity did not differ between the sexes (**Figure 3.23 A-D**). Furthermore, the number of GFAP$^+$ astrocytes (for total, distal or proximal astrocytes) or GFAP staining intensity (for total or proximal astrocytes) did not differ between the sexes (**Figure 3.24 A-E**).

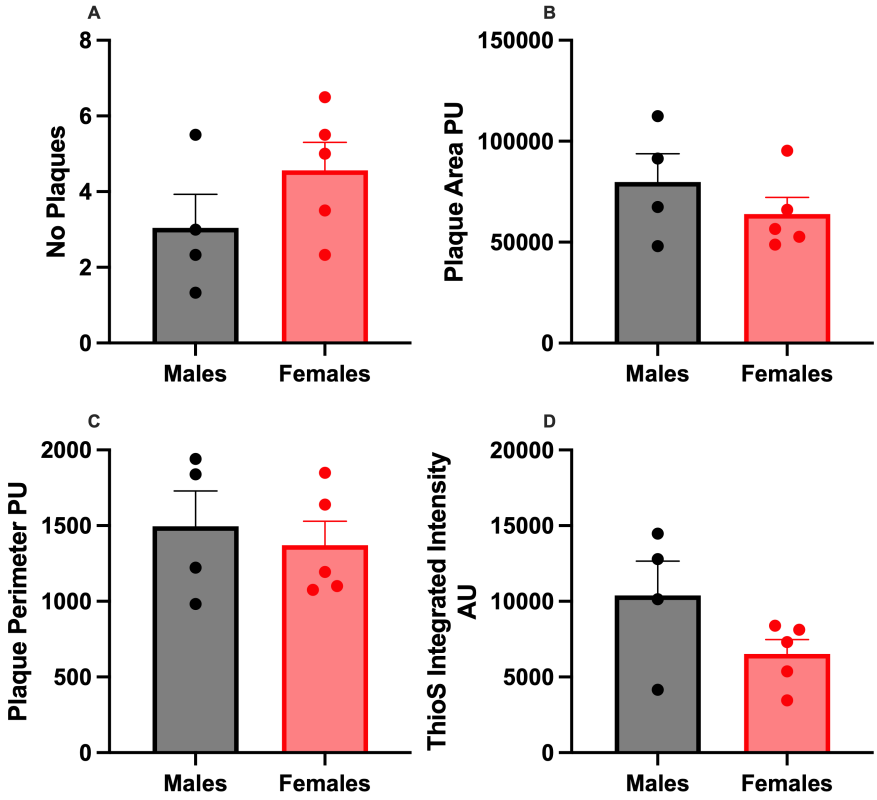


Figure 3.23 Investigation of plaque abundance and profile in the dentate gyrus of the hippocampus of APP/PS1 males and females using immunofluorescence

*The total number of plaques (**A**), plaque area (**B**), plaque perimeter (**C**) and Thioflavin S intensity (**D**) in the dentate gyrus of the hippocampus in 13-15 month old APP/PS1 males (n=4) and females (n=5). Data, presented as mean +/- SEM, were analysed by unpaired t-tests or Mann Whitney when appropriate for non-parametric data.*

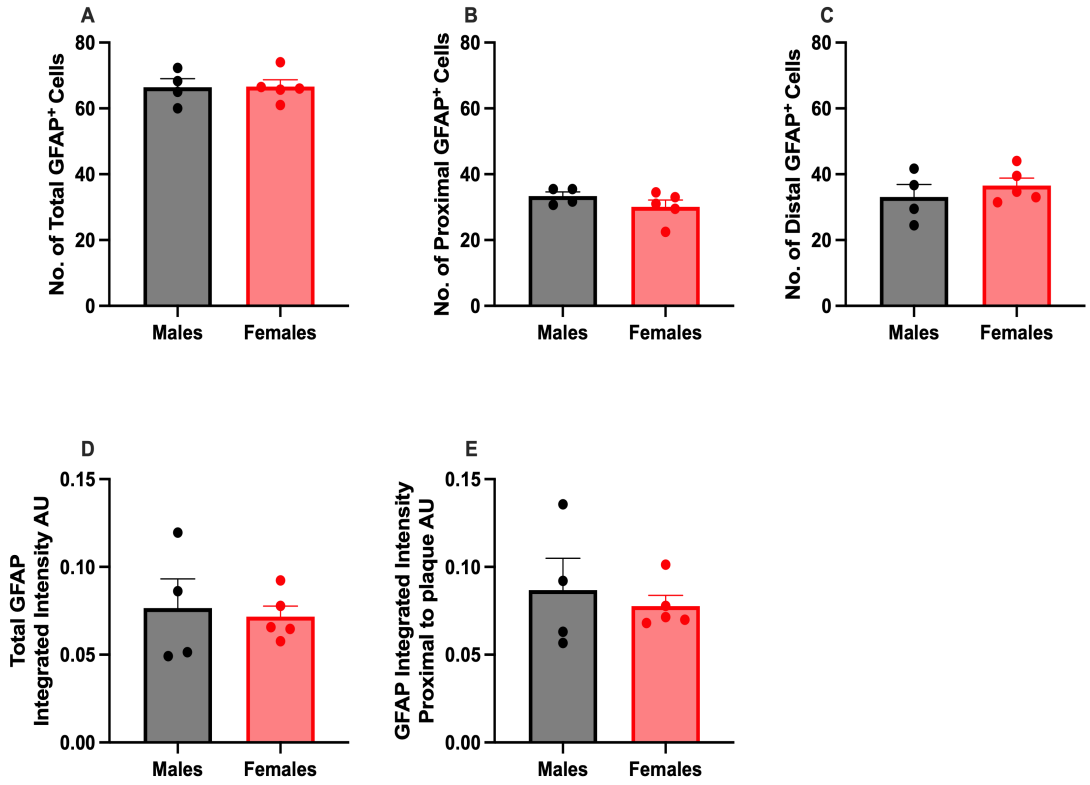


Figure 3.24 Investigation of astrocyte abundance and reactivity in the dentate gyrus of the hippocampus of APP/PS1 males and females using immunofluorescence

*The total number of astrocytes and GFAP intensity (**A and D**), numbers of astrocytes and GFAP intensity proximal to plaques (**B and E**) and number of astrocytes distal to plaques (**C**) in the dentate gyrus of the hippocampus in 13-15 month old APP/PS1 males (n=4) and females (n=5). Data, presented as mean +/- SEM, were analysed by unpaired t-tests or Mann Whitney when appropriate for non-parametric data.*

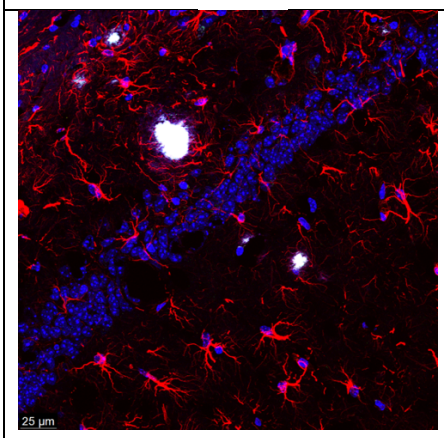
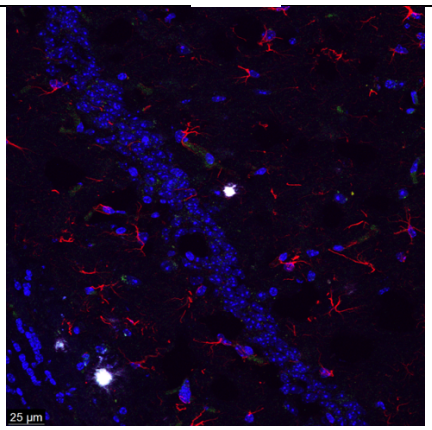
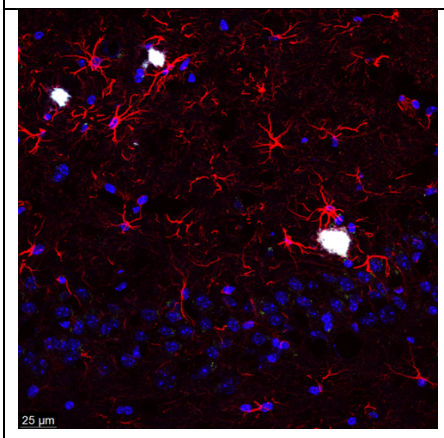
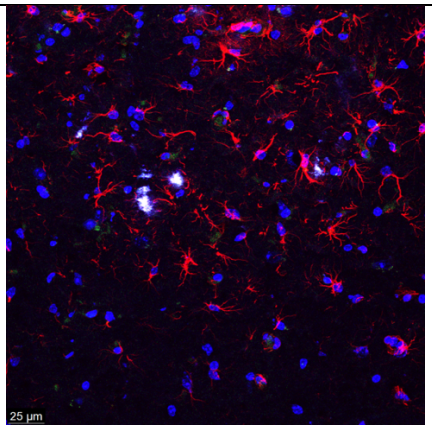
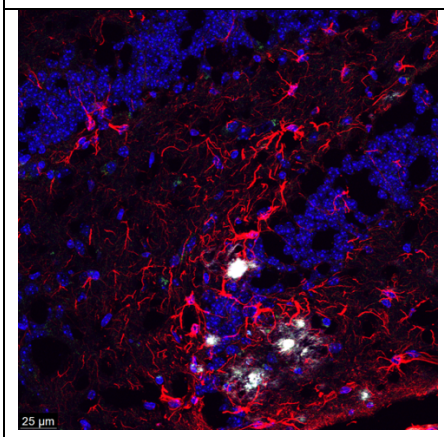
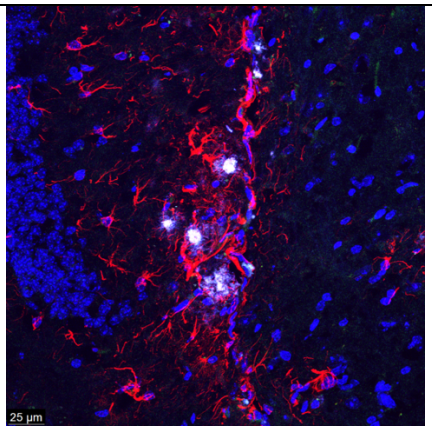
APP/PS1 Female	APP/PS1 Male
CA1 A	B
	
CA3 C	D
	
E Dentate Gyrus	F
	

Figure 3.25 Representative images of APP/PS1 40µm sections of the CA1, CA3 and the dentate gyrus of the hippocampus

*Representative images of 40µm brain sections of the hippocampus sub regions in APP/PS1 female and male: CA1 (**A-B**), CA3 (**C-D**) and the dentate gyrus (**E-F**). Images were taken at 40X magnification. Astrocytes (red), plaque (white) and nuclei (blue).*

Summary of results obtained while assessing the impact of sex and the APP/PS1 transgene on plaque abundance and GFAP$^+$ astrocytes

- APP/PS1 females have a significant increase in GFAP staining intensity (for total and proximal astrocytes) in the CA3 region of the hippocampus compared to males
- APP/PS1 females have a significant increase in plaque perimeter in the CA1 region of the hippocampus compared to males

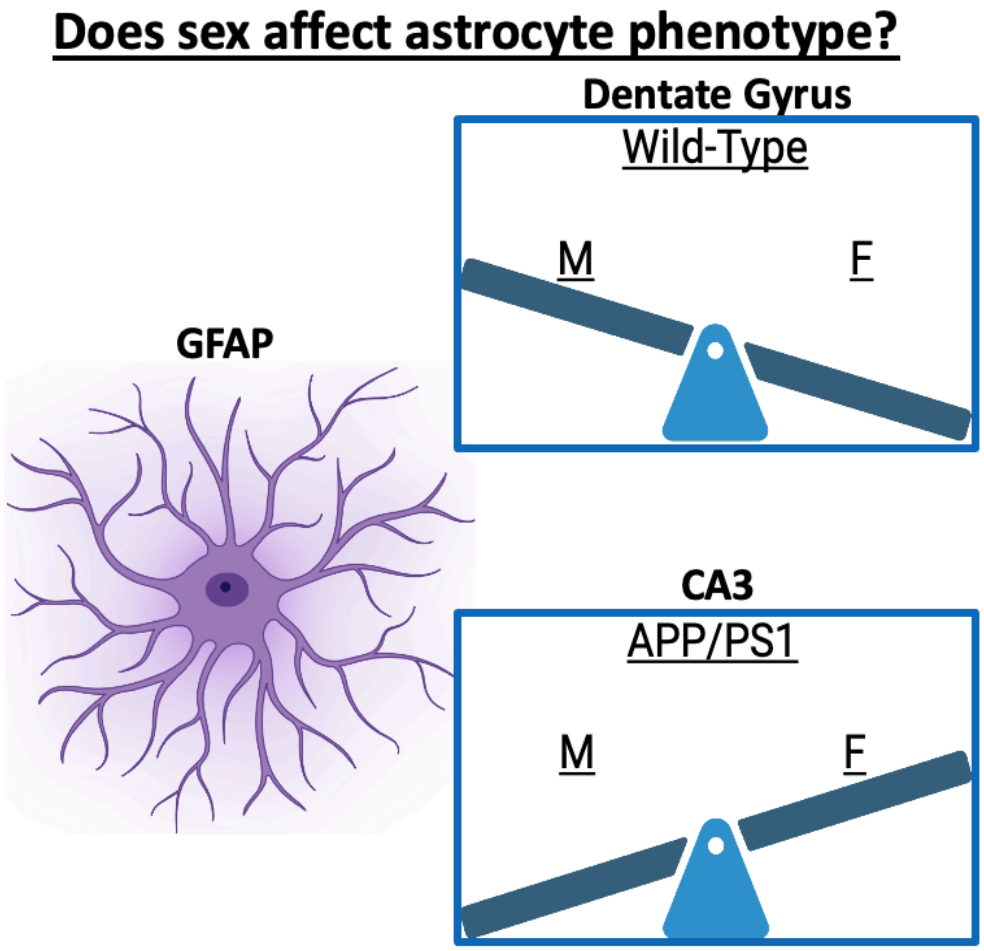


Figure 3.26 Abstract summary of GFAP immunohistochemistry analysis in male and female APP/PS1 and wild-type littermates

The effect of sex on astrocyte GFAP expression was region dependent. In the wild-type cohort, there was a significant decrease in number of GFAP$^+$ astrocytes in the dentate gyrus of the hippocampus which was not observed in the APP/PS1 cohort. In the APP/PS1 cohort, there was a significant increase in GFAP integrated intensity in APP/PS1 females compared to males, this was not observed in the wild-type cohort.

3.4 Discussion

The aim of this study is to understand the interplay between the innate and adaptive immune systems during the progression of AD and how sex may be a contributing factor to pathogenesis. Various studies have used immunisation strategies in AD mouse models to enhance Treg or Th17 cells populations and assess their effect on AD development, however producing conflicting results. Some have shown that increasing Treg abundance can lead to partial resolution of AD-like pathology (Faridar et al., 2020, Dansokho et al., 2016, Baek et al., 2016, Faridar et al., 2022, Yeapuri et al., 2023) whereas other studies have claimed Treg to be detrimental (Casares et al., 2023, Baruch et al., 2015, Di Benedetto et al., 2019). In humans, data suggest that Treg from AD patients compared to MCI patients have an impaired ability to supress Teff cells (Faridar et al., 2020). Additionally, Treg suppression and consequently Teff proliferation has been linked to detrimental effects in an AD mouse model including an increase in amyloidosis and microgliosis (Machhi et al., 2021). However, the interplay between the adaptive and the innate immune systems is less understood. Additionally, the question of sex variability and the baseline T cell populations in these studies has been largely neglected. The data I show here attempts to highlight some aspects of the interaction between adaptive and innate immune cells as the pathology progresses in APP/PS1 mice with sex accounted as a biological variable.

We report that changes in proportion of $CD4^+$ T cells in APP/PS1 males and females does not translate to changes in $CD4^+$ cytokine response or Tregs in secondary lymphoid tissue. In relation to cytokine expression, $CD8^+$ T cells are affected by sex in both wild-type and APP/PS1 cohorts. However, alterations in $CD8^+$ T cell cytokine responses in this study are identified in the lymph nodes but not in the spleen. The spleen is considered the secondary lymphoid organ of the circulatory system which indicates that it is presented with antigens from the blood. Conversely, lymph nodes are presented with antigens present in lymphatic fluid drained from tissue (Lewis et al., 2019). Thus, this indicates that antigen(s) are likely derived from tissue rather than circulating in the blood in this animal study.

We then must question where the antigen may be coming from to be presented to T cells in the lymph nodes. The cervical lymph nodes have been proposed to be involved in draining from the CNS (Louveau et al., 2015). It was reported that initial drainage from the CNS occurs in the deep cervical lymph nodes followed by subsequent drainage into the superficial cervical lymph nodes (Louveau et al., 2015). Thus, the alterations in cytokine expression we have reported here in superficial cervical lymph nodes may be in response to antigens drained from the CNS. However, the antigen in question has not been identified. Furthermore, the stronger $CD8^+$ T cells response in APP/PS1 males compared to females could be influencing the pathology seen in the APP/PS1. Additionally, a beneficial role for the cervical LNs has been reported in relation to Aß plaques and $IBA1^+$ and GFAP expression in the APP/PS1 model (Wang et al., 2019). As the $CD8^+$ T cell responses in the cervical lymph nodes are weakened in females this could indicate a potential dysfunction in cervical lymph node drainage in females. Subsequently, sex differences reported in females such as increased plaque load and microgliosis (Guillot-Sestier et al., 2021) could be influenced by this inefficient drainage and T cell response in females. However, this requires further investigation to understand the mechanism at play.

Furthermore, it could be argued that as the $CD8^+$ response in the cervical lymph nodes is altered in both WT and APP/PS1 cohorts, Aß is unlikely to be the antigen causing the significant changes in $CD8^+$ IFN-γ and IL-17 expression. It would be useful to investigate potential antigens responsible for T cell response by carrying out TCR sequencing similar to that conducted by Gate et al., (2020) to investigate potential antigens in both WT and APP/PS1 groups. It would further clarify if the same antigen or different antigens are causing the alteration reported in $CD8^+$ T cells in this study. However, this would need to be verified with further studies isolating T cells from cervical lymph nodes and stimulating with possible antigens including Aß to investigate if it leads to a response from $CD8^+$ T cells.

Additionally, it would be helpful to further elucidate whether the expression $CD8^+$ IFN-γ or $CD8^+$ IL-17 are beneficial or detrimental. This could be carried out by undergoing $CD8^+$ IFN-γ or $CD8^+$ IL-17 peripheral enhancement or suppression to see the effect this has on pathology and memory retention and whether it is more

effective in one sex. In previous studies, suppression of IL-17 γδ T and $CD4^+$ T cells led to improvements in AD pathogenesis (Brigas et al., 2021, Machhi et al., 2021, Li et al., 2023). Whereas a Aß specific $CD8^+$ T cell vaccination was neither detrimental or beneficial in APP/PS1 model (Rosset et al., 2015) indicating that the relationship between $CD8^+$ cytokines and AD pathogenesis in males and females requires further investigation.

In this study we have also reported a sexual dimorphism in the Treg population present in the brain. In APP/PS1 males there is a significant decrease compared to WT males indicating that pathology affects the proportion of Tregs present in the CNS. However in females, the WT cohort do not possess large proportions of Tregs. As Tregs are considered an anti-inflammatory subset of $CD4^+$ T cells the decrease in APP/PS1 male mice and an overall small Treg population in females regardless of pathology indicates a potential increase in inflammation. There have been studies that argue that Tregs ameliorate AD pathology (Faridar et al., 2020, Dansohko et., 2016, Yeapuiri et al., 2023) and others that refute this claim (Baruch et al., 2015, Benedetto et., 2019). Hence, the implication of this sexual dimorphic response should be investigated further to understand the potential benefit or harm related to AD pathogenesis. Furthermore, by not separating cohorts by sex the effect of increasing or decreasing Tregs in AD models may be lost or overestimated and could explain the contradictory findings reported in Treg studies. Additionally, the immunosuppressive function of Tregs could also be investigated as both animal studies (Abdelmoaty et al., 2023) and human studies (Faridar et al., 2020) have reported compromised Treg suppression in AD cohorts. This could be carried out by isolating Tregs from the spleen of APP/PS1 mice and co-culturing with Teff to assess their ability to inhibit Teff proliferation.

T cells isolated from PBMCs, have revealed significant increases in $CD8^+$ $CD27^-$ T_{EMRA} (Gate et al., 2020), $PD1^-$ $CD57^+$ $CD8^+$ and $PD1^+$ $CD57^+$ $CD8^+$ T_{EMRA} (van Olst et al., 2024) in AD patients compared to controls. Hence, another component that would be useful to study in relation to T cell response is senescence and exhaustion markers in T cells from male and female WT and APP/PS1 mice. In relation to glia-T cell crosstalk, CXCL16–CXCR6 has been identified as a key pathway in $CD8^+$ T cell signalling with microglia in 5XFAD mouse model (Su et al., 2023). Investigating

expression of chemokine receptor expression on T cells isolated from lymph nodes could help identify potential sex differences in glia T cell crosstalk.

We also reported alterations in $CD8^+$ T cells isolated from the inguinal and axillary lymph nodes. As these are not defined as the draining lymph nodes of the CNS there are some possible explanations for this observation;

As the study defining the cervical LNs as the draining LNs of the CNS (Louveau et al., 2015) was carried out in non-transgenic C57Bl/6J mice and not carried out in the APP/PS1 model it is possible that dysfunctional draining into different lymph node regions occurs in the APP/PS1 model. Additionally, BBB integrity maintained by markers such as ZO-1 and occludin (Jiao et al., 2011) are decreased in APP/PS1 model of AD (Zhang et al., 2018) indicating another component in drainage dysfunction. Furthermore, the animals in this study are aged between 16-17 months old when pathology has been established for several months thus the systemic immune response to Alzheimer's may be affected. It would be useful to include ages before pathology has been established and early stage pathology to see if these T cell alterations are present in the inguinal and axillary lymph nodes or is this a consequence of systemic inflammation brought on by long term AD pathology. Overall, the results reported in this study highlight the necessity to interrogate the potential role of sex in AD pathogenesis in T cell subsets.

Another key component to understanding the pathogenesis of AD is investigating the role of the innate immune system in the CNS. Microglia are the primary innate immune cell of the CNS and recent studies revealed specific sexual dimorphism in microglial phenotype and function. $APP_{swe}/PS1_{dE9}$ females have impaired phagocytic ability, altered metabolism and consequently an increased plaque load compared to their male counterparts (Guillot-Sestier et al., 2021). In particular, morphological changes between microglia from females and males have also been reported in several AD mouse models ($APP_{swe}PSEN1_{\Delta E9}$ and $App^{NL\text{-}G\text{-}F}$) and in AD postmortem tissue, which is accompanied by an alteration in phagocytic capacity (Sala Frigerio et al., 2019, Guillot-Sestier et al., 2021, O'Neill et al., 2022). Although they are not considered the primary immune cell of the CNS, astrocytes also play a role in immune response in the CNS (Colombo and Farina, 2016). Therefore, the intention of our study was to report potential sex differences present in astrocyte

phenotype and the implication this may have on inflammation in the CNS and plaque load.

This data reports sexual dimorphisms that are region specific and change with pathology. In wild-type aged animals, there is a sexual dimorphism in number of $GFAP^+$ cells present in DG with females having less $GFAP^+$ astrocytes compared to males. There are no studies that have highlighted this finding with studies mainly focusing on the difference in $GFAP^+$ cells with age in the hippocampus. This indicates that the effect of age on the number of $GFAP^+$ astrocytes is not uniform between males and females. The implication of increased $GFAP^+$ astrocytes indicates a more reactive phenotype (Ceyzériat et al., 2018) in the DG for WT males compared to females. Furthermore C3 expression is also correlated with GFAP expression on astrocytes (Liddelow et., 2017) therefore it would be useful to co-stain for C3 to further elucidate sex differences in astrocyte reactivity in wild-type cohorts. Consequently, reactive astrocytes are less capable of phagocytosing synaptosomes (Sanchez-Mico et al., 2021) hence it could also indicate an impairment in phagocytosis in WT male astrocytes that females are able to conserve. Cognitive decline could also be assessed to investigate if there is a correlation between GFAP expression and cognitive capabilities and if this is impaired in male WTs due to this GFAP increase.

Previous work has reported differences in astrocytic distribution identified in AD donors, with astrogliosis (determined by GFAP staining) significantly higher in the CA1 and CA3 regions compared to non-AD donors (Gonzalez-Rodriguez et al., 2021). We report additional results that indicate a sexual dimorphic GFAP expression in APP/PS1 males and females in response to pathology. Astrocyte GFAP expression decreases in response to pathology in the CA3 of male APP/PS1 brains which is not reported in females. However, APP/PS1 females respond to pathology in the DG with an increase in the number of $GFAP^+$ astrocytes which is not observed in the male cohort. This could imply that the response to pathology is not uniform in the sexes with males opting for a less reactive phenotype whereas females increase reactivity by increasing the number of $GFAP^+$ astrocytes present.

Within the APP/PS1 cohort, GFAP expression of astrocytes in response to Aß plaques is also heterogenous and region dependent. Female astrocytes are more

reactive in the CA3 region compared to male APP/PS1 astrocytes. The CA3 is an important component for memory and learning and is necessary for connection to the entorhinal cortex and the CA1 (Witter, 2007, Squire et al., 2004), therefore impairments due to increased inflammatory responses could have a negative impact on connectivity and lead to synaptic dysfunction. Due to the sexual dimorphic response reported, it would be beneficial to investigate markers such as C3 and C1q which have been reported to be increased in AD patients (Liddelow et al., 2017) and AD models (Wu et al., 2019). As inflammatory cytokine such as IL-1β, CCL2, CCL4 and CCL6 are known to increase with reactivity in AD (Ceyzériat et al., 2018) this could imply astrocytes from female APP/PS1 mice have increased inflammatory responses which would require further investigation.

The release of TNF-α, IL-1α and the complement component 1q (C1q) by microglia has been proven to induce a reactive phenotype in astrocytes (Liddelow et al., 2017). At 16–18 month APPswePSEN1$_{\Delta E9}$ microglia from female mice had a significant increase in expression of genes associated with DAMs and ARMs such as *TYROBP, CTSD* and *CCL6* compared to male APP$_{swe}$PSEN1$_{\Delta E9}$ mice (Guillot-Sestier et al., 2021). Thus the reactivity that we report in female APP/PS1 astrocytes may be induced by the increased reactivity seen in microglia in female APP/PS1 mice. Taken together this would indicate that both glial populations are more reactive in females compared to males in the APP/PS1 cohort.

Additionally, the effect of the APP/PS1 transgene is sexually dimorphic in relation to gene expression of glia. The effect of the APP/PS1 transgene is observed only in male microglial gene expression with a significant decrease in *MHC-II*, *CD86* and *TNF-α* in male APP/PS1 compared to wild-type. Conversely, the effect of the APP/PS1 transgene is observed in female astrocytes with an increase gene expression of *MHC-II* and *CD86* indicating a sexual dimorphic response by glia in relation to pathology and antigen presentation capacity. It is interesting that as well as male microglia adopting a less inflamed phenotype (Guillot-Sestier et al., 2021), the antigen presentation capacity in response to pathology is also decreased. Although as mentioned previously astrocytes are not the primary immune cell of the CNS their role in immunity has been identified with MHC-II expression on astrocytes

previously reported in Parkinson's brains (Rostami et al., 2020) and more recently in AD brains (Beretta et al., 2025). In our report, the MHC-II expression at gene level did not translate to protein level as $GFAP^+$ astrocytes did not co-stain for MHC-II. However, Beretta et al., 2025 reported that MHC-II^+ astrocytes are located close to $CD4^+$ T cells in post-mortem AD brains. As $CD4^+$ T cell staining was not carried out in our study it would be important to investigate this claim. Additionally, it has been reported that hiPSC derived astrocytes incubated with Aß had a decrease in MHC-II expression (Beretta et al., 2025). Thus a potential explanation for the lack of MHC-II expression in astrocytes immunolabelled in our study could be due to Aß load. This could be further investigated by staining MHC-II with GFAP and $CD4^+$ T cell markers together at different age points to see if astrocytes lose MHC-II expression as Aß load increases. It is interesting however that MHC-II expression at gene level is significantly increased only in female APP/PS1 mice indicating that the interaction with the adaptive immune system may be stronger in females than in males. This could be further elucidated by investigating potential sex differences in $CD4^+$ and $CD8^+$ T cell populations present in the brain.

Furthermore, any treatments aiming at modulating astrocyte reactivity would need to take into consideration the sexual dimorphism reported in astrocytes. As males and females do not uniformly respond to AD pathology in the APP/PS1 mouse model it would be important to segregate cohorts based on sex to further elucidate the benefit of treatments on groups.

In relation to plaque load, previous studies have reported that females have an increase in Aß deposition compared to males (Guillot-Sestier et al., 2021, Oveisgharan et al., 2018, Luchsinger et al., 2020, Wang et al., 2003). To have a more complete understanding of the plaque profile present in this study plaque area, perimeter and thioflavin S staining intensity was also considered. Again, a sex difference that is region specific was observed. In the CA1, males have a significant increase in plaque number. However, plaques are significantly larger in females with a significantly larger perimeter and a trend toward significance for females with an increase in plaque area as well ($p=0.0691$). This indicates the plaque profile between the sexes is not uniform in the APP/PS1 mouse model.

Overall, these results highlight the sexual dimorphism within the adaptive and the innate immune system in males and females at baseline (where no disease is present), in response to AD pathology (wild-type versus APP/PS1) and between APP/PS1 males and APP/PS1 females. This highlights how imperative it is to take sex differences into consideration at each level of studies to have a complete and thorough comprehension of disease progression and appropriate timing for therapeutic interventions.

4 Chapter 4: Investigating sex differences in T cells and cytokine concentration in the cerebrospinal fluid of Alzheimer's disease patients

4.1 Introduction

AD diagnosis was originally determined from a clinical phenotype without the use of biomarkers and categorised into mild, moderate or severe (McKhann et al., 1984). However, issues arise when up to one-third of patients were being misdiagnosed with AD, as it can only be confirmed with post-mortem investigation (Beach et al., 2012); therefore the criteria for diagnosis of AD has evolved overtime to include biomarkers in tandem with an initial clinical phenotype (Dubois et al., 2021). Initial investigations into the potential use of biomarkers in AD diagnosis reported a negative correlation with CSF $A\beta_{1-42}$ levels and positive correlation with CSF tau levels in patients with probable AD (Galasko et al., 1998). Additionally, the use of positron emission tomography (PET) scans of the Pittsburgh Compound B (PiB) (radiotracer that can bind to Aß) with CSF analysis reported an inverse relationship between PiB^+ patients and CSF $A\beta_{1-42}$ concentration (Fagan et al., 2006). Taken together these studies suggested alterations in CSF concentrations of $A\beta_{1-42}$ and tau do occur in patients with AD.

One major issue identified with CSF analysis as a tool for diagnosis is the variance between different assays (Lewczuk et al., 2006). To combat this more recent work has investigated potential "cut-off" points in relation to CSF $A\beta_{1-42}$, total tau (t-tau) and phosphorylated tau (p-tau) along with biomarker ratios such as $A\beta_{42}$/tau and $A\beta_{42}$/ $A\beta_{40}$ as indicators of AD pathology using Elecsys immunoassays (Roche Diagnostics) (Bittner et al., 2016, Schindler et al., 2018, Hansson et al., 2018, Doecke et al., 2020). High concordance between PET Aß imaging and Elecsys immunoassay assessing $A\beta_{1-42}$ CSF concentration (Roche Diagnostics) has illustrated the reliability of this assay to correctly identify AD patients (Schindler et al., 2018, Hansson et al., 2018, Doecke et al., 2020). Additionally, biomarker ratios such as $A\beta_{42}$/t-tau, $A\beta_{42}$/p-tau and $A\beta_{42}$/ $A\beta_{40}$ reported better concordance than a single biomarker (Schindler et al., 2018, Hansson et al., 2018, Doecke et al., 2020). The values for diagnosis cut-off points do differ between studies however with one study suggesting a cut off of CSF $A\beta_{1-42}$ < 1100pg/mL (Hansson et al., 2018) and another reporting the cut off CSF $A\beta_{1-42}$ < 1054pg/mL (Doecke et al., 2020).

CSF analysis in the prodromal stage of AD has also been investigated with reports of a greater risk of developing AD in MCI patients with a higher ratio of $A\beta_{42}$/t-tau (Hansson et al., 2006, Fagan et al., 2007, Duits et al., 2014). In individuals with dominantly inherited AD, CSF $A\beta_{42}$ levels started to decline up to 25 years prior to predicted disease onset (determined by parent's age of disease onset) whereas $A\beta^+$ PET results were reported 15 years prior to expected disease onset (Bateman et al., 2012). Alterations in CSF $A\beta_{1\text{-}42}$ concentration were interrogated prior to dementia diagnosis using cognitively healthy controls along with early or late MCI patients (Palmqvist et al., 2016). Patients pre-determined to have a decreased concentrations of $A\beta_{1\text{-}42}$ (<182.4 ng/l) but $A\beta^-$ PET results had the highest rate of Aß accumulation over 2 years, which was 3 times higher than patients with an initial CSF $A\beta^-$ PET $A\beta^-$ result (Palmqvist et al., 2016). This indicates CSF $A\beta_{42}$ concentrations could be useful as a preclinical marker.

One limitation of these studies is the accessibility of a lumbar puncture and PET scans compared to blood drawn analysis of AD biomarkers. In recent studies the pursuit of blood biomarkers for AD diagnosis has revealed modulations in tau and Aß concentrations. The use of immunoassays and immunoprecipitation mass spectrometry analysis has investigated the ability of plasma p-tau_{217} and p-tau_{181} to predict Aß results of PET scans and CSF results. It has been reported that plasma p-tau_{217} is greater at predicting MCI progression to AD in patients compared to p-tau_{181} or p-tau_{231} (Janelidze et al., 2023). A^+ patients with MCI (abnormal CSF $A\beta_{42}$/ $A\beta_{40}$ results but not diagnosed with AD) had greater concentrations of all three plasma p-tau levels (181, 217 and 231) compared to A^- MCI patients (Janelidze et al., 2023). In relation to clinical progression of MCI to MCI-AD, plasma p-tau_{217} significantly increased in MCI AD patients compared to MCI non-AD patients (Janelidze et al., 2023). These findings were corroborated in another study that also showed that plasma p-tau_{217} and p-tau_{181} both strongly correlated with amyloid status determined by CSF analysis (Arranz et al., 2024, Kivisäkk et al., 2024, Dyer et al., 2024). Additionally, in Aß and tau positive PET patients (A^+ T^+) plasma p-tau_{217} was significantly higher in A^+T^+ patients (Ashton et al., 2024). Moreover, plasma p-tau_{217} was a better predictor of abnormal Aß PET status than hippocampal atrophy, tau PET and CSF p-tau_{181} analysis (Ashton et al., 2024).

Recent studies have reported high performance of plasma $Aß_{42}$ using immunoprecipitation mass spectrometry to determine Aß status (Nakamura et al., 2018). Plasma $Aß_{42}/Aß_{40}$ ratio had the greatest correspondence with amyloid PET status and CSF p-$tau_{181}/Aß_{42}$ with an enhance correspondence when the age and *APOE* status of the individual was included (Schindler et al., 2019). This study also highlighted the potential predictive capacity of plasma $Aß_{42}/Aß_{40}$ as patients with an initial negative amyloid PET status but a high plasma $Aß_{42}/Aß_{40}$ ratio had a 15 fold risk of amyloid PET positive conversion compared to individuals with low plasma $Aß_{42}/Aß_{40}$ ratio (Schindler et al., 2019). The predictive potential of a combination of plasma Aß, plasma p-tau derivatives, *APOE* status and age have also been investigated. Studies have reported that plasma p-tau_{181}, p-tau_{217} and *APOE4* status could potentially predict AD dementia status in cognitively unimpaired individuals within 6 years whereas plasma p-tau_{181}, p-tau_{217} and $Aß_{42}/Aß_{40}$ ratio could predict MCI status (Palmqvist et al., 2023). This was further corroborated in a predictive model produced by (Rissman et al., 2024) including; plasma p-tau_{217} /non-phosphorylated tau_{217}, $Aß_{42}/Aß_{40}$, age and *APOE* status to predict amyloid PET status.

Another important component of these biomarker assays is their use in clinical trials to ensure appropriate patients can be included or excluded. If we rely solely on the clinical phenotype presentation of AD, we increase the risk of including patients that do not have AD and thus a drug designed to target an AD related protein may be deemed inefficient, when the appropriate cohort is not chosen.

Subsequently, as well as CSF and blood from AD patients being used for biomarker analysis, samples have also been utilised to identify potential changes in pro-inflammatory cytokine levels, GFAP expression and NfL in the CSF (Taipa et al., 2019, Johnson et al., 2020). Additionally, PBMCs isolated from the blood of AD patients have been utilised to further elucidate the mechanisms at play with regard to the immune system in AD (see section 1.5)

Therefore the aims of this study are to investigate the effect of sex on:

1) T cell cytokine response in PBMCs isolated from AD patients
2) T cell activation, senescence and Treg population in AD patient blood
3) Cytokines present in the CSF of AD patients

4.2 Methods

4.2.1 Patient Overview

PBMCs were isolated as outlined in 2.7. The total number of patients per group, mean age (+/- standard deviation) and female: male ratio for PBMCs and CSF are outlined below. Please refer to section 2.6.1 for categorisation of AD versus non-AD/MCI patients.

PBMCs Flow cytometry	Non-AD/MCI N=7	AD N=19
Age (Mean)	67.2 +/- 7.4	68.9 +/- 7.5
Sex (Female : Male)	3: 4	11:8
PBMCs Con media	N=8	N=18
Age (Mean)	68.2 +/- 7.4	69.1 +/- 6.9
Sex (Female : Male)	3:5	11:7
CSF	N=8	N=17
Age (Mean)	68.2 +/- 7.4	68.5 +/- 6.5
Sex (Female : Male)	3:5	12:5

Table 4.1 Mean age +/- standard deviation of non-AD/MCI and AD patients samples including PBMCs isolated from blood, conditioned media from stimulated PBMCS and cerebrospinal fluid.

Please note, Con Media refers to conditioned media supernatant collected after PBMCs were isolated and stimulated for 5 days with anti-CD3 and anti-CD28

4.2.2 PBMCs conditioned media

24 well plates were pre-coated with anti-CD3 (1µg/mL in PBS; 37°C; 5% CO_2; overnight; eBioscience™; Cat Code: 16-0037-81). The following day, PBMCs were thawed and seeded at 1 million cells/mL in each well in cRPMI containing anti-CD28 (0.5µg/mL; eBioscience™; Cat Code: 16-0289-81). Cells were incubated for 5 days (37°C; 5% CO_2) before collecting the conditioned media and storing at -20°C before processing.

4.2.3 PBMCs Flow Cytometry

PBMCs were thawed and resuspended in cRPMI (10% (v/v) foetal bovine serum (FBS), 1% (v/v) penicillin streptomycin, 1% (v/v) glutaMAX and RPMI; ThermoFisher) (1 mL). Cell suspensions were split into two (500 µL per panel) and

immunolabelled with antibodies investigating cytokine response (**Table 4.2**) or antibodies investigating activation, senescence and regulatory T cells populations (**Table 4.3**).

4.2.3.1 Stimulation

PBMCs immunolabelled for the cytokine panel were stimulated with phorbol 12-myristate 13-acetate (PMA; 50ng/mL), ionomycin (0.5μg/mL) and brefeldin A (5μg/mL) in cRPMI with each sample also having an unstimulated control using just brefeldin A (5μg/mL) (37°C; 5% CO_2; 5 hours). To identify the stimulated cytokine response the unstimulated sample paired with the corresponding stimulated sample were analysed side by side to ensure baseline stimulation was not included and strictly PMA and Ionomycin induced stimulation was accounted for.

4.2.3.2 Cell staining and immunolabelling T cells

All samples were immunolabelled with Live Dead Aqua stain (LIVE/DEAD™ Fixable Aqua Dead Cell Stain Kit, for 405 nm excitation; ThermoFisher; Cat Code: L34957) in PBS (1X; 1:500; 100 μL; 15 minutes; RT; in the dark). Extracellular and intracellular staining was carried out to detect the presence of T cell subsets. The antibodies conjugated with fluorophores used in both panels are outlined in **Table 4.2** and **Table 4.3**. Extracellular antibodies were diluted in Brilliant Stain Buffer (1:33; BD Pharmingen; Cat Code: 563794) and FcBlock (1:50; BioLegend; Cat Code: 422302) and added to the samples (50 μL; 20 minutes; RT; in the dark). After incubation, cells were washed with FACs Buffer (200 μL), centrifuged (340 x *g*; 5 minutes; RT) and the supernatant was decanted. Cells were fixed and permeabilized using the FoxP3 staining kit (eBioscience™ Foxp3 / Transcription Factor Staining Buffer Set; Invitrogen). Fixation concentrate solution was diluted in the perm dilute solution (1:4) and added to each sample (100 μL; in the dark; RT; 20 minutes). Cells were centrifuged (340 x *g*; 5 minutes; 4°C) and supernatant decanted. The intracellular antibodies were diluted (1:33) in 1X permeabilisation buffer (1:10; 10X perm buffer (Invitrogen); H_2O) and added to the samples (50 μL; 1 hour; 4°C; in the dark). Samples were washed with diluted permeabilisation buffer (1X; 200 μL) and centrifuged (340 x *g*; 5 minutes; 4°C). The supernatant was decanted and samples were washed with FACs buffer (1000 μL; 340 x *g*; 5 minutes; 4°C). Samples were

resuspended in FACs buffer (200 µL). Compensation beads (40 µL; OneComp eBeads™ Compensation Beads; Invitrogen and 160 µL FACs Buffer) and single stain samples were immunolabelled with one specific antibody from the antibody panel to account for wavelength overlap between antibodies. Negative controls consisted of samples immunolabelled with all fluorescent antibodies minus one (FMO). Samples were processed on the Aurora Cytometer (Cytek Biosciences) in TCD Flow cytometry core facility.

Emission Peak (approx.)	Channel	Fluorophore	Target	Species	Manufacturer and catalogue No.
720	V13	BV711	IFN-γ	Mouse	BD Horizon 564039
750	V14	BV750	IL-17A	Mouse	BD Horizon 566358
720	B10	PerCP-eF710	IL-2	Mouse	Invitrogen 46-7029-42
542	B3	SparkBlue 550	CD3	Mouse	BioLegend 344852
615	B6	BB630	CD4	Mouse	BD Horizon 624294
812	B14	BB790	CD8	Mouse	BD Horizon 624296
780	YG9	PE-Cy7	TNF-α	Mouse	BD Horizon 557647

Table 4.2 Flow cytometry antibodies used to investigate cytokine expression

Emission Peak (approx.)	Channel	Fluorophore	Target	Species	Manufacturer And Catalogue No.
720	V13	BV711	CD28	Mouse	BD Horizon 563131
780	V15	BV786	CD25	Mouse	BD Horizon 563701
508	B1	BB515	CD27	Mouse	BD Horizon 564642
542	B3	SparkBlue 550	CD3	Mouse	BioLegend 344852
615	B6	BB630	CD4	Mouse	BD Horizon 624294
812	B14	BB790	CD8	Mouse	BD Horizon 624296
615	YG3	PE-CF594	CD57	Mouse	BD Horizon 562488
661	R1	APC	KLRG1	Mouse	Invitrogen 17-9488-41
692	R3	Spark NIR 685	CD127	Mouse	BioLegend 351361
738	R5	R718	FoxP3	Mouse	BD Horizon 566935
812	R8	APC-Fire 810	CD45	Mouse	BioLegend 304076

Table 4.3 Flow cytometry antibodies used to investigate activation, senescence and regulatory T cells

4.2.4 Meso-Scale Discovery (MSD) assays for the detection of cytokines

MSD assays were carried out in accordance with manufacturing instructions (Meso Scale Diagnostics, UK). MSD plates were purchased with pre-coated capture antibodies present (See **Table 4.4** for list of V-plex plates used). Plates were washed

with wash buffer (0.5% Tween in PBS; 3 times). Samples and standards were added to the MSD plate and incubated on a plate rocker (2 hours; RT). The samples and standards were removed and washed with wash buffer (3 times). The detection antibody was added and incubated on a plate rocker (2 hours; RT). The detection antibody was removed and washed with wash buffer (3 times). 2X read buffer T (4X read buffer in deionised water (1:2)) was added to the plate. The read buffer is necessary to generate the electrochemiluminescence (ECL) signal for detection. The plate was analysed on the MSD plate reader (MESO QuickPlex SQ 120MM, UK). Concentrations of the samples were derived from the standard curve.

V-Plex Plate	Cat Code
Eotaxin, MIP-1β, IP-10, IL-8, MCP1	K15047D
IFN-γ, IL-6, IL-10, IL-12p70, TNF-α	K15049D
IL-17A	K151RFD
IL-1Rα	K151WTD

Table 4.4 List of V-Plex plates used for meso-scale discovery analysis

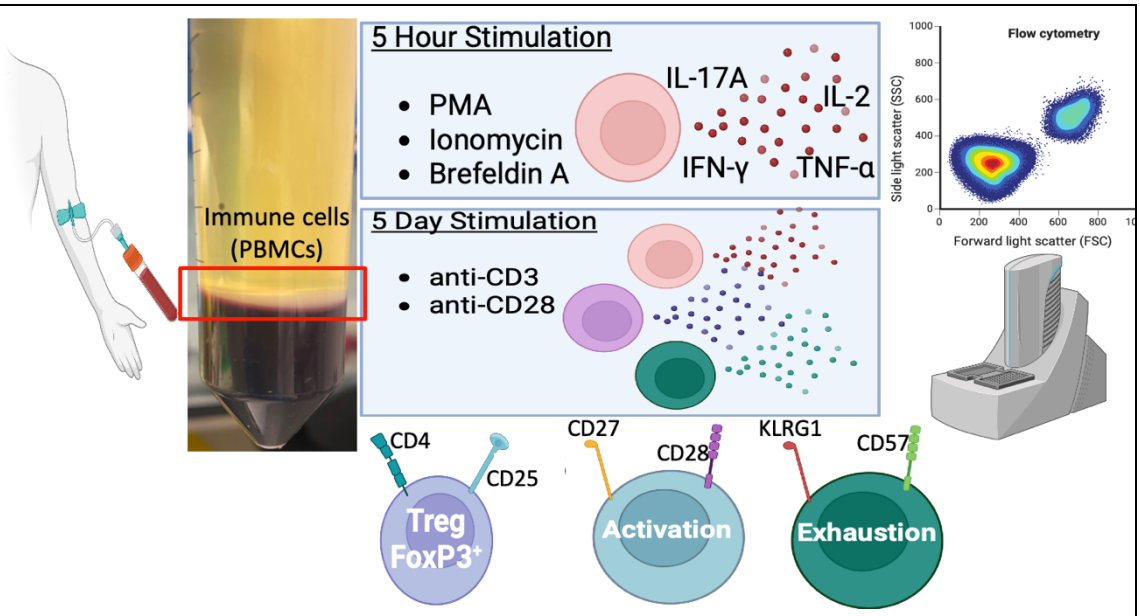


Figure 4.1 Schematic diagram of the methods carried out on PBMCs isolated from non-AD/MCI and AD patients

Blood was collected from non-AD/MCI and AD patients and PBMCs were isolated. PBMCs were then stimulated with:

i) *stimulated with phorbol 12-myristate 13-acetate (PMA; 50ng/mL), ionomycin (0.5μg/mL) and brefeldin A (5μg/mL) and incubated for 5 hours (37°C; 5% CO_2) and immunolabeled for flow cytometry to investigate cytokine response in T cells*

ii) *stimulated with anti-CD3 (1*μg/mL*) and anti-CD28 (0.5*μg/mL*) for 5 days (37°C; 5% CO_2) with supernatant collected for Meso-Scale Discovery*

iii) *immunolabelled for flow cytometry to investigate proportions of regulatory T cells, activated $CD4^+$ and $CD8^+$ T cells and exhausted $CD4^+$ and $CD8^+$ T cells.*

4.3 Results

4.3.1 Investigation of T cell populations in peripheral blood mononuclear cells of Non Alzheimer's Disease/MCI and Alzheimer's Disease patients using flow cytometry

Alterations in $CD4^+$ and $CD8^+$ T cells were initially investigated by isolating PBMCs from non-Alzheimer's disease/MCI (non-AD) and Alzheimer's disease (AD) patients. PBMCs were stimulated with phorbol 12-myristate 13-acetate (PMA; 50ng/mL), ionomycin (0.5µg/mL) and brefeldin A (5µg/mL) to investigate cytokine release (see **Figure 4.2** for gating strategy applied). The proportion of $CD4^+$ and $CD8^+$ T cells did not differ between non-AD/MCI and AD patients (**Figure 4.3**). When separated by sex (**Figure 4.4**), neither sex nor AD pathology impacted the proportion of $CD4^+$ and $CD8^+$ T cells present.

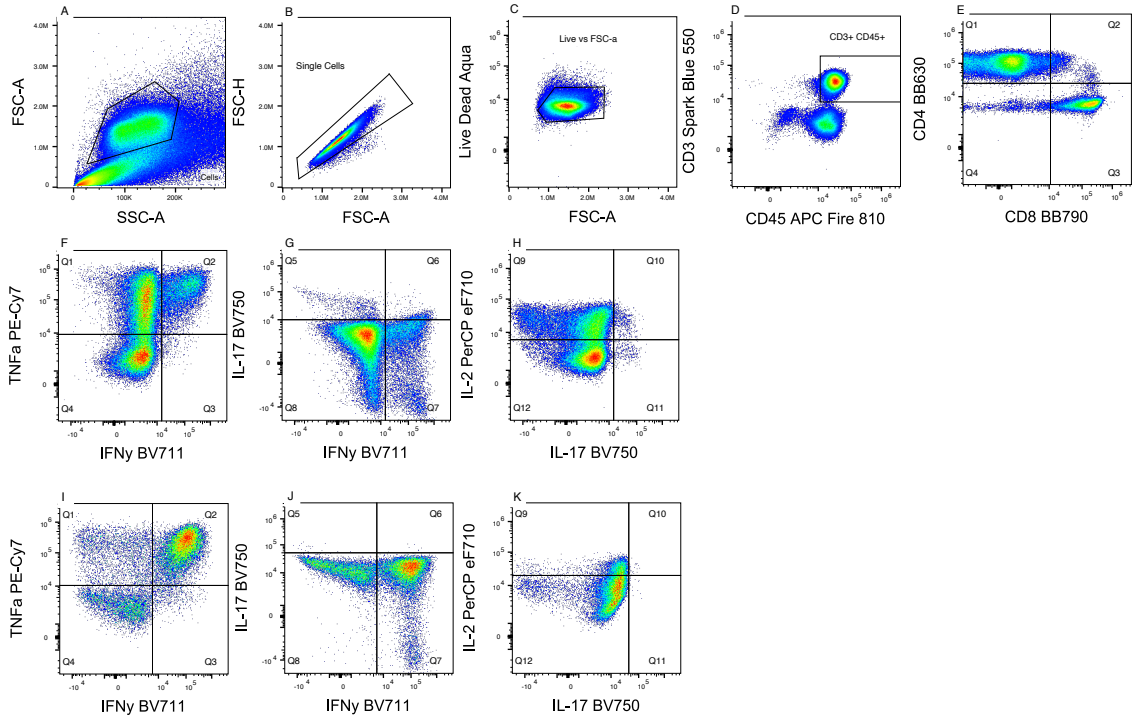


Figure 4.2 Outline of flow cytometry gating strategy for cytokine response in $CD4^+$ and $CD8^+$ T cells

*PBMCs were stimulated with phorbol 12-myristate 13-acetate (PMA; 50ng/mL), ionomycin (0.5µg/mL) and brefeldin A (5µg/mL) with each sample also having an unstimulated control using brefeldin A (5µg/mL) alone. All samples for the cytokine panel were incubated for 5 hours (37°C; 5% CO_2). Lymphocytes were gated front scatter area (FSC-A) vs side scatter area (SSC-A) (**A**), single*

*cells were gated FSC-H vs FSC-A (**B**) and live cells were gated on live dead stain vs FSC-A (**C**). T lymphocytes were gated CD3 vs CD45 (**D**) and T cells were gated on CD4 vs CD8 (**E**). $CD4^+$ and $CD8^+$ cytokine expression was gated for TNFα (**F and I**), IFNγ (**F and I**), IL-17 (**G and J**) and IL-2 (**H and K**). Gating was established using single stain and fluorescent minus one (FMO) controls*

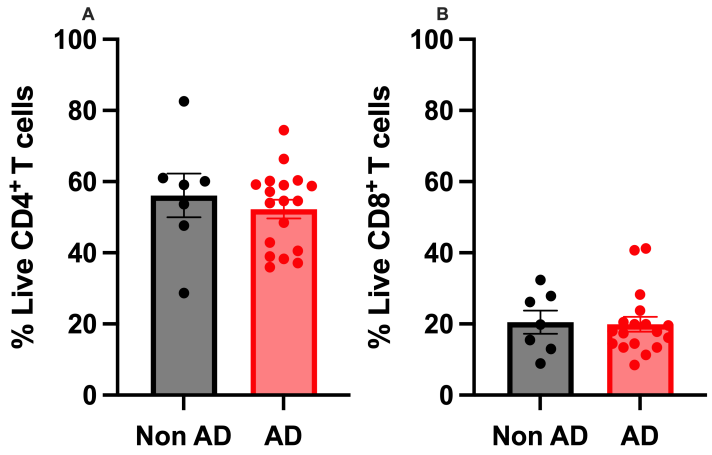


Figure 4.3 Analysis of T cell populations in non-Alzheimer's Disease/MCI and Alzheimer's Disease patients

*Flow cytometry analysis of the percentage of $CD4^+$ (**A**) and $CD8^+$ (**B**) T cells identified in PBMCs of non-Alzheimer's Disease/MCI (N=7) and Alzheimer's disease (N=18) patients stimulated with phorbol 12-myristate 13-acetate (PMA; 50ng/mL), ionomycin (0.5μg/mL) and brefeldin A (5μg/mL) and incubated for 5 hours (37°C; 5% CO_2). See Figure 4.2 for the gating strategy applied. Data, presented as mean +/- SEM, were analysed by unpaired t-tests or Mann Whitney when appropriate for non-parametric data.*

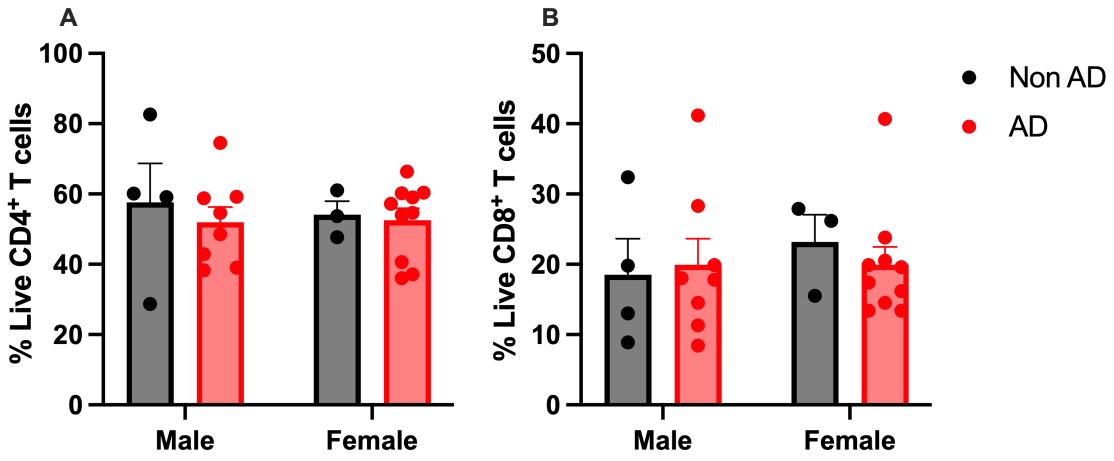


Figure 4.4 Analysis of T cell populations in male and female non-Alzheimer's Disease/MCI and Alzheimer's Disease patients

*Flow cytometry analysis of the percentage of $CD4^+$ (**A**) and $CD8^+$ (**B**) T cells identified in PBMCs of male (N=4) and female (N=3) non-Alzheimer's Disease/MCI and male (N=8) and female (N=10) Alzheimer's disease patients. Cells were stimulated with phorbol 12-myristate 13-acetate (PMA; 50ng/mL), ionomycin (0.5μg/mL) and brefeldin A (5μg/mL) and incubated for 5 hours (37°C; 5% CO_2). See Figure 4.2 for the gating strategy applied. Data, presented as mean +/- SEM, were analysed by two-way ANOVA and Šidák's post-hoc multiple comparison tests.*

$CD4^+$ and $CD8^+$ T cell cytokine response of TNF-α, TNF-α IFN-γ, IFN-γ, IL-17 and IL-2 following stimulation was subsequently analysed (**Figure 4.5**). In $CD4^+$ T cells, there was no difference observed in cytokine response between non-AD and AD patients (**Figure 4.5 A-E**). In $CD8^+$ T cells, TNF-α response trended towards a significant decrease in AD patients compared to non-AD/MCI patients (**Figure 4.5 F**, p=0.097). The proportion of TNF-α IFN-γ, IFN-γ, IL-17 or IL-2 $CD8^+$ T cells did not differ between non-AD/MCI and AD patients (**Figure 4.5 G-J**).

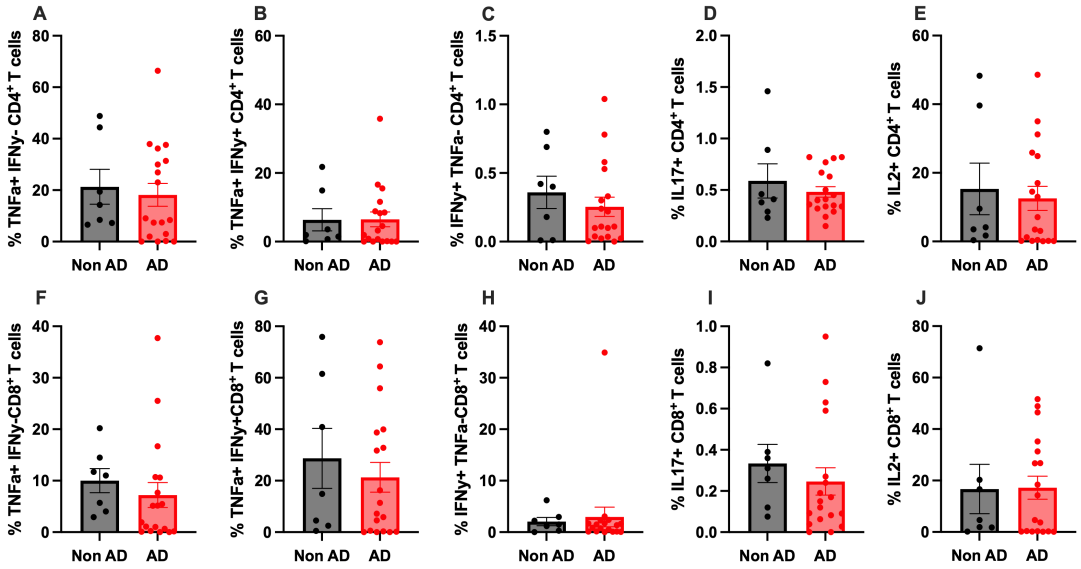


Figure 4.5 Analysis of Cytokine Expression in T cell populations of non-Alzheimer's Disease/MCI and Alzheimer's Disease patients

*Flow cytometry analysis of the percentage of intracellular cytokines in $CD4^+$ and $CD8^+$ T cells in PBMCs of non-Alzheimer's Disease/MCI (N=7) and Alzheimer's disease (N=18) patients. Cells were stimulated with phorbol 12-myristate 13-acetate (PMA; 50ng/mL), ionomycin (0.5μg/mL) and brefeldin A (5μg/mL) and incubated for 5 hours (37°C; 5% CO_2). No statistically significant differences in the proportion of $CD4^+$ TNF-α (**A**), TNF-α IFNγ (**B**), IFNγ (**C**), IL-17 (**D**) or IL-2 (**E**) cells were reported. No statistically significant differences in the proportion of $CD8^+$ TNF-α (**F**), TNF-α IFNγ (**G**), IFNγ (**H**), IL-17 (**I**) or IL-2 (**J**) cells were reported. See Figure 4.2 for the gating strategy applied. Data, presented as mean +/- SEM, were analysed by unpaired t-tests or Mann Whitney when appropriate for non-parametric data.*

We then analysed cytokine expression in $CD4^+$ T cells based on sex in non-AD/MCI and AD patients (**Figure 4.6 A-E**). Two-way ANOVA reported a significant sex *x* pathology interaction on the proportion of $CD4^+$ $IL\text{-}17^+$ cells (**Figure 4.6 A**, p=0.0091). AD females had a significant decrease in $CD4^+$ IL17 cells compared to non-AD/MCI females (**Figure 4.6 A**; p=0.0495) according to Šidák's post-hoc multiple comparison tests. A trending increase in $CD4^+$ $IL\text{-}17^+$ cells was observed in non-AD/MCI females compared to non-AD/MCI males but did not reach significance (**Figure 4.6 A**, p=0.0977). The effect of sex or AD pathology was not observed in the proportion of $CD4^+$ IL-2, TNF-α, TNF-α IFN-γ or IFN-γ cells (**Figure 4.6 B-E**).

Potential sex differences in non-AD/MCI and AD $CD8^+$ T cell cytokine expression was also investigated (**Figure 4.7 A-E**). No effect of sex or AD pathology on $CD8^+$ cytokine response was observed.

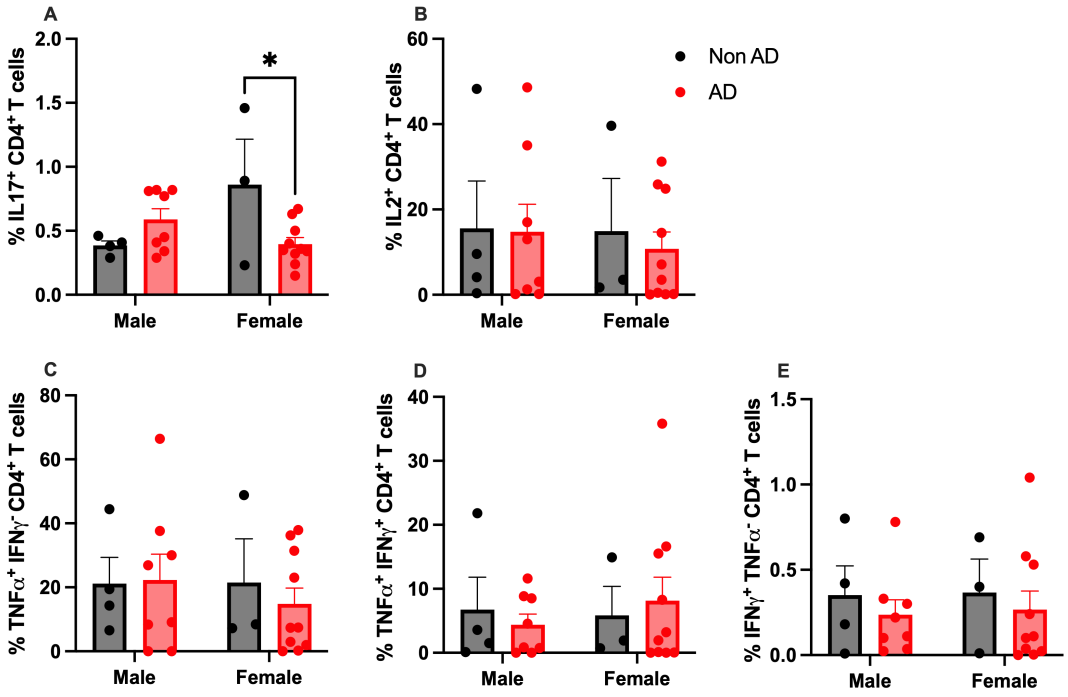


Figure 4.6 Analysis of Cytokine Expression in $CD4^+$ T cell populations of male and female non-Alzheimer's Disease/MCI and Alzheimer's Disease patients

*Flow cytometry analysis of the percentage of intracellular cytokines in $CD4^+$ T cells in PBMCs of male (N=4) and female (N=3) non-Alzheimer's Disease/MCI and male (N=8) and female (N=10) Alzheimer's disease patients. Cells were stimulated with phorbol 12-myristate 13-acetate (PMA; 50ng/mL), ionomycin (0.5μg/mL) and brefeldin A (5μg/mL) and incubated for 5 hours (37°C; 5% CO_2). Two-way ANOVA reported a significant sex x pathology interaction on $CD4^+$ IL-17 response (**A**, p=0.0091). There was a significant decrease in $CD4^+$ IL-17 cells in AD females versus non-AD females (p=0.0495). No statistically significant differences in the proportion of $CD4^+$ IL-2 (**B**) TNF-α (**C**), TNF-α IFNγ (**D**) or IFNγ (**E**) cells were reported. See Figure 4.2 for the gating strategy applied. Data, presented as mean +/- SEM, were analysed by two-way ANOVA and Šidák's post-hoc multiple comparison tests.*

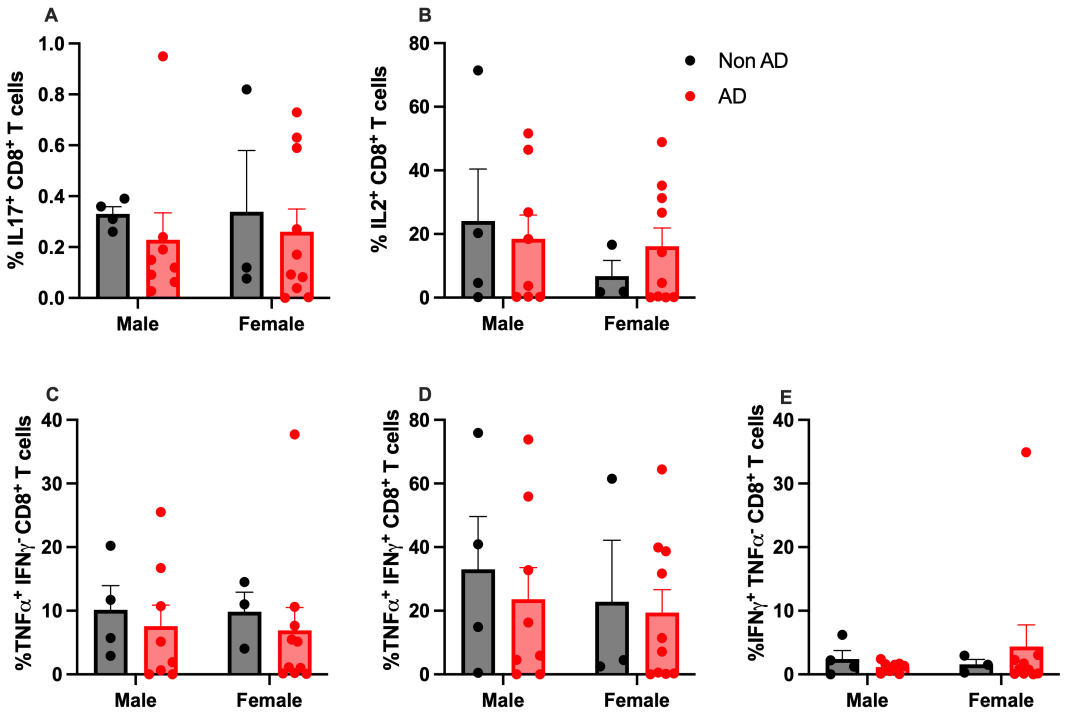


Figure 4.7 Analysis of Cytokine Expression in CD8⁺ T cell populations of male and female non-Alzheimer's Disease/MCI and Alzheimer's Disease patients

*Flow cytometry analysis of the percentage of intracellular cytokines in CD8⁺ T cells in PBMCs of male (N=4) and female (N=3) non-Alzheimer's Disease/MCI and male (N=8) and female (N=10) Alzheimer's disease patients. Cells were stimulated with phorbol 12-myristate 13-acetate (PMA; 50ng/mL), ionomycin (0.5μg/mL) and brefeldin A (5μg/mL) and incubated for 5 hours (37°C; 5% CO_2). No statistically significant differences in the proportion of CD8⁺ IL-17 (**A**), IL-2 (**B**) TNF-α (**C**), TNF-α IFNγ (**D**) or IFNγ (**E**) cells were reported. See Figure 4.2 for the gating strategy applied. Data, presented as mean +/- SEM, were analysed by two-way ANOVA and Šidák's post-hoc multiple comparison tests.*

Additionally, the effect of AD pathology and sex on CD4⁺ and CD8⁺ T cell activation (CD27 and CD28), senescence (CD57 and KLRG1) and regulatory T cells ($CD4^+FoxP3^+$ $CD127_{lo}$) (Tregs) were investigated using PBMCs from non-AD/MCI and AD patients (see **Figure 4.8** for gating strategy applied).

In non-AD and AD patients, there was no significant difference between the percentage of CD4⁺ T cells (**Figure 4.9 A**). There was no difference observed in the percentage of Tregs between non-AD and AD patients (**Figure 4.9 B**). In relation to T cell activation, there was a significant increase in $CD4^+$ $CD27^+$ $CD28^-$ T cells in AD compared to non-AD patients (**Figure 4.9 C**; p=0.0285). The proportion of $CD4^+$ $CD27^+$

CD28$^+$, CD4$^+$ CD28$^+$ CD27$^-$ or CD4$^+$ CD27$^-$ CD28$^-$ did not differ between non-AD/MCI and AD patients (**Figure 4.9 D-F**). Regarding T cell senescence, there was a slight decline observed in CD4$^+$ CD57$^+$ KLRG1$^-$ expression in AD patients compared to non-AD/MCI patients (**Figure 4.9 G**, p=0.0829) this however did not reach statistical significance. There was no difference observed between non-AD/MCI and AD patients in relation to CD4$^+$ CD57$^+$ KLRG1$^+$, KLRG1$^+$ or CD57$^-$ KLRG1$^-$ expression (**Figure 4.9 H-J**).

In non-AD/MCI and AD patients, there was no significant difference between the percentage of CD8$^+$ T cells, CD8$^+$ T cell activation (CD27 CD28) or CD8$^+$ T cell senescence (CD57 KLRG1) (**Figure 4.10 A-I**).

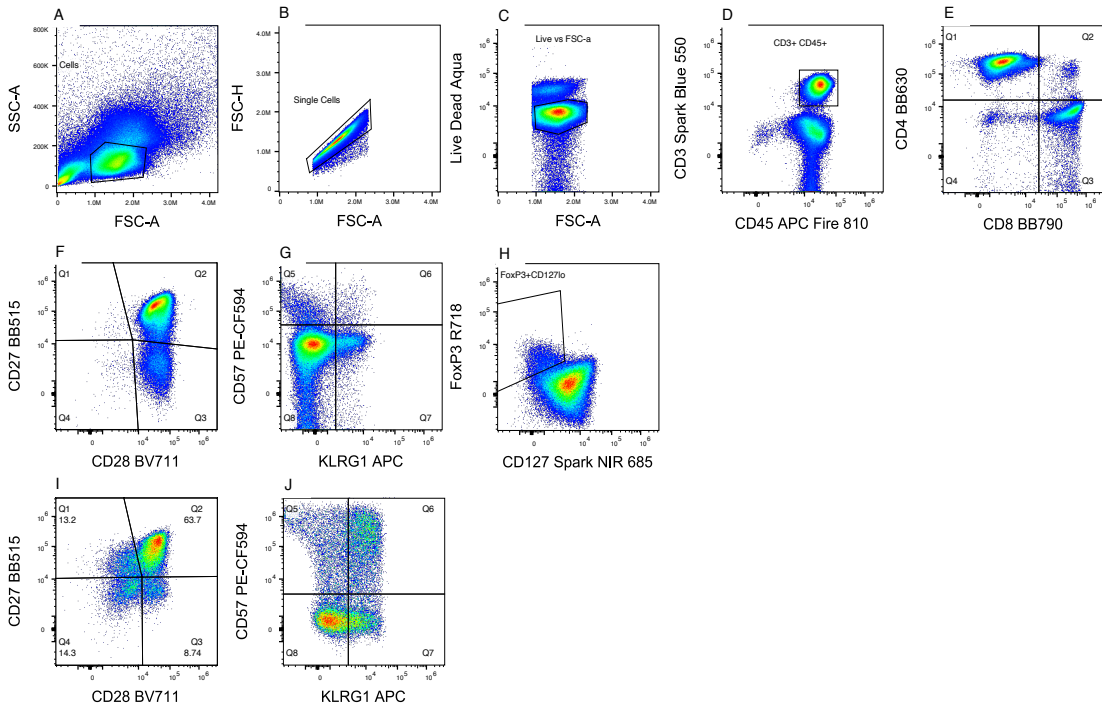


Figure 4.8 Outline of flow cytometry gating strategy for activation and senescent markers and regulatory T cells in peripheral blood mononuclear cells

*Lymphocytes were gated side scatter area (SSC-A) vs front scatter area (FSC-A) (**A**), single cells were gated FSC-H vs FSC-A (**B**) and live cells were gated on live dead stain vs FSC-A (**C**). T lymphocytes were gated CD3 vs CD45 (**D**) and T cells were gated on CD4 vs CD8 (**E**). CD27 and CD28 (**F and I**) were used to identify activated CD4$^+$ and CD8$^+$ T cells and CD57 and KLRG1(**G and J**) were used to identify senescence in CD4$^+$ and CD8$^+$ T cells. FoxP3$^+$ and CD127$_{lo}$ were used to identify regulatory CD4$^+$ Tregs (**H**). Gating was established using single stain and fluorescent minus one (FMO) controls.*

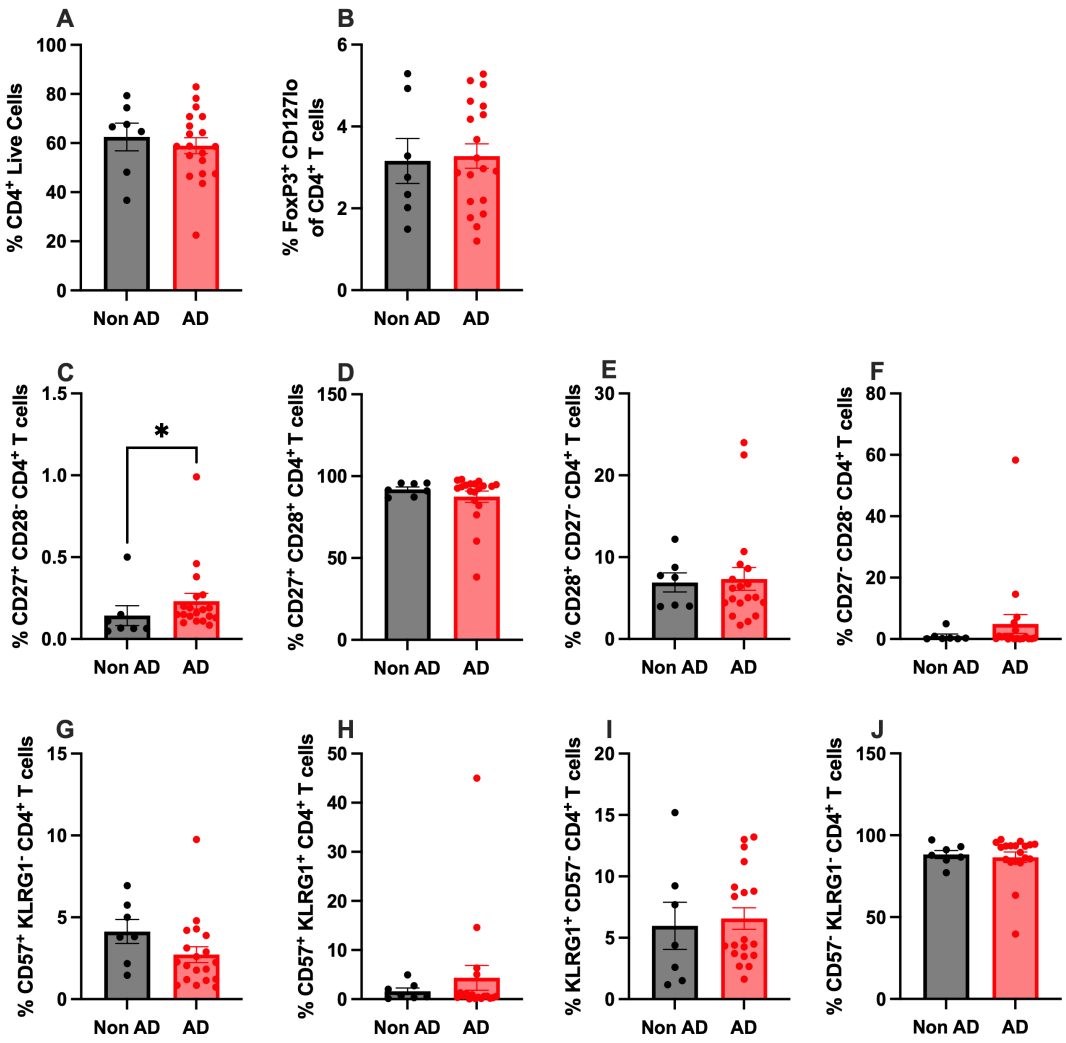


Figure 4.9 Analysis of activation, senescence and regulatory CD4⁺ T cells in non-Alzheimer's Disease/MCI and Alzheimer's Disease patients

*Flow cytometry analysis of the percentage of senescent and activated CD4⁺ T cells and regulatory T cells in PBMCs of non-Alzheimer's Disease/MCI (N=7) and Alzheimer's disease (N=19) patients. No statistically significant differences in the proportion of CD4⁺ Live cells (**A**) or regulatory T cells CD4⁺ FoxP3⁺ CD127$_{lo}$ (**B**) between non-AD and AD patients were reported. There was a significant increase in CD4⁺CD28⁺CD28⁻ T cells in AD patients compared to non-AD patients (**C**, *p=0.0285). No statistically significant differences in the proportion of activated T cells: CD27 (**C**) CD27 CD28 (**D**), CD28 (**E**), CD27⁻CD28⁻ (**F**), or senescent T cells: CD57 (**G**), CD57 KLRG1 (**H**), KLRG1 (**I**) and CD57⁻ KLRG1⁻ (**J**) were reported. See Figure 4.8 for the gating strategy applied. Data, presented as mean +/- SEM, were analysed by unpaired t-tests or Mann Whitney when appropriate for non-parametric data.*

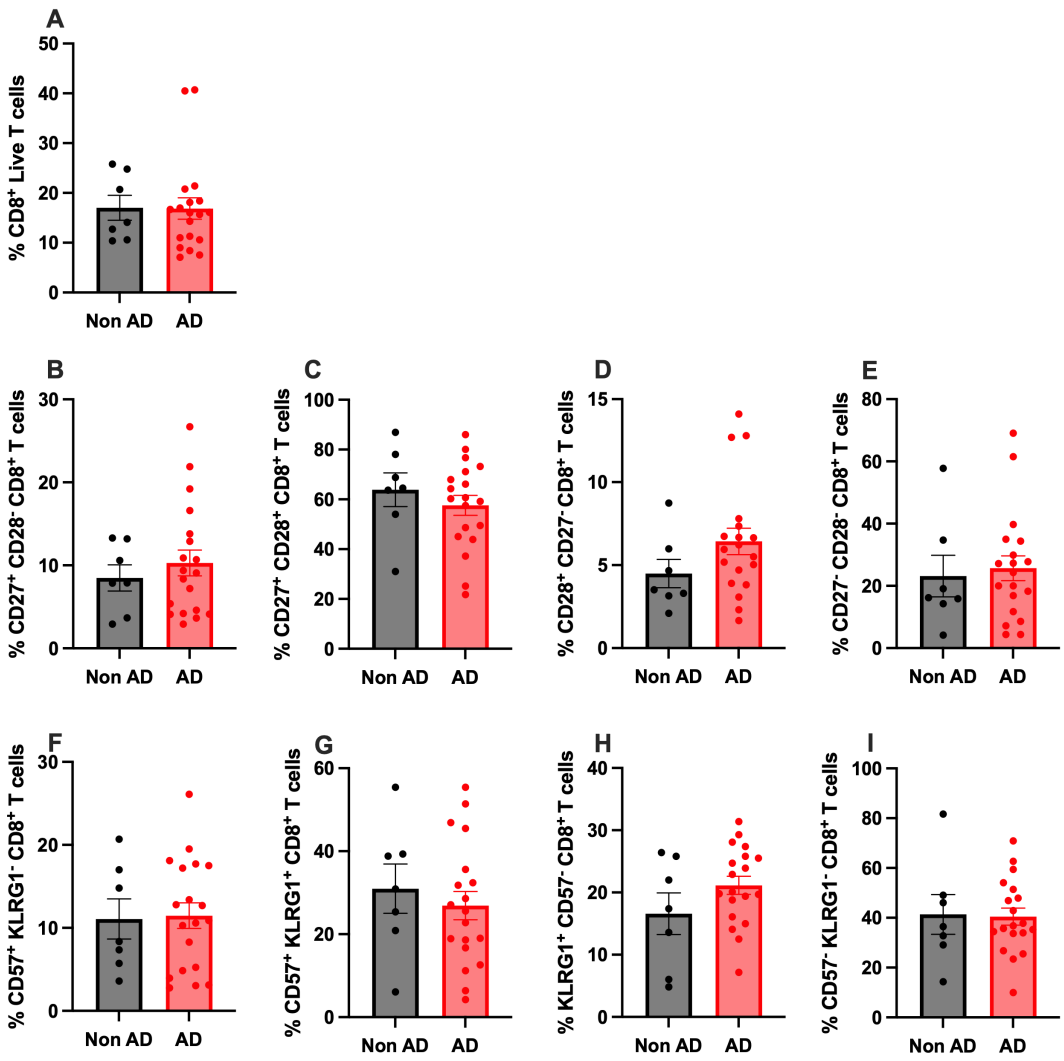


Figure 4.10 ***Analysis of activation and senescence in CD8⁺ T cells in non-Alzheimer's Disease/MCI and Alzheimer's Disease patients***

*Flow cytometry analysis of the percentage of senescent and activated CD8⁺ T cells in PBMCs of non-Alzheimer's Disease/MCI (N=7) and Alzheimer's disease (N=19) patients. No statistically significant differences in the proportion of CD8⁺ Live cells (**A**), activated T cells: CD27 (**B**) CD27 CD28 (**C**), CD28 (**D**), CD27⁻CD28⁻ (**E**), senescent T cells: CD57 (**F**), CD57 KLRG1 (**G**), KLRG1 (**H**) and CD57⁻ KLRG1⁻ (**I**) were reported. See Figure 4.8 for the gating strategy applied. Data, presented as mean +/- SEM, were analysed by unpaired t-tests or Mann Whitney when appropriate for non-parametric data.*

We next analysed the proportion of activated CD4⁺ T cells, senescent CD4⁺ T cells and Tregs segregated by sex in non-AD/MCI and AD patients (**Figure 4.11**). There was no effect of sex or AD pathology on the proportion of CD4⁺ cells, Tregs, CD4⁺ CD27⁺ CD28⁻, CD4⁺ CD27⁺ CD28⁺, CD4⁺ CD28⁺ CD27⁻ or CD4⁺ CD27⁻ CD28⁻ cells observed between any of the groups (**Figure 4.11 A-F**). Sex as a main effect trended

towards significance in relation to the proportion of $CD4^+$ $CD57^+$ $KLRG1^-$ cells (**Figure 4.11 G**, p=0.0693). Neither sex nor AD pathology impacted on the proportion of $CD4^+$ $CD57^+$ $KLRG1^+$, $CD4^+$ $KLRG1^+$ $CD57^-$ or $CD4^+$ $CD57^-$ $KLRG1^-$ cells (**Figure 4.11 H-J**).

T cell activation and senescence in $CD8^+$ T cells segregated by sex in non-AD/MCI and AD patients was also investigated (**Figure 4.12**). There was no effect of sex or AD pathology on the proportion of $CD8^+$ T cells, $CD8^+$ $CD27^+$ $CD28^-$, $CD8^+$ $CD27^+$ $CD28^+$, $CD8^+$ $CD28^+$ $CD27^-$ or $CD8^+$ $CD27^-$ $CD28^-$ cells observed (**Figure 4.12 A-E**). Two-way ANOVA reported a main effect of sex on $CD8^+$ $CD57^+$ $KLRG1^+$ T cells (**Figure 4.12 G**, p=0.0234). However, Šidák's post-hoc multiple comparison tests did not report a significant difference in any of the groups. There was no effect of sex or AD pathology observed on the proportion of $CD8^+$ $CD57^+$ $KLRG1^-$, $CD8^+$ $KLRG1^+$ $CD57^-$ or $CD8^+$ $CD57^-$ $KLRG1^-$ cells (**Figure 4.12 F, H and I**).

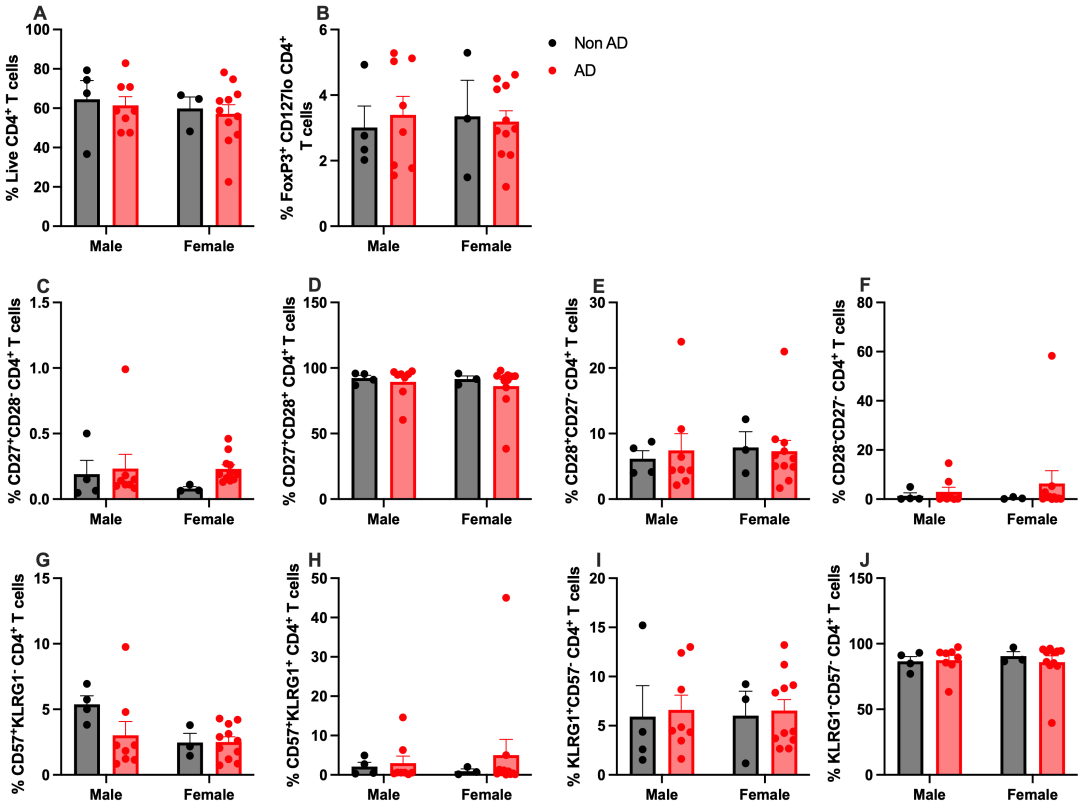


Figure 4.11 Analysis of activation, senescence and regulatory CD4⁺ T cells in male and female non-Alzheimer's Disease/MCI and Alzheimer's Disease patients

*Flow cytometry analysis of the percentage of senescent and activated CD4⁺ T cells and regulatory T cells in PBMCs of male (N=4) and female (N=3) non-Alzheimer's Disease/MCI and male (N=8) and female (N=11) Alzheimer's disease patients. No statistically significant differences in the proportion of CD4⁺ Live cells (**A**), regulatory T cells CD4⁺ FoxP3⁺ CD127$_{lo}$ (**B**), Activated T cells: CD27 (**C**) CD27 CD28 (**D**), CD28 (**E**), CD27⁻CD28⁻ (**F**) or senescent T cells: CD57 (**G**), CD57 KLRG1 (**H**), KLRG1 (**I**) or CD57⁻ KLRG1⁻ (**J**) were reported. See Figure 4.8 for the gating strategy applied. Data, presented as mean +/- SEM, were analysed by two-way ANOVA and Šidák's post-hoc multiple comparison tests.*

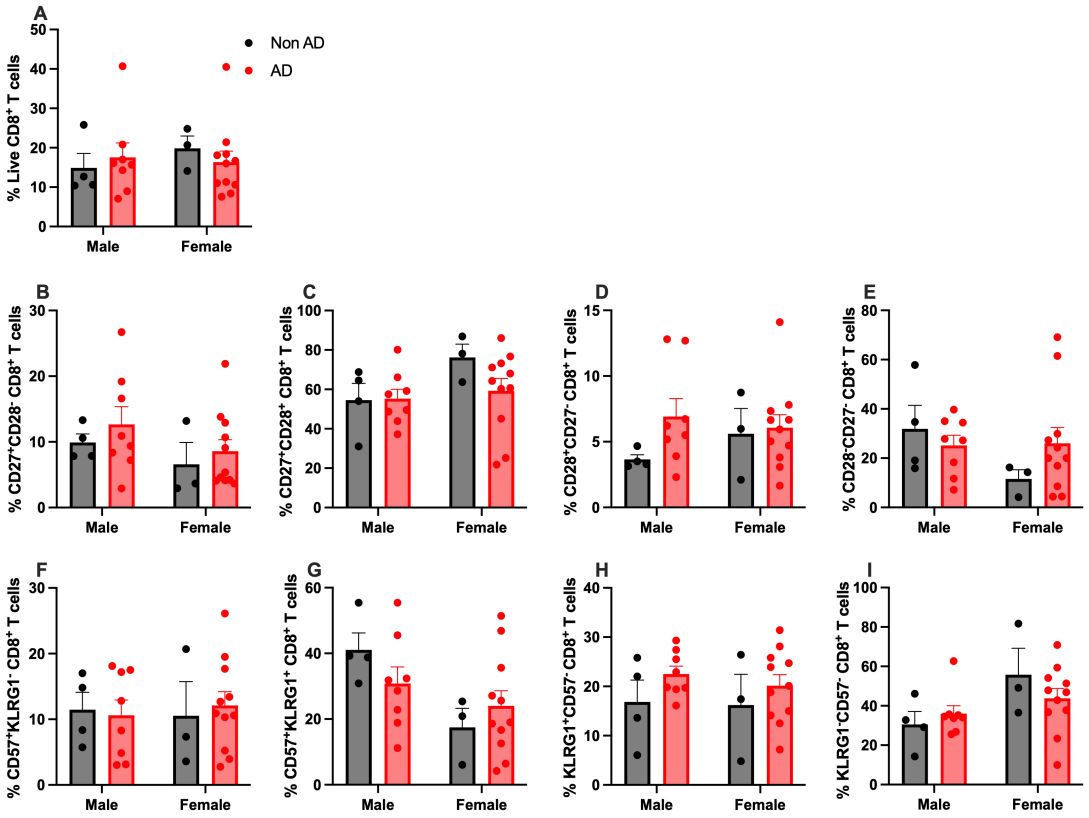


Figure 4.12 Analysis of activation and senescence CD8⁺ T cells in male and female non-Alzheimer's Disease/MCI and Alzheimer's Disease patients

*Flow cytometry analysis of the percentage of senescent and activated CD8⁺ T cells in PBMCs of male (N=4) and female (N=3) non-Alzheimer's Disease/MCI and male (N=8) and female (N=11) Alzheimer's disease patients. No statistically significant differences in the proportion of CD8⁺ Live cells (**A**), Activated T cells: CD27 (**B**) CD27 CD28 (**C**), CD28 (**D**), CD27⁻CD28⁻ (**E**) or senescent T cells: CD57 (**F**), KLRG1 (**H**) or CD57⁻ KLRG1⁻ (**I**)* were reported. Two-way ANOVA reported a main effect of sex on CD8⁺ CD57⁺ KLRG1⁺ T cells (**G**, p=0.0234). However Šidák's post-hoc multiple comparison tests did not report a significant difference in any of the groups. *See Figure 4.8 for the gating strategy applied. Data, presented as mean +/- SEM, were analysed by two-way ANOVA and Šidák's post-hoc multiple comparison tests.*

Summary of results obtained while assessing the impact of sex and the AD pathology on $CD4^+$ and $CD8^+$ T cell populations:

- Neither sex nor AD pathology affects the proportion of $CD4^+$ and $CD8^+$ T cells in PBMCs.
- There is a significant decrease in $CD4^+$ IL-17 cells in AD females compared to non-AD females. This not observed in the male cohort of this study.
- There is a significant increase in $CD4^+$ $CD27^+$ $CD28^-$ cells in AD compared to non-AD/MCI patients which is not reported when cohorts are separated by sex.
- Neither sex nor AD pathology affects the proportion of $CD8^+$ cytokine response, senescent or activated $CD8^+$ T cells.

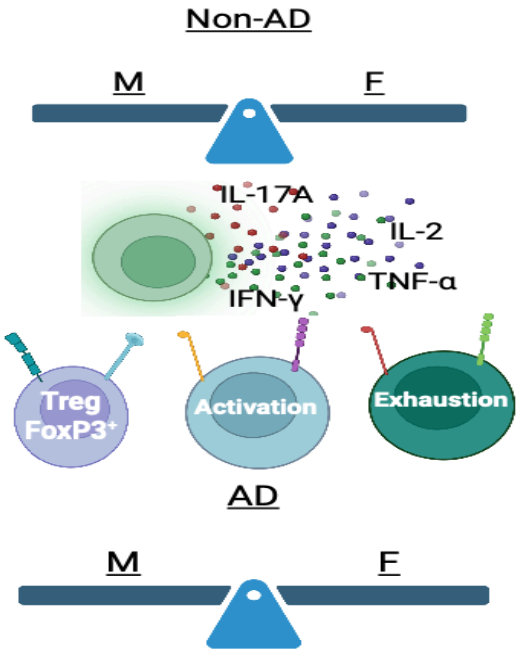


Figure 4.13 Abstract summary of flow cytometry results investigating sex differences in cytokine and T cell subsets in male and female non-AD and AD patients' PBMCs

In non-AD male and female patients, there was no significant increase or decrease in $CD4^+$ and $CD8^+$ cytokine response, in regulatory T cells, in activated T cells or exhausted T cells. In AD male and female patients, there was no significant increase or decrease in $CD4^+$ and $CD8^+$ cytokine response, in regulatory T cells, in activated T cells or exhausted T cells.

4.3.2 Investigation of cytokines released by stimulated peripheral blood mononuclear cells and cerebrospinal fluid in non-Alzheimer's/MCI and Alzheimer's disease patients using meso-scale discovery

Next, the effect of AD pathology and sex on cytokine concentrations were investigated in PBMCs and CSF from non-AD/MCI and AD patients using meso-scale discovery (MSD). PBMCs were stimulated with anti-CD3 (1µg/mL) and anti-CD28 (0.5µg/mL) for 5 days. The supernatant was then collected for MSD analysis. CSF was collected by Dr. Adam Dyer, Dr. Helena Dolphin and Dr. Sarah Fullam during the patient's lumbar puncture for MSD analysis.

Initially, we investigated potential differences in cytokine concentrations secreted from PBMCs of non-AD/MCI and AD patients (**Figure 4.14**). There was no difference observed in PBMCs cytokine secretion from non-AD and AD patients (**Figure 4.14 A-L**). We then investigated potential differences in male and female non-AD/MCI and AD patients cytokine concentrations from PBMCs (**Figure 4.15**). The effect of sex or AD pathology on PBMCs cytokine secretion in male or female non-AD/MCI and AD patients was not observed (**Figure 4.15 A-K**).

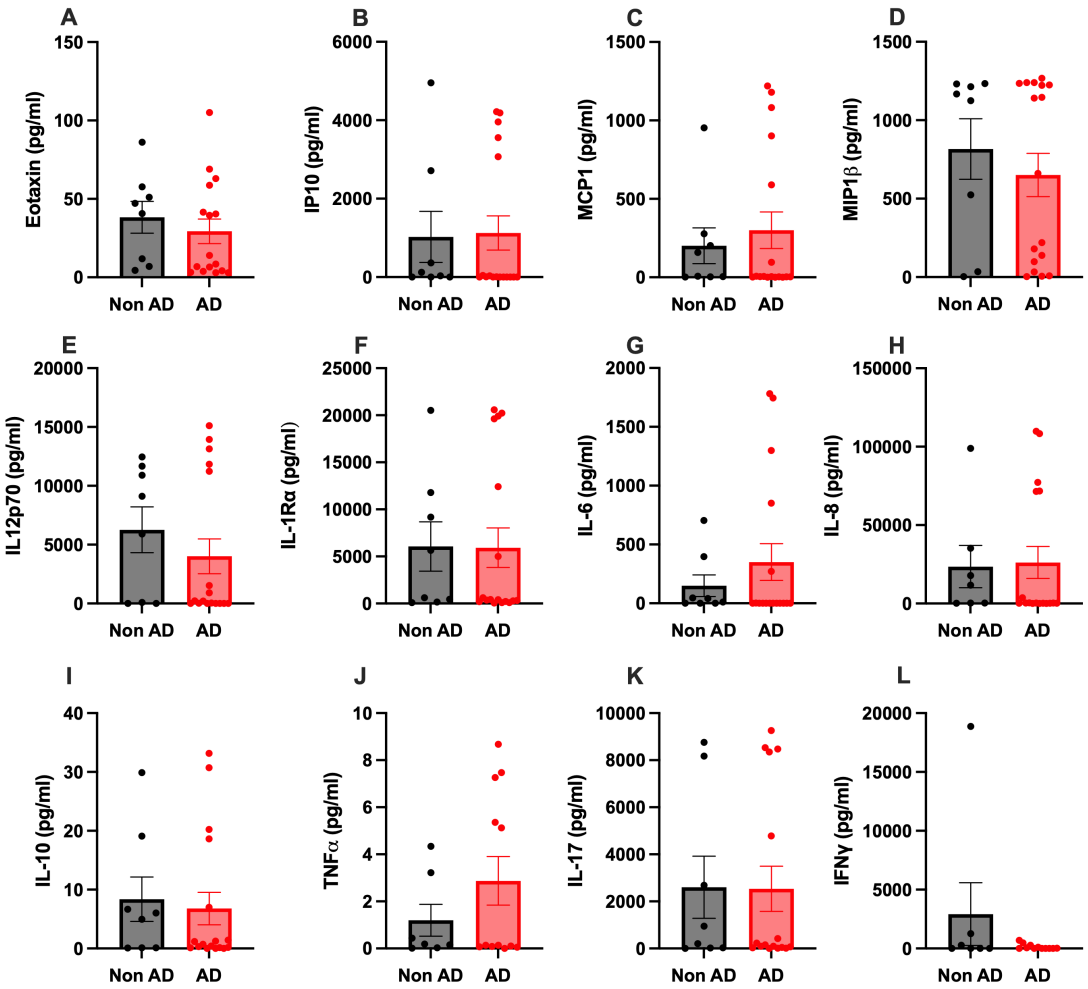


Figure 4.14 MSD Analysis of cytokines released by stimulated peripheral blood mononuclear cells in non-Alzheimer's Disease/MCI and Alzheimer's Disease patients

*Analysis of cytokine protein expression in PBMCs of non-Alzheimer's Disease/MCI (N=7-8) and Alzheimer's disease (N=12-17) patients by meso-scale discovery. PBMCs were stimulated with anti CD3 (1µg/mL) and anti-CD28 (0.5µg/mL) and incubated for 5 days (37°C; 5% CO_2). Expression of Eotaxin (**A**), IP10 (**B**), MCP1 (**C**), MIP1β (**D**), IL12p70 (**E**), IL-1Rα (**F**), IL-6 (**G**), IL-8 (**H**), IL-10 (**I**), TNF-α (**J**), IL-17 (**K**) and IFNγ (**L**) was reported. Data, presented as mean +/- SEM, were analysed by unpaired t-tests or Mann Whitney when appropriate for non-parametric data*

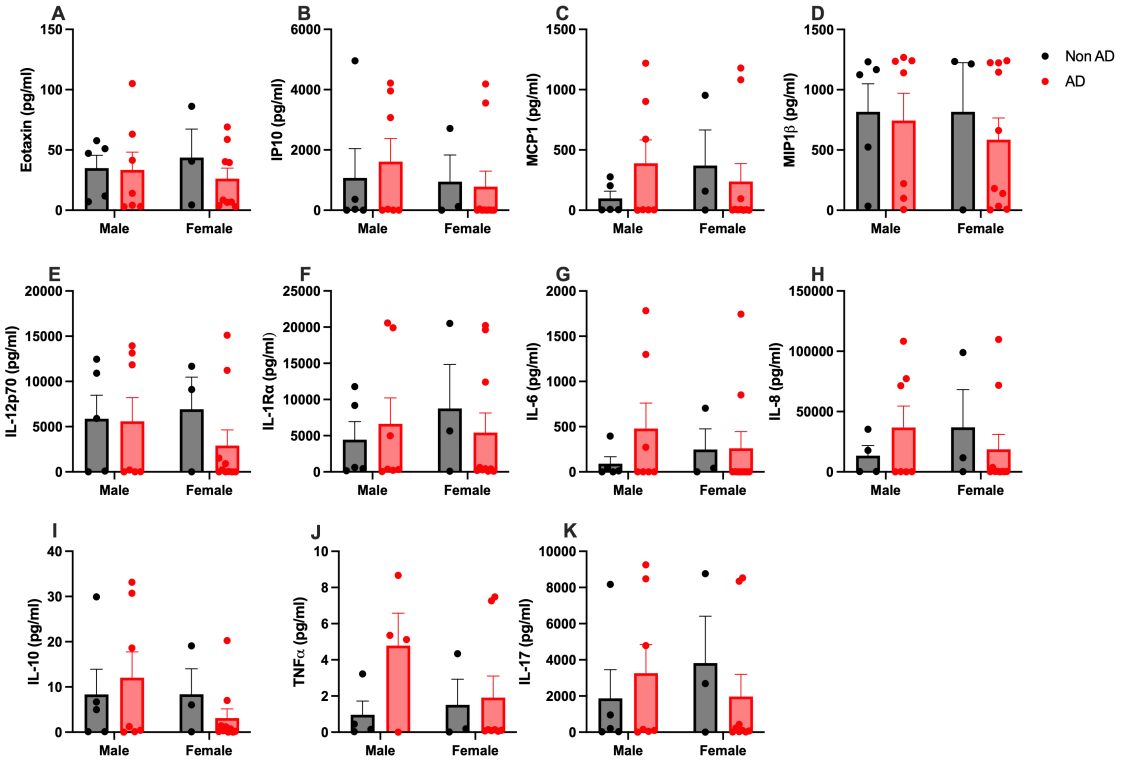


Figure 4.15 MSD Analysis of cytokines released by stimulated peripheral blood mononuclear cells in male and female Non-Alzheimer's Disease/MCI and Alzheimer's Disease patients

*Analysis of cytokine protein expression in PBMCs of male (N=3-5) and female (N=3) non-Alzheimer's Disease/MCI and male (N=4-7) and female (N=8-10) Alzheimer's disease patients by meso-scale discovery. PBMCs were stimulated with anti CD3 (1µg/mL) and anti-CD28 (0.5µg/mL) and incubated for 5 days (37°C; 5% CO_2). Expression of Eotaxin (**A**), IP10 (**B**), MCP1 (**C**), MIP1β (**D**), IL12p70 (**E**), IL-1Rα (**F**), IL-6 (**G**), IL-8 (**H**), IL-10 (**I**), TNF-α (**J**) and IL-17 (**K**) was reported. Please note IFN-γ is not reported due to low sample numbers. Data, presented as mean +/- SEM, were analysed by two-way ANOVA and Šidák's post-hoc multiple comparison tests.*

We also investigated changes in cytokine concentrations in non-AD/MCI and AD patients' CSF samples (**Figure 4.16**). Eotaxin concentration in CSF trended toward an increase in AD patients compared to non-AD/MCI patients but did not reach significance (**Figure 4.16 A**, p=0.1056). IP10 and MCP1 CSF concentration did not differ between non-AD/MCI and AD patients (**Figure 4.16 B and C**). There was a significant increase in MIP1β concentration in AD compared to non-AD/MCI patients (**Figure 4.16 D**; p=0.0421). There was no significant changes observed in IL12p70 concentration (**Figure 4.16 E**). IL-1Rα concentration trended toward an increase in AD compared to non-AD/MCI patients, however this did not reach significance (**Figure 4.16 F**, p=0.0702). Changes in IL-6, IL-8, IL-10 or IL-17 concentration were not

observed between non-AD/MCI and AD patients (**Figure 4.16 G-J**). There was a significant decrease in IFN-γ concentration in AD compared to non-AD/MCI patients (**Figure 4.16 K**; p=0.0036).

We then separated non-AD/MCI and AD groups by sex to further investigate any potential sexual dimorphisms in CSF cytokine concentrations **(Figure 4.17**). The effect of AD pathology or sex was not observed in Eotaxin, IP10 or MCP1 CSF concentration (**Figure 4.17 A-C**). Two-way ANOVA reported a significant main effect of AD pathology on MIP1β concentration (**Figure 4.17 D**; p=0.0409), however no significance between male and female non-AD and AD cohorts were reported by Šidák's post-hoc multiple comparison tests. The effect of sex or AD pathology was not observed in IL12p70 CSF concentration (**Figure 4.17 E**). Two-way ANOVA reported a significant effect of the interaction of sex *x* pathology on IL-1Rα concentration (**Figure 4.17 F**; p=0.0149) with a significant increase in IL-1rα concentration in AD males compared to non-AD/MCI males **(Figure 4.17 F**; p=0.0125). IL-1rα CSF concentration trended toward a decrease in AD females compared to AD males however significance was not reached (**Figure 4.17 F**; p=0.0878). Two-way ANOVA revealed a significant effect of sex *x* pathology on IL-6 concentration (**Figure 4.17 G**; p=0.0052) with a significant decrease in IL-6 secretion observed in AD females compared to non-AD/MCI females (**Figure 4.17 G**; p=0.0121). The change in IL-6 concentration was not observed in the male cohort. The interaction of sex *x* AD pathology in IL-8 CSF concentration trended towards significance (**Figure 4.17 H**, p=0.103). IL-10 secretion (**Figure 4.17 J**) did not observe any alterations in concentration between male and female non-AD/MCI and AD patients. The effect of AD pathology on IFN-γ concentration was observed (**Figure 4.17 J**; p=0.0272), with a significant decrease in IFN-γ concentration in male AD compared to male non-AD/MCI patients (**Figure 4.17 J**; p=0.0362).

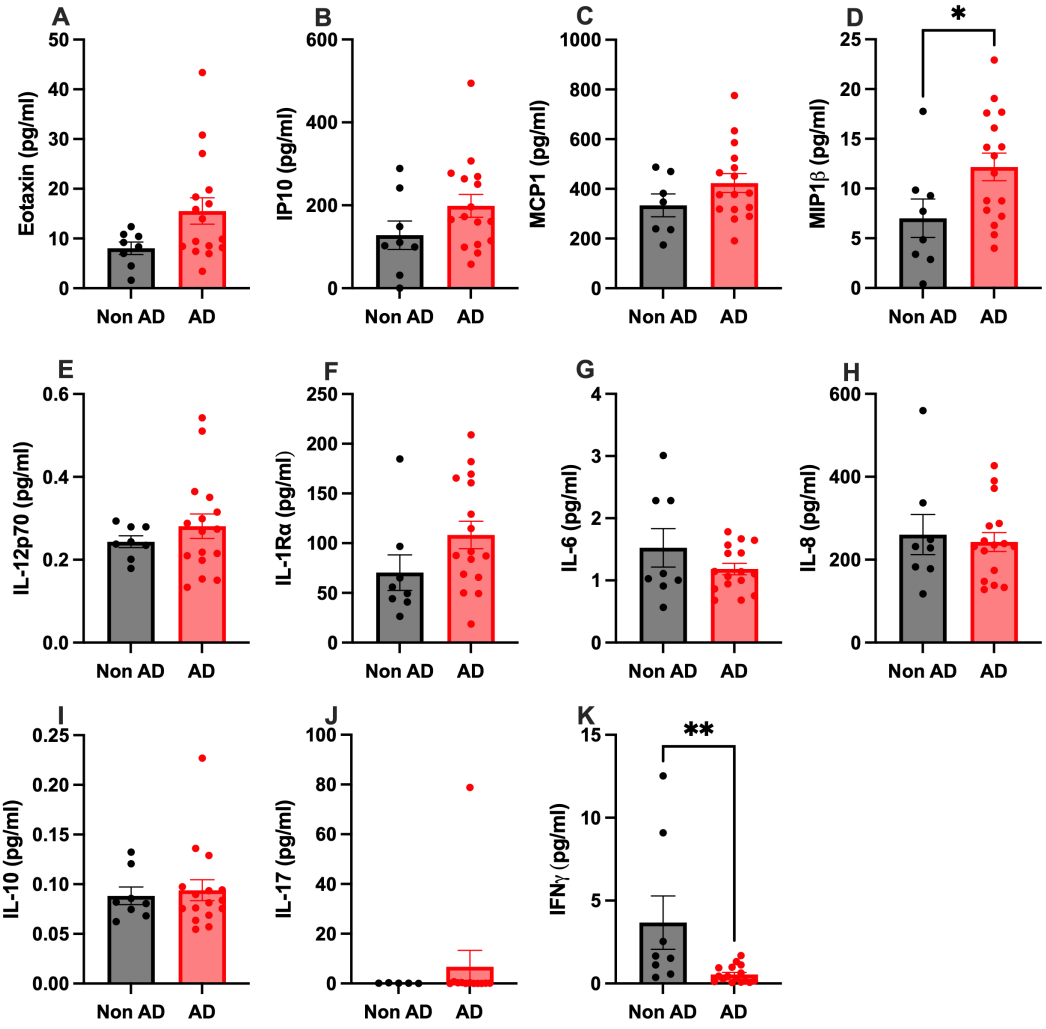


Figure 4.16 MSD Analysis of cytokines in cerebrospinal fluid of non-Alzheimer's Disease/MCI and Alzheimer's Disease patients

*Analysis of cytokine concentration in cerebrospinal fluid (CSF) of non-Alzheimer's Disease/MCI (N=5-8) and Alzheimer's disease (N=12-16) patients by meso-scale discovery. Expression of Eotaxin (**A**), IP10 (**B**), MCP1 (**C**), MIP1β (**D**), IL12p70(**E**), IL-1Rα(**F**), IL-6 (**G**), IL-8 (**H**), IL-10 (**I**), IL-17 (**J**) and IFNγ (**K**) was reported. There was a significant increase in MIP1β (**D**) in AD patients (*p=0.04). There was a significant decrease in IFNγ (**K**) in AD patients (**p=0.0036). Please note TNF-α was not reported due to concentration levels being undetectable. Data, presented as mean +/- SEM, were analysed by unpaired t-tests or Mann Whitney when appropriate for non-parametric data.*

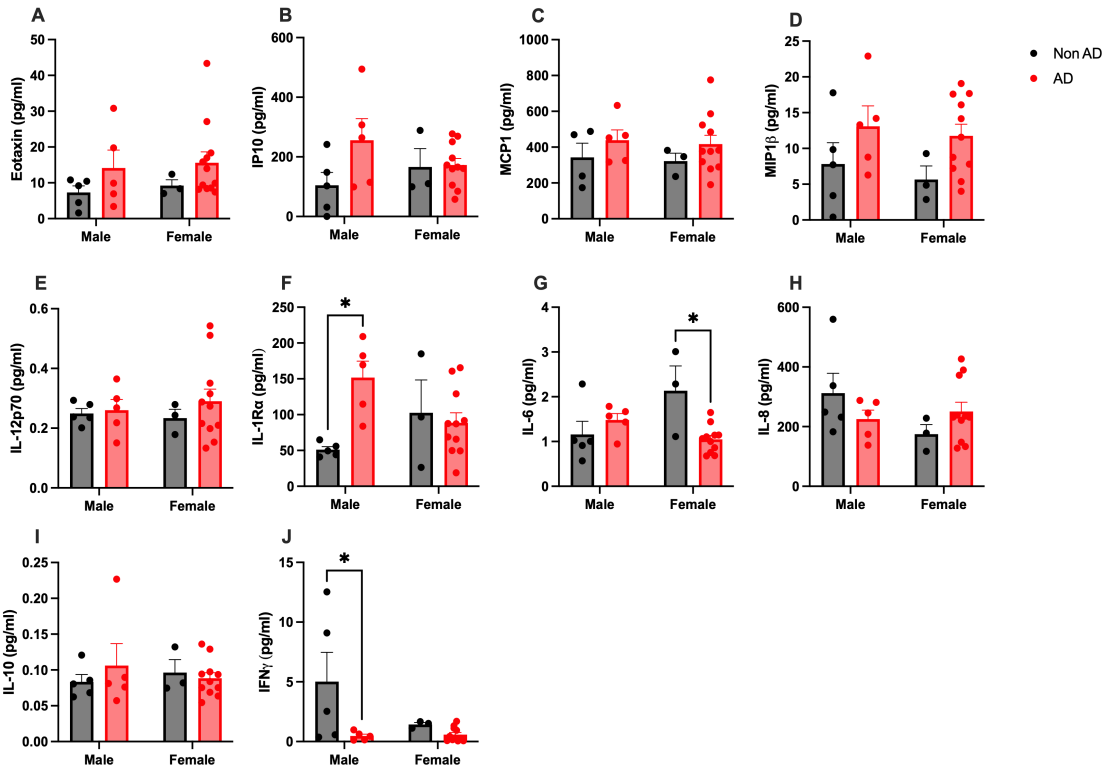


Figure 4.17 MSD Analysis of cytokines in cerebrospinal fluid of male and female non-Alzheimer's Disease/MCI and Alzheimer's Disease patients

*Analysis of cytokine concentration in CSF of male (N=4-5) and female (N=3) non-Alzheimer's Disease/MCI and male (N=5) and female (N=11-12) and Alzheimer's disease patients by meso-scale discovery. Expression of Eotaxin (**A**), IP10 (**B**), MCP1 (**C**), MIP1β (**D**), IL12p70 (**E**), IL-1Rα (**F**), IL-6 (**G**), IL-8 (**H**), IL-10 (**I**), and IFNγ (**J**) was reported. Two-way ANOVA reported a significant main effect of AD pathology on MIP1β concentration (**D**; p=0.0409). Šidák's post-hoc multiple comparison tests reported no significance between male and female non-AD and AD cohorts for MIP1β concentration. In male non-AD and AD patients, two-way ANOVA reported a significant effect of pathology on and IL-rα (**F**; p=0.0149) and IFN-γ (**J**; p=0.0272) concentration. Šidák's post-hoc multiple comparison tests reported a significant increase in IL-1rα (**F**) (*p=0.0125) and a significant decrease in IFNγ (**J**) (*p=0.0362) in AD males. Two-way ANOVA reported a significant effect of sex x pathology on IL-6 concentration (**G**; p=0.0052). There was a significant decrease in IL-6 (**G**) in AD females compared to non-AD females (*p=0.0121). Please note TNF-α was not reported due to concentration levels being undetectable and IL-17 was not reported due to low sample numbers. Data, presented as mean +/- SEM, were analysed by two-way ANOVA and Šidák's post-hoc multiple comparison tests.*

Summary of results obtained while assessing the impact of sex and the AD pathology on CSF and PBMC cytokine concentration

- Neither sex nor AD pathology affects the concentration of cytokines present in PBMCs of male and female non-AD/MCI and AD patients.
- In the CSF;
- There is a significant increase in MIP1β concentration in AD compared to non-AD/MCI patients. This is not observed once patients were separated by sex.
- There is a significant decrease in IFN-γ concentration in AD compared to non-AD/MCI patients. This is observed specifically in male AD patients, but not female AD patients once separated by sex.
- There is a significant increase in IL-1Rα concentration in AD males compared to non-AD/MCI males. This is not observed in the female cohort of the study.
- There is a significant decrease in IL-6 concentration in AD females compared to non-AD/MCI females. This is not observed in the male cohort of this study.

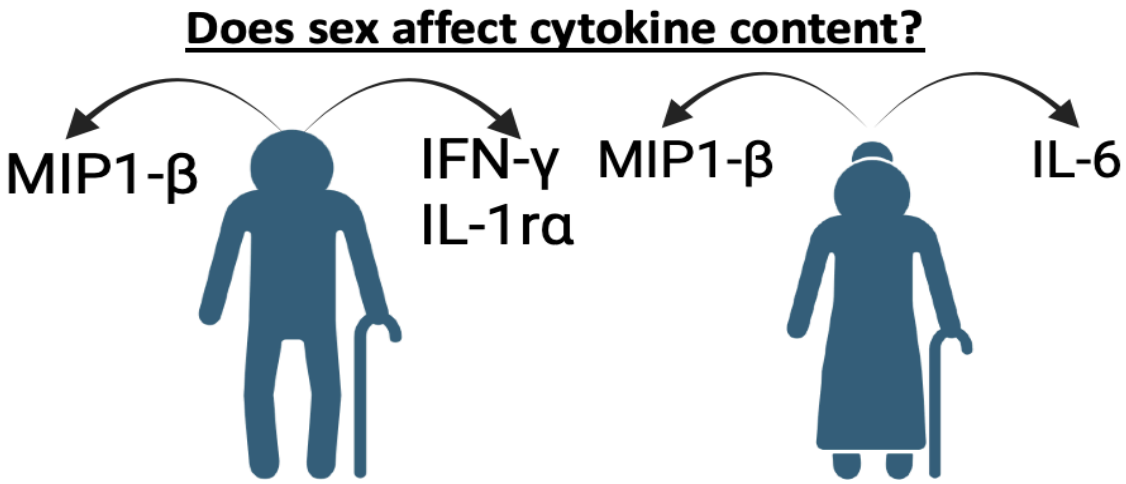


Figure 4.18 Abstract summary of sex differences reported in the cytokines present in the CSF of AD patients

***Males**: Using MSD assays, the concentration of MIP1-ß and IL-1Rα were significantly increased in the CSF of male AD patients. The concentration of IFN-γ was significantly decreased in the CSF of male AD patients.*

***Females**: Using MSD assays, the concentration of MIP1-ß was significantly increased in the CSF of female AD patients. The concentration of IL-6 was significantly decreased in the CSF of female AD patients. This indicates sexual dimorphic cytokine responses in AD patients.*

4.4 Discussion

One of the aims of this study was to elucidate the potential sexual bias in $CD4^+$ and $CD8^+$ T cell populations in response to AD pathology through the analysis of cytokine expressions and proportions of activated, senescent and regulatory T cells present in PBMCs.

Previous work on T cell cytokine responses from AD patients PBMCs have reported increases in Th1 cells and $CD8^+$ IFN-γ T cells compared to healthy controls (Zhang and Niu, 2022, Li et al., 2023, Gate et al., 2020). In our analysis however we found no differences in $CD4^+$ and $CD8^+$ cytokine response between non-AD/MCI and AD patients. Therefore to include an age match group that has no cognitive impairments and considered healthy would be useful to see if this alteration occurs prior to AD symptoms and diagnosis in this cohort.

Previous studies have also reported increases in Th17 cells in PBMCs isolated from MCI AD patients compared to healthy controls (Oberstein et al., 2018, Zeng et al., 2022, Li et al., 2023, Cao et al., 2023). It has been reported using BV2 murine microglial cell line that IL-17A can enhance TNF-α secretion by stimulating TLR4 signalling pathway in microglia and exacerbate neuroinflammation indicating a detrimental role for IL-17 in AD progression (Cao et al., 2023). Additionally, Th-17 cells have been reported to correlate with cognitive impairment in AD patients (Zeng et al., 2022).

However, it is surprising when sex is introduced as a second biological variable we report a significant decrease in $CD4^+$ $IL\text{-}17^+$ in AD females compared to non-AD females which is not observed in males. The suggestion of a “blunted” Th17 response in females with MCI but not males has been reported by Bachstetter and colleagues previously. Furthermore, low Th17 response was observed to correlate with low Montreal cognitive assessment scores only in women and not men (Bachstetter et al., 2023). In relation to other plasma biomarkers, the correlation between low levels of Th17 and low $A\beta_{40}$ plasma levels was only observed in MCI females (Bachstetter et al., 2023). It was suggested that the decrease in Th17 population in cognitively impaired females could be explained by the significant decrease in $CD4^+$ T cells (Bachstetter et al., 2023). As we saw no significant difference in the proportion of

$CD4^+$ T cells present in males or females with AD the lower Th17 response reported in our study cannot be explained by an overall decrease in $CD4^+$ T cells. Our study adds on to the initial observation of a "blunted" Th17 response in MCI females as we now report this occurs in AD females and not AD males.

The cause of this decrease in Th17 response was not identified in our study. Interestingly, GFAP plasma levels negatively correlated with Th17 response specifically in females (Bachstetter et al., 2023) therefore it would be helpful to assess the concentration of GFAP along with other biomarkers (NfL, $A\beta_{40}$, $A\beta_{42}$, p-tau) in both plasma and the CSF in our study to elucidate a potential relationship between Th17 response and biomarkers. Additionally, we saw no difference in male or female Treg proportions in our study, therefore the decline of Th17 cells in AD females cannot be explained by the proportion of Tregs present. A future experiment consisting of isolating Tregs from PBMCs of AD males and females to assess their immunosuppressive function on Teff or Th17 cells specifically could assist in elucidating the blunted Th17 response reported. Furthermore, this could give us an insight into the potential sex difference in suppressive activity of Tregs and help explain what mechanisms are at play that cause this Th17 "blunted" response in females. Overall, the role of Th17 in relation to AD progression is not clearly defined and therefore the consequences of this female specific decreased Th17 response is not totally understood and requires further investigation. It does however highlight once again that the immune response to AD is not homogenous between the sexes. It also highlights the importance of investigating sex as a second biological variable as the alteration in Th17 response would have been omitted if we only separated the patients into non-AD and AD groups and disregarded sex.

In relation to senescence and activation in T cells, previous studies have reported alterations in expression of markers such as significant increases in $CD8^+$ $CD27^-$ T_{EMRA} (Gate et al., 2020), $PD1^+$ $CD57^+$ $CD8^+$ T_{EMRA} (van Olst et al., 2024) in MCI and AD patients compared to controls. Analysis of senescent and activation profiles of T cells from our study, reported an increase in $CD4^+CD27^+CD28^-$ compared to non-AD patients. This could indicate a weaker immune response compared to non-AD patients and a reduced ability to proliferate (Moro-García et al., 2013).

Furthermore, the loss of CD28 expression on $CD4^+$ T cells has been reported to be altered with AD progression as only AD patients with severe AD had a significant decrease in $CD4^+$ $CD28^+$ T cells compared to age matched controls (Busse et al., 2022). Any AD cohort prior to severe AD did not have altered CD28 expression compared to control highlighting the modulatory response of T cells as AD progresses (Busse et al., 2022). Additionally, loss of $CD4^+$ $CD28^+$ expression correlated with total tau present in the CSF in a stage dependent manner with mild AD patients possessing a stronger correlation with total tau levels compared to moderate AD patients (Busse et al., 2022). In moderate AD patients it was reported that a higher proportion of CD4 CD28 T cells corelated with a greater $Aß_{40}/Aß_{42}$ ratio in the CSF (Busse et al., 2022). Taken together these results illustrate the modulatory effect of T cells in AD progression.

However, Buuse and colleagues did not categorise CD27 and CD28 expression on T cells so a more complete picture is required to understand the consequences of changes in CD27 and CD28 expression on T cells as the disease progresses. Therefore, it would be useful to map out the changes in $CD4^+$ and $CD8^+$ CD27 CD28 expression from the prodromal stage of AD all the way to severe AD diagnosis and how this correlates with biomarkers in the CSF and plasma to pinpoint when modulations occur and comprehend the consequences of such alterations in relation to overall inflammatory responses in AD.

PD-1 is known to play a role in T cell inhibition prior to antigen stimulation (Chikuma et al., 2009), thus it would be important to include the marker PD-1 in future experiments as it has been implicated in AD T cell response (van Olst et al., 2024). Furthermore, as TEM and TEMRA T cell subsets have been reported to be altered in AD patients (Wang et al., 2024b, Gate et al., 2020, van Olst et al., 2024) it would be helpful to investigate these T cell subsets with regards to sex as a second variable in this study by adding markers such as CD45RA and CD45RO.

Another aim of this study was to investigate the effect of AD pathology and sex on cytokine concentrations present in the CSF. Our findings reported AD specific changes with an increase in MIP1ß (also known as CCL4 (Maurer and von Stebut, 2004)) and a decrease in IFN-γ in the CSF of patients with AD.

Interestingly, in other studies MIP1ß CSF levels have been reported to be increased in patients with idiopathic normal pressure hydrocephalus from neurodegenerative diseases compared to healthy controls (Braun et al., 2023). Additionally, primary cultures of human brain micro vessel endothelial cells (HBMEC) following MIP1ß treatment reported an increase in CCR5 expression, induced P38 mitogen-activated kinase known to regulate neurovascular function and decreased tight junction protein ZO-1 expression indicating a role for MIP1ß in BBB permeability (Estevao et al., 2021). Conversely in AD studies, using plasma albumin quotient (Qalb) to assess BBB integrity, MCI and early AD patients with higher MIP1ß expression had a negative correlation with BBB permeability (Bruno et al., 2024). Furthermore, MIP1ß was reported to positively correlate with cognitive status in AD patients indicating a potentially beneficial role of MIP1ß in the CSF of AD patients (Taipa et al., 2019). Our result therefore could indicate a harmful or protective role for MIP1ß in BBB integrity and cognition in AD. When segregated by sex MIP1B was not strongly associated with one sex which would imply that it is related to AD pathology and not influenced by sex.

The decrease in IFN-γ seen in the CSF of AD patients, was only reported in male AD patients once segregated by sex. Differences in IFN-γ levels between non AD and AD female patients were minimal. This would indicate a potential sexual dimorphic response to AD. IFN-γ has been reported to have an integral role in T cell migration across the choroid plexus (Kunis et al., 2013). In the APP Tg CRND8 AD mouse model, IFN-γ was suggested to improve Aß clearance and enhanced expression of MHC-II and CD11c in microglia indicating a beneficial role in AD pathogenesis (Chakrabarty et al., 2010). However, another study in the IFN-γ KO mouse model, reported that the presence of IFN-γ led to cognitive decline and neuronal impairment (Monteiro et al., 2016). Additionally, in HBMEC studies, IFN-γ has been reported to disrupt BBB integrity due to rapid tight junction disassembly (Rahman et al., 2018). Conversely, IFN-γ levels were reported to negatively correlate with cognitive decline over one year in AD patients (Taipa et al., 2019). Thus the decrease observed in our study could indicate an improved BBB integrity, a reduction in T cell infiltration into the brain or reduced cognitive decline in AD males.

Additionally, the cytokines IL-1Rα and IL-6 were observed to respond to AD in a sexually dimorphic manner in this study. IL-1Rα significantly increased in the CSF of AD male patients compared to non-AD males, which was not observed in females. An increase in IL-1Rα CSF levels has been previously reported in AD patients compared to healthy controls (Taipa et al., 2019, Wang et al., 2021b), however sexual dimorphic observations were not reported. Furthermore, IL-1rα was reported to positively correlate with cognitive status in AD patients (Taipa et al., 2019) thus the results we report here imply a potentially beneficial role of IL-1rα in the CSF of male AD patients.

In our study IL-6 is significantly decreased in the CSF of AD females compared to non-AD females, this alteration is not observed in male patients. As we only obtained n=3 for AD females these findings were preliminary and required more samples in this cohort to confirm this observation. IL-6 has been reported to exacerbate AD pathology in both human and animal studies. In previous work, IL-6 CSF concentrations in AD patients have correlated with neuronal damage marker NfL (Plantone et al., 2025). Additionally, plasma IL-6 levels negatively correlated with MMSE scores (Lyra e Silva et al., 2021). Female patients in the prodromal phase of AD (CSF $A\beta_{42}/A\beta_{40}$ positive score) that have an increased risk of developing AD, reported a significant decrease in IL-6 compared to males (Knudtzon et al., 2025). Therefore, our reported decrease in IL-6 concentration aligns with previous reports. The consequences of this decrease however requires further investigation to understand it's contribution to AD pathogenesis.

To achieve a better understanding of the implications of changes in cytokine concentrations it would be important to assess the correlation of MIP1ß, IFN-γ, IL-1rα and IL-6 with $A\beta_{42}$,p-tau, GFAP and NfL CSF concentrations along with cognitive scores of patients in male and female patients.

Overall, differences in cytokine response were more apparent in CSF samples compared to PBMCs isolated from AD patients. As the PBMCs were stimulated with anti-CD3 and anti-CD28 a direct comparison between baseline CSF and PBMC cytokine release is not appropriate. It would be helpful to include plasma analysis to

understand the baseline cytokine concentration in patients and if this correlates with CSF cytokine concentrations.

Additionally, a more distinct difference in the CSF rather than the blood of AD patients compared to non-AD patients may be explained by the potential response to biomarkers present in the CSF. These could include GFAP, NfL, total tau, p-tau and amyloid. As we did not assess the concentrations of these biomarkers it would be helpful to understand the impact they may be having in cytokine responses in the CSF of AD patients in our cohort.

Limitations of our study should be highlighted; Segregating cohorts based on sex as well as AD pathology led to a small sample size especially in the non-AD cohort. This may contribute to the overall minimal changes observed in T cell cytokine response and T cell phenotype subsets. Therefore, we would require more samples in each cohort to fully comprehend potential sex differences present in T cell subsets. It is important to note that the non-AD cohort have reported to the memory clinic and have undergone diagnosis assessment for some cognitive impairment and could potentially go on to develop AD or another neurodegenerative disease. This impacts the segregation of the groups based on pathology as the differences in T cell responses may be occurring at an earlier prodromal stage of AD prior to clinical manifestations of cognitive decline. Furthermore, patients may go on to develop a different neurodegenerative disease and therefore would be excluded from this analysis.

Moreover, it has recently been reported that male and female T cell subsets differ throughout AD progression (van Olst et al., 2024). Increases in $CD8^+$ $CD57^+$ TEMRA and $PD1^-$ $CD57^+$ $CD8^+$ TEMRA cells are more apparent at the MCI AD stage for females whereas this does not occur until the AD Dementia stage for males (van Olst et al., 2024). Therefore, the timepoint investigated in our study may explain the minimal changes in T cell phenotype between our non-AD and AD cohort. Thus, a more expansive non AD and AD cohort with prodromal, early and late stage patients may achieve more significant findings. There are logistical difficulties acquiring such samples as prodromal alterations in AD in the CSF have been reported as up to 10-20 years prior to clinical manifestations in familial AD and up to 2 years prior to Aß PET positive results in sporadic cases (Bateman et al., 2012, Palmqvist et al., 2016).

Therefore, the study design would require a longitudinal setup following patients throughout the prodromal phase and post diagnosis before analysis could be fully understood. Additionally, investigating the role of sex as a biological variable would increase the number of participants required to appropriately report sex differences throughout.

5 Chapter 5: Investigating the effect of sex specific differences in Alzheimer's disease patients' cerebrospinal fluid and PBMCs on iPSC derived cortical astrocytes

5.1 Introduction

In more recent years, advances in our understanding of developmental biology and stem cell research has led to the establishment of an extremely useful model of induced pluripotent stem cells (iPSCs) which can be used to investigate a wide range of physiological and pathological questions.

The injection of mRNA into frog oocytes to investigate translation was one of the initial investigations into the production of exogenous genetic material first reported by Gordon et al., (1971). Seminal work carried out in mouse embryos, demonstrated that prior to embryo implantation, cells were the most pluripotent (Evans and Kaufman, 1981). Additionally, blastocysts isolated prior to implantation in this study were successfully used to generate mouse embryonic stem (ES) cell lines (Evans and Kaufman, 1981). The successful birth of lambs (Dolly the sheep), derived from adult mammary glands indicated the totipotency of adult somatic cells (Wilmut et al., 1997). It further highlighted that differentiation of cells was achieved by systemic and sequential signalling between the nucleus and the cytoplasmic environment (Wilmut et al., 1997). One of the first human embryonic stem cell lines were successfully developed by Thomson et al., (1998) using fresh or frozen cleavage stage embryos donated from in-vitro fertilisation (IVF) patients. This study successfully established 5 ES cell lines from 5 different embryos with undifferentiated proliferation maintained for 5-6 months (Thomson et al., 1998).

The beginning of the 21st century saw an increase in attempts to reprogramme adult somatic cells into pluripotent stem cells. Key work carried out identified 4 genes required to induce pluripotency in somatic adult cells from mice (Takahashi and Yamanaka, 2006). Via retroviral transduction, the genes Oct 3/4, Sox2, c-Myc and Klf4 were all identified as key genes required to induce pluripotency in adult somatic cells (Takahashi and Yamanaka, 2006). Furthermore, this study successfully generated iPSCs using retroviral transduction of the 4 gene factors from tail tip fibroblasts of 7 week old mice which were morphologically and genetically indistinguishable from ES cells (Takahashi and Yamanaka, 2006). A follow-up study successfully induced pluripotency in human adult somatic dermal fibroblasts via retroviral transduction using the 4 genes (Takahashi et al., 2007). These iPSCs had exponential proliferation

abilities up to 4 months and morphological and DNA microarray analysis confirmed their similarity to ES cells (Takahashi et al., 2007). This study also reported the capability of iPSCs to differentiate into the three germ layers and successfully differentiate into neurons and cardiac myocytes indicating their downstream use for future studies (Takahashi et al., 2007). The introduction of Nanog into subsequent iPSC studies were successful in developing adult chimeras and were more alike to ES cells than previous iPSC lines that did not include Nanog (Okita et al., 2007).

Obstacles that have been overcome more recently is the use of alternatives to retroviral transduction to induce pluripotency (Yu et al., 2009, Okita et al., 2011). The use of retroviral transduction causes the transgene to be inserted into the host genome which increases the risk of insertional mutations and downstream impacts on differentiated cell lineages (Yu et al., 2007). To overcome this, Yu and colleagues successfully generated iPSCs using episomal vectors which replicate in the host cells without being incorporated into the host genome permanently (Yu et al., 2009). This was further enhanced by incorporating p53 short hairpin RNA (shRNA), Lin28 and l-Myc instead of c-Myc into an episomal vector to induce pluripotency in somatic cells (Okita et al., 2011). Further optimisations in cell mediums used to culture iPSCs led to the removal of bovine serum albumin on Matrigel and ß-mercaptaethonol and defined the 8 components required to sustain iPSCs. These included insulin, selenium, transferrin, L-ascorbic acid, FGF2 and TGF-ß in DMEM/F-12 (Chen et al., 2011). This study also identified vitronectin (Vtn) coated plates as key to supporting initial attachment and survival of iPSCs (Chen et al., 2011).

The successful induction of pluripotent stem cells from human adult somatic cells has now opened up a possibility to differentiate cells into different cell fates. Studies investigating neurodegeneration require the ability to differentiate iPSCs into cell specific (neurons, glia) and region specific (cortical, midbrain) lineages. The SMAD inhibitors, Noggin and SB431542, were identified as key factors required to induce rapid neural conversion in human ES cells and iPSCs (Chambers et al., 2009). Neural conversion was achieved by these two factors with SB431542 blocking TGF-ß pathways thus preventing pluripotency and Noggin decreasing bone morphogenic protein (BMP) signalling required for the trophoblast lineage (Chambers et al., 2009). The introduction of a different SMAD inhibitor LDN193189 instead of Noggin and

including retinoid led to differentiation towards cortical lineage for neurons (Shi et al., 2012).

Additionally, the successful differentiation of neural progenitor cells (NPCs) to astrocyte progenitor cells (APCs) has also been reported (Crompton et al., 2021, Perriot et al., 2021). The introduction of epidermal growth factor (EGF) and human leukaemia inhibitory factor (hLIF) have been identified as key to astrocyte differentiation. It is suggested that these two factors accelerate the glial switch with hLIF activating the JAK/STAT pathway and EGF preventing premature differentiation of NPCs to neurons to drive their cell fate towards astrocyte formation (Perriot et al., 2021, Bonni et al., 1997). Finally, BMP4 in combination with hLIF has been identified as necessary to drive astrocyte maturation (Nakashima et al., 1999, Serio et al., 2013). The use of iPSC derived astrocytes allows for further elucidation of their role in the pathogenesis of many neurodegenerative diseases including AD and overcoming potential translation issues when using animal models. Recently, it has been confirmed that mature astrocytes derived from iPSC treated with TIC factors generate a reactive phenotype (McComish et al., 2024). TIC factors refer to microglia related cytokines TNF-α (30ng/mL), IL-1α (3ng/mL) and C1q (400ng/mL) that have been shown to be released and generate a reactive astrocyte phenotype in mice treated with LPS (Liddelow et al., 2017). Thus, it is imperative to assess astrocyte response to these TIC factors to ensure an appropriate mature astrocyte has been differentiated.

Therefore, the aims of this study are to:

1) Confirm mature astrocytes derived from iPSC adopt a reactive phenotype when treated with TIC factors
2) Investigate the effect of AD pathology and sex on iPSC derived astrocytes treated with conditioned media from PBMCs of non-AD/MCI and AD patients
3) Investigate the effect of AD pathology and sex on iPSC derived astrocytes treated with CSF from non-AD/MCI and AD patients

5.2 Methods

5.2.1 Cell Line

Non-affecting sibling 2 (NAS2) induced pluripotent stem cells (iPSC) were gifted by Dr. Tilo Kunath (University of Edinburgh, UK). Fibroblast of the dermis of the patient donor were reprogrammed using retroviral transduction with Yamanaka reprogramming factors (OCT4, SOX2, KLF4 and c-MYC). The donor was female aged between 30-34 years. The genotyping of the cell line reported the line to be E3E3 homozygous. The cell line can now be purchased via the European Bank for Induced pluripotent Stem Cells (Ref Code: EDi002-A; https://ebisc.org/EDi002-A/).

5.2.2 iPSC Cell Culture

NAS2 iPSC were thawed, resuspended in Essential 8 Flex (E8) media (ThermoFisher, USA) and plated on vitronectin (Vtn; 0.5μg/cm^2; ThermoFisher Scientific, USA) coated 6 well plates (Nunc by ThermoFisher Scientific, USA). E8 media was changed every 1-2 days (2-3 mL) in accordance with Chen et al., protocol (2011). In the initial thaw and following cell passages E8 media was supplemented with the ROCK inhibitor Y-27632 (10μM; 24 hours; Bio-Techne, USA) to aid cell survival (Watanabe et al., 2007).

Once cells reached 80% confluency they were passaged. E8 media was removed and the well was washed with PBS (1X) and ethylenediaminetetraacetic acid (EDTA (0.5 mM; ThermoFisher Scientific, USA) and then incubated in EDTA (0.5 mM; 3-4 minutes; RT). EDTA was removed and the cells were washed with E8 media (1 mL). Cells were detached from the well with E8 media and collected. Cells were split at a 1:4 or 1:5 ratio and plated onto a new Vtn coated 6 well plate.

5.2.3 Neural Progenitor Cell (NPC) Culture

iPSCs were passaged on a Vtn coated 12 well plate (Nunc by ThermoFisher Scientific, USA) at lower densities (1:6, 1:8 and 1:10) and maintained in E8 media. Once cells were 80% confluent, E8 media was removed, cells were washed with PBS (1X) and neural maintenance media (NMM) was added (1:1 Dulbecco's Modified Eagle Medium (DMEM)/F12 with GlutaMAX and Neurobasal media, 1% B-27, 1% non-essential amino acids (NEAA), 1% penicillin streptomycin, 0.5% N2, 0.5% GlutaMAX,

75μM β-mercaptaethanol and 5μg/mL insulin). Media was supplemented with the mesoderm differentiation inhibitor LDN193189 (100 nM; Sigma Aldrick, UK) and pluripotency inhibitor SB431542 (10 μM; Bio-Techne, USA). Cells were incubated in NMM with LDN and SB43 for 10 days. On day 3 and day 6, laminin (0.1μg/cm^2) was added to assist with cell adherence. On day 10, NMM with LDN and SB43 was removed and cells were incubated in NMM without LDN and SB43. On day 11, media was removed, cells were washed with PBS (1X) and incubated with Accutase™ (2-3 minutes). Cells were detached and collected in NMM and passaged on 6 well plates. The 6 well plates had been previously coated with poly-L-ornithine (1μg/cm^2; 1 hour; 37°C), poly-L- ornithine was removed, the well was washed with PBS (1X) and laminin was added (1μg/cm^2; 2 hours; 37°C). Media was supplemented with the ROCK inhibitor Y-27632 (10 μM; 24 hours; Bio-Techne, USA) to aid cell survival. Cells were fed with NMM every 1-2 days (initial volumes 3-4 mL with increasing volume of NMM as cells become more confluent).

Once cells had reached 100% confluency, ROCK inhibitor Y-27632 (10 μM) was added at least two hours before passaging cells to aid cell survival. After two hours, media was removed, cells were washed with PBS (1X) and incubated with Accutase™ (2-3 minutes). Cells were detached and collected in NMM and passaged on 6 well plates coated poly-L-ornithine and laminin (1μg/cm^2) in NMM media. Media was supplemented with the ROCK inhibitor Y-27632 (10 μM; 24 hours; Bio-Techne, USA) to aid cell survival. NPCs were also seeded for characterisation on UV sterilised coverslips coated in poly-L-ornithine (1μg/cm^2; 1 hour; 37°C) followed by laminin (1μg/cm^2; 2 hours; 37°C). The same method to collect NPCs for passaging was followed as above. Cells were collected and centrifuged (200 x *g*; 3 minutes; RT). The supernatant was removed and the cell pellet were resuspended in NMM (1 mL). 50 μL and 100 μL droplets of cell suspension were seeded on the pre-coated coverslips and incubated overnight (37°C). The following day once the cells had adhered to the coverslips, wells were flooded with NMM (400 μL).

5.2.4 Astrocyte Progenitor Cell (APC) Culture

Before day 30, neurons were confirmed to be a pure culture. Once neurons reached confluency, NMM media was removed, cells were washed with PBS (1X) and

astrocyte maintenance media (Advanced DMEM/F12 (ThermoFisher Scientific, USA), 1% GlutaMAX, 1% penicillin streptomycin, 1% N2, 1% NEAA and 0.2% B27) referred to as Serio supplemented with epidermal growth factor (EGF; 20ng/mL; Sigma Aldrick, UK) human leukaemia inhibitory factor (hLIF; 20ng/mL; Sigma Aldrich, UK) (SerioEL) was added (2 mL/well). This induces the gliogenic switch of NPCs to gliogenic precursors by inhibiting neurogenesis (Bonni et al., 1997) and activating the JAK/STAT pathway, specifically the STAT3 signalling pathway, mediated via gp-130 activation inducing astrogliosis (Sriram et al., 2004). After 3 days, cells were passaged by removing SerioEL, washing the cells with PBS (1X) and incubating with Accutase™ (2-3 minutes; RT). Cells were collected using SerioEL and passaged onto pre-coated Geltrex (1X; ThermoFisher Scientific, USA) 6 well plate. Media was supplemented with the ROCK inhibitor Y-27632 (10μM; 24 hours; Bio-Techne, USA) to aid cell survival. Cells were fed every second day (2 mL/well) and extra media was given at the weekend period (4 mL/well).

Passaging and expanding the cells was carried out when the cells were 100% confluent up to day 80. On day 80, APCs could be seeded for characterisation by immunocytochemistry to ensure the population was not mixed before maturing. SerioEL was removed, cells were washed with PBS (1X) and incubated in Accutase™ (2-3 minutes; RT). Cells were collected in Serio and centrifuged (200 x *g*; 3 minutes). The supernatant was removed and the cells were resuspended in SerioEL (1 mL). 50μl and 100μl droplets of cell suspension were seeded on UV sterilised Geltrex pre-coated coverslips. The following day, the coverslips were flooded with SerioEL (400 μL) and incubated (37°C) until cells were fixed and immunolabelled for immunocytochemistry.

After D80 once confluent, APCs were plated for terminal differentiation on 24 well plates. Cells were collected and centrifuged as mentioned above and counted (outlined in 2.8). For immunocytochemistry, APCs were seeded at a density of 50,000 cells/coverslip on UV sterilised Geltrex pre-coated coverslips in SerioEL. The following day, coverslips were flooded with SerioEL (400 μL). For enzyme linked immunosorbent assay (ELISA) and RT-qPCR cells were seeded at a density of 100,000 cells/well on Geltrex precoated wells in SerioEL (500 μL). Once cells were confluent,

SerioEL was exchanged for Serio supplemented with BMP4 (20ng/mL; R&D Systems, UK) and hLIF (20ng/mL) referred to as SerioBL. APCs were matured for 7 days in SerioBL. On day 8, SerioBL was removed and replaced with plain Serio for 3 days and were then considered mature astrocytes. Mature astrocytes could be used for experimentation up to day 120.

5.2.5 Treatment of mature cortical astrocytes with microglial factors (TIC)

Mature astrocytes seeded for ELISA, RT-qPCR and immunocytochemistry were treated with TIC factors, (TNF-α, IL-1α, C1q), initially identified by Liddelow et., al (2017) to generate a reactive phenotype in astrocytes. Plain Serio was removed from cells and replaced with Serio supplemented with TNF-α (30ng/mL; Cell Signalling Technology, USA), IL-1α (3ng/mL; PeproTech, UK) and C1q (400ng/mL; MyBioSource, USA) (TIC) factors. The control group were treated with plain Serio. Cells were incubated for 24 hours (5% CO_2; 37°C). After 24 hours, conditioned media was collected from treated and control groups and stored (-20°C) for later ELISA experiments. Cells were washed with PBS (1X) and lysed with RA1 buffer and stored (-80°C) for later RNA isolation and subsequent RT-qPCR. Treatment was removed from cells seeded on coverslips and cells were fixed with PFA (4%; 30 minutes; RT) and stored in PBS (1X) before staining (4°C).

5.2.6 Treatment of mature cortical astrocytes with CSF and PBMCs conditioned media

Mature astrocytes were treated with plain serio supplemented with non-AD/MCI and AD patients:

1) 10% (v/v) conditioned media from PBMCs stimulated with anti-CD3 and anti-CD28

2) 1:1 CSF

Please refer to section 2.6.1 for categorisation of AD versus non-AD/MCI patients. Controls were treated with plain Serio and will be referred to as control in all experiments in this study. Astrocytes were incubated for 24 hours (5% CO_2; 37°C). After 24 hours, conditioned media was collected from treated and control groups and

stored (-20°C) for later ELISA experiments. Cells were washed with PBS (1X) and lysed with RA1 buffer and stored (-80°C) for later RNA isolation and subsequent RT-qPCR.

5.2.7 Enzyme linked immunosorbent assay (ELISA)

ELISAs were carried out in accordance with manufacturing instructions (R&D Systems, USA) to investigate astrocyte IL-6, CXCL10, GMCSF and RANTES protein secretion on single ELISA plates per protein of interest. Plates were incubated overnight with capture antibody (capture antibody diluted in PBS; RT). The capture antibody was removed and washed with wash buffer (0.5% (v/v)Tween in PBS; 3 times). Plates were blocked in reagent diluent (1% (v/v) bovine serum albumin in PBS) (1 hour; RT). The blocking buffer was removed and washed in washing buffer (3 times). Samples and standards of specific known concentration (R&D systems, USA specifications) were diluted in reagent diluent and incubated on a plate rocker (RT; 2 hours). The samples and standards were removed and washed with wash buffer (3 times). The detection antibody was added to the plate (2 hours; RT). The detection antibody was removed from the plate and washed with wash buffer (3 times). Streptavidin-horse radish peroxidase (HRP) (1:40 diluted in reagent diluent) was added (20 minutes; in the dark; RT). Streptavidin-HRP was removed and the plate was washed with wash buffer (3 times). 3,3',5,5'-Tetramethylbenzidine (TMB), was added to the plate (7-10 minutes; in the dark; RT). Stop buffer (1M Sulfuric Acid) was added to stop the reaction. Plates were read with absorbance values reported at the 450nm and 540nm wavelengths (Synergy HT, BioTek Instruments, USA). Concentrations of samples were derived from the standard curve.

5.2.8 Immunocytochemistry

Section 2.3 outlines the steps followed for immunocytochemistry on NPCs, APCs and reactive astrocytes. NPCs were immunolabelled for the cortical marker TBR1 and neuronal marker β-tubulin-III. APCS were immunolabelled for astrocyte marker GFAP and β-tubulin-III. Mature and reactive astrocytes were immunolabelled for GFAP, S100β, EAAT1 and Connexin-43.

Primary Antibody	Manufacturer	Dilution
Rabbit anti-TBR1	Abcam, UK; ab183032	1:1500
Mouse anti-β- Tubulin III	Merck-Millipore, USA; T8578	1:1000
Chicken anti-GFAP	Sigma Aldrich, UK; AB5541	1:1000
Mouse anti-S100β	Sigma Aldrich, UK; S2532	1:1000
Rabbit anti-EAAT1	Bio-Techne; NBPI-20135	1:1500
Rabbit anti-Connexin-43	Sigma Aldrick, UK; C6219	1:1500

Table *5.1* Primary antibodies for immunocytochemistry

Secondary Antibody	Manufacturer	Dilution
Goat Anti-chicken 488	Abcam; ab150169	1:500
Donkey Anti-mouse 488	ThermoFisher Scientific, USA; A21202	1:500
Donkey anti-mouse 594	ThermoFisher Scientific, USA; A21202	1:500
Donkey Anti-mouse 647	ThermoFisher Scientific, USA; A31571	1:500
Donkey Anti-rabbit 594	ThermoFisher Scientific, USA; A21207	1:500
Donkey Anti-rabbit 647	ThermoFisher Scientific, USA; A31573	1:500

Table 5.2 Secondary antibodies for immunocytochemistry

5.2.9 RT-qPCR

Section 2.5.3 outlines RNA isolation, cDNA synthesis and RT-qPCR method carried out. See below for genes investigated in astrocytes treated with TIC. See **Table 5.3** for genes investigated (all sourced from ThermoFisher Scientific) in astrocytes treated with patients PBMC conditioned media or CSF.

Primer	Gene Name	Gene Code
Gapdh	Glyceraldehyde-3-phosphate dehydrogenase	Hs02786624_g1
C3	Complement Component 3	Hs00163811_m1
CCL5	C-C motif chemokine ligand 5	Hs00982282_m1
CSF2	Colony stimulating factor 2	Hs00929873_m1
CXCL10	C-X-C motif chemokine ligand 10	Hs00171042_m1
GFAP	Glial fibrillary acidic protein	Hs00909233_m1
GJA1	Gap junction protein alpha 1	Hs00748445_s1
IL-1β	Interleukin 1 beta	Hs01555410_m1
IL-6	Interleukin 6	Hs00174131_m1
IL-17RA	Interleukin 17 receptor A	Hs01056316_m1
LCN2	Lipocalin 2	Hs01008571_m1
SLC1A3	Solute carrier family 1 member 3	Hs00904823_g1
TLR4	Toll-like receptor 4	Hs00152939_m1

Table 5.3 TaqMan primers used for RT-qPCR

5.2.10 Statistical Methods

In relation to immunocytochemistry analysis, nested t-test was used for cell profiler analysis of astrocytes seeded on coverslips and immunolabelled with astrocyte markers. For control and treated groups, 100 cells were analysed per n. Data, presented as mean +/- SEM.

5.3 Results

5.3.1 iPSC derived cortical astrocytes develop a reactive phenotype when treated with TIC factors

Mature astrocytes were treated with TIC factors, (TNF-α, IL-1α, C1q), to generate a reactive phenotype. Mature cortical astrocytes post treatment were assessed by immunocytochemistry, ELISA and qPCR. We used the astrocyte markers GFAP (**Figure 5.1**) and S100β (**Figure 5.2**) to investigate changes in morphology. The integrated intensity of the astrocytic markers GFAP, S100β, Connexin-43 and EAAT1 were also investigated (**Figure 5.1** and **Figure 5.2**). Utilising GFAP as a cytoskeleton marker (**Figure 5.1**), there was a no change reported in cell area in treated versus control (**Figure 5.1 A**). There was a significant decrease in cell eccentricity in treated versus control astrocytes (**Figure 5.1 B**; p=0.008). There were no alterations observed in cell circularity, maximum feret diameter, minimum feret diameter or perimeter between control and treated cortical astrocytes **(Figure 5.1 C-F**). There was a significant decrease in Connexin-43 intensity in treated astrocytes compared to control (**Figure 5.1 G**; p=0.0013). GFAP intensity trended towards a decrease in treated astrocytes versus the control group (**Figure 5.1 H**; p=0.0973) but it did not reach statistical significance. There was a significant decrease in S100β intensity in treated astrocytes compared to control (**Figure 5.1 I**; p=0.0174).

Additionally, we utilised another astrocyte marker S100β to assess morphological changes (**Figure 5.2**). A decrease in cell area was observed in treated astrocytes compared to control, however this did not reach statistical significance (**Figure 5.2 A**; p=0.0668). There was a significant decrease in cell eccentricity in treated versus control astrocytes (**Figure 5.2 B**; p=0.0277). There was no change in cell circularity reported (**Figure 5.2 C**). There was a significant decrease in maximum feret diameter in treated astrocytes (**Figure 5.2 D**; p=0.0477). Minimum feret diameter trended towards a decrease in treated astrocytes however, this did not reach significance (Figure 5.2 E, p=0.108). There was no change in perimeter observed between control and treated astrocytes (**Figure 5.2 F**). Treated astrocytes had a significant decrease in EAAT1 (**Figure 5.2 G**; p=0.0229) and S100β (**Figure 5.2 H**; p=0.0239).

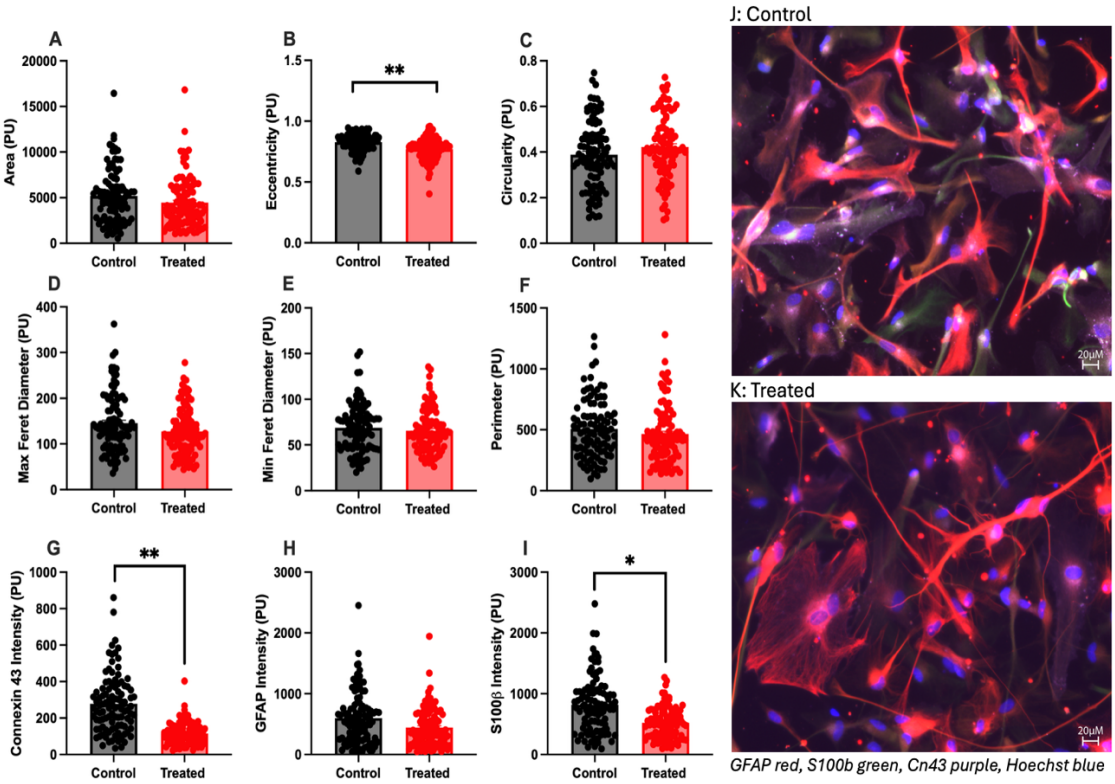


Figure 5.1 Differentiated NAS2 cortical astrocytes respond to TIC factors to adopt a reactive phenotype using GFAP expression to assess morphology

*Analysis of morphological alterations in NAS2 cortical astrocytes treated with TIC factors (TNFα (30ng/mL), IL-1α (3ng/mL) and C1q (400ng/mL)) versus control (mature astrocytes treated with plain serio) after 24-hour treatment using Cell Profiler software. Graphical representation of morphological features; area (**A**), eccentricity (**B**), circularity (**C**), maximum feret diameter (**D**), minimum feret diameter (**E**), perimeter (**F**) and quantification of intensity of connexin-43 (**G**), GFAP (**H**) and S100β (**I**). Representative images of GFAP (red), Connexin-43 (purple), S100β (green) and Hoechst (blue) expression in NAS2 cortical astrocytes post 24-hour treatment; control (**J**) and treated (**K**). There was a significant decrease in eccentricity in treated astrocytes (**p=0.008). Intensity of connexin-43 (**G**) and S100β (**I**) were significantly decreased in treated astrocytes (**p=0.0013) and (*p=0.0174) respectively. Data, presented as mean +/- SEM, were analysed by nested t test (n=3 per group; 100 cells were analysed per N).*

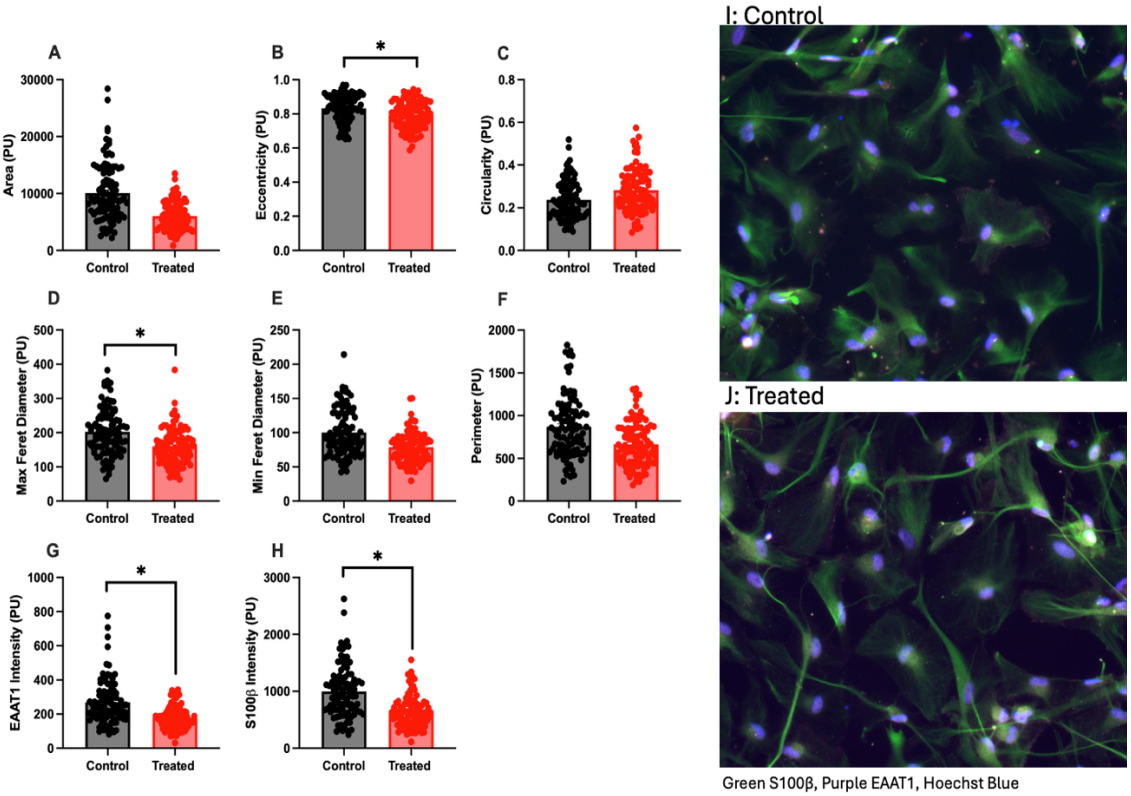


Figure 5.2 Differentiated NAS2 cortical astrocytes respond to TIC factors to adopt a reactive phenotype using S100β expression to assess morphology

*Analysis of morphological alterations in NAS2 cortical astrocytes treated with TIC factors (TNFα (30ng/mL), IL-1α(3ng/mL) and C1q (400ng/mL)) versus control (mature astrocytes treated with plain serio) after 24-hour treatment using Cell Profiler software. Graphical representation of morphological features; area (**A**), eccentricity (**B**), circularity (**C**), maximum feret diameter (**D**), minimum feret diameter (**E**), perimeter (**F**) and quantification of intensity of EAAT1 (**G**) and S100β (**H**). Representative images of EAAT1 (purple), S100β (green) and Hoechst (blue) expression in NAS2 cortical astrocytes post 24 hour treatment; control (**I**) and treated (**J**). There was a significant decrease in eccentricity in treated astrocytes (*p=0.0277) and max feret diameter (*p=0.0447) respectively. Intensity of EAAT1 (**G**) and S100β (**H**) were significantly decreased in treated astrocytes (*p=0.0229) and (*p=0.0239) respectively. Data, presented as mean +/- SEM, were analysed by nested t test (n=3 per group; 100 cells were analysed per N)*

We then investigated protein secretion of treated versus control astrocytes for IL-6, CXCL10, GMCSF and RANTES using ELISA **(Figure 5.3**). Treated astrocytes had a significant increase in IL-6 (**Figure 5.3 A**; p<0.0001), CXCL10 (**Figure 5.3 B**; p<0.0001), GMCSF (**Figure 5.3 C**; p=0.0011) and RANTES secretion (**Figure 5.3 D**; p=0.0004).

We also investigated gene expression in treated and control astrocytes for *GJA1, CCL5, CXCL10* and *IL-6* (**Figure 5.4**). There was a significant decrease in *GJA1* gene expression in treated astrocytes (**Figure 5.4 A**; p=0.0196). There was a significant increase in *CCL5* (**Figure 5.4 B**; p=0.0314), *CXCL10* (**Figure 5.4 C**; p=0.0421) and *IL-6* (**Figure 5.4 D**; p=0.0327) gene expression in treated astrocytes. These results indicate that mature astrocytes differentiated from iPSCs possess the ability to become reactive when treated with TIC factors.

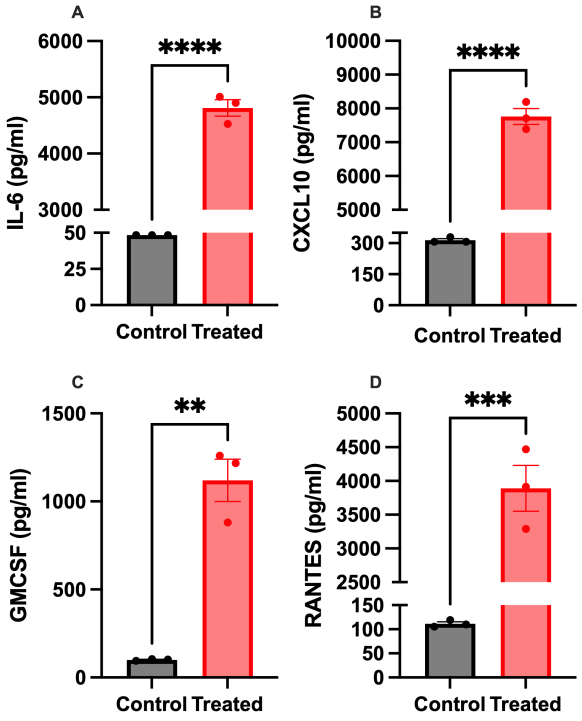


Figure 5.3 NAS2 cortical astrocytes increase cytokine protein secretion in response to TIC factors

*NAS2 astrocytes secrete pro-inflammatory cytokines when induced by TIC factors ((TNFα (30ng/mL), IL-1α (3ng/mL) and C1q (400ng/mL)) versus control (mature astrocytes treated with plain serio) after 24-hour treatment confirmed by ELISA. Graphical representation of protein secretion (pg/mL) of IL-6 (**A**), CXCL10 (**B**), GMCSF (**C**) and RANTES (**D**) in control versus treated astrocytes. There was a significant increase in IL-6 (****p<0.0001), CXCL10 (****p<0.0001), GMCSF (**p=0.0011) and RANTES (*** p=0.0004) secretion in treated astrocytes compared to control. Data, presented as mean +/- SEM, were analysed by unpaired t test (n=3 per group).*

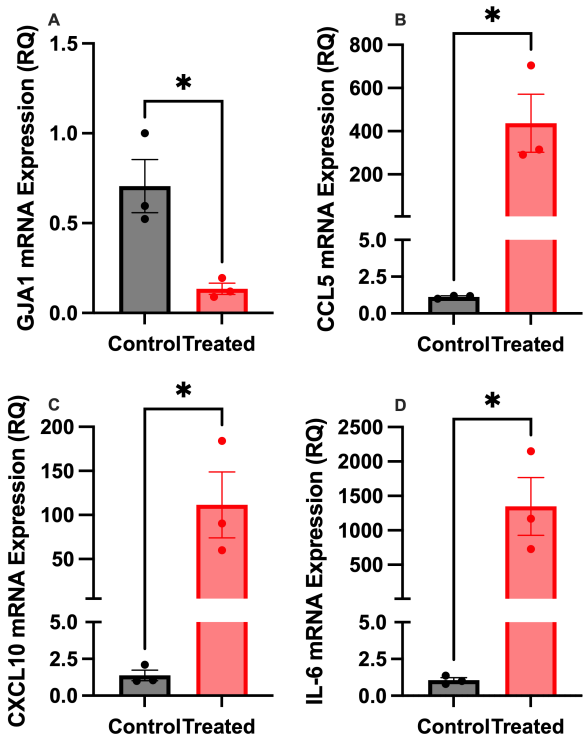


Figure 5.4 NAS2 cortical astrocytes undergo altered gene expression in response to TIC factors

*NAS2 astrocytes treated with TIC factors (TNFα (30ng/mL), IL-1α (3ng/mL) and C1q (400ng/mL)) versus control (mature astrocytes treated with plain serio) after 24-hour treatment undergo altered gene expression confirmed by RT-qPCR. Graphical representation of alterations in gene expression (RQ) of GJA1 (**A**), CCL5 (**B**), CXCL10 (**C**) and IL-6 (**D**) in control versus treated astrocytes. There was a significant decrease in GJA1 gene expression in treated astrocytes vs control (*p=0.0196). There was a significant increase in expression of CCL5 (*p=0.0314), CXCL10 (*p=0.0421) and IL-6 (*p=0.0327) genes in treated astrocytes compared to control. Data, presented as mean +/- SEM, were analysed by unpaired t test (n=3 per group).*

Summary of results obtained while assessing iPSC derived astrocytes response to TIC factors

- When treated with TIC factors;
- Mature astrocytes undergo morphological changes such as decreased eccentricity and max feret diameter compared to control.
- Mature astrocytes adopt a reactive phenotype consisting of increased secretion of IL-6, CXCL10, GMCSF and RANTES compared to control.

- Mature astrocytes alter their gene expression with an increase in CCL5, CXCL10 and IL-6 and a decrease in GJA1 expression compared to control.

5.3.2 The effect of PBMCs conditioned media and CSF on cortical astrocytes' protein secretion and gene expression

Following confirmation that we had successfully differentiated functional astrocytes we then investigated the effect of AD pathology and sex on astrocytes. Astrocytes were treated with 10% (v/v) PBMC conditioned media (CM) or CSF (1:1) diluted in plain serio for 24 hours (37°C; 5% CO_2) from non-AD/MCI and AD patients. Protein secretion via ELISA and gene expression by RT-qPCR were utilised post treatment to investigate any potential differences between the groups.

In astrocytes treated with 10% CM there was no change observed in CXCL10 or IL-6 secretion astrocytes treated with non-AD/MCI or AD CM, compared to control (**Figure 5.5 A and B**). There was a significant increase in RANTES secretion in astrocytes treated with non-AD/MCI and AD patients' CM (**Figure 5.5 C**; p=0.0167 and p=0.0044 respectively). There was no differences in RANTES secretion observed between astrocytes treated with non-AD/MCI or AD CM. There was a significant increase in GMCSF secretion in astrocytes treated with AD CM compared to control (**Figure 5.5 D**; p=0.0484). There was no difference in GMCSF secretion reported between non-AD/MCI CM and control or between non-AD/MCI and AD CM treated astrocytes (**Figure 5.5 D**).

We then investigated the effect of sex on astrocytes treated with CM from male and female non-AD/MCI and AD patients (**Figure 5.6**). Two-way ANOVA reported no main effect of AD pathology or sex on astrocyte CXCL10, IL-6 , RANTES or GMCSF secretion in any of the groups (**Figure 5.6 A-D**).

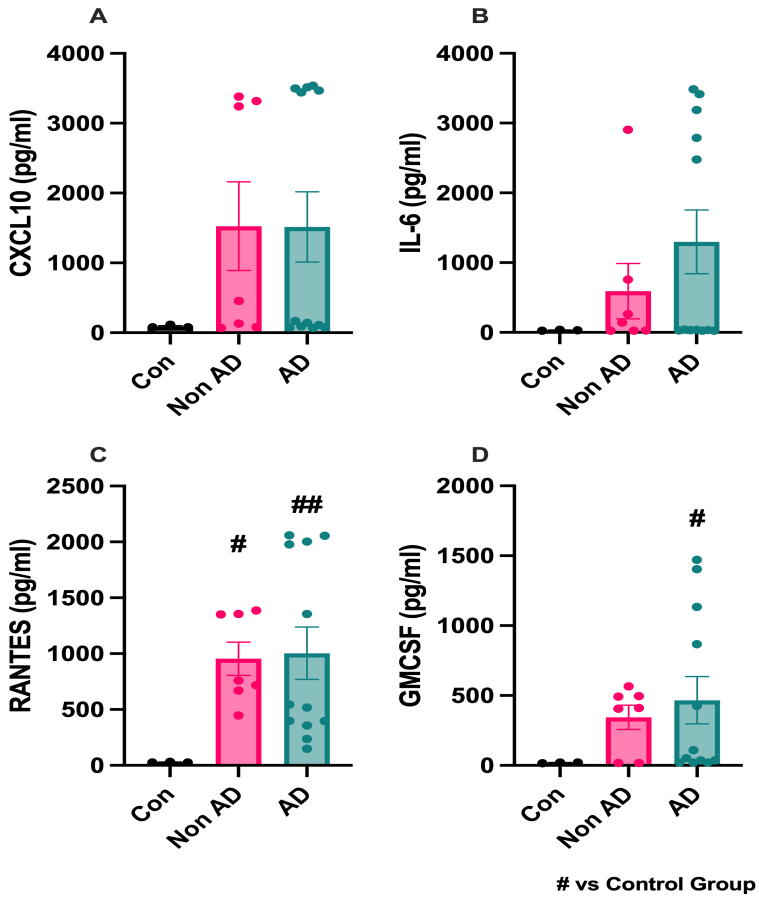


Figure 5.5 NAS2 cortical astrocytes increase cytokine protein expression in response to stimulated PBMCs conditioned media from non-Alzheimer's disease/MCI and Alzheimer's disease patients

*NAS2 astrocytes release pro-inflammatory cytokines when treated with 10% (v/v) conditioned PBMCs media from non-AD/MCI (N=7) and AD patients (N=12) for 24 hours versus control (mature astrocytes treated with plain serio) confirmed by ELISA. Graphical representation of protein secretion (pg/mL) of CXCL10 (**A**), IL-6 (**B**), RANTES (**C**) and GMCSF (**D**) in control versus treated astrocytes. In astrocytes treated with non-AD patients conditioned media there was a significant increase in RANTES (#p=0.0167) compared to control. In astrocytes treated with AD patients conditioned media there was a significant increase in RANTES (##p=0.0044) and GMCSF (#p=0.0484) secretion compared to control. Data, presented as mean +/- SEM, were analysed by unpaired t test* or *Mann Whitney when appropriate for non-parametric data.*

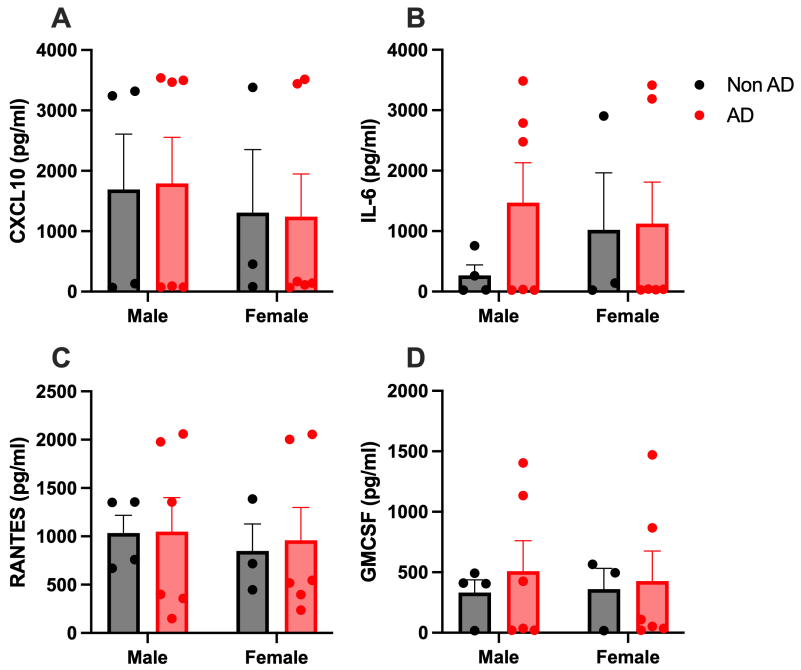


Figure 5.6 NAS2 cortical astrocytes cytokine protein expression in response to stimulated PBMCs conditioned media from male and female non-Alzheimer's disease/MCI and Alzheimer's disease patients

*NAS2 astrocytes were treated with 10% (v/v) conditioned PBMCs media from male (N=4) and female (N=3) non-AD/MCI and male (N=6) and female (N=6) AD patients for 24 hours and protein secretion was confirmed by ELISA. Graphical representation of protein secretion (pg/mL) of CXCL10 (**A**), IL-6 (**B**), RANTES (**C**) and GMCSF (**D**). Data, presented as mean +/- SEM, were analysed by two-way ANOVA and Šidák's post-hoc multiple comparison tests.*

We then investigated alterations in protein secretion of astrocytes treated with CSF diluted with plain serio (1:1) from non-AD/MCI or AD patients (**Figure 5.7**). There was a significant increase in CXCL10 secretion in astrocytes treated with non-AD/MCI or AD CSF compared to control (**Figure 5.7 A**; p=0.0013 and p=0.0236 respectively). There was also a significant decrease in CXCL10 secretion in astrocytes treated with AD CSF compared to non-AD/MCI CSF (**Figure 5.7 A**, p=0.0471). There was a significant increase in IL-6 secretion in astrocytes treated with non-AD/MCI or AD CSF compared to control (**Figure 5.7 B**; p=0.0119 and p=0.0055 respectively). There was no difference observed in IL-6 secretion in astrocytes treated with non-AD/MCI or AD CSF. RANTES and GMCSF secretion in astrocytes treated with non-AD/MCI or AD CSF did not differ from astrocytes treated with control (**Figure 5.7 C and D**).

Next we investigated alterations in astrocyte protein secretion when separated based on sex and AD pathology (**Figure 5.8**). Two-way ANOVA reported a significant main effect of AD pathology on CXCL10 secretion by astrocytes (**Figure 5.8 A**; p=0.0498). Šidák's post-hoc multiple comparison tests however revealed no significance between the groups. Two-way ANOVA reported a significant effect of sex x pathology in IL-6 secretion by astrocytes (**Figure 5.8 B**; p=0.046). Šidák's post-hoc multiple comparison tests however revealed no significance between the groups. Neither AD pathology nor sex impacted on RANTES or GMCSF astrocyte secretion in any of the groups (**Figure 5.8 C and D**).

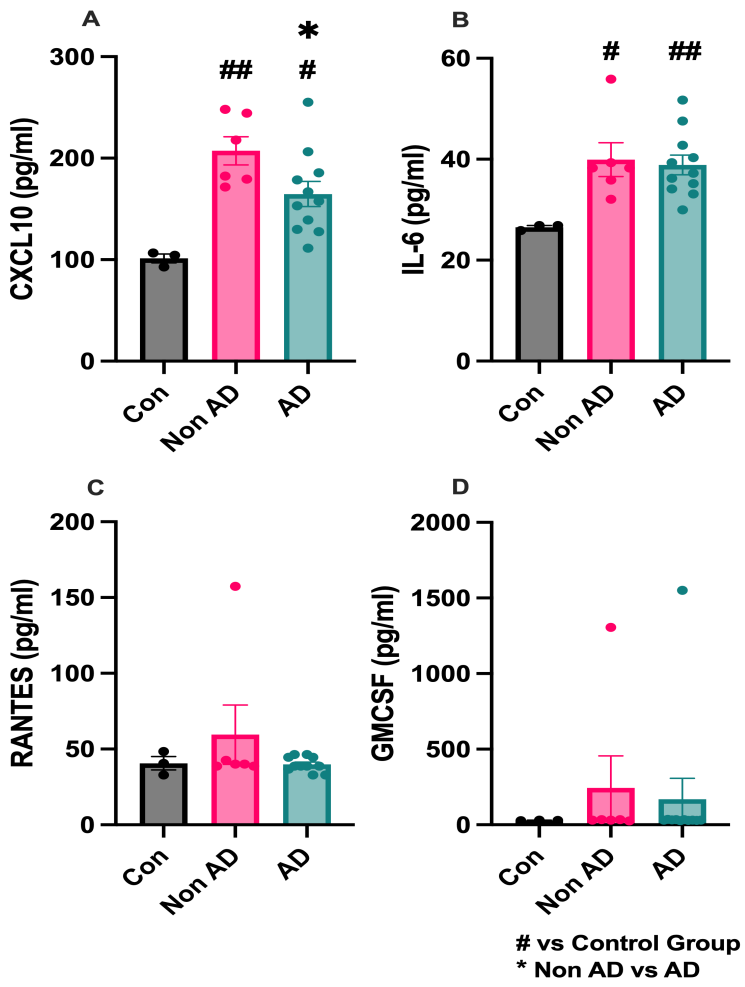


Figure 5.7 CSF-induced increased expression of CXCL10, IL-6, RANTES and GMCSF in NAS2 cortical astrocytes from non-Alzheimer's disease/MCI and Alzheimer's disease patients

*NAS2 astrocytes release pro-inflammatory cytokines when treated with CSF diluted in plain Serio (1:1) from non-AD/MCI (N=6) and AD patients (N=11) for 24 hours versus control (mature astrocytes treated with plain serio) confirmed by ELISA. Graphical representation of protein secretion (pg/mL) of CXCL10 (**A**), IL-6 (**B**), RANTES (**C**) and GMCSF (**D**). In astrocytes treated with non-AD patients' CSF there was a significant increase in CXCL10 (##p=0.0013) and IL-6 (#p=0.0119) compared to control. In astrocytes treated with AD patients' CSF there was a significant increase in CXCL10 (#p=0.0236) and IL-6 (##p=0.0055) secretion compared to control. Astrocytes treated with AD patients' CSF had a significant decrease in CXCL10 compared to astrocytes treated with non-AD CSF (*p=0.0471). Data, presented as mean +/- SEM, were analysed by unpaired t test or Mann Whitney when appropriate for non-parametric data.*

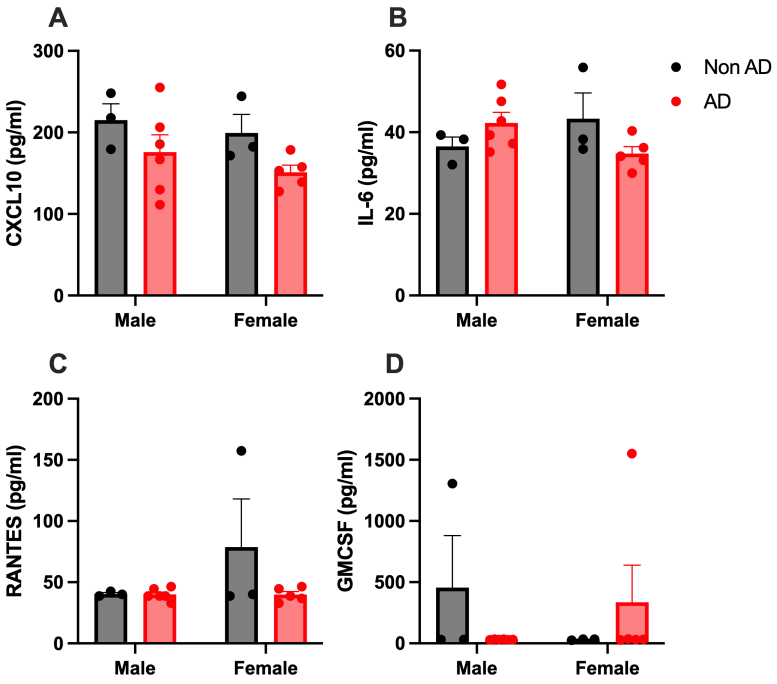


Figure 5.8 CSF-induced increased expression of CXCL10, IL-6, RANTES and GMCSF in NAS2 cortical astrocytes from male and female non-Alzheimer's disease/MCI and Alzheimer's disease patients

*NAS2 astrocytes were treated with CSF diluted in plain serio (1:1) from male (N=3) and female (N=3) non-AD/MCI and male (N=6) and female (N=5) AD patients for 24 hours and protein secretion was confirmed by ELISA. Graphical representation of protein secretion (pg/mL) of CXCL10 (**A**), IL-6 (**B**), RANTES (**C**) and GMCSF (**D**). Two-way ANOVA reported a significant main effect of pathology on CXCL10 secretion by astrocytes (**A**; p=0.0498). Two-way ANOVA reported a significant effect of sex x pathology in IL-6 secretion by astrocytes (**B**; p=0.046). Šidák's post-hoc multiple comparison tests however revealed no significance between the groups. Data, presented as mean +/- SEM, were analysed by two-way ANOVA and Šidák's post-hoc multiple comparison tests.*

Subsequently, alterations in gene expression in astrocytes treated with PBMCs CM or CSF from non-AD/MCI and AD patients was investigated.

Astrocytes treated with PBMCs CM from non-AD/MCI or AD patients reported no change in gene expression for *C3, CCL5, CSF2, CXCL10, GFAP, GJA1, IL-1β* or *IL-6* (**Figure 5.9 A-H**). There was a trending decrease in *IL-17RA* gene expression in astrocytes treated with AD CM compared to non-AD/MCI CM but this did not reach statistical significance (**Figure 5.9 I**, p=0.0516). There was no change in *LCN2, SLC1A3* or *TLR4* gene expression in astrocytes treated with non-AD/MCI or AD CM (**Figure 5.9 J-L**).

Furthermore, the effect of sex on astrocyte gene expression was then analysed (**Figure 5.10**). The effect of AD pathology or sex on *C3*, *CCl5, CSF2, CXCL10, GFAP, GJA1, IL-1β* or *IL-6* gene expression from astrocytes treated with non-AD/MCI or AD CM from males or females was not observed (**Figure 5.10 A-H**). A trending decrease in *IL-17RA* expression was observed in astrocytes treated with AD CM however, this did not reach significance (**Figure 5.10 I**, p=0.0682). Astrocytes treated with male or female non-AD/MCI or AD CM reported no significant change in expression of *LCN2, SLC1A3* or *TLR4* genes (**Figure 5.9 J-L**).

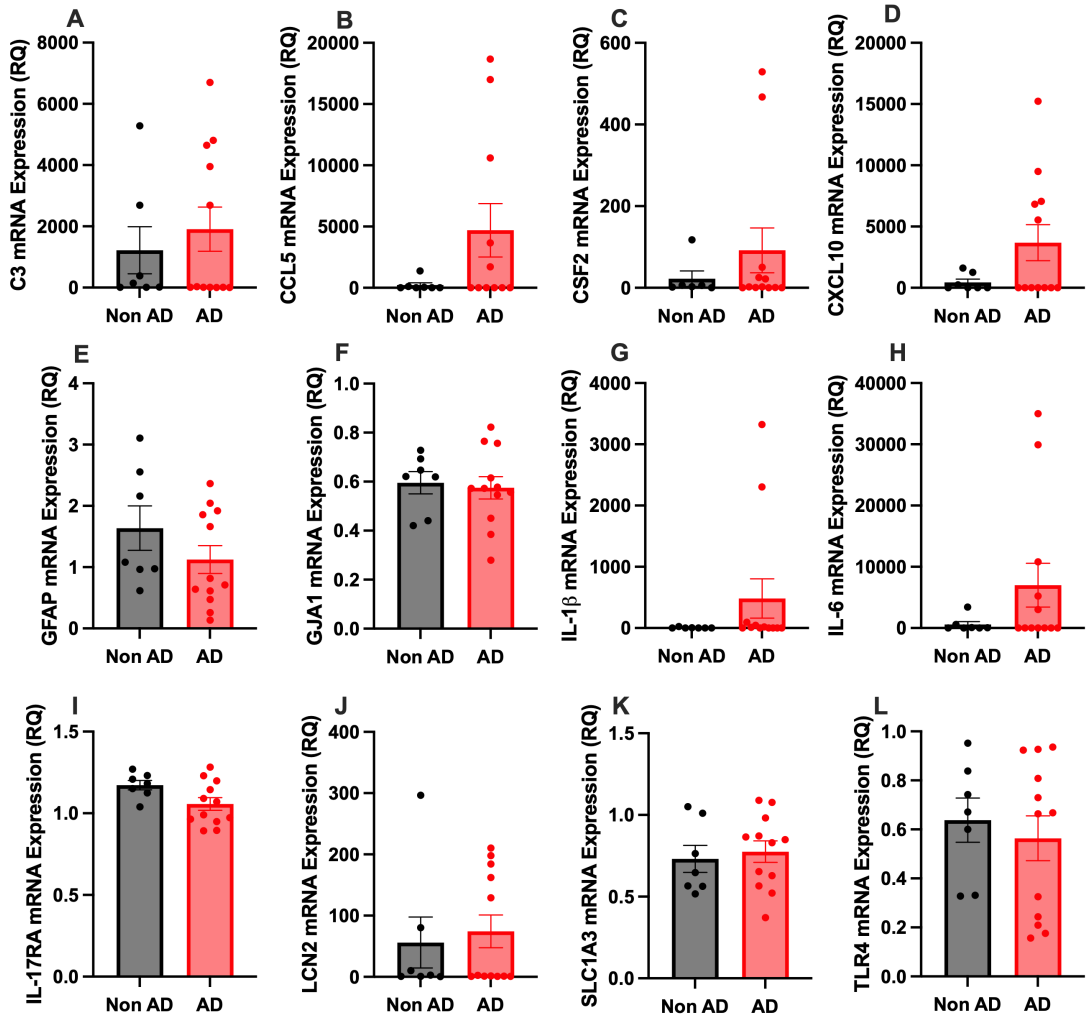


Figure 5.9 NAS2 cortical astrocytes gene expression in response to stimulated PBMCs conditioned media from non-Alzheimer's disease /MCI and Alzheimer's disease patients

*NAS2 astrocyte gene expression (RQ) when treated with 10% (v/v) conditioned PBMCs media from non-AD/MCI (N=6-7) and AD patients (N=11-12) for 24 hours was confirmed by RT-qPCR. Graphical representation of mRNA expression (RQ) of C3 (**A**), CCL5 (**B**), CSF2 (**C**), CXCL10 (**D**), GFAP (**E**), GJA1*

*(**F**), IL-1β (**G**), IL-6 (**H**), IL-17RA (**I**), LCN2 (**J**), SLC1A3 (**K**) and TLR4 (**L**) in treated astrocytes. Data, presented as mean +/- SEM, were analysed by unpaired t test or Mann Whitney when appropriate for non-parametric data.*

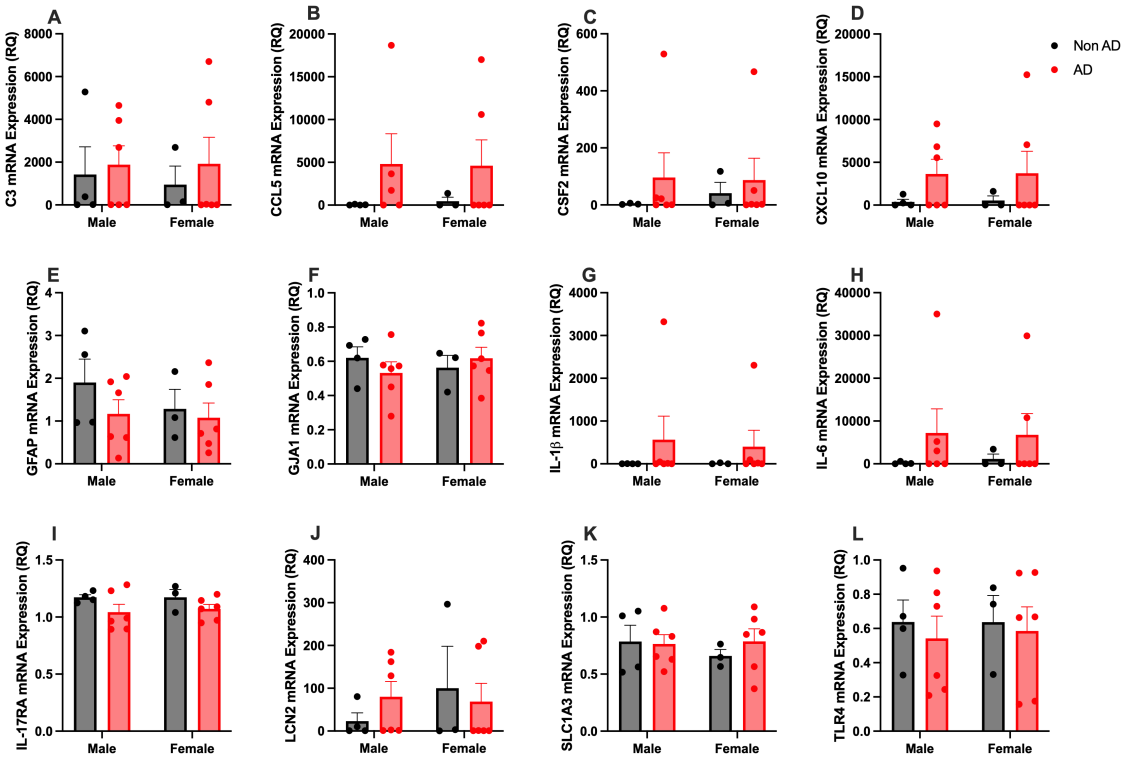


Figure 5.10 NAS2 cortical astrocytes mRNA gene expression in response to stimulated PBMCs conditioned media from male and female non-Alzheimer's disease/MCI and Alzheimer's disease patients

*NAS2 astrocytes gene expression (RQ) when treated with 10% (v/v) conditioned PBMCs media from male (N=4) and female (N=3) non-AD/MCI and male (N=5-6) and female (N=6) AD patients for 24 hours was confirmed by RT-qPCR. Graphical representation of mRNA expression (RQ) of C3 (**A**), CCL5 (**B**), CSF2 (**C**), CXCL10 (**D**), GFAP (**E**), GJA1 (**F**), IL-1β (**G**), IL-6 (**H**), IL-17RA (**I**), LCN2 (**J**), SLC1A3 (**K**) and TLR4 (**L**) in treated astrocytes. Data, presented as mean +/- SEM, were analysed by two-way ANOVA and Šidák's post-hoc multiple comparison tests.*

Additionally, the effect of non-AD/MCI and AD CSF treatment on astrocyte gene expression was investigated. Astrocytes treated with diluted CSF from non-AD/MCI or AD patients reported no change in *C3, CCL5, CSF2, CXCL10* or *GFAP* gene expression (**Figure 5.11 A-E**). There was a trending decrease in *GJA1* expression in astrocytes treated with AD CSF but this did not reach statistical significance (**Figure**

5.11 F, p=0.0775). Astrocytes treated with CSF from non-AD/MCI or AD patients reported no change in *IL-1β, IL-6, IL-17RA, LCN2, SLC1A3* or *TLR4* gene expression (**Figure 5.11 G-L**).

Additionally, modulation of gene expression in astrocytes treated with male or female non-AD/MCI or AD CSF was then investigated (**Figure 5.12**). Two-way ANOVA reported no effect of AD pathology or sex on *C3, CCL5, CSF2, CXCL10* or *GFAP* expression in astrocytes treated with non-AD/MCI or AD CSF from males or females (**Figure 5.12 A-E**). According to two-way ANOVA, there was a trending decrease in *GJA1* gene expression with AD pathology reported as the main effect, however this did not reach significance (**Figure 5.12 F**, p=0.0698). Two-way ANOVA reported no effect of AD pathology or sex on *IL-1β, IL-6, IL-17RA, LCN2, SLC1A3* or *TLR4* gene expression in astrocytes treated with male or female non-AD/MCI or AD CSF (**Figure 5.12 G-L**).

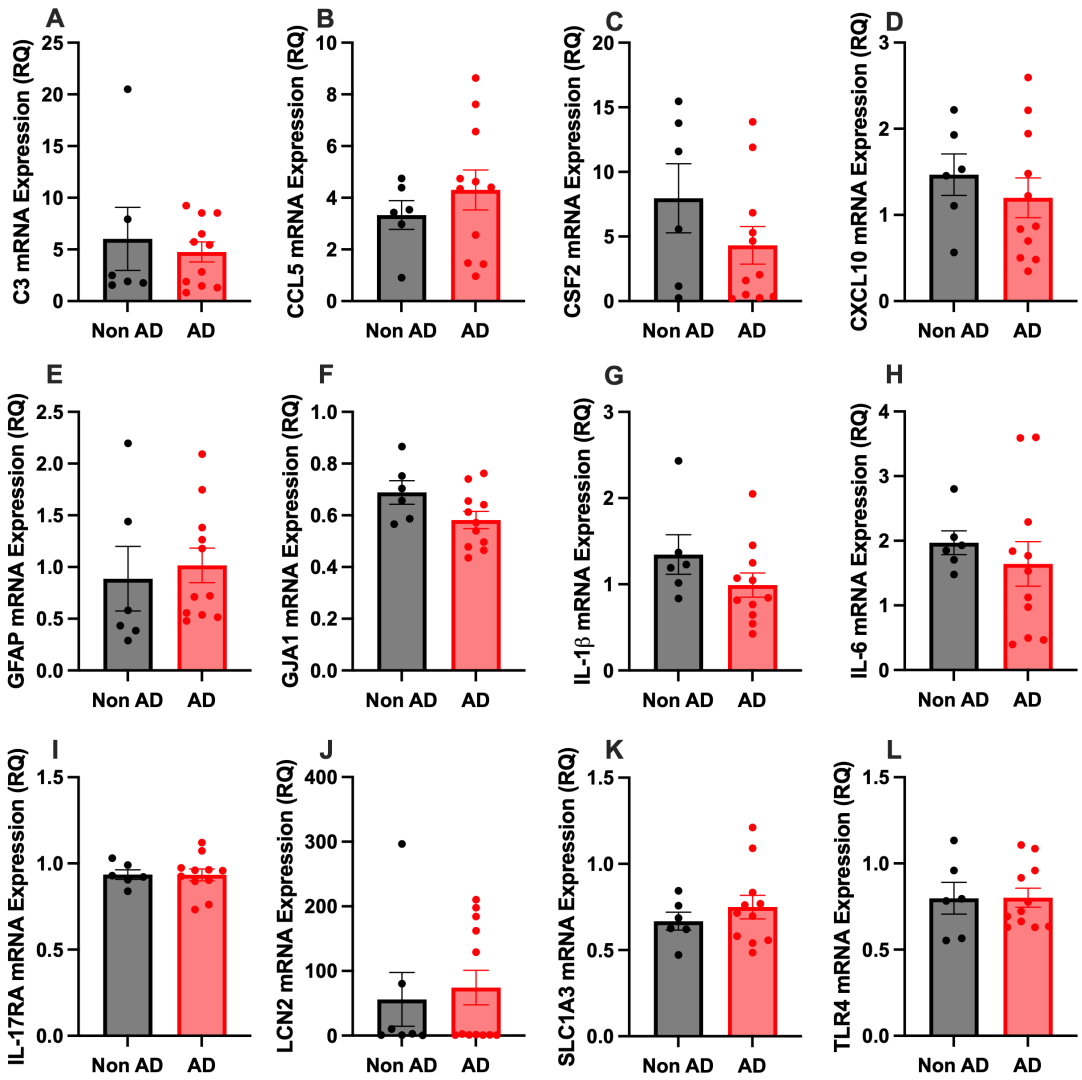


Figure 5.11 NAS2 cortical astrocytes mRNA gene expression in response to cerebrospinal fluid from non-Alzheimer's disease/MCI and Alzheimer's disease patients

*NAS2 astrocyte gene expression (RQ) when treated with 1:1 CSF media from non-AD/MCI (N=6) and AD (N=11) patients for 24 hours was confirmed by RT-qPCR. Graphical representation of mRNA expression (RQ) of C3 (**A**), CCL5 (**B**), CSF2 (**C**), CXCL10 (**D**), GFAP (**E**), GJA1 (**F**), IL-1β (**G**), IL-6 (**H**), IL-17RA (**I**), LCN2 (**J**), SLC1A3 (**K**) and TLR4 (**L**) in treated astrocytes. Data, presented as mean +/- SEM, were analysed by unpaired t test or Mann Whitney when appropriate for non-parametric data.*

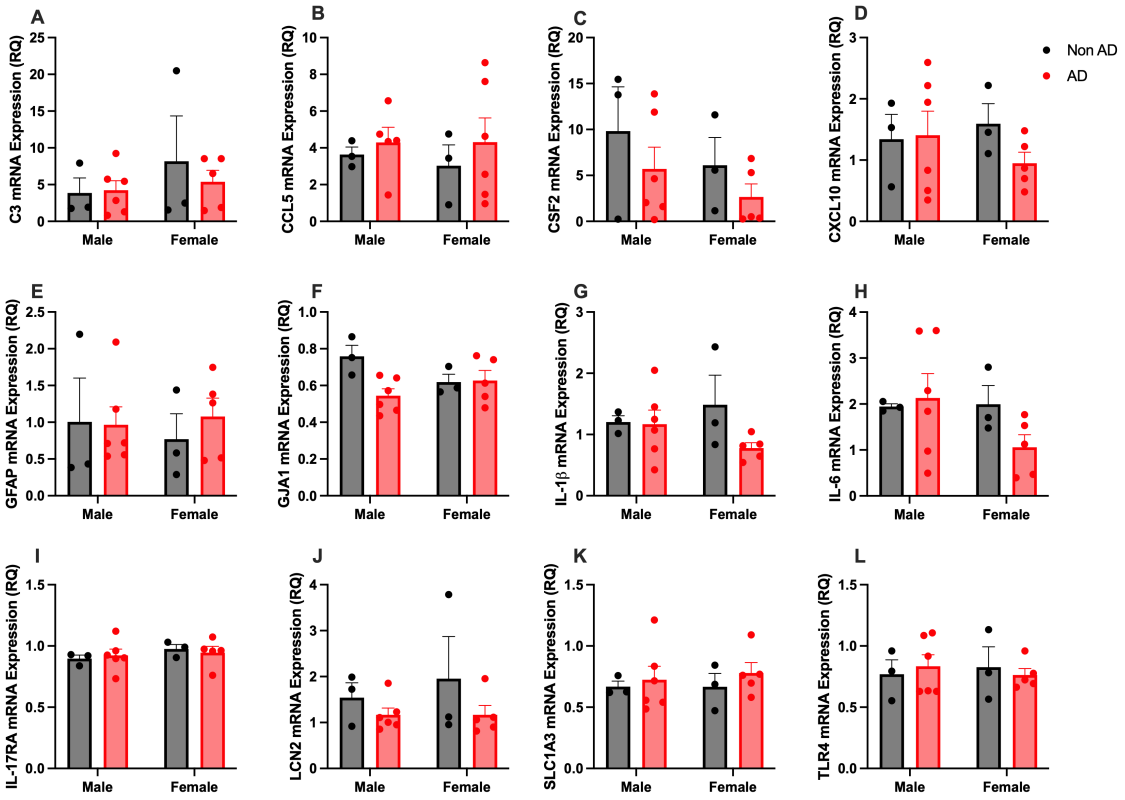


Figure 5.12 NAS2 cortical astrocytes mRNA gene expression in response to cerebrospinal fluid from male and female non-Alzheimer's disease/MCI and Alzheimer's disease patients

*NAS2 astrocyte gene expression (RQ) when treated with 1:1 CSF media from male (N=3) and female (N=3) non-AD/MCI and male (N=5-6) and female (N=5-6) AD patients for 24 hours was confirmed by RT-qPCR. Graphical representation of mRNA expression (RQ) of C3 (**A**), CCL5 (**B**), CSF2 (**C**), CXCL10 (**D**), GFAP (**E**), GJA1 (**F**), IL-1β (**G**), IL-6 (**H**), IL-17RA (**I**), LCN2 (**J**), SLC1A3 (**K**) and TLR4 (**L**) in treated astrocytes. Data, presented as mean +/- SEM, were analysed by two-way ANOVA and Šidák's post-hoc multiple comparison tests.*

Summary of results obtained while assessing the effects of PBMCs CM and CSF treatment from non-AD/MCI and AD male and female patients on iPSC derived astrocyte

- Mature astrocytes treated with PBMCs CM from non-AD/MCI or AD patients had a significant increase in RANTES compared to control. This was not observed once groups were separated by sex.
- Mature astrocytes treated with PBMCs CM from AD patients had a significant increase in GMCSF compared to control. This was not observed once groups were separated by sex.
- Mature astrocytes treated with CSF from non-AD/MCI or AD patients had a significant increase in IL-6 and CXCL10 secretion compared to control. This was not observed once groups were separated by sex.
- Mature astrocytes treated with AD CSF had a significant decrease in CXCL10 secretion compared to non-AD/MCI CSF treated astrocytes. This was not observed once groups were separated by sex.
- The effect of sex or AD pathology was not reported in astrocyte gene expression from either PBMC CM or CSF treatment.

iPSC derived Astrocytes treated with PBMCs CM	**Non-AD/MCI**	**AD**
Male	**RANTES**	**RANTES and GMCSF**
Female	**RANTES**	**RANTES and GMCSF**
iPSC derived Astrocytes treated with CSF	**Non-AD/MCI**	**AD**
Male	**IL-6 and CXCL10**	**IL-6, decrease in CXCL10**
Female	**IL-6 and CXCL10**	**IL-6, decrease in CXCL10**

Table 5.4 Summary of ELISA results of iPSC derived astrocytes treated with PBMCs conditioned media or CSF from non-AD/MCI or AD patients

5.4 Discussion

The first aim of this study was to confirm mature astrocytes derived from iPSCs adopt a reactive phenotype when treated with TIC factors. The increase in pro-inflammatory cytokine secretion and gene expression confirmed astrocytes had adopted a reactive phenotype which has been previously observed in (McComish et al., 2024).

Following on from this we could then investigate the response of astrocytes when treated with PBMC conditioned media or CSF from male and female non-AD/MCI and AD patients.

When treated with PBMCs CM from non-AD/MCI or AD patients, astrocytes had a significant increase in RANTES secretion compared to control. An increase in GMCSF was observed only in astrocytes treated with AD PBMCs CM compared to control. Increase in GMCSF and RANTES release from astrocytes has been reported in iPSC derived astrocytes treated with the TIC factors (McComish et al., 2024), hence this would indicate that the astrocytes have adopted a reactive phenotype when treated with patients' PBMCs CM.

Several studies have highlighted the potential neuroprotective effect of GMCSF in AD. GMCSF subcutaneous injections in APP_{V717F} $PS1_{M146L}$ mice has been reported to cause a significant decrease in amyloid burden, improvements in behavioural scores and an increase in microglia located in the hippocampus and entorhinal cortex (Boyd et al., 2010). Furthermore, daily subcutaneous injection of the drug sargramostim (GMCSF drug) for three weeks in mild to moderate AD patients reported immunomodulatory effects with increases in IL-6, TNF-α, IL-10 and decrease in IL-8 in the blood and a significant improvement in MMSE scores during follow up appointments (Potter et al., 2021). Intraperitoneal injections of GMCSF have also been reported to increase migration of Tregs into the CNS of $APP/PS1_{M146L}$ mice and lead to improvements in cognition (Kiyota et al., 2018). This treatment however did not affect Aß load but did cause a decrease in NOS2 expression in microglia indicating it may effect neuroinflammation in the CNS (Kiyota et al., 2018). In other studies the effect of GMCSF has been reported to be potentially harmful. GMCSF has been reported to exacerbate murine microglial responses to LPS insults with

increased TNF-α, IL-6 and NOS2 released from GMCSF 'primed' microglia compared to 'unprimed' microglia (Parajuli et al., 2012). This study also identified that GMCSF stimulation of microglia led to TLR4 activation via the ERK 1/2 pathway and CD14 activation via the p38 pathway (Parajuli et al., 2012). Thus, the increase of GMCSF reported in our study could potentially improve AD pathology due to Treg migration into CNS and reduction NOS microglial expression or it could also exacerbate inflammatory microglial responses in AD. As the increase in GMCSF was only identified in astrocytes treated with AD patients PBMCs CM compared to control, it would be prudent to explore more cytokines specifically altered in the AD CM including C1q and IL-1α as our MSD analysis of PBMCs CM (**Figure 4.14**) reported no difference between cytokine concentrations of non-AD and AD individuals.

In relation to RANTES, it has been reported to contribute to the transmigration of T cells across the BBB (Lanfranco et al., 2018, Ubogu et al., 2006). In an astrocyte specific RANTES KO mouse model after stroke, a significant decrease in $CD8^+$ but not $CD4^+$ T cells was reported in the CNS (Zhou et al., 2024). Additionally, in relation to BBB, astrocyte specific RANTES KO mice had increased expression of tight junction markers such as ZO-1 and occludin after stroke indicating the potential role RANTES can play in BBB integrity (Zhou et al., 2024). One of the receptors that RANTES can bind to is CCR5 which has also been shown to be expressed by microglia (Fantuzzi et al., 2019) and significantly increased in AD post mortem brains (Xia et al., 1998). Furthermore, the use of a CCR5 antagonist in a rat model of AD reported a reduction in microglia and astrocytes in the hippocampus (Rosi et al., 2005). Therefore the increase in RANTES released by astrocytes in our study could play a role in microglial migration, BBB integrity and potentially increase the transmigration of other immune cells into the CNS including Tregs and $CD8^+$ T cells.

As RANTES secretion is significantly increased in both astrocytes treated with non-AD and AD PBMCs CM, it is difficult to decipher which cytokine(s) may be causing RANTES secretion. As has been previously reported, iPSC derived astrocytes treated with the TIC factors TNF-α, IL-1α and C1q, revealed a significant increase in RANTES secretion (McComish et al., 2024). In our study, TNF-α concentration was not significantly different between non-AD and AD patients according to MSD

analysis in Chapter 4 (**Figure 4.14**). Hence, TNF-α present in the CM could potentially contribute to the increase in RANTES secretion observed in our study. It would be helpful to assess the presence of C1q, IL-1α or IL-1ß via ELISA or MSD analysis to further elucidate the synergistic relationship of these cytokines in relation to RANTES astrocyte secretion.

Astrocytes treated with CSF from non-AD/MCI or AD patients had a significant increase in IL-6 and CXCL10 compared to control. Additionally, CXCL10 secretion from astrocytes treated with AD CSF had a significant decrease compared to astrocytes treated with non-AD CSF, indicating a specific astrocyte response to AD pathology.

With regards to IL-6, studies have reported the detrimental effect of IL-6 in relation to neuroinflammation and BBB integrity. In a recent study, iPSC derived reactive astrocytes treated with TIC factors had a significant increase in IL-6 secretion (McComish et al., 2024) indicating that astrocytes in our study treated with non-AD and AD CSF adopt a similar reactive phenotype. In one mouse study, IL-6 production restricted to exclusively astrocytes led to a significant increase in the number of microglia, macrophages and T cell infiltration (Recasens et al., 2021). Furthermore, IL-6 released from astrocytes had an effect on microglial morphology with a more ramified rounded shape adopted compared to control (Recasens et al., 2021). Perforant pathway transection lesions in this IL-6 mouse model also led to a significant increase in macrophage and microglial proliferation and a decrease in collateral sprouting of mossy fibres around the lesion site (Recasens et al., 2021). The effect of IL-6 on the BBB has also been investigated. Immortalised mouse brain endothelial cells treated with IL-6 for 24 hours led to a significant decrease in protein expression of BBB tight junction markers ZO-1 and claudin-5 and increased permeability using a sodium-fluoride assay (Voirin et al., 2020). Therefore, the increased expression of IL-6 by astrocytes reported in our study could potentially impact on BBB integrity, infiltration of immune cells along with an increased inflammatory response.

As IL-6 secretion is significantly increased in both astrocytes treated with non-AD and AD CSF it is difficult to decipher which cytokine(s) or potentially other biomarkers (total tau, p-tau, GFAP, NfL or amyloid) may be causing this IL-6

induction. IL-6 astrocyte secretion has been suggested to be mediated through the presence of TNF-α and IL-1ß (Van Wagoner et al., 1999) and the TIC factors TNF-α, IL-1α and C1q (McComish et al., 2024). It is interesting that TNF-α was not detected in the CSF in this study Chapter 4 (**Figure 4.16**) which may indicate that this IL-6 response is mediated through other cytokines present. It would be helpful to assess the presence of C1q, IL-1α or IL-1ß via ELISA or MSD analysis to further elucidate the cause of this IL-6 secretion.

With regards to CXCL10, studies have reported a significant increase in $CXCL10^+$ astrocytes located near senile plaques (Xia et al., 2000) suggesting CXCL10 expression increases migration of astrocytes to the plaque region (Lai et al., 2013). In other models of CNS pathology, astrocyte mediated CXCL10 secretion has led to BBB disruption and pyroptosis of endothelial cells (binding to CXCR3) via the cGAS/AIM2 signalling pathway in a mouse model of cerebral haemorrhage (Sheng et al., 2025). Additionally, in a mouse model of TBI the recruitment of $CD8^+$ T cells into the CNS was mediated by a subpopulation of astrocytes expressing IFN regulatory factor 1 and secreting CXCL10 leading to BBB dysfunction (Cui et al., 2025). Therefore the increase in CXCL10 secretion observed in our study would suggest a potential role in BBB disruption and T cell migration.

Additionally, we reported a decrease in CXCL10 secretion in astrocytes treated with AD CSF compared to non-AD/MCI CSF. It could be postulated that the significant decrease in IFN-γ in CSF from AD patients reported in Chapter 4 (**Figure 4.16**) could cause this decrease in CXCL10 secretion in astrocytes which has been reported to be a key stimulator of CXCL10 astrocyte secretion in human and mouse cell culture studies (Bakmiwewa et al., 2016). The implication of this CXCL10 decrease in astrocytes treated with AD CSF, could be a reduced migration of immune cells across the BBB.

Whether the alterations in these cytokine responses are beneficial or detrimental however remains to be seen. Future studies could co-culture iPSC derived microglia and astrocytes or astrocytes and T cells from non-AD and AD patients to investigate the expression of CXCR3 on these immune cells and if this is altered in AD patients. Additionally using the conditioned media from these co-

culture experiments on iPSC derived neurons could further elucidate the harm or benefit of these synergistic cytokine relationships in AD.

With regards to RT-qPCR analysis there was no significant difference detected in astrocytes treated with non-AD/MCI or AD PBMCs CM or CSF. Therefore it would be prudent to incorporate different incubation times with CSF and PBMC CM to investigate changes in gene expression before and after 24 hours. Furthermore the antigen capacity of astrocytes could be assessed at the gene level by investigating genes such *MHC-I, MHC-II, CD40, CD80* and *CD86* to understand any possible changes in gene expression when astrocytes are treated with CSF or PBMC CM and how it differs between the sexes.

It is worth noting as seen in the ELISA analysis PBMC CM and CSF treatment did not warrant the same response in astrocyte gene expression. Furthermore, the gene that was trending towards a decrease in astrocytes treated with AD PBMCs CM was *IL-17RA* whereas astrocytes treated with CSF from AD patients trended towards a decrease in *GJA1* compare to non-AD/MCI CSF. As they did not reach statistical significance conclusions cannot be drawn from these findings yet.

It is important to note, that segregating based on sex as well as AD pathology led to a small sample size in all of the astrocyte treatment groups. Therefore, the addition of more non-AD/MCI and AD male and female samples would allow the effect of sex on astrocyte response to be further understood.

Furthermore the addition of cognitively normal individuals would be necessary to expand our comprehension of the modulatory effect of cytokines on astrocytes through the AD timeline. A better understanding of when astrocytes begin to react to AD pathology and how it may differ between males and females in turn would help determine potential timings for pharmaceutical interventions to have the most substantial effect on disease pathology.

6 Final Discussion

6.1 Introduction

AD is the most common cause of dementia with 55 million people worldwide living with dementia currently (Alzheimer's Disease International). Additionally, AD affects approximately 5% of the over 65 population (AAR, 2023) with dementia cases projected to reach up to 152.8 million by 2050 (Nichols et al., 2022). Furthermore, females are at a greater risk of developing AD with females making up two thirds of AD patients in Europe and North America (Gustavsson et al., 2022). These figures indicate the rationale for investigating the role that immune cells such as T cells and glial cells such as astrocytes play in AD pathogenesis and how sex may contribute to the overall risk of AD diagnosis. It has also been discussed that "pure" AD is usually the exception rather than the rule with the majority of patients presenting with co-morbidities to clinicians (Dolphin et al., 2024). Consequently, the multifactorial nature of this disease implies many components can play a role in an individual's risk such as genetics, environment and sex.

6.2 Findings and future directions

The aim of this project was to understand the immunomodulatory effect that sex can play in AD progression in both animal models using the APP/PS1 model, patient samples and induced pluripotent stem cell derived astrocytes.

Our initial investigation in the APP/PS1 animal model reported sexual dimorphic responses in T cell subsets along with alterations in astrocyte GFAP expression and antigen presenting capacity. This highlights the role that sex can play in the progression of the disease as males and females from this cohort did not respond uniformly. The limitation in this study was using only one age group when AD pathology is established. It would be prudent therefore to add younger age groups such as young adult and middle-age adult mice to further elucidate changes in T cell and astrocyte response to AD prior to the presence of extensive plaque deposition.

By including a younger age group (2-3 months), we could identify potential sex differences in astrocyte GFAP expression along with antigen presentation capacity at baseline prior to disease onset. Additionally, the proportion of T cell subsets in $CD4^+$ and $CD8^+$ T cells could also be determined to identify if any potential sex differences exist in young APP/PS1 adults. This would allow us to understand the biological

foundation in relation to astrocytes and T cells that males and females possess and how this may protect or harm against AD pathogenesis. For example if GFAP expression is greater in males or females prior to the presence of Aß plaques that would highlight a potential predisposition one sex may have to enhanced astrocyte reactivity at AD onset.

As AD is a progressive disease the responses of astrocytes and T cells at the onset of AD when plaque deposition has just begun versus at the later stages of AD pathology may also differ. Therefore the inclusion of a middle-aged cohort (6-9 months), would grant us the opportunity to elucidate how males and females respond to counteract the onset of AD pathology. Additionally, the consequences of these T cell or astrocyte responses in early stages of AD may help us understand features identified in later stages of AD such as a higher plaque load in females and decreased proportion of Tregs in the brain of APP/PS1 males.

If specific sexual dimorphisms are identified in the early stages of AD pathology (6-9 months), this could open up avenues to assess certain therapeutics that may be more appropriate in one sex at a certain time rather than treating both sexes uniformly. For example, we identified a significant increase in the proportion of $CD8^+$ TNF-α^+ cells in APP/PS1 females compared to APP/PS1 males at 16-17 months. If an increase in this T cell subset was also identified only in females at the early stage of AD, this could offer an appropriate therapeutic window to decrease the proportion of this T cell subset at the onset of AD and may improve AD pathogenesis for females. This potentially could improve the efficaciousness of the chosen drug which perhaps could be lost if the treatment was given at the later AD stage or given to males when it appears to be unique to APP/PS1 females.

Currently, the majority of immunotherapies undergoing clinical trials are only suitable for early stages of AD (van Dyck et al., 2023, Sims et al., 2023). Consequently this indicates that the onset of AD may be more malleable to pharmaceutical interventions to slow down AD progression and perhaps improve disease severity. Thus the inclusion of young adult and middle-aged APP/PS1 mice would be very helpful in understanding the predispositions and alterations in astrocytes and T cells throughout AD progression and how they may be targeted in AD treatments.

We then investigated the T cell and cytokine profile of non-AD and AD male and female patients using PBMCs and CSF samples. Due to the low sample size the findings were less informative in relation to T cell subsets compared to other studies identifying changes in T cells in AD patients (Gate et al., 2020, van Olst et al., 2024). However data obtained while analysing CSF samples revealed more changes in cytokine expression between male and female patients compared to analysis from cytokine expression in PBMC samples. A common issue with human studies is the inherent variability between individuals which must be overcome with large sample sizes and identifying more homogenous cohorts to reduce variability.

Future studies could also include plasma isolated from blood samples to investigate the baseline cytokine concentration along with AD biomarkers such as p-tau, GFAP and S100ß which have been shown to increase in AD patients (Dyer et al., 2024, Nehra et al., 2025). This would allow us to elucidate how changes in plasma contents may correlate with T cell subsets in AD patients and how it may differ between the sexes. It would also improve our understanding of the synergistic relationship of the CSF and the blood in relation to the BBB and potential dysfunction identified in AD (Kurz et al., 2022).

Furthermore a longitudinal study with the inclusion of cognitively normal individuals from middle age onwards would further our understanding of the preclinical and prodromal alterations of the adaptive and innate immune profile in individuals that may go on to develop AD. This would offer a retrospective opportunity to map modulations in the innate and adaptive immune system and inform us on timepoints that are crucial for pharmaceutical intervention and how that is determined.

The effect of treating iPSC derived astrocytes with CSF and PBMC conditioned media gave us an opportunity to understand both of these mediums' role in AD pathology and their interaction with the most abundant cell in the CNS which forms a key part of the neurovascular unit (Gong et al., 2025, Nehra et al., 2022).

In this study, we identified a reduction in CXCL10 expression in astrocytes treated with CSF from AD patients compared to non-AD patients. In future studies, it would be helpful to widen our analysis of the CSF contents by investigating the

presence of biomarkers such as tau, amyloid, GFAP and NfL present in the CSF and how that may be impacting astrocyte cytokine modulation.

We also reported a heterogenous response from astrocytes treated with conditioned media versus CSF. Therefore this would justify the continued use of both PBMCs conditioned media and CSF in relation to AD studies to further ameliorate both of their roles in AD pathogenesis. With the increase of sample size overtime trends observed here may reach statistical significance and the cytokine profile of male and females in relation to AD will become more apparent. Additionally, by generating iPSC derived microglia and neurons to attempt co-cultures we could identify synergistic mechanisms at play in AD. The inclusion of iPSC lines from different male and female *APOE* alleles (E2, E3 and E4) would be helpful to investigate the role *APOE* plays in AD pathology and add a genetic component to the overall study.

6.3 Is sex a risk factor?

Sex differences are not unique to AD with other diseases reported to have disparity between the sexes with some treatments having better outcomes for females or males. In the case of vaccinations against viruses, females are reported to possess an enhanced response with protective antibodies twice as high in females compared to age matched males (Klein et al., 2010). This enhanced vaccine-induced immune response in females has been suggested to be related to circulating oestradiol levels and is lost in post-menopausal women when circulating estrogen is reduced (Potluri et al., 2019). Therefore the similar post-vaccination immune response observed in males and females older than 65 can be explained by the loss of circulating oestradiol in females and indicates the significant role that sex steroid hormones can play in immune modulation (Potluri et al., 2019).

However, there are other conditions where being female can lead to less effective treatments such as rheumatoid arthritis and psoriatic arthritis where males have better treatment outcomes compared to females when using TNF inhibitors (Lee et al., 2014) (Højgaard et al., 2018). Sex is also reported to contribute to an individual's risk of developing an autoimmune disease with females making up a greater proportion of autoimmune cases such as systemic lupus erythematosus

(SLE) (Kronzer et al., 2021, Lovell and Anguera, 2025). The evasion of certain X linked genes such as TLR7 has been reported in women with SLE and men with SLE and Klinefelter syndrome (carry one or more supernumerary X chromosomes) (Souyris et al., 2018). This highlights the risk of potential aberrant X-linked gene expression in relation to immune responses and how it can contribute to the female bias observed in autoimmune diseases (Kronzer et al., 2021, Lovell and Anguera, 2025).

Another area of disease treatment where sex differences are observed is the use of checkpoint inhibitors in cancer treatments. It has been reported that the inclusion of checkpoint inhibitors in cancer treatment has led to improvements in overall survival and progression free survival in both male and female patients (Klein and Flanagan, 2016). However, the efficacy of these inhibitors is greater in males than females for cancers such as melanoma and non-small cell lung cancer (Klein and Flanagan, 2016, Grassadonia et al., 2018).

Other neurological conditions and diseases report a sex disparity among patients with a higher prevalence of Parkinson's disease in males compared to females (Baldereschi et al., 2000) and a greater proportion of females diagnosed with Multiple Sclerosis (Koch-Henriksen and Sørensen, 2010). Taken together these studies bring our attention to the broad effect sex has on many conditions and diseases. Hence it should not come as a surprise to observe differences in the prevalence of AD among the sexes (Gustavsson et al., 2022). It has been reported that sex can also modulate the duration of stages of AD with females progressing from mild to moderate AD at a higher rate than males (Vermunt et al., 2019). In more recent years sex differences in microglia in AD have identified key changes in male and female microglial phenotypes in AD mouse models (Guillot-Sestier et al., 2021, O'Neill et al., 2022, Mela et al., 2023) and human studies (Sala Frigerio et al., 2019, Sanfilippo et al., 2022). Other studies reported differences in immune cell populations at different disease stages depending on the sex of the patient (van Olst et al., 2024). In females, $CD8^+$, $CD57^+$ $CD8^+$ TEMRA (reduced proliferative ability susceptible to cell death (Verma et al., 2017)) and $PD1^-$ $CD57^+$ $CD8^+$ TEMRA (reduced immunosuppression and enhanced cytotoxic ability (van Olst et al., 2024) T cell populations increased at an earlier stage of disease progression (MCI-AD transition

stage) compared to males where these cell populations only appeared once AD dementia was established (van Olst et al., 2024).

Thus, further examination of cytokines and biomarkers present in the CSF and the blood and alterations in T cell populations in patients at different stages of AD from prodromal to severe AD could open up avenues for timing of treatment driven by the sex differences in AD rather than pathology based timepoints or cognitive scores. Additionally, the access to iPSC derived astrocytes garners an opportunity to include another cell implicated in this multifactorial disease. Promising work carried out by Vatine and colleagues successfully generated a human iPSC derived BBB chip in recent years (Vatine et al., 2019). In this study iPSC derived brain microvascular endothelial like cells successfully emulated the transendothelial electrical resistance of the BBB and predicted blood-to-brain permeability of pharmaceutical drugs (Vatine et al., 2019). This study was also successful in generating a BBB Huntington's Disease model with disease related BBB features detected (Vatine et al., 2019). We could apply this model in our study to treat an iPSC derived BBB including iPSC derived brain microvascular endothelial cells, astrocytes and neurons with the CSF and conditioned media of AD patients to obtain a better understanding of each cell's role in AD pathology. Additionally, by including both males and females in the study we could identify the modulatory role that sex can play in BBB integrity and how this can harm or protect against AD progression.

Another key area that was not addressed in our study was the potential role that menopause plays in AD and immune response. Hormonal replacement therapy (HRT) in women to counteract the loss of circulating estrogen has reported to affect the immune system, resulting in an increase in lymphocytes (T cells, B cells and natural killer cells) compared to post-menopausal women not receiving HRT (Kamada et al., 2000) and circulating levels of monocytes increasing to levels reported in menstruating females (Ben-Hur et al., 1995). Recent systematic and meta-analysis in relation to HRT, has reported a 32% decrease in the risk of developing AD with the use of estrogen in midlife (Nerattini et al., 2023). However the use of estrogen in late life did indicate a potential increased risk in developing AD but did not reach significance (Nerattini et al., 2023). Once again this highlights the modulatory effect of sex steroid hormones throughout a women's progression through menopause.

Furthermore, the combined effect of genotype (*APOE4*) and menopause also illustrates the multifactorial nature of AD. The administration of HRT in *APOE4* females (above the age of 50 not diagnosed with AD but carrier of *APOE4* allele) has been reported to improve cognition scores and increase the size of brain regions affected by AD such as the amygdala and entorhinal cortex compared to *APOE4* carriers not using HRT (Saleh et al., 2023). Consequently, it highlights the complex convergence of genetics, hormones and the immune system in AD and proposes that a multifactorial disease requires several components working synergistically to achieve an overall reduction in AD risk.

6.4 The prospect of immunotherapies

Until recently, the only drugs prescribed to treat Alzheimer's disease addressed symptoms related to AD. For mild to moderate AD a family of drugs related to cholinesterase inhibition were licensed to prevent the breakdown of acetylcholine suggested to help with the noted neuronal loss and hence reduction of acetylcholine present in AD (Long and Holtzman, 2019). In moderate to severe cases of AD, the glutamate inhibitor memantine has been licensed to reduce the amount of glutamate release suggested to protect against neurotoxicity which leads to neuronal loss (Long and Holtzman, 2019). However, both these treatments do not cure or prevent the progression of AD and can only treat AD symptoms.

For many years immunotherapies for AD treatment such as Bapineuzumab (Salloway et al., 2014), Solnezumab (Doody et al., 2014) and Crenezumab (Cummings et al., 2018) failed to report a significant difference in cognitive scores compared to placebo. However, Lecanemab was the first drug to report an efficacious result after 18 months of treatment in mild AD patients cognitive scores in phase III clinical trial (van Dyck et al., 2023). Additionally, another immunotherapy Donanemab has now also reported a significant slowing down of cognitive decline in mild AD patients (Sims et al., 2023). Just this year the European Medicines Agency licensed the use of Lecanemab to treat patients diagnosed with mild AD (Agency, 2025). This is a promising development in AD treatment however it should be noted that stringent guidance has been outlined with regards to APOE4 homozygous patients. Due to the increased risk observed in this cohort in potential amyloid related

imaging abnormalities (ARIA) individuals with E4E4 allele are not eligible for this treatment in Europe (van Dyck et al., 2023). Furthermore, patients with later stages of AD are also not eligible for this treatment which means current pre-clinical and prodromal screening will become more crucial to ensure patients can enrol in therapies at the appropriate time. As more patients begin to be treated with immunotherapies the underlying contributions of innate and adaptive immune cells in the periphery and the CNS can be further interrogated. As has been reported above in immunotherapies for other diseases, Lecanemab did report a sex difference in the initial phase III study. The efficaciousness of the drug was more pronounced in males than females (van Dyck et al., 2023). This once again highlights the need for future studies interrogating the possible underpinnings of the sex disparity in treatment. Considering females make up a larger proportion of AD patients in Europe and North America (Gustavsson et al., 2022) this could possibly lead to a disappointing outcome in relation to treatment. It is also reported that females progress into moderate AD quicker than males (Vermunt et al., 2019) therefore the window of treatment to use this disease modifying drug is also smaller for females.

Additionally, the costs of immunotherapies like Lecanemab to health services has been estimated to be approximately €133 billion for the European union (Jönsson et al., 2023). Due to the nature of immunotherapies which in the case of Lecanemab involves intravenous administration every two weeks and several MRI scans it has also been suggested that trials should report quality of life indicators as well as clinical outcomes and broaden the scope of assessment to be more patient centred (Dolphin et al., 2024).

Another potential immunotherapy that has been suggested to treat AD is vaccines. One of the first attempts of this however was pulled from clinical trials after inducing meningoencephalitis in a subset of AD patients (Orgogozo et al., 2003). However, in more recent times the safety and tolerability of active Aß40 vaccine was achieved indicating that is possible to generate safer vaccines in the AD field (Lacosta et al., 2018). As vaccines offer a less invasive and demanding schedule compared to passive immunotherapies they could be an attractive alternative if deemed effective. However, this would also open up the issue reported with older age individuals in relation to their reduced ability to mount immune responses after vaccination caused

by immunosenescence in B and T cells (Crooke et al., 2019, Wagner et al., 2018). Therefore, vaccine treatments for AD may involve assessing antibody titres of individuals to determine if they have developed a response or if booster doses are required which is seen in other vaccination programmes in the elderly.

6.5 Conclusions

The intention of this study was to contribute to our understanding of the role T cells and astrocytes play in AD and elucidate the modulatory factor of sex. Ultimately a key area of focus for developing precision medicine for AD and other CNS disorders is the identification of sex-dependant phenotypic variability for the important cell players reported: microglia, astrocytes and T cells. While AD symptoms manifest in old age, deciphering the early cellular changes in the prodromal stage of AD is paramount and warrants the development of more impactful therapeutic interventions with hopes to preserve brain health in both males and females.

7 Bibliography

AAR 2023. 2023 Alzheimer's disease facts and figures. *Alzheimers Dement,* 19**,** 1598-1695.

ABBAS, S., BELLAVER, B., FERREIRA, P. C. L., POVALA, G., FERRARI-SOUZA, J. P., LUSSIER, F. Z., ZALZALE, H., LEMAIRE, P. C., SOARES, C., ROHDEN, F., AGUZZOLI, C. S., CABRERA, A., LEFFA, D. T., THERRIAULT, J., TISSOT, C., SERVAES, S., MACEDO, A. C., CHAMOUN, M., BEZGIN, G., STEVENSON, J., STEVENSON, A., RAHMOUNI, N., PALLEN, V., KARIKARI, T. K., ASHTON, N. J., BENEDET, A. L., ZETTERBERG, H., BLENNOW, K., ROSA-NETO, P. & PASCOAL, T. A. 2023. Sex impacts the association of plasma Glial Fibrillary Acidic Protein with neurodegeneration in Alzheimer's disease. *Alzheimer's & Dementia,* 19**,** e076402.

ABDELMOATY, M. M., YEAPURI, P., MACHHI, J., LU, Y., NAMMINGA, K. L., KADRY, R., LU, E., BHATTARAI, S., MOSLEY, R. L. & GENDELMAN, H. E. 2023. Immune senescence in aged APP/PS1 mice. *NeuroImmune Pharm Ther,* 2**,** 317-330.

AFSHAN, G., AFZAL, N. & QURESHI, S. 2012. CD4+CD25(hi) regulatory T cells in healthy males and females mediate gender difference in the prevalence of autoimmune diseases. *Clin Lab,* 58**,** 567-71.

AGENCY, E. M. 2025. *Leqembi* [Online]. Available: https://www.ema.europa.eu/en/medicines/human/EPAR/leqembi [Accessed 18/09/2025 2025].

AHN, K.-C., LEARMAN, C. R., DUNBAR, G. L., MAITI, P., JANG, W.-C., CHA, H.-C. & SONG, M.-S. 2018. Characterization of Impaired Cerebrovascular Structure in APP/PS1 Mouse Brains. *Neuroscience,* 385**,** 246-254.

ALI, M., GARCIA, P., LUNKES, L. P., SCIORTINO, A., THOMAS, M., HEURTAUX, T., GRZYB, K., HALDER, R., COOWAR, D., SKUPIN, A., BUÉE, L., BLUM, D., BUTTINI, M. & GLAAB, E. 2024. Single cell transcriptome analysis of the THY-Tau22 mouse model of Alzheimer's disease reveals sex-dependent dysregulations. *Cell Death Discov,* 10**,** 119.

ALI, M., HUARTE, O. U., HEURTAUX, T., GARCIA, P., RODRIGUEZ, B. P., GRZYB, K., HALDER, R., SKUPIN, A., BUTTINI, M. & GLAAB, E. 2022. Single-Cell Transcriptional Profiling and Gene Regulatory Network Modeling in Tg2576 Mice Reveal Gender-Dependent Molecular Features Preceding Alzheimer-Like Pathologies. *Mol Neurobiol*.

ALLEN, N. J., BENNETT, M. L., FOO, L. C., WANG, G. X., CHAKRABORTY, C., SMITH, S. J. & BARRES, B. A. 2012. Astrocyte glypicans 4 and 6 promote formation of excitatory synapses via GluA1 AMPA receptors. *Nature,* 486**,** 410-4.

ALPÍZAR-RODRÍGUEZ, D., PLUCHINO, N., CANNY, G., GABAY, C. & FINCKH, A. 2017. The role of female hormonal factors in the development of rheumatoid arthritis. *Rheumatology (Oxford),* 56**,** 1254-1263.

ALTENDORFER, B., UNGER, M. S., POUPARDIN, R., HOOG, A., ASSLABER, D., GRATZ, I. K., MROWETZ, H., BENEDETTI, A., BESSA DE SOUSA, D. M., GREIL, R., EGLE, A., GATE, D., WYSS-CORAY, T. & AIGNER, L. 2022. Transcriptomic Profiling Identifies CD8⁺ T Cells in the Brain of Aged and Alzheimer's Disease Transgenic Mice as Tissue-Resident Memory T Cells. *The Journal of Immunology***,** ji2100737.

ALVES, S., CHURLAUD, G., AUDRAIN, M., MICHAELSEN-PREUSSE, K., FOL, R., SOUCHET, B., BRAUDEAU, J., KORTE, M., KLATZMANN, D. & CARTIER, N. 2017. Interleukin-2 improves amyloid pathology, synaptic failure and memory in Alzheimer's disease mice. *Brain,* 140**,** 826-842.

ARRANZ, J., ZHU, N., RUBIO-GUERRA, S., RODRÍGUEZ-BAZ, Í., FERRER, R., CARMONA-IRAGUI, M., BARROETA, I., ILLÁN-GALA, I., SANTOS-SANTOS, M., FORTEA, J., LLEÓ, A., TONDO, M. & ALCOLEA, D. 2024. Diagnostic performance of plasma pTau(217), pTau(181), Aβ(1-42) and Aβ(1-40) in the LUMIPULSE automated platform for the detection of Alzheimer disease. *Alzheimers Res Ther,* 16**,** 139.

ASHTON, N. J., BRUM, W. S., DI MOLFETTA, G., BENEDET, A. L., ARSLAN, B., JONAITIS, E., LANGHOUGH, R. E., CODY, K., WILSON, R., CARLSSON, C. M., VANMECHELEN, E., MONTOLIU-GAYA, L., LANTERO-RODRIGUEZ, J., RAHMOUNI, N., TISSOT, C., STEVENSON, J., SERVAES, S., THERRIAULT, J., PASCOAL, T., LLEÓ, A., ALCOLEA, D., FORTEA, J., ROSA-NETO, P., JOHNSON, S., JEROMIN, A., BLENNOW, K. & ZETTERBERG, H. 2024. Diagnostic Accuracy of a Plasma Phosphorylated Tau 217 Immunoassay for Alzheimer Disease Pathology. *JAMA Neurol,* 81**,** 255-263.

BACHSTETTER, A. D., LUTSHUMBA, J., WINFORD, E., ABNER, E. L., MARTIN, B. J., HARP, J. P., VAN ELDIK, L. J., SCHMITT, F. A., WILCOCK, D. M., STOWE, A. M., JICHA, G. A. & NIKOLAJCZYK, B. S. 2023. A blunted T(H)17 cytokine signature in women with mild cognitive impairment: insights from inflammatory profiling of a community-based cohort of older adults. *Brain Commun,* 5**,** fcad259.

BAEK, H., YE, M., KANG, G. H., LEE, C., LEE, G., CHOI, D. B., JUNG, J., KIM, H., LEE, S., KIM, J. S., LEE, H. J., SHIM, I., LEE, J. H. & BAE, H. 2016. Neuroprotective effects of CD4+CD25+Foxp3+ regulatory T cells in a 3xTg-AD Alzheimer's disease model. *Oncotarget,* 7**,** 69347-69357.

BAKMIWEWA, S. M., WEISER, S., GREY, M., HENG, B., GUILLEMIN, G. J., BALL, H. J. & HUNT, N. H. 2016. Synergistic induction of CXCL10 by interferon-gamma and lymphotoxin-alpha in astrocytes: Possible role in cerebral malaria. *Cytokine,* 78**,** 79-86.

BALDERESCHI, M., DI CARLO, A., ROCCA, W. A., VANNI, P., MAGGI, S., PERISSINOTTO, E., GRIGOLETTO, F., AMADUCCI, L. & INZITARI, D. 2000. Parkinson's disease and parkinsonism in a longitudinal study: two-fold higher incidence in men. ILSA Working Group. Italian Longitudinal Study on Aging. *Neurology,* 55**,** 1358-63.

BANERJEE, S., WEBBER, C. & POOLE, A. R. 1992. The induction of arthritis in mice by the cartilage proteoglycan aggrecan: roles of CD4+ and CD8+ T cells. *Cell Immunol,* 144**,** 347-57.

BANIK, A., BROWN, R. E., BAMBURG, J., LAHIRI, D. K., KHURANA, D., FRIEDLAND, R. P., CHEN, W., DING, Y., MUDHER, A., PADJEN, A. L., MUKAETOVA-LADINSKA, E., IHARA, M., SRIVASTAVA, S., PADMA SRIVASTAVA, M. V., MASTERS, C. L., KALARIA, R. N. & ANAND, A. 2015. Translation of Pre-Clinical Studies into Successful Clinical Trials for Alzheimer's Disease: What are the Roadblocks and How Can They Be Overcome? *J Alzheimers Dis,* 47**,** 815-43.

BARUCH, K., ROSENZWEIG, N., KERTSER, A., DECZKOWSKA, A., SHARIF, A. M., SPINRAD, A., TSITSOU-KAMPELI, A., SAREL, A., CAHALON, L. & SCHWARTZ, M. 2015. Breaking immune tolerance by targeting Foxp3(+) regulatory T cells mitigates Alzheimer's disease pathology. *Nature communications,* 6**,** 7967-7967.

BATEMAN, R. J., XIONG, C., BENZINGER, T. L., FAGAN, A. M., GOATE, A., FOX, N. C., MARCUS, D. S., CAIRNS, N. J., XIE, X., BLAZEY, T. M., HOLTZMAN, D. M., SANTACRUZ, A., BUCKLES, V., OLIVER, A., MOULDER, K., AISEN, P. S., GHETTI, B., KLUNK, W. E., MCDADE, E., MARTINS, R. N., MASTERS, C. L., MAYEUX, R., RINGMAN, J. M., ROSSOR, M. N., SCHOFIELD, P. R., SPERLING, R. A., SALLOWAY, S. & MORRIS, J. C. 2012. Clinical and biomarker changes in dominantly inherited Alzheimer's disease. *N Engl J Med,* 367**,** 795-804.

BEACH, T. G., MONSELL, S. E., PHILLIPS, L. E. & KUKULL, W. 2012. Accuracy of the clinical diagnosis of Alzheimer disease at National Institute on Aging Alzheimer Disease Centers, 2005-2010. *J Neuropathol Exp Neurol,* 71**,** 266-73.

BEHAIRI, N., BELKHELFA, M., MESBAH-AMROUN, H., RAFA, H., BELARBI, S., TAZIR, M. & TOUIL-BOUKOFFA, C. 2015. All-trans-Retinoic Acid Modulates Nitric Oxide and Interleukin-17A Production by Peripheral Blood Mononuclear Cells from Patients with Alzheimer's Disease. *Neuroimmunomodulation,* 22**,** 385-393.

BELFIORE, R., RODIN, A., FERREIRA, E., VELAZQUEZ, R., BRANCA, C., CACCAMO, A. & ODDO, S. 2019. Temporal and regional progression of Alzheimer's disease-like pathology in 3xTg-AD mice. *Aging Cell,* 18**,** e12873.

BELLAVER, B., POVALA, G., FERREIRA, P. C. L., FERRARI-SOUZA, J. P., LEFFA, D. T., LUSSIER, F. Z., BENEDET, A. L., ASHTON, N. J., TRIANA-BALTZER, G., KOLB, H. C., TISSOT, C., THERRIAULT, J., SERVAES, S., STEVENSON, J., RAHMOUNI, N., LOPEZ, O. L., TUDORASCU, D. L., VILLEMAGNE, V. L., IKONOMOVIC, M. D., GAUTHIER, S., ZIMMER, E. R., ZETTERBERG, H., BLENNOW, K., AIZENSTEIN, H. J., KLUNK, W. E., SNITZ, B. E., MAKI, P., THURSTON, R. C., COHEN, A. D., GANGULI, M., KARIKARI, T. K., ROSA-NETO, P. & PASCOAL, T. A. 2023. Astrocyte reactivity influences amyloid-β effects on tau pathology in preclinical Alzheimer's disease. *Nature Medicine*.

BELONWU, S. A., LI, Y., BUNIS, D., RAO, A. A., SOLSBERG, C. W., TANG, A., FRAGIADAKIS, G. K., DUBAL, D. B., OSKOTSKY, T. & SIROTA, M. 2022. Sex-Stratified Single-Cell RNA-Seq Analysis Identifies Sex-Specific and Cell Type-Specific Transcriptional Responses in Alzheimer's Disease Across Two Brain Regions. *Mol Neurobiol,* 59**,** 276-293.

BEN-HUR, H., MOR, G., INSLER, V., BLICKSTEIN, I., AMIR-ZALTSMAN, Y., SHARP, A., GLOBERSON, A. & KOHEN, F. 1995. Menopause is associated with a significant increase in blood monocyte number and a relative decrease in the expression of estrogen receptors in human peripheral monocytes. *Am J Reprod Immunol,* 34**,** 363-9.

BENEDET, A. L., MILÀ-ALOMÀ, M., VRILLON, A., ASHTON, N. J., PASCOAL, T. A., LUSSIER, F., KARIKARI, T. K., HOURREGUE, C., COGNAT, E., DUMURGIER, J., STEVENSON, J., RAHMOUNI, N., PALLEN, V., POLTRONETTI, N. M., SALVADÓ, G., SHEKARI, M., OPERTO, G., GISPERT, J. D., MINGUILLON, C.,

FAURIA, K., KOLLMORGEN, G., SURIDJAN, I., ZIMMER, E. R., ZETTERBERG, H., MOLINUEVO, J. L., PAQUET, C., ROSA-NETO, P., BLENNOW, K. & SUÁREZ-CALVET, M. 2021. Differences Between Plasma and Cerebrospinal Fluid Glial Fibrillary Acidic Protein Levels Across the Alzheimer Disease Continuum. *JAMA Neurol,* 78**,** 1471-1483.

BERETTA, C., DAKHEL, A., ELTOM, K., ROSQVIST, F., UZONI, S., MOTHES, T., FLETCHER, J. S., RISÉRUS, U., SEHLIN, D., ROSTAMI, J., MICHNO, W. P. & ERLANDSSON, A. 2025. Astrocytic lipid droplets contain MHCII and may act as cogs in the antigen presentation machinery. *Journal of Neuroinflammation,* 22**,** 117.

BETTCHER, B. M., OLSON, K. E., CARLSON, N. E., MCCONNELL, B. V., BOYD, T., ADAME, V., SOLANO, D. A., ANTON, P., MARKHAM, N., THAKER, A. A., JENSEN, A. M., DALLMANN, E. N., POTTER, H. & COUGHLAN, C. 2021. Astrogliosis and episodic memory in late life: higher GFAP is related to worse memory and white matter microstructure in healthy aging and Alzheimer's disease. *Neurobiol Aging,* 103**,** 68-77.

BETTELLI, E., CARRIER, Y., GAO, W., KORN, T., STROM, T. B., OUKKA, M., WEINER, H. L. & KUCHROO, V. K. 2006. Reciprocal developmental pathways for the generation of pathogenic effector TH17 and regulatory T cells. *Nature,* 441**,** 235-238.

BILLINGS, L. M., ODDO, S., GREEN, K. N., MCGAUGH, J. L. & LAFERLA, F. M. 2005. Intraneuronal Aβ Causes the Onset of Early Alzheimer's Disease-Related Cognitive Deficits in Transgenic Mice. *Neuron,* 45**,** 675-688.

BIRD, T. D., NOCHLIN, D., POORKAJ, P., CHERRIER, M., KAYE, J., PAYAMI, H., PESKIND, E., LAMPE, T. H., NEMENS, E., BOYER, P. J. & SCHELLENBERG, G. D. 1999. A clinical pathological comparison of three families with frontotemporal dementia and identical mutations in the tau gene (P301L). *Brain,* 122 (Pt 4)**,** 741-56.

BITTNER, T., ZETTERBERG, H., TEUNISSEN, C. E., OSTLUND, R. E., JR., MILITELLO, M., ANDREASSON, U., HUBEEK, I., GIBSON, D., CHU, D. C., EICHENLAUB, U., HEISS, P., KOBOLD, U., LEINENBACH, A., MADIN, K., MANUILOVA, E., RABE, C. & BLENNOW, K. 2016. Technical performance of a novel, fully automated electrochemiluminescence immunoassay for the quantitation of β-amyloid (1-42) in human cerebrospinal fluid. *Alzheimers Dement,* 12**,** 517-26.

BOCCALINI, C., PERETTI, D. E., SCHEFFLER, M., MU, L., GRIFFA, A., TESTART, N., ALLALI, G., PRIOR, J. O., ASHTON, N. J., ZETTERBERG, H., BLENNOW, K., FRISONI, G. B. & GARIBOTTO, V. 2025. Sex differences in the association of Alzheimer's disease biomarkers and cognition in a multicenter memory clinic study. *Alzheimer's Research & Therapy,* 17**,** 46.

BONNEH-BARKAY, D., BISSEL, S. J., KOFLER, J., STARKEY, A., WANG, G. & WILEY, C. A. 2012. Astrocyte and Macrophage Regulation of YKL-40 Expression and Cellular Response in Neuroinflammation. *Brain Pathology,* 22**,** 530-546.

BONNI, A., SUN, Y., NADAL-VICENS, M., BHATT, A., FRANK, D. A., ROZOVSKY, I., STAHL, N., YANCOPOULOS, G. D. & GREENBERG, M. E. 1997. Regulation of gliogenesis in the central nervous system by the JAK-STAT signaling pathway. *Science,* 278**,** 477-83.

BORCHELT, D. R., RATOVITSKI, T., VAN LARE, J., LEE, M. K., GONZALES, V., JENKINS, N. A., COPELAND, N. G., PRICE, D. L. & SISODIA, S. S. 1997. Accelerated amyloid deposition in the brains of transgenic mice coexpressing mutant presenilin 1 and amyloid precursor proteins. *Neuron,* 19**,** 939-45.

BOYD, T. D., BENNETT, S. P., MORI, T., GOVERNATORI, N., RUNFELDT, M., NORDEN, M., PADMANABHAN, J., NEAME, P., WEFES, I., SANCHEZ-RAMOS, J., ARENDASH, G. W. & POTTER, H. 2010. GM-CSF upregulated in rheumatoid arthritis reverses cognitive impairment and amyloidosis in Alzheimer mice. *J Alzheimers Dis,* 21**,** 507-18.

BOYLES, J. K., PITAS, R. E., WILSON, E., MAHLEY, R. W. & TAYLOR, J. M. 1985. Apolipoprotein E associated with astrocytic glia of the central nervous system and with nonmyelinating glia of the peripheral nervous system. *J Clin Invest,* 76**,** 1501-13.

BRAUN, M., BOSTRÖM, G., INGELSSON, M., KILANDER, L., LÖWENMARK, M., NYHOLM, D., BURMAN, J., NIEMELÄ, V., FREYHULT, E., KULTIMA, K. & VIRHAMMAR, J. 2023. Levels of inflammatory cytokines MCP-1, CCL4, and PD-L1 in CSF differentiate idiopathic normal pressure hydrocephalus from neurodegenerative diseases. *Fluids Barriers CNS,* 20**,** 72.

BREEDVELD, F. C., DYNESIUS-TRENTHAM, R., DE SOUSA, M. & TRENTHAM, D. E. 1989. Collagen arthritis in the rat is initiated by CD4+ T cells and can be amplified by iron. *Cell Immunol,* 121**,** 1-12.

BRIGAS, H. C., RIBEIRO, M., COELHO, J. E., GOMES, R., GOMEZ-MURCIA, V., CARVALHO, K., FAIVRE, E., COSTA-PEREIRA, S., DARRIGUES, J., DE ALMEIDA, A. A., BUÉE, L., DUNOT, J., MARIE, H., POUSINHA, P. A., BLUM, D., SILVA-SANTOS, B., LOPES, L. V. & RIBOT, J. C. 2021. IL-17 triggers the onset of cognitive and synaptic deficits in early stages of Alzheimer's disease. *Cell Rep,* 36**,** 109574.

BROEKMANS, F. J., SOULES, M. R. & FAUSER, B. C. 2009. Ovarian aging: mechanisms and clinical consequences. *Endocr Rev,* 30**,** 465-93.

BRUNO, M., BONOMI, C. G., RICCI, F., DI DONNA, M. G., MERCURI, N. B., KOCH, G., MARTORANA, A. & MOTTA, C. 2024. Blood-brain barrier permeability is associated with different neuroinflammatory profiles in Alzheimer's disease. *Eur J Neurol,* 31**,** e16095.

BUSSE, S., VON HOFF, F., MICHLER, E., HARTIG, R., BOGERTS, B. & BUSSE, M. 2022. Altered expression of costimulatory molecules in dementias. *European Archives of Psychiatry and Clinical Neuroscience,* 272**,** 807-815.

CAO, M., LIU, J., ZHANG, X., WANG, Y., HOU, Y., SONG, Q., CUI, Y., ZHAO, Y. & WANG, P. 2023. IL-17A promotes the progression of Alzheimer's disease in APP/PS1 mice. *Immun Ageing,* 20**,** 74.

CARRASQUILLO, M. M., ALLEN, M., BURGESS, J. D., WANG, X., STRICKLAND, S. L., ARYAL, S., SIUDA, J., KACHADOORIAN, M. L., MEDWAY, C., YOUNKIN, C. S., NAIR, A., WANG, C., CHANANA, P., SERIE, D., NGUYEN, T., LINCOLN, S., MALPHRUS, K. G., MORGAN, K., GOLDE, T. E., PRICE, N. D., WHITE, C. C., DE JAGER, P. L., BENNETT, D. A., ASMANN, Y. W., CROOK, J. E., PETERSEN, R. C., GRAFF-RADFORD, N. R., DICKSON, D. W., YOUNKIN, S. G. & ERTEKIN-TANER, N. 2017. A candidate regulatory variant at the TREM gene cluster

associates with decreased Alzheimer's disease risk and increased TREML1 and TREM2 brain gene expression. *Alzheimers Dement,* 13**,** 663-673.
CASARES, N., ALFARO, M., CUADRADO-TEJEDOR, M., LASARTE-CIA, A., NAVARRO, F., VIVAS, I., ESPELOSIN, M., CARTAS-CEJUDO, P., FERNÁNDEZ-IRIGOYEN, J., SANTAMARÍA, E., GARCÍA-OSTA, A. & LASARTE, J. J. 2023. Improvement of cognitive function in wild-type and Alzheimer´s disease mouse models by the immunomodulatory properties of menthol inhalation or by depletion of T regulatory cells. *Front Immunol,* 14**,** 1130044.
CEYZÉRIAT, K., BEN HAIM, L., DENIZOT, A., POMMIER, D., MATOS, M., GUILLEMAUD, O., PALOMARES, M. A., ABJEAN, L., PETIT, F., GIPCHTEIN, P., GAILLARD, M. C., GUILLERMIER, M., BERNIER, S., GAUDIN, M., AURÉGAN, G., JOSÉPHINE, C., DÉCHAMPS, N., VERAN, J., LANGLAIS, V., CAMBON, K., BEMELMANS, A. P., BAIJER, J., BONVENTO, G., DHENAIN, M., DELEUZE, J. F., OLIET, S. H. R., BROUILLET, E., HANTRAYE, P., CARRILLO-DE SAUVAGE, M. A., OLASO, R., PANATIER, A. & ESCARTIN, C. 2018. Modulation of astrocyte reactivity improves functional deficits in mouse models of Alzheimer's disease. *Acta Neuropathol Commun,* 6**,** 104.
CHAKRABARTY, P., CEBALLOS-DIAZ, C., BECCARD, A., JANUS, C., DICKSON, D., GOLDE, T. E. & DAS, P. 2010. IFN-gamma promotes complement expression and attenuates amyloid plaque deposition in amyloid beta precursor protein transgenic mice. *J Immunol,* 184**,** 5333-43.
CHAKRABARTY, P., LI, A., CEBALLOS-DIAZ, C., EDDY, J. A., FUNK, C. C., MOORE, B., DINUNNO, N., ROSARIO, A. M., CRUZ, P. E., VERBEECK, C., SACINO, A., NIX, S., JANUS, C., PRICE, N. D., DAS, P. & GOLDE, T. E. 2015. IL-10 alters immunoproteostasis in APP mice, increasing plaque burden and worsening cognitive behavior. *Neuron,* 85**,** 519-33.
CHAMBERS, S. M., FASANO, C. A., PAPAPETROU, E. P., TOMISHIMA, M., SADELAIN, M. & STUDER, L. 2009. Highly efficient neural conversion of human ES and iPS cells by dual inhibition of SMAD signaling. *Nature Biotechnology,* 27**,** 275-280.
CHATTERJEE, P., PEDRINI, S., STOOPS, E., GOOZEE, K., VILLEMAGNE, V. L., ASIH, P. R., VERBERK, I. M. W., DAVE, P., TADDEI, K., SOHRABI, H. R., ZETTERBERG, H., BLENNOW, K., TEUNISSEN, C. E., VANDERSTICHELE, H. M. & MARTINS, R. N. 2021. Plasma glial fibrillary acidic protein is elevated in cognitively normal older adults at risk of Alzheimer's disease. *Transl Psychiatry,* 11**,** 27.
CHEN, G., GULBRANSON, D. R., HOU, Z., BOLIN, J. M., RUOTTI, V., PROBASCO, M. D., SMUGA-OTTO, K., HOWDEN, S. E., DIOL, N. R., PROPSON, N. E., WAGNER, R., LEE, G. O., ANTOSIEWICZ-BOURGET, J., TENG, J. M. & THOMSON, J. A. 2011. Chemically defined conditions for human iPSC derivation and culture. *Nat Methods,* 8**,** 424-9.
CHEN, J.-M., JIANG, G.-X., LI, Q.-W., ZHOU, Z.-M. & CHENG, Q. 2014. Increased Serum Levels of Interleukin-18, -23 and -17 in Chinese Patients with Alzheimer's Disease. *Dementia and Geriatric Cognitive Disorders,* 38**,** 321-329.
CHEN, X., FIRULYOVA, M., MANIS, M., HERZ, J., SMIRNOV, I., ALADYEVA, E., WANG, C., BAO, X., FINN, M. B., HU, H., SHCHUKINA, I., KIM, M. W., YUEDE, C. M., KIPNIS, J., ARTYOMOV, M. N., ULRICH, J. D. & HOLTZMAN, D. M. 2023.

Microglia-mediated T cell infiltration drives neurodegeneration in tauopathy. *Nature,* 615**,** 668-677.

CHIKUMA, S., TERAWAKI, S., HAYASHI, T., NABESHIMA, R., YOSHIDA, T., SHIBAYAMA, S., OKAZAKI, T. & HONJO, T. 2009. PD-1-mediated suppression of IL-2 production induces CD8+ T cell anergy in vivo. *J Immunol,* 182**,** 6682-9.

CICCOCIOPPO, F., LANUTI, P., PIERDOMENICO, L., SIMEONE, P., BOLOGNA, G., ERCOLINO, E., BUTTARI, F., FANTOZZI, R., THOMAS, A., ONOFRJ, M., CENTONZE, D., MISCIA, S. & MARCHISIO, M. 2019. The Characterization of Regulatory T-Cell Profiles in Alzheimer's Disease and Multiple Sclerosis. *Sci Rep,* 9**,** 8788.

CITRON, M., OLTERSDORF, T., HAASS, C., MCCONLOGUE, L., HUNG, A. Y., SEUBERT, P., VIGO-PELFREY, C., LIEBERBURG, I. & SELKOE, D. J. 1992. Mutation of the beta-amyloid precursor protein in familial Alzheimer's disease increases beta-protein production. *Nature,* 360**,** 672-4.

CLARK, R. F., HUTTON, M., FULDNER, M., FROELICH, S., KARRAN, E., TALBOT, C., CROOK, R., LENDON, C., PRIHAR, G., HE, C., KORENBLAT, K., MARTINEZ, A., WRAGG, M., BUSFIELD, F., BEHRENS, M. I., MYERS, A., NORTON, J., MORRIS, J., MEHTA, N., PEARSON, C., LINCOLN, S., BAKER, M., DUFF, K., ZEHR, C., PEREZ-TUR, J., HOULDEN, H., RUIZ, A., OSSA, J., LOPERA, F., ARCOS, M., MADRIGAL, L., COLLINGE, J., HUMPHREYS, C., ASHWORTH, A., SARNER, S., FOX, N., HARVEY, R., KENNEDY, A., ROQUES, P., CLINE, R. T., PHILIPS, C. A., VENTER, J. C., FORSELL, L., AXELMAN, K., LILIUS, L., JOHNSTON, J., COWBURN, R., VIITANEN, M., WINBLAD, B., KOSIK, K., HALTIA, M., POYHONEN, M., DICKSON, D., MANN, D., NEARY, D., SNOWDEN, J., LANTOS, P., LANNFELT, L., ROSSOR, M., ROBERTS, G. W., ADAMS, M. D., HARDY, J. & GOATE, A. 1995. The structure of the presenilin 1 (S182) gene and identification of six novel mutations in early onset AD families. *Nature Genetics,* 11**,** 219-222.

COALES, I., TSARTSALIS, S., FANCY, N., WEINERT, M., CLODE, D., OWEN, D. & MATTHEWS, P. M. 2022. Alzheimer's disease-related transcriptional sex differences in myeloid cells. *Journal of Neuroinflammation,* 19**,** 247.

CORDER, E. H., SAUNDERS, A. M., STRITTMATTER, W. J., SCHMECHEL, D. E., GASKELL, P. C., SMALL, G. W., ROSES, A. D., HAINES, J. L. & PERICAK-VANCE, M. A. 1993. Gene dose of apolipoprotein E type 4 allele and the risk of Alzheimer's disease in late onset families. *Science,* 261**,** 921-3.

CROMPTON, L. A., MCCOMISH, S. F., STATHAKOS, P., CORDERO-LLANA, O., LANE, J. D. & CALDWELL, M. A. 2021. Efficient and Scalable Generation of Human Ventral Midbrain Astrocytes from Human-Induced Pluripotent Stem Cells. *J Vis Exp*.

CROOKE, S. N., OVSYANNIKOVA, I. G., POLAND, G. A. & KENNEDY, R. B. 2019. Immunosenescence and human vaccine immune responses. *Immun Ageing,* 16**,** 25.

CUI, W., BAI, H., GUO, C., ZHOU, J., FENG, D., ZHANG, S., GAO, F., HAN, L., TIAN, Y., DONG, J., WEI, F., BAI, J., WU, X., SHI, Y., GUO, H., WANG, L., LI, Z., GUO, W., ZHAO, T., HENG, L., CAI, Q., LIU, H., GE, S. & QU, Y. 2025. Interferon regulatory factor-1–expressing astrocytes are epigenetically controlled and

exacerbate TBI-associated pathology in mice. *Science Translational Medicine,* 17**,** eadr5300.
CUMMINGS, J. L., COHEN, S., VAN DYCK, C. H., BRODY, M., CURTIS, C., CHO, W., WARD, M., FRIESENHAHN, M., RABE, C., BRUNSTEIN, F., QUARTINO, A., HONIGBERG, L. A., FUJI, R. N., CLAYTON, D., MORTENSEN, D., HO, C. & PAUL, R. 2018. ABBY: A phase 2 randomized trial of crenezumab in mild to moderate Alzheimer disease. *Neurology,* 90**,** e1889-e1897.
CUMMINGS, J. L., MORSTORF, T. & ZHONG, K. 2014. Alzheimer's disease drug-development pipeline: few candidates, frequent failures. *Alzheimers Res Ther,* 6**,** 37.
DANSOKHO, C., AIT AHMED, D., AID, S., TOLY-NDOUR, C., CHAIGNEAU, T., CALLE, V., CAGNARD, N., HOLZENBERGER, M., PIAGGIO, E., AUCOUTURIER, P. & DOROTHÉE, G. 2016. Regulatory T cells delay disease progression in Alzheimer-like pathology. *Brain,* 139**,** 1237-51.
DARNELL, J. E., JR., KERR, I. M. & STARK, G. R. 1994. Jak-STAT pathways and transcriptional activation in response to IFNs and other extracellular signaling proteins. *Science,* 264**,** 1415-21.
DAS, H. K., MCPHERSON, J., BRUNS, G. A., KARATHANASIS, S. K. & BRESLOW, J. L. 1985. Isolation, characterization, and mapping to chromosome 19 of the human apolipoprotein E gene. *J Biol Chem,* 260**,** 6240-7.
DI BENEDETTO, G., BURGALETTO, C., CARTA, A. R., SACCONE, S., LEMPEREUR, L., MULAS, G., LORETO, C., BERNARDINI, R. & CANTARELLA, G. 2019. Beneficial effects of curtailing immune susceptibility in an Alzheimer's disease model. *J Neuroinflammation,* 16**,** 166.
DI ROSA, M., DELL'OMBRA, N., ZAMBITO, A. M., MALAGUARNERA, M., NICOLETTI, F. & MALAGUARNERA, L. 2006. Chitotriosidase and inflammatory mediator levels in Alzheimer's disease and cerebrovascular dementia. *European Journal of Neuroscience,* 23**,** 2648-2656.
DINIZ, L. P., ALMEIDA, J. C., TORTELLI, V., VARGAS LOPES, C., SETTI-PERDIGÃO, P., STIPURSKY, J., KAHN, S. A., ROMÃO, L. F., DE MIRANDA, J., ALVES-LEON, S. V., DE SOUZA, J. M., CASTRO, N. G., PANIZZUTTI, R. & GOMES, F. C. 2012. Astrocyte-induced synaptogenesis is mediated by transforming growth factor β signaling through modulation of D-serine levels in cerebral cortex neurons. *J Biol Chem,* 287**,** 41432-45.
DOECKE, J. D., WARD, L., BURNHAM, S. C., VILLEMAGNE, V. L., LI, Q. X., COLLINS, S., FOWLER, C. J., MANUILOVA, E., WIDMANN, M., RAINEY-SMITH, S. R., MARTINS, R. N. & MASTERS, C. L. 2020. Elecsys CSF biomarker immunoassays demonstrate concordance with amyloid-PET imaging. *Alzheimers Res Ther,* 12**,** 36.
DOLFI, D. V. & KATSIKIS, P. D. 2007. CD28 and CD27 costimulation of CD8+ T cells: a story of survival. *Adv Exp Med Biol,* 590**,** 149-70.
DOLPHIN, H., DYER, A. H., MORRISON, L., SHENKIN, S. D., WELSH, T. & KENNELLY, S. P. 2024. New horizons in the diagnosis and management of Alzheimer's Disease in older adults. *Age Ageing,* 53.
DOODY, R. S., THOMAS, R. G., FARLOW, M., IWATSUBO, T., VELLAS, B., JOFFE, S., KIEBURTZ, K., RAMAN, R., SUN, X., AISEN, P. S., SIEMERS, E., LIU-SEIFERT,

H. & MOHS, R. 2014. Phase 3 trials of solanezumab for mild-to-moderate Alzheimer's disease. *N Engl J Med,* 370**,** 311-21.

DUARTE-GUTERMAN, P., ALBERT, A. Y., INKSTER, A. M., BARHA, C. K., GALEA, L. A. M. & ON BEHALF OF THE ALZHEIMER'S DISEASE NEUROIMAGING, I. 2020. Inflammation in Alzheimer's Disease: Do Sex and APOE Matter? *Journal of Alzheimer's Disease,* 78**,** 627-641.

DUBENKO, O. E., CHYNIAK, O. S. & POTAPOV, O. O. 2021. LEVELS OF PROINFLAMMATORY CYTOKINES IL-17 AND IL-23 IN PATIENTS WITH ALZHEIMER'S DISEASE, MILD COGNITIVE IMPAIRMENT AND VASCULAR DEMENTIA. *Wiad Lek,* 74**,** 68-71.

DUBOIS, B., VILLAIN, N., FRISONI, G. B., RABINOVICI, G. D., SABBAGH, M., CAPPA, S., BEJANIN, A., BOMBOIS, S., EPELBAUM, S., TEICHMANN, M., HABERT, M. O., NORDBERG, A., BLENNOW, K., GALASKO, D., STERN, Y., ROWE, C. C., SALLOWAY, S., SCHNEIDER, L. S., CUMMINGS, J. L. & FELDMAN, H. H. 2021. Clinical diagnosis of Alzheimer's disease: recommendations of the International Working Group. *Lancet Neurol,* 20**,** 484-496.

DUITS, F. H., TEUNISSEN, C. E., BOUWMAN, F. H., VISSER, P. J., MATTSSON, N., ZETTERBERG, H., BLENNOW, K., HANSSON, O., MINTHON, L., ANDREASEN, N., MARCUSSON, J., WALLIN, A., RIKKERT, M. O., TSOLAKI, M., PARNETTI, L., HERUKKA, S. K., HAMPEL, H., DE LEON, M. J., SCHRÖDER, J., AARSLAND, D., BLANKENSTEIN, M. A., SCHELTENS, P. & VAN DER FLIER, W. M. 2014. The cerebrospinal fluid "Alzheimer profile": easily said, but what does it mean? *Alzheimers Dement,* 10**,** 713-723.e2.

DUMANCHIN, C., CAMUZAT, A., CAMPION, D., VERPILLAT, P., HANNEQUIN, D., DUBOIS, B., SAUGIER-VEBER, P., MARTIN, C., PENET, C., CHARBONNIER, F., AGID, Y., FREBOURG, T. & BRICE, A. 1998. Segregation of a missense mutation in the microtubule-associated protein tau gene with familial frontotemporal dementia and parkinsonism. *Hum Mol Genet,* 7**,** 1825-9.

DYER, A. H., DOLPHIN, H., O'CONNOR, A., MORRISON, L., SEDGWICK, G., MCFEELY, A., KILLEEN, E., GALLAGHER, C., DAVEY, N., CONNOLLY, E., LYONS, S., YOUNG, C., GAFFNEY, C., ENNIS, R., MCHALE, C., JOSEPH, J., KNIGHT, G., KELLY, E., O'FARRELLY, C., BOURKE, N. M., FALLON, A., O'DOWD, S. & KENNELLY, S. P. 2023. Protocol for the Tallaght University Hospital Institute for Memory and Cognition-Biobank for Research in Ageing and Neurodegeneration. *BMJ Open,* 13**,** e077772.

DYER, A. H., DOLPHIN, H., O'CONNOR, A., MORRISON, L., SEDGWICK, G., YOUNG, C., KILLEEN, E., GALLAGHER, C., MCFEELY, A., CONNOLLY, E., DAVEY, N., CLAFFEY, P., DOYLE, P., LYONS, S., GAFFNEY, C., ENNIS, R., MCHALE, C., JOSEPH, J., KNIGHT, G., KELLY, E., O'FARRELLY, C., FALLON, A., O'DOWD, S., BOURKE, N. M. & KENNELLY, S. P. 2024. Performance of plasma p-tau217 for the detection of amyloid-β positivity in a memory clinic cohort using an electrochemiluminescence immunoassay. *Alzheimers Res Ther,* 16**,** 186.

ECKMAN, C. B., MEHTA, N. D., CROOK, R., PEREZ-TUR, J., PRIHAR, G., PFEIFFER, E., GRAFF-RADFORD, N., HINDER, P., YAGER, D., ZENK, B., REFOLO, L. M., PRADA, C. M., YOUNKIN, S. G., HUTTON, M. & HARDY, J. 1997. A new pathogenic mutation in the APP gene (I716V) increases the relative proportion of A beta 42(43). *Hum Mol Genet,* 6**,** 2087-9.

EISENBERG, D. T., KUZAWA, C. W. & HAYES, M. G. 2010. Worldwide allele frequencies of the human apolipoprotein E gene: climate, local adaptations, and evolutionary history. *Am J Phys Anthropol,* 143**,** 100-11.

ENDO, F., KASAI, A., SOTO, J. S., YU, X., QU, Z., HASHIMOTO, H., GRADINARU, V., KAWAGUCHI, R. & KHAKH, B. S. 2022. Molecular basis of astrocyte diversity and morphology across the CNS in health and disease. *Science,* 378**,** eadc9020.

ENDO, T. A., MASUHARA, M., YOKOUCHI, M., SUZUKI, R., SAKAMOTO, H., MITSUI, K., MATSUMOTO, A., TANIMURA, S., OHTSUBO, M., MISAWA, H., MIYAZAKI, T., LEONOR, N., TANIGUCHI, T., FUJITA, T., KANAKURA, Y., KOMIYA, S. & YOSHIMURA, A. 1997. A new protein containing an SH2 domain that inhibits JAK kinases. *Nature,* 387**,** 921-4.

ESTEVAO, C., BOWERS, C. E., LUO, D., SARKER, M., HOEH, A. E., FRUDD, K., TUROWSKI, P. & GREENWOOD, J. 2021. CCL4 induces inflammatory signalling and barrier disruption in the neurovascular endothelium. *Brain Behav Immun Health,* 18**,** 100370.

EVANS, M. J. & KAUFMAN, M. H. 1981. Establishment in culture of pluripotential cells from mouse embryos. *Nature,* 292**,** 154-156.

FAGAN, A. M., MINTUN, M. A., MACH, R. H., LEE, S. Y., DENCE, C. S., SHAH, A. R., LAROSSA, G. N., SPINNER, M. L., KLUNK, W. E., MATHIS, C. A., DEKOSKY, S. T., MORRIS, J. C. & HOLTZMAN, D. M. 2006. Inverse relation between in vivo amyloid imaging load and cerebrospinal fluid Abeta42 in humans. *Ann Neurol,* 59**,** 512-9.

FAGAN, A. M., ROE, C. M., XIONG, C., MINTUN, M. A., MORRIS, J. C. & HOLTZMAN, D. M. 2007. Cerebrospinal fluid tau/beta-amyloid(42) ratio as a prediction of cognitive decline in nondemented older adults. *Arch Neurol,* 64**,** 343-9.

FANG, D. & ZHU, J. 2017. Dynamic balance between master transcription factors determines the fates and functions of CD4 T cell and innate lymphoid cell subsets. *J Exp Med,* 214**,** 1861-1876.

FANTUZZI, L., TAGLIAMONTE, M., GAUZZI, M. C. & LOPALCO, L. 2019. Dual CCR5/CCR2 targeting: opportunities for the cure of complex disorders. *Cell Mol Life Sci,* 76**,** 4869-4886.

FARIDAR, A., GAMEZ, N., LI, D., WANG, Y., BORADIA, R., THOME, A. D., ZHAO, W., BEERS, D. R., THONHOFF, J. R., NAKAWAH, M. O., ROMÁN, G. C., VOLPI, J. J., TOLEDO, J. B., GEORGE, M., DAVIS, C. S., PASCUAL, B., GRUNDMAN, M., MASDEU, J. C. & APPEL, S. H. 2025. Low-dose interleukin-2 in patients with mild to moderate Alzheimer's disease: a randomized clinical trial. *Alzheimer's Research & Therapy,* 17**,** 146.

FARIDAR, A., THOME, A. D., ZHAO, W., THONHOFF, J. R., BEERS, D. R., PASCUAL, B., MASDEU, J. C. & APPEL, S. H. 2020. Restoring regulatory T-cell dysfunction in Alzheimer's disease through ex vivo expansion. *Brain communications,* 2**,** fcaa112-fcaa112.

FARIDAR, A., VASQUEZ, M., THOME, A. D., YIN, Z., XUAN, H., WANG, J. H., WEN, S., LI, X., THONHOFF, J. R., ZHAO, W., ZHAO, H., BEERS, D. R., WONG, S. T. C., MASDEU, J. C. & APPEL, S. H. 2022. Ex vivo expanded human regulatory T cells modify neuroinflammation in a preclinical model of Alzheimer's disease. *Acta Neuropathol Commun,* 10**,** 144.

FERRARI-SOUZA, J. P., FERREIRA, P. C. L., BELLAVER, B., TISSOT, C., WANG, Y.-T., LEFFA, D. T., BRUM, W. S., BENEDET, A. L., ASHTON, N. J., DE BASTIANI, M. A., ROCHA, A., THERRIAULT, J., LUSSIER, F. Z., CHAMOUN, M., SERVAES, S., BEZGIN, G., KANG, M. S., STEVENSON, J., RAHMOUNI, N., PALLEN, V., POLTRONETTI, N. M., KLUNK, W. E., TUDORASCU, D. L., COHEN, A. D., VILLEMAGNE, V. L., GAUTHIER, S., BLENNOW, K., ZETTERBERG, H., SOUZA, D. O., KARIKARI, T. K., ZIMMER, E. R., ROSA-NETO, P. & PASCOAL, T. A. 2022. Astrocyte biomarker signatures of amyloid-β and tau pathologies in Alzheimer's disease. *Molecular Psychiatry,* 27**,** 4781-4789.

FERRETTI, M. T., MERLINI, M., SPÄNI, C., GERICKE, C., SCHWEIZER, N., ENZMANN, G., ENGELHARDT, B., KULIC, L., SUTER, T. & NITSCH, R. M. 2016. T-cell brain infiltration and immature antigen-presenting cells in transgenic models of Alzheimer's disease-like cerebral amyloidosis. *Brain, Behavior, and Immunity,* 54**,** 211-225.

FÖRSTER, R., DAVALOS-MISSLITZ, A. C. & ROT, A. 2008. CCR7 and its ligands: balancing immunity and tolerance. *Nat Rev Immunol,* 8**,** 362-71.

FU, J., DUAN, J., MO, J., XIAO, H., HUANG, Y., CHEN, W., XIANG, S., YANG, F., CHEN, Y. & XU, S. 2020. Mild Cognitive Impairment Patients Have Higher Regulatory T-Cell Proportions Compared With Alzheimer's Disease-Related Dementia Patients. *Front Aging Neurosci,* 12**,** 624304.

GALASKO, D., CHANG, L., MOTTER, R., CLARK, C. M., KAYE, J., KNOPMAN, D., THOMAS, R., KHOLODENKO, D., SCHENK, D., LIEBERBURG, I., MILLER, B., GREEN, R., BASHERAD, R., KERTILES, L., BOSS, M. A. & SEUBERT, P. 1998. High cerebrospinal fluid tau and low amyloid beta42 levels in the clinical diagnosis of Alzheimer disease and relation to apolipoprotein E genotype. *Arch Neurol,* 55**,** 937-45.

GALLAGHER, J. J., MINOGUE, A. M. & LYNCH, M. A. 2013. Impaired performance of female APP/PS1 mice in the Morris water maze is coupled with increased Aβ accumulation and microglial activation. *Neurodegener Dis,* 11**,** 33-41.

GAMES, D., ADAMS, D., ALESSANDRINI, R., BARBOUR, R., BERTHELETTE, P., BLACKWELL, C., CARR, T., CLEMENS, J., DONALDSON, T., GILLESPIE, F. & ET AL. 1995. Alzheimer-type neuropathology in transgenic mice overexpressing V717F beta-amyloid precursor protein. *Nature,* 373**,** 523-7.

GAO, Z., ZHU, Q., ZHANG, Y., ZHAO, Y., CAI, L., SHIELDS, C. B. & CAI, J. 2013. Reciprocal modulation between microglia and astrocyte in reactive gliosis following the CNS injury. *Mol Neurobiol,* 48**,** 690-701.

GATE, D., SALIGRAMA, N., LEVENTHAL, O., YANG, A. C., UNGER, M. S., MIDDELDORP, J., CHEN, K., LEHALLIER, B., CHANNAPPA, D., DE LOS SANTOS, M. B., MCBRIDE, A., PLUVINAGE, J., ELAHI, F., TAM, G. K., KIM, Y., GREICIUS, M., WAGNER, A. D., AIGNER, L., GALASKO, D. R., DAVIS, M. M. & WYSS-CORAY, T. 2020. Clonally expanded CD8 T cells patrol the cerebrospinal fluid in Alzheimer's disease. *Nature,* 577**,** 399-404.

GIUNTI, D., BORSELLINO, G., BENELLI, R., MARCHESE, M., CAPELLO, E., VALLE, M. T., PEDEMONTE, E., NOONAN, D., ALBINI, A., BERNARDI, G., MANCARDI, G. L., BATTISTINI, L. & UCCELLI, A. 2003. Phenotypic and functional analysis of T cells homing into the CSF of subjects with inflammatory diseases of the CNS. *J Leukoc Biol,* 73**,** 584-90.

GLENNER, G. G. 1979. Congophilic microangiopathy in the pathogenesis of Alzheimer's syndrome (presenile dementia). *Medical Hypotheses,* 5**,** 1231-1236.

GOATE, A., CHARTIER-HARLIN, M. C., MULLAN, M., BROWN, J., CRAWFORD, F., FIDANI, L., GIUFFRA, L., HAYNES, A., IRVING, N., JAMES, L. & ET AL. 1991. Segregation of a missense mutation in the amyloid precursor protein gene with familial Alzheimer's disease. *Nature,* 349**,** 704-6.

GONG, Y., WU, M., HUANG, Y., HE, X., YUAN, J. & DANG, B. 2025. Research developments in the neurovascular unit and the blood-brain barrier (Review). *Biomed Rep,* 22**,** 88.

GONZALEZ-RODRIGUEZ, M., VILLAR-CONDE, S., ASTILLERO-LOPEZ, V., VILLANUEVA-ANGUITA, P., UBEDA-BANON, I., FLORES-CUADRADO, A., MARTINEZ-MARCOS, A. & SAIZ-SANCHEZ, D. 2021. Neurodegeneration and Astrogliosis in the Human CA1 Hippocampal Subfield Are Related to hsp90ab1 and bag3 in Alzheimer's Disease. *Int J Mol Sci,* 23.

GRASSADONIA, A., SPERDUTI, I., VICI, P., IEZZI, L., BROCCO, D., GAMUCCI, T., PIZZUTI, L., MAUGERI-SACCÀ, M., MARCHETTI, P., COGNETTI, G., DE TURSI, M., NATOLI, C., BARBA, M. & TINARI, N. 2018. Effect of Gender on the Outcome of Patients Receiving Immune Checkpoint Inhibitors for Advanced Cancer: A Systematic Review and Meta-Analysis of Phase III Randomized Clinical Trials. *J Clin Med,* 7.

GRATUZE, M., SCHLACHETZKI, J. C. M., D'OLIVEIRA ALBANUS, R., JAIN, N., NOVOTNY, B., BRASE, L., RODRIGUEZ, L., MANSEL, C., KIPNIS, M., O'BRIEN, S., PASILLAS, M. P., LEE, C., MANIS, M., COLONNA, M., HARARI, O., GLASS, C. K., ULRICH, J. D. & HOLTZMAN, D. M. 2022. TREM2-independent microgliosis promotes tau-mediated neurodegeneration in the presence of ApoE4. *Neuron*.

GUERREIRO, R., WOJTAS, A., BRAS, J., CARRASQUILLO, M., ROGAEVA, E., MAJOUNIE, E., CRUCHAGA, C., SASSI, C., KAUWE, J. S., YOUNKIN, S., HAZRATI, L., COLLINGE, J., POCOCK, J., LASHLEY, T., WILLIAMS, J., LAMBERT, J. C., AMOUYEL, P., GOATE, A., RADEMAKERS, R., MORGAN, K., POWELL, J., ST GEORGE-HYSLOP, P., SINGLETON, A. & HARDY, J. 2013. TREM2 variants in Alzheimer's disease. *N Engl J Med,* 368**,** 117-27.

GUERREIRO, R. J., BAQUERO, M., BLESA, R., BOADA, M., BRÁS, J. M., BULLIDO, M. J., CALADO, A., CROOK, R., FERREIRA, C., FRANK, A., GÓMEZ-ISLA, T., HERNÁNDEZ, I., LLEÓ, A., MACHADO, A., MARTÍNEZ-LAGE, P., MASDEU, J., MOLINA-PORCEL, L., MOLINUEVO, J. L., PASTOR, P., PÉREZ-TUR, J., RELVAS, R., OLIVEIRA, C. R., RIBEIRO, M. H., ROGAEVA, E., SA, A., SAMARANCH, L., SÁNCHEZ-VALLE, R., SANTANA, I., TÀRRAGA, L., VALDIVIESO, F., SINGLETON, A., HARDY, J. & CLARIMÓN, J. 2010. Genetic screening of Alzheimer's disease genes in Iberian and African samples yields novel mutations in presenilins and APP. *Neurobiol Aging,* 31**,** 725-31.

GUILLOT-SESTIER, M. V., ARAIZ, A. R., MELA, V., GABAN, A. S., O'NEILL, E., JOSHI, L., CHOUCHANI, E. T., MILLS, E. L. & LYNCH, M. A. 2021. Microglial metabolism is a pivotal factor in sexual dimorphism in Alzheimer's disease. *Commun Biol,* 4**,** 711.

GUILLOT-SESTIER, M. V., DOTY, K. R., GATE, D., RODRIGUEZ, J., JR., LEUNG, B. P., REZAI-ZADEH, K. & TOWN, T. 2015. Il10 deficiency rebalances innate immunity to mitigate Alzheimer-like pathology. *Neuron,* 85**,** 534-48.

GUO, T., LI, A., SUN, P., HE, Z., CAI, Y., LAN, G., LIU, L., LI, J., YANG, J., ZHU, Y., ZHAO, R., CHEN, X., SHI, D., LIU, Z., WANG, Q., XU, L., ZHOU, L., RAN, P., WANG, X., SUN, K., LU, J. & HAN, Y. 2024. Astrocyte reactivity is associated with tau tangle load and cortical thinning in Alzheimer's disease. *Mol Neurodegener,* 19**,** 58.

GURDON, J. B., LANE, C. D., WOODLAND, H. R. & MARBAIX, G. 1971. Use of Frog Eggs and Oocytes for the Study of Messenger RNA and its Translation in Living Cells. *Nature,* 233**,** 177-182.

GUSTAVSSON, A., NORTON, N., FAST, T., FRÖLICH, L., GEORGES, J., HOLZAPFEL, D., KIRABALI, T., KROLAK-SALMON, P., ROSSINI, P. M., FERRETTI, M. T., LANMAN, L., CHADHA, A. S. & VAN DER FLIER, W. M. 2022. Global estimates on the number of persons across the Alzheimer's disease continuum. *Alzheimer's & Dementia,* n/a.

GUTTENPLAN, K. A., WEIGEL, M. K., ADLER, D. I., COUTHOUIS, J., LIDDELOW, S. A., GITLER, A. D. & BARRES, B. A. 2020. Knockout of reactive astrocyte activating factors slows disease progression in an ALS mouse model. *Nat Commun,* 11**,** 3753.

HABIB, N., MCCABE, C., MEDINA, S., VARSHAVSKY, M., KITSBERG, D., DVIR-SZTERNFELD, R., GREEN, G., DIONNE, D., NGUYEN, L., MARSHALL, J. L., CHEN, F., ZHANG, F., KAPLAN, T., REGEV, A. & SCHWARTZ, M. 2020. Disease-associated astrocytes in Alzheimer's disease and aging. *Nat Neurosci,* 23**,** 701-706.

HANSSON, O., SEIBYL, J., STOMRUD, E., ZETTERBERG, H., TROJANOWSKI, J. Q., BITTNER, T., LIFKE, V., CORRADINI, V., EICHENLAUB, U., BATRLA, R., BUCK, K., ZINK, K., RABE, C., BLENNOW, K. & SHAW, L. M. 2018. CSF biomarkers of Alzheimer's disease concord with amyloid-β PET and predict clinical progression: A study of fully automated immunoassays in BioFINDER and ADNI cohorts. *Alzheimers Dement,* 14**,** 1470-1481.

HANSSON, O., ZETTERBERG, H., BUCHHAVE, P., LONDOS, E., BLENNOW, K. & MINTHON, L. 2006. Association between CSF biomarkers and incipient Alzheimer's disease in patients with mild cognitive impairment: a follow-up study. *Lancet Neurol,* 5**,** 228-34.

HARDY, J. A. & HIGGINS, G. A. 1992. Alzheimer's Disease: The Amyloid Cascade Hypothesis. *Science,* 256**,** 184-185.

HAROLD, D., ABRAHAM, R., HOLLINGWORTH, P., SIMS, R., GERRISH, A., HAMSHERE, M. L., PAHWA, J. S., MOSKVINA, V., DOWZELL, K., WILLIAMS, A., JONES, N., THOMAS, C., STRETTON, A., MORGAN, A. R., LOVESTONE, S., POWELL, J., PROITSI, P., LUPTON, M. K., BRAYNE, C., RUBINSZTEIN, D. C., GILL, M., LAWLOR, B., LYNCH, A., MORGAN, K., BROWN, K. S., PASSMORE, P. A., CRAIG, D., MCGUINNESS, B., TODD, S., HOLMES, C., MANN, D., SMITH, A. D., LOVE, S., KEHOE, P. G., HARDY, J., MEAD, S., FOX, N., ROSSOR, M., COLLINGE, J., MAIER, W., JESSEN, F., SCHÜRMANN, B., HEUN, R., VAN DEN BUSSCHE, H., HEUSER, I., KORNHUBER, J., WILTFANG, J., DICHGANS, M., FRÖLICH, L., HAMPEL, H., HÜLL, M., RUJESCU, D., GOATE,

A. M., KAUWE, J. S., CRUCHAGA, C., NOWOTNY, P., MORRIS, J. C., MAYO, K., SLEEGERS, K., BETTENS, K., ENGELBORGHS, S., DE DEYN, P. P., VAN BROECKHOVEN, C., LIVINGSTON, G., BASS, N. J., GURLING, H., MCQUILLIN, A., GWILLIAM, R., DELOUKAS, P., AL-CHALABI, A., SHAW, C. E., TSOLAKI, M., SINGLETON, A. B., GUERREIRO, R., MÜHLEISEN, T. W., NÖTHEN, M. M., MOEBUS, S., JÖCKEL, K. H., KLOPP, N., WICHMANN, H. E., CARRASQUILLO, M. M., PANKRATZ, V. S., YOUNKIN, S. G., HOLMANS, P. A., O'DONOVAN, M., OWEN, M. J. & WILLIAMS, J. 2009. Genome-wide association study identifies variants at CLU and PICALM associated with Alzheimer's disease. *Nat Genet,* 41**,** 1088-93.

HERCULANO-HOUZEL, S. 2014. The glia/neuron ratio: how it varies uniformly across brain structures and species and what that means for brain physiology and evolution. *Glia,* 62**,** 1377-91.

HEWAGAMA, A., PATEL, D., YARLAGADDA, S., STRICKLAND, F. M. & RICHARDSON, B. C. 2009. Stronger inflammatory/cytotoxic T-cell response in women identified by microarray analysis. *Genes Immun,* 10**,** 509-16.

HILL, E. J., SOJKA, C., SAMPSON, M. M., WANG, H. L., KING, A. T., SING, A. D., FAUNDEZ, V. & SLOAN, S. A. 2025. Temporal regulation of human reactive astrocytes reveals their capacity for antigen presentation. *bioRxiv*.

HIRATA, K., MATSUOKA, K., TAGAI, K., ENDO, H., TATEBE, H., ONO, M., KOKUBO, N., OYAMA, A., SHINOTOH, H., TAKAHATA, K., OBATA, T., DEHGHANI, M., NEAR, J., KAWAMURA, K., ZHANG, M.-R., SHIMADA, H., YOKOTA, T., TOKUDA, T., HIGUCHI, M. & TAKADO, Y. 2024. Altered Brain Energy Metabolism Related to Astrocytes in Alzheimer's Disease. *Annals of Neurology,* 95**,** 104-115.

HØJGAARD, P., BALLEGAARD, C., CORDTZ, R., ZOBBE, K., CLAUSEN, M., GLINTBORG, B., KRISTENSEN, L. E. & DREYER, L. 2018. Gender differences in biologic treatment outcomes-a study of 1750 patients with psoriatic arthritis using Danish Health Care Registers. *Rheumatology (Oxford),* 57**,** 1651-1660.

HOSTENBACH, S., CAMBRON, M., D'HAESELEER, M., KOOIJMAN, R. & DE KEYSER, J. 2014. Astrocyte loss and astrogliosis in neuroinflammatory disorders. *Neurosci Lett,* 565**,** 39-41.

HUANG, Z., CHEN, B., LIU, X., LI, H., XIE, L., GAO, Y., DUAN, R., LI, Z., ZHANG, J., ZHENG, Y. & SU, W. 2021. Effects of sex and aging on the immune cell landscape as assessed by single-cell transcriptomic analysis. *Proc Natl Acad Sci U S A,* 118.

IMTIAZ, B., TAIPALE, H., TANSKANEN, A., TIIHONEN, M., KIVIPELTO, M., HEIKKINEN, A. M., TIIHONEN, J., SOININEN, H., HARTIKAINEN, S. & TOLPPANEN, A. M. 2017. Risk of Alzheimer's disease among users of postmenopausal hormone therapy: A nationwide case-control study. *Maturitas,* 98**,** 7-13.

ITAGAKI, S., MCGEER, P. L. & AKIYAMA, H. 1988. Presence of T-cytotoxic suppressor and leucocyte common antigen positive cells in Alzheimer's disease brain tissue. *Neuroscience Letters,* 91**,** 259-264.

ITO, M., KOMAI, K., MISE-OMATA, S., IIZUKA-KOGA, M., NOGUCHI, Y., KONDO, T., SAKAI, R., MATSUO, K., NAKAYAMA, T., YOSHIE, O., NAKATSUKASA, H., CHIKUMA, S., SHICHITA, T. & YOSHIMURA, A. 2019. Brain regulatory T cells suppress astrogliosis and potentiate neurological recovery. *Nature,* 565**,** 246-250.

JANELIDZE, S., BALI, D., ASHTON, N. J., BARTHÉLEMY, N. R., VANBRABANT, J., STOOPS, E., VANMECHELEN, E., HE, Y., DOLADO, A. O., TRIANA-BALTZER, G., PONTECORVO, M. J., ZETTERBERG, H., KOLB, H., VANDIJCK, M., BLENNOW, K., BATEMAN, R. J. & HANSSON, O. 2023. Head-to-head comparison of 10 plasma phospho-tau assays in prodromal Alzheimer's disease. *Brain,* 146**,** 1592-1601.

JANKOWSKY, J. L., FADALE, D. J., ANDERSON, J., XU, G. M., GONZALES, V., JENKINS, N. A., COPELAND, N. G., LEE, M. K., YOUNKIN, L. H., WAGNER, S. L., YOUNKIN, S. G. & BORCHELT, D. R. 2004. Mutant presenilins specifically elevate the levels of the 42 residue beta-amyloid peptide in vivo: evidence for augmentation of a 42-specific gamma secretase. *Hum Mol Genet,* 13**,** 159-70.

JANKOWSKY, J. L. & ZHENG, H. 2017. Practical considerations for choosing a mouse model of Alzheimer's disease. *Mol Neurodegener,* 12**,** 89.

JAY, T. R., HIRSCH, A. M., BROIHIER, M. L., MILLER, C. M., NEILSON, L. E., RANSOHOFF, R. M., LAMB, B. T. & LANDRETH, G. E. 2017. Disease Progression-Dependent Effects of TREM2 Deficiency in a Mouse Model of Alzheimer's Disease. *J Neurosci,* 37**,** 637-647.

JIAO, H., WANG, Z., LIU, Y., WANG, P. & XUE, Y. 2011. Specific role of tight junction proteins claudin-5, occludin, and ZO-1 of the blood-brain barrier in a focal cerebral ischemic insult. *J Mol Neurosci,* 44**,** 130-9.

JIWAJI, Z., TIWARI, S. S., AVILÉS-REYES, R. X., HOOLEY, M., HAMPTON, D., TORVELL, M., JOHNSON, D. A., MCQUEEN, J., BAXTER, P., SABARI-SANKAR, K., QIU, J., HE, X., FOWLER, J., FEBERY, J., GREGORY, J., ROSE, J., TULLOCH, J., LOAN, J., STORY, D., MCDADE, K., SMITH, A. M., GREER, P., BALL, M., KIND, P. C., MATTHEWS, P. M., SMITH, C., DANDO, O., SPIRES-JONES, T. L., JOHNSON, J. A., CHANDRAN, S. & HARDINGHAM, G. E. 2022. Reactive astrocytes acquire neuroprotective as well as deleterious signatures in response to Tau and Aß pathology. *Nat Commun,* 13**,** 135.

JOHNSON, E. C. B., DAMMER, E. B., DUONG, D. M., PING, L., ZHOU, M., YIN, L., HIGGINBOTHAM, L. A., GUAJARDO, A., WHITE, B., TRONCOSO, J. C., THAMBISETTY, M., MONTINE, T. J., LEE, E. B., TROJANOWSKI, J. Q., BEACH, T. G., REIMAN, E. M., HAROUTUNIAN, V., WANG, M., SCHADT, E., ZHANG, B., DICKSON, D. W., ERTEKIN-TANER, N., GOLDE, T. E., PETYUK, V. A., DE JAGER, P. L., BENNETT, D. A., WINGO, T. S., RANGARAJU, S., HAJJAR, I., SHULMAN, J. M., LAH, J. J., LEVEY, A. I. & SEYFRIED, N. T. 2020. Large-scale proteomic analysis of Alzheimer's disease brain and cerebrospinal fluid reveals early changes in energy metabolism associated with microglia and astrocyte activation. *Nat Med,* 26**,** 769-780.

JÖNSSON, L., WIMO, A., HANDELS, R., JOHANSSON, G., BOADA, M., ENGELBORGHS, S., FRÖLICH, L., JESSEN, F., KEHOE, P. G., KRAMBERGER, M., DE MENDONΣA, A., OUSSET, P. J., SCARMEAS, N., VISSER, P. J., WALDEMAR, G. & WINBLAD, B. 2023. The affordability of lecanemab, an amyloid-targeting therapy for Alzheimer's disease: an EADC-EC viewpoint. *Lancet Reg Health Eur,* 29**,** 100657.

JONSSON, T., STEFANSSON, H., STEINBERG, S., JONSDOTTIR, I., JONSSON, P. V., SNAEDAL, J., BJORNSSON, S., HUTTENLOCHER, J., LEVEY, A. I., LAH, J. J.,

RUJESCU, D., HAMPEL, H., GIEGLING, I., ANDREASSEN, O. A., ENGEDAL, K., ULSTEIN, I., DJUROVIC, S., IBRAHIM-VERBAAS, C., HOFMAN, A., IKRAM, M. A., VAN DUIJN, C. M., THORSTEINSDOTTIR, U., KONG, A. & STEFANSSON, K. 2012. Variant of TREM2 Associated with the Risk of Alzheimer's Disease. *New England Journal of Medicine,* 368**,** 107-116.

JUNG, M., LEE, S., PARK, S., HONG, J., KIM, C., CHO, I., SOHN, H. S., KIM, K., PARK, I. W., YOON, S., KWON, S., SHIN, J., LEE, D., KANG, M., GO, S., MOON, S., CHUNG, Y., KIM, Y. & KIM, B. S. 2023. A Therapeutic Nanovaccine that Generates Anti-Amyloid Antibodies and Amyloid-specific Regulatory T Cells for Alzheimer's Disease. *Adv Mater,* 35**,** e2207719.

KAMADA, M., IRAHARA, M., MAEGAWA, M., YASUI, T., TAKEJI, T., YAMADA, M., TEZUKA, M., KASAI, Y. & AONO, T. 2000. Effect of hormone replacement therapy on post-menopausal changes of lymphocytes and T cell subsets. *J Endocrinol Invest,* 23**,** 376-82.

KAMPHUIS, W., MIDDELDORP, J., KOOIJMAN, L., SLUIJS, J. A., KOOI, E. J., MOETON, M., FRERIKS, M., MIZEE, M. R. & HOL, E. M. 2014. Glial fibrillary acidic protein isoform expression in plaque related astrogliosis in Alzheimer's disease. *Neurobiol Aging,* 35**,** 492-510.

KEREN-SHAUL, H., SPINRAD, A., WEINER, A., MATCOVITCH-NATAN, O., DVIR-SZTERNFELD, R., ULLAND, T. K., DAVID, E., BARUCH, K., LARA-ASTAISO, D., TOTH, B., ITZKOVITZ, S., COLONNA, M., SCHWARTZ, M. & AMIT, I. 2017. A Unique Microglia Type Associated with Restricting Development of Alzheimer's Disease. *Cell,* 169**,** 1276-1290.e17.

KILGORE, M., MILLER, C. A., FASS, D. M., HENNIG, K. M., HAGGARTY, S. J., SWEATT, J. D. & RUMBAUGH, G. 2010. Inhibitors of class 1 histone deacetylases reverse contextual memory deficits in a mouse model of Alzheimer's disease. *Neuropsychopharmacology,* 35**,** 870-80.

KIPNIS, J., AVIDAN, H., CASPI, R. R. & SCHWARTZ, M. 2004. Dual effect of CD4+CD25+ regulatory T cells in neurodegeneration: a dialogue with microglia. *Proc Natl Acad Sci U S A,* 101 Suppl 2**,** 14663-9.

KIVISÄKK, P., FATIMA, H. A., CAHOON, D. S., OTIENO, B., CHACKO, L., MINOOEI, F., DEMOS, C., STENGELIN, M., SIGAL, G., WOHLSTADTER, J. & ARNOLD, S. E. 2024. Clinical evaluation of a novel plasma pTau217 electrochemiluminescence immunoassay in Alzheimer's disease. *Sci Rep,* 14**,** 629.

KIYOTA, T., MACHHI, J., LU, Y., DYAVARSHETTY, B., NEMATI, M., YOKOYAMA, I., MOSLEY, R. L. & GENDELMAN, H. E. 2018. Granulocyte-macrophage colony-stimulating factor neuroprotective activities in Alzheimer’s disease mice. *Journal of Neuroimmunology,* 319**,** 80-92.

KLEIN, S. L. & FLANAGAN, K. L. 2016. Sex differences in immune responses. *Nature Reviews Immunology,* 16**,** 626-638.

KLEIN, S. L., JEDLICKA, A. & PEKOSZ, A. 2010. The Xs and Y of immune responses to viral vaccines. *Lancet Infect Dis,* 10**,** 338-49.

KNUDTZON, S., NORDENGEN, K., PÅLHAUGEN, L., GÍSLADÓTTIR, B., JARHOLM, J., BRÅTHEN, G., SKOGSETH, R. E., WATERLOO, K., SELNES, P., FLADBY, T. & KIRSEBOM, B. E. 2025. Sexual dimorphisms in innate immune activation markers in predementia Alzheimer's disease. *Brain Commun,* 7**,** fcaf161.

KOCH-HENRIKSEN, N. & SØRENSEN, P. S. 2010. The changing demographic pattern of multiple sclerosis epidemiology. *Lancet Neurol,* 9**,** 520-32.

KRASEMANN, S., MADORE, C., CIALIC, R., BAUFELD, C., CALCAGNO, N., EL FATIMY, R., BECKERS, L., O'LOUGHLIN, E., XU, Y., FANEK, Z., GRECO, D. J., SMITH, S. T., TWEET, G., HUMULOCK, Z., ZRZAVY, T., CONDE-SANROMAN, P., GACIAS, M., WENG, Z., CHEN, H., TJON, E., MAZAHERI, F., HARTMANN, K., MADI, A., ULRICH, J. D., GLATZEL, M., WORTHMANN, A., HEEREN, J., BUDNIK, B., LEMERE, C., IKEZU, T., HEPPNER, F. L., LITVAK, V., HOLTZMAN, D. M., LASSMANN, H., WEINER, H. L., OCHANDO, J., HAASS, C. & BUTOVSKY, O. 2017. The TREM2-APOE Pathway Drives the Transcriptional Phenotype of Dysfunctional Microglia in Neurodegenerative Diseases. *Immunity,* 47**,** 566-581.e9.

KROCZYNSKA, B., RAFIDI, R. L., MAJCHRZAK-KITA, B., KOSCIUCZUK, E. M., BLYTH, G. T., JEMIELITY, J., WARMINSKA, Z., SALEIRO, D., MEHROTRA, S., ARSLAN, A. D., FISH, E. N. & PLATANIAS, L. C. 2016. Interferon γ (IFNγ) Signaling via Mechanistic Target of Rapamycin Complex 2 (mTORC2) and Regulatory Effects in the Generation of Type II Interferon Biological Responses. *J Biol Chem,* 291**,** 2389-96.

KRONZER, V. L., BRIDGES, S. L., JR. & DAVIS, J. M., 3RD 2021. Why women have more autoimmune diseases than men: An evolutionary perspective. *Evol Appl,* 14**,** 629-633.

KUNIS, G., BARUCH, K., ROSENZWEIG, N., KERTSER, A., MILLER, O., BERKUTZKI, T. & SCHWARTZ, M. 2013. IFN-γ-dependent activation of the brain's choroid plexus for CNS immune surveillance and repair. *Brain,* 136**,** 3427-40.

KURZ, C., WALKER, L., RAUCHMANN, B. S. & PERNECZKY, R. 2022. Dysfunction of the blood-brain barrier in Alzheimer's disease: Evidence from human studies. *Neuropathol Appl Neurobiol,* 48**,** e12782.

LABONTE, J., SUGARMAN, M. A., PETTWAY, E., ZETTERBERG, H., BLENNOW, K., ASHTON, N. J., KARIKARI, T. K., APARICIO, H. J., FRANK, B., TRIPODIS, Y., MARTIN, B., PALMISANO, J. N., STEINBERG, E. G., SIMKIN, I., FARRER, L. A., JUN, G. R., TURK, K. W., BUDSON, A. E., O'CONNOR, M. K., AU, R., GOLDSTEIN, L. E., STERN, R. A., STEIN, T. D., MCKEE, A. C., QIU, W. Q., MEZ, J., BANKS, S. J. & ALOSCO, M. L. 2025. Sex differences on tau, astrocytic, and neurodegenerative plasma biomarkers. *J Alzheimers Dis,* 105**,** 443-452.

LACOSTA, A. M., PASCUAL-LUCAS, M., PESINI, P., CASABONA, D., PÉREZ-GRIJALBA, V., MARCOS-CAMPOS, I., SARASA, L., CANUDAS, J., BADI, H., MONLEÓN, I., SAN-JOSÉ, I., MUNUERA, J., RODRÍGUEZ-GÓMEZ, O., ABDELNOUR, C., LAFUENTE, A., BUENDÍA, M., BOADA, M., TÁRRAGA, L., RUIZ, A. & SARASA, M. 2018. Safety, tolerability and immunogenicity of an active anti-Aβ(40) vaccine (ABvac40) in patients with Alzheimer's disease: a randomised, double-blind, placebo-controlled, phase I trial. *Alzheimers Res Ther,* 10**,** 12.

LAI, W., WU, J., ZOU, X., XIE, J., ZHANG, L., ZHAO, X., ZHAO, M., WANG, Q. & JI, J. 2013. Secretome analyses of Aβ(1-42) stimulated hippocampal astrocytes reveal that CXCL10 is involved in astrocyte migration. *J Proteome Res,* 12**,** 832-43.

LALONDE, R., KIM, H. D., MAXWELL, J. A. & FUKUCHI, K. 2005. Exploratory activity and spatial learning in 12-month-old APP(695)SWE/co+PS1/DeltaE9 mice with amyloid plaques. *Neurosci Lett,* 390**,** 87-92.

LANFRANCO, M. F., MOCCHETTI, I., BURNS, M. P. & VILLAPOL, S. 2018. Glial- and Neuronal-Specific Expression of CCL5 mRNA in the Rat Brain. *Frontiers in Neuroanatomy,* Volume 11 - 2017.

LARBI, A. & FULOP, T. 2014. From "truly naïve" to "exhausted senescent" T cells: when markers predict functionality. *Cytometry A,* 85**,** 25-35.

LARBI, A., PAWELEC, G., WITKOWSKI, J. M., SCHIPPER, H. M., DERHOVANESSIAN, E., GOLDECK, D. & FULOP, T. 2009. Dramatic Shifts in Circulating CD4 but not CD8 T Cell Subsets in Mild Alzheimer's Disease. *Journal of Alzheimer's Disease,* 17**,** 91-103.

LEE, B. W., YAP, H. K., CHEW, F. T., QUAH, T. C., PRABHAKARAN, K., CHAN, G. S., WONG, S. C. & SEAH, C. C. 1996. Age- and sex-related changes in lymphocyte subpopulations of healthy Asian subjects: from birth to adulthood. *Cytometry,* 26**,** 8-15.

LEE, C. Y. D., DAGGETT, A., GU, X., JIANG, L. L., LANGFELDER, P., LI, X., WANG, N., ZHAO, Y., PARK, C. S., COOPER, Y., FERANDO, I., MODY, I., COPPOLA, G., XU, H. & YANG, X. W. 2018. Elevated TREM2 Gene Dosage Reprograms Microglia Responsivity and Ameliorates Pathological Phenotypes in Alzheimer's Disease Models. *Neuron,* 97**,** 1032-1048.e5.

LEE, J., MASON, R., MARTIN, L. & BARNABE, C. 2014. Biologic therapy response and drug survival for females compared to males with rheumatoid arthritis: a cohort study. *Rheumatol Int,* 34**,** 1449-53.

LEE, S.-H., REZZONICO, M. G., FRIEDMAN, B. A., HUNTLEY, M. H., MEILANDT, W. J., PANDEY, S., CHEN, Y.-J. J., EASTON, A., MODRUSAN, Z., HANSEN, D. V., SHENG, M. & BOHLEN, C. J. 2021. TREM2-independent oligodendrocyte, astrocyte, and T cell responses to tau and amyloid pathology in mouse models of Alzheimer disease. *Cell Reports,* 37.

LEVY-LAHAD, E., WASCO, W., POORKAJ, P., ROMANO, D. M., OSHIMA, J., PETTINGELL, W. H., YU, C. E., JONDRO, P. D., SCHMIDT, S. D., WANG, K. & ET AL. 1995. Candidate gene for the chromosome 1 familial Alzheimer's disease locus. *Science,* 269**,** 973-7.

LEWCZUK, P., BECK, G., GANSLANDT, O., ESSELMANN, H., DEISENHAMMER, F., REGENITER, A., PETEREIT, H. F., TUMANI, H., GERRITZEN, A., OSCHMANN, P., SCHRÖDER, J., SCHÖNKNECHT, P., ZIMMERMANN, K., HAMPEL, H., BÜRGER, K., OTTO, M., HAUSTEIN, S., HERZOG, K., DANNENBERG, R., WURSTER, U., BIBL, M., MALER, J. M., REUBACH, U., KORNHUBER, J. & WILTFANG, J. 2006. International quality control survey of neurochemical dementia diagnostics. *Neurosci Lett,* 409**,** 1-4.

LEWIS, S. M., WILLIAMS, A. & EISENBARTH, S. C. 2019. Structure and function of the immune system in the spleen. *Sci Immunol,* 4.

LI, Y., FAN, H., HAN, X., SUN, J., NI, M., ZHANG, L., FANG, F., ZHANG, W. & MA, P. 2023. PR-957 Suppresses Th1 and Th17 Cell Differentiation via Inactivating PI3K/AKT Pathway in Alzheimer’s Disease. *Neuroscience,* 510**,** 82-94.

LIDDELOW, S. A., GUTTENPLAN, K. A., CLARKE, L. E., BENNETT, F. C., BOHLEN, C. J., SCHIRMER, L., BENNETT, M. L., MÜNCH, A. E., CHUNG, W. S., PETERSON,

T. C., WILTON, D. K., FROUIN, A., NAPIER, B. A., PANICKER, N., KUMAR, M., BUCKWALTER, M. S., ROWITCH, D. H., DAWSON, V. L., DAWSON, T. M., STEVENS, B. & BARRES, B. A. 2017. Neurotoxic reactive astrocytes are induced by activated microglia. *Nature,* 541**,** 481-487.

LIN, M., YU, J. X., ZHANG, W. X., LAO, F. X. & HUANG, H.-C. 2024. Roles of TREM2 in the Pathological Mechanism and the Therapeutic Strategies of Alzheimer's Disease. *The Journal of Prevention of Alzheimer's Disease,* 11**,** 1682-1695.

LIU, C. C., ZHAO, N., FU, Y., WANG, N., LINARES, C., TSAI, C. W. & BU, G. 2017. ApoE4 Accelerates Early Seeding of Amyloid Pathology. *Neuron,* 96**,** 1024-1032.e3.

LONG, J. M. & HOLTZMAN, D. M. 2019. Alzheimer Disease: An Update on Pathobiology and Treatment Strategies. *Cell,* 179**,** 312-339.

LOUVEAU, A., SMIRNOV, I., KEYES, T. J., ECCLES, J. D., ROUHANI, S. J., PESKE, J. D., DERECKI, N. C., CASTLE, D., MANDELL, J. W., LEE, K. S., HARRIS, T. H. & KIPNIS, J. 2015. Structural and functional features of central nervous system lymphatic vessels. *Nature,* 523**,** 337-341.

LOVELL, C. D. & ANGUERA, M. C. 2025. More X's, more problems: how contributions from the X chromosomes enhance female predisposition for autoimmunity. *Current Opinion in Immunology,* 93**,** 102543.

LUCHSINGER, J. A., PALTA, P., RIPPON, B., SOTO, L., CEBALLOS, F., PARDO, M., LAING, K., IGWE, K., JOHNSON, A., TOMLJANOVIC, Z., HE, H., REITZ, C., KREISL, W., RAZLIGHI, Q., TERESI, J., MORENO, H. & BRICKMAN, A. M. 2020. Sex Differences in in vivo Alzheimer's Disease Neuropathology in Late Middle-Aged Hispanics. *J Alzheimers Dis,* 74**,** 1243-1252.

LUEG, G., GROSS, C. C., LOHMANN, H., JOHNEN, A., KEMMLING, A., DEPPE, M., GROGER, J., MINNERUP, J., WIENDL, H., MEUTH, S. G. & DUNING, T. 2015. Clinical relevance of specific T-cell activation in the blood and cerebrospinal fluid of patients with mild Alzheimer's disease. *Neurobiol Aging,* 36**,** 81-9.

LYRA E SILVA, N. M., GONÇALVES, R. A., PASCOAL, T. A., LIMA-FILHO, R. A. S., RESENDE, E. D. P. F., VIEIRA, E. L. M., TEIXEIRA, A. L., DE SOUZA, L. C., PENY, J. A., FORTUNA, J. T. S., FURIGO, I. C., HASHIGUCHI, D., MIYA-COREIXAS, V. S., CLARKE, J. R., ABISAMBRA, J. F., LONGO, B. M., DONATO, J., FRASER, P. E., ROSA-NETO, P., CARAMELLI, P., FERREIRA, S. T. & DE FELICE, F. G. 2021. Pro-inflammatory interleukin-6 signaling links cognitive impairments and peripheral metabolic alterations in Alzheimer's disease. *Translational Psychiatry,* 11**,** 251.

MACHHI, J., YEAPURI, P., LU, Y., FOSTER, E., CHIKHALE, R., HERSKOVITZ, J., NAMMINGA, K. L., OLSON, K. E., ABDELMOATY, M. M., GAO, J., QUADROS, R. M., KIYOTA, T., JINGJING, L., KEVADIYA, B. D., WANG, X., LIU, Y., POLUEKTOVA, L. Y., GURUMURTHY, C. B., MOSLEY, R. L. & GENDELMAN, H. E. 2021. CD4+ effector T cells accelerate Alzheimer's disease in mice. *Journal of Neuroinflammation,* 18**,** 272.

MAHAN, T. E., WANG, C., BAO, X., CHOUDHURY, A., ULRICH, J. D. & HOLTZMAN, D. M. 2022. Selective reduction of astrocyte apoE3 and apoE4 strongly reduces Aβ accumulation and plaque-related pathology in a mouse model of amyloidosis. *Mol Neurodegener,* 17**,** 13.

MAHLEY, R. W. 1988. Apolipoprotein E: cholesterol transport protein with expanding role in cell biology. *Science,* 240**,** 622-30.
MAHNKE, Y. D., BRODIE, T. M., SALLUSTO, F., ROEDERER, M. & LUGLI, E. 2013. The who's who of T-cell differentiation: human memory T-cell subsets. *Eur J Immunol,* 43**,** 2797-809.
MAKARAVA, N., MYCHKO, O., MOLESWORTH, K., CHANG, J. C.-Y., HENRY, R. J., TSYMBALYUK, N., GERZANICH, V., SIMARD, J. M., LOANE, D. J. & BASKAKOV, I. V. 2023. Region-specific homeostatic identity of astrocytes is essential for defining their reactive phenotypes following pathological insults. *bioRxiv***,** 2023.02.01.526708.
MANDALA, W., HARAWA, V., MUNYENYEMBE, A., SOKO, M. & LONGWE, H. 2021. Optimization of stimulation and staining conditions for intracellular cytokine staining (ICS) for determination of cytokine-producing T cells and monocytes. *Curr Res Immunol,* 2**,** 184-193.
MANGOLD, C. A., WRONOWSKI, B., DU, M., MASSER, D. R., HADAD, N., BIXLER, G. V., BRUCKLACHER, R. M., FORD, M. M., SONNTAG, W. E. & FREEMAN, W. M. 2017. Sexually divergent induction of microglial-associated neuroinflammation with hippocampal aging. *J Neuroinflammation,* 14**,** 141.
MATHYS, H., BOIX, C. A., AKAY, L. A., XIA, Z., DAVILA-VELDERRAIN, J., NG, A. P., JIANG, X., ABDELHADY, G., GALANI, K., MANTERO, J., BAND, N., JAMES, B. T., BABU, S., GALIANA-MELENDEZ, F., LOUDERBACK, K., PROKOPENKO, D., TANZI, R. E., BENNETT, D. A., TSAI, L. H. & KELLIS, M. 2024. Single-cell multiregion dissection of Alzheimer's disease. *Nature,* 632**,** 858-868.
MATHYS, H., DAVILA-VELDERRAIN, J., PENG, Z., GAO, F., MOHAMMADI, S., YOUNG, J. Z., MENON, M., HE, L., ABDURROB, F., JIANG, X., MARTORELL, A. J., RANSOHOFF, R. M., HAFLER, B. P., BENNETT, D. A., KELLIS, M. & TSAI, L. H. 2019. Single-cell transcriptomic analysis of Alzheimer's disease. *Nature,* 570**,** 332-337.
MAURER, M. & VON STEBUT, E. 2004. Macrophage inflammatory protein-1. *Int J Biochem Cell Biol,* 36**,** 1882-6.
MAYO, L., CUNHA, A. P., MADI, A., BEYNON, V., YANG, Z., ALVAREZ, J. I., PRAT, A., SOBEL, R. A., KOBZIK, L., LASSMANN, H., QUINTANA, F. J. & WEINER, H. L. 2016. IL-10-dependent Tr1 cells attenuate astrocyte activation and ameliorate chronic central nervous system inflammation. *Brain,* 139**,** 1939-57.
MCCOMISH, S. F., O'SULLIVAN, J., COPAS, A. M. M., IMIOLEK, M., BOYLE, N. T., CROMPTON, L. A., LANE, J. D. & CALDWELL, M. A. 2024. Reactive astrocytes generated from human iPSC are pro-inflammatory and display altered metabolism. *Exp Neurol,* 382**,** 114979.
MCKHANN, G., DRACHMAN, D., FOLSTEIN, M., KATZMAN, R., PRICE, D. & STADLAN, E. M. 1984. Clinical diagnosis of Alzheimer's disease: report of the NINCDS-ADRDA Work Group under the auspices of Department of Health and Human Services Task Force on Alzheimer's Disease. *Neurology,* 34**,** 939-44.
MCQUADE, A., KANG, Y. J., HASSELMANN, J., JAIRAMAN, A., SOTELO, A., COBURN, M., SHABESTARI, S. K., CHADAREVIAN, J. P., FOTE, G., TU, C. H., DANHASH, E., SILVA, J., MARTINEZ, E., COTMAN, C., PRIETO, G. A., THOMPSON, L. M.,

STEFFAN, J. S., SMITH, I., DAVTYAN, H., CAHALAN, M., CHO, H. & BLURTON-JONES, M. 2023. Author Correction: Gene expression and functional deficits underlie TREM2-knockout microglia responses in human models of Alzheimer's disease. *Nature Communications,* 14**,** 1194.

MELA, V., GABAN, A. S., SHATZ, P. M., GUILLOT-SESTIER, M. V. & LYNCH, M. A. 2023. Acute Stress, Induced by IFNγ + Aβ, and Chronic Stress, Induced by Age, Affect Microglia in a Sex-Specific Manner. *Mol Neurobiol*.

MELNIKOVA, T., PARK, D., BECKER, L., LEE, D., CHO, E., SAYYIDA, N., TIAN, J., BANDEEN-ROCHE, K., BORCHELT, D. R. & SAVONENKO, A. V. 2016. Sex-related dimorphism in dentate gyrus atrophy and behavioral phenotypes in an inducible tTa:APPsi transgenic model of Alzheimer's disease. *Neurobiology of Disease,* 96**,** 171-185.

MEYER-LUEHMANN, M., MIELKE, M., SPIRES-JONES, T. L., STOOTHOFF, W., JONES, P., BACSKAI, B. J. & HYMAN, B. T. 2009. A Reporter of Local Dendritic Translocation Shows Plaque- Related Loss of Neural System Function in APP-Transgenic Mice. *The Journal of Neuroscience,* 29**,** 12636-12640.

MHATRE-WINTERS, I., EID, A., HAN, Y., TIEU, K. & RICHARDSON, J. R. 2022. Sex and APOE Genotype Alter the Basal and Induced Inflammatory States of Primary Microglia from APOE Targeted Replacement Mice. *Int J Mol Sci,* 23.

MISHRA, A., SHANG, Y., WANG, Y., BACON, E. R., YIN, F. & BRINTON, R. D. 2020. Dynamic Neuroimmune Profile during Mid-life Aging in the Female Brain and Implications for Alzheimer Risk. *iScience,* 23**,** 101829.

MITTAL, K., EREMENKO, E., BERNER, O., ELYAHU, Y., STROMINGER, I., APELBLAT, D., NEMIROVSKY, A., SPIEGEL, I. & MONSONEGO, A. 2019. CD4 T Cells Induce A Subset of MHCII-Expressing Microglia that Attenuates Alzheimer Pathology. *iScience,* 16**,** 298-311.

MOEHLMANN, T., WINKLER, E., XIA, X., EDBAUER, D., MURRELL, J., CAPELL, A., KAETHER, C., ZHENG, H., GHETTI, B., HAASS, C. & STEINER, H. 2002. Presenilin-1 mutations of leucine 166 equally affect the generation of the Notch and APP intracellular domains independent of their effect on Abeta 42 production. *Proc Natl Acad Sci U S A,* 99**,** 8025-30.

MONTAGNE, A., NATION, D. A., SAGARE, A. P., BARISANO, G., SWEENEY, M. D., CHAKHOYAN, A., PACHICANO, M., JOE, E., NELSON, A. R., D'ORAZIO, L. M., BUENNAGEL, D. P., HARRINGTON, M. G., BENZINGER, T. L. S., FAGAN, A. M., RINGMAN, J. M., SCHNEIDER, L. S., MORRIS, J. C., REIMAN, E. M., CASELLI, R. J., CHUI, H. C., TCW, J., CHEN, Y., PA, J., CONTI, P. S., LAW, M., TOGA, A. W. & ZLOKOVIC, B. V. 2020. APOE4 leads to blood-brain barrier dysfunction predicting cognitive decline. *Nature,* 581**,** 71-76.

MONTEIRO, S., FERREIRA, F. M., PINTO, V., ROQUE, S., MORAIS, M., DE SÁ-CALÇADA, D., MOTA, C., CORREIA-NEVES, M. & CERQUEIRA, J. J. 2016. Absence of IFNγ promotes hippocampal plasticity and enhances cognitive performance. *Transl Psychiatry,* 6**,** e707.

MORO-GARCÍA, M. A., ALONSO-ARIAS, R. & LÓPEZ-LARREA, C. 2013. When Aging Reaches CD4+ T-Cells: Phenotypic and Functional Changes. *Front Immunol,* 4**,** 107.

MOSCONI, L., BERTI, V., QUINN, C., MCHUGH, P., PETRONGOLO, G., VARSAVSKY, I., OSORIO, R. S., PUPI, A., VALLABHAJOSULA, S., ISAACSON, R. S., DE

LEON, M. J. & BRINTON, R. D. 2017. Sex differences in Alzheimer risk: Brain imaging of endocrine vs chronologic aging. *Neurology,* 89**,** 1382-1390.
MUCHAMUEL, T., BASLER, M., AUJAY, M. A., SUZUKI, E., KALIM, K. W., LAUER, C., SYLVAIN, C., RING, E. R., SHIELDS, J., JIANG, J., SHWONEK, P., PARLATI, F., DEMO, S. D., BENNETT, M. K., KIRK, C. J. & GROETTRUP, M. 2009. A selective inhibitor of the immunoproteasome subunit LMP7 blocks cytokine production and attenuates progression of experimental arthritis. *Nature Medicine,* 15**,** 781-787.
MULLAN, M., CRAWFORD, F., AXELMAN, K., HOULDEN, H., LILIUS, L., WINBLAD, B. & LANNFELT, L. 1992. A pathogenic mutation for probable Alzheimer's disease in the APP gene at the N-terminus of beta-amyloid. *Nat Genet,* 1**,** 345-7.
MURRELL, J., FARLOW, M., GHETTI, B. & BENSON, M. D. 1991. A mutation in the amyloid precursor protein associated with hereditary Alzheimer's disease. *Science,* 254**,** 97-9.
NAJ, A. C., JUN, G., BEECHAM, G. W., WANG, L. S., VARDARAJAN, B. N., BUROS, J., GALLINS, P. J., BUXBAUM, J. D., JARVIK, G. P., CRANE, P. K., LARSON, E. B., BIRD, T. D., BOEVE, B. F., GRAFF-RADFORD, N. R., DE JAGER, P. L., EVANS, D., SCHNEIDER, J. A., CARRASQUILLO, M. M., ERTEKIN-TANER, N., YOUNKIN, S. G., CRUCHAGA, C., KAUWE, J. S., NOWOTNY, P., KRAMER, P., HARDY, J., HUENTELMAN, M. J., MYERS, A. J., BARMADA, M. M., DEMIRCI, F. Y., BALDWIN, C. T., GREEN, R. C., ROGAEVA, E., ST GEORGE-HYSLOP, P., ARNOLD, S. E., BARBER, R., BEACH, T., BIGIO, E. H., BOWEN, J. D., BOXER, A., BURKE, J. R., CAIRNS, N. J., CARLSON, C. S., CARNEY, R. M., CARROLL, S. L., CHUI, H. C., CLARK, D. G., CORNEVEAUX, J., COTMAN, C. W., CUMMINGS, J. L., DECARLI, C., DEKOSKY, S. T., DIAZ-ARRASTIA, R., DICK, M., DICKSON, D. W., ELLIS, W. G., FABER, K. M., FALLON, K. B., FARLOW, M. R., FERRIS, S., FROSCH, M. P., GALASKO, D. R., GANGULI, M., GEARING, M., GESCHWIND, D. H., GHETTI, B., GILBERT, J. R., GILMAN, S., GIORDANI, B., GLASS, J. D., GROWDON, J. H., HAMILTON, R. L., HARRELL, L. E., HEAD, E., HONIG, L. S., HULETTE, C. M., HYMAN, B. T., JICHA, G. A., JIN, L. W., JOHNSON, N., KARLAWISH, J., KARYDAS, A., KAYE, J. A., KIM, R., KOO, E. H., KOWALL, N. W., LAH, J. J., LEVEY, A. I., LIEBERMAN, A. P., LOPEZ, O. L., MACK, W. J., MARSON, D. C., MARTINIUK, F., MASH, D. C., MASLIAH, E., MCCORMICK, W. C., MCCURRY, S. M., MCDAVID, A. N., MCKEE, A. C., MESULAM, M., MILLER, B. L., et al. 2011. Common variants at MS4A4/MS4A6E, CD2AP, CD33 and EPHA1 are associated with late-onset Alzheimer's disease. *Nat Genet,* 43**,** 436-41.
NAKAMURA, A., KANEKO, N., VILLEMAGNE, V. L., KATO, T., DOECKE, J., DORÉ, V., FOWLER, C., LI, Q.-X., MARTINS, R., ROWE, C., TOMITA, T., MATSUZAKI, K., ISHII, K., ISHII, K., ARAHATA, Y., IWAMOTO, S., ITO, K., TANAKA, K., MASTERS, C. L. & YANAGISAWA, K. 2018. High performance plasma amyloid-β biomarkers for Alzheimer’s disease. *Nature,* 554**,** 249-254.
NAKASHIMA, K., WIESE, S., YANAGISAWA, M., ARAKAWA, H., KIMURA, N., HISATSUNE, T., YOSHIDA, K., KISHIMOTO, T., SENDTNER, M. & TAGA, T. 1999. Developmental requirement of gp130 signaling in neuronal survival and astrocyte differentiation. *J Neurosci,* 19**,** 5429-34.

NATION, D. A., SWEENEY, M. D., MONTAGNE, A., SAGARE, A. P., D'ORAZIO, L. M., PACHICANO, M., SEPEHRBAND, F., NELSON, A. R., BUENNAGEL, D. P., HARRINGTON, M. G., BENZINGER, T. L. S., FAGAN, A. M., RINGMAN, J. M., SCHNEIDER, L. S., MORRIS, J. C., CHUI, H. C., LAW, M., TOGA, A. W. & ZLOKOVIC, B. V. 2019. Blood-brain barrier breakdown is an early biomarker of human cognitive dysfunction. *Nat Med,* 25**,** 270-276.

NEHRA, G., BAUER, B. & HARTZ, A. M. S. 2022. Blood-brain barrier leakage in Alzheimer's disease: From discovery to clinical relevance. *Pharmacology & Therapeutics,* 234**,** 108119.

NEHRA, G., MALONEY, B. J., SMITH, R. R., CHUMBOATONG, W., ABNER, E. L., NELSON, P. T., BAUER, B. & HARTZ, A. M. S. 2025. Plasma S100β is a predictor for pathology and cognitive decline in Alzheimer's disease. *Fluids and Barriers of the CNS,* 22**,** 4.

NERATTINI, M., JETT, S., ANDY, C., CARLTON, C., ZARATE, C., BONEU, C., BATTISTA, M., PAHLAJANI, S., LOEB-ZEITLIN, S., HAVRYULIK, Y., WILLIAMS, S., CHRISTOS, P., FINK, M., BRINTON, R. D. & MOSCONI, L. 2023. Systematic review and meta-analysis of the effects of menopause hormone therapy on risk of Alzheimer's disease and dementia. *Front Aging Neurosci,* 15**,** 1260427.

NICHOLS, E., STEINMETZ, J. D., VOLLSET, S. E., FUKUTAKI, K., CHALEK, J., ABD-ALLAH, F., ABDOLI, A., ABUALHASAN, A., ABU-GHARBIEH, E., AKRAM, T. T., AL HAMAD, H., ALAHDAB, F., ALANEZI, F. M., ALIPOUR, V., ALMUSTANYIR, S., AMU, H., ANSARI, I., ARABLOO, J., ASHRAF, T., ASTELL-BURT, T., AYANO, G., AYUSO-MATEOS, J. L., BAIG, A. A., BARNETT, A., BARROW, A., BAUNE, B. T., BÉJOT, Y., BEZABHE, W. M. M., BEZABIH, Y. M., BHAGAVATHULA, A. S., BHASKAR, S., BHATTACHARYYA, K., BIJANI, A., BISWAS, A., BOLLA, S. R., BOLOOR, A., BRAYNE, C., BRENNER, H., BURKART, K., BURNS, R. A., CÁMERA, L. A., CAO, C., CARVALHO, F., CASTRO-DE-ARAUJO, L. F. S., CATALÁ-LÓPEZ, F., CERIN, E., CHAVAN, P. P., CHERBUIN, N., CHU, D.-T., COSTA, V. M., COUTO, R. A. S., DADRAS, O., DAI, X., DANDONA, L., DANDONA, R., DE LA CRUZ-GÓNGORA, V., DHAMNETIYA, D., DIAS DA SILVA, D., DIAZ, D., DOUIRI, A., EDVARDSSON, D., EKHOLUENETALE, M., EL SAYED, I., EL-JAAFARY, S. I., ESKANDARI, K., ESKANDARIEH, S., ESMAEILNEJAD, S., FARES, J., FARO, A., FAROOQUE, U., FEIGIN, V. L., FENG, X., FERESHTEHNEJAD, S.-M., FERNANDES, E., FERRARA, P., FILIP, I., FILLIT, H., FISCHER, F., GAIDHANE, S., GALLUZZO, L., GHASHGHAEE, A., GHITH, N., GIALLUISI, A., GILANI, S. A., GLAVAN, I.-R., GNEDOVSKAYA, E. V., GOLECHHA, M., GUPTA, R., GUPTA, V. B., GUPTA, V. K., HAIDER, M. R., HALL, B. J., HAMIDI, S., HANIF, A., HANKEY, G. J., HAQUE, S., HARTONO, R. K., HASABALLAH, A. I., HASAN, M. T., HASSAN, A., et al. 2022. Estimation of the global prevalence of dementia in 2019 and forecasted prevalence in 2050: an analysis for the Global Burden of Disease Study 2019. *The Lancet Public Health,* 7**,** e105-e125.

O'NEILL, E., MELA, V., GABAN, A. S., BECHET, S., MCGRATH, A., WALSH, A., MCINTOSH, A. & LYNCH, M. A. 2022. Sex-Related Microglial Perturbation Is Related to Mitochondrial Changes in a Model of Alzheimer's Disease. *Front Cell Neurosci,* 16**,** 939830.

OAKLEY, H., COLE, S. L., LOGAN, S., MAUS, E., SHAO, P., CRAFT, J., GUILLOZET-BONGAARTS, A., OHNO, M., DISTERHOFT, J., VAN ELDIK, L., BERRY, R. & VASSAR, R. 2006. Intraneuronal beta-amyloid aggregates, neurodegeneration, and neuron loss in transgenic mice with five familial Alzheimer's disease mutations: potential factors in amyloid plaque formation. *J Neurosci,* 26**,** 10129-40.

OBERSTEIN, T. J., TAHA, L., SPITZER, P., HELLSTERN, J., HERRMANN, M., KORNHUBER, J. & MALER, J. M. 2018. Imbalance of Circulating T(h)17 and Regulatory T Cells in Alzheimer's Disease: A Case Control Study. *Front Immunol,* 9**,** 1213.

ODDO, S., CACCAMO, A., SHEPHERD, J. D., MURPHY, M. P., GOLDE, T. E., KAYED, R., METHERATE, R., MATTSON, M. P., AKBARI, Y. & LAFERLA, F. M. 2003. Triple-transgenic model of Alzheimer's disease with plaques and tangles: intracellular Abeta and synaptic dysfunction. *Neuron,* 39**,** 409-21.

OKADA, S., NAKAMURA, M., KATOH, H., MIYAO, T., SHIMAZAKI, T., ISHII, K., YAMANE, J., YOSHIMURA, A., IWAMOTO, Y., TOYAMA, Y. & OKANO, H. 2006. Conditional ablation of Stat3 or Socs3 discloses a dual role for reactive astrocytes after spinal cord injury. *Nature Medicine,* 12**,** 829-834.

OKITA, K., ICHISAKA, T. & YAMANAKA, S. 2007. Generation of germline-competent induced pluripotent stem cells. *Nature,* 448**,** 313-317.

OKITA, K., MATSUMURA, Y., SATO, Y., OKADA, A., MORIZANE, A., OKAMOTO, S., HONG, H., NAKAGAWA, M., TANABE, K., TEZUKA, K.-I., SHIBATA, T., KUNISADA, T., TAKAHASHI, M., TAKAHASHI, J., SAJI, H. & YAMANAKA, S. 2011. A more efficient method to generate integration-free human iPS cells. *Nature Methods,* 8**,** 409-412.

OLAH, M., PATRICK, E., VILLANI, A.-C., XU, J., WHITE, C. C., RYAN, K. J., PIEHOWSKI, P., KAPASI, A., NEJAD, P., CIMPEAN, M., CONNOR, S., YUNG, C. J., FRANGIEH, M., MCHENRY, A., ELYAMAN, W., PETYUK, V., SCHNEIDER, J. A., BENNETT, D. A., DE JAGER, P. L. & BRADSHAW, E. M. 2018. A transcriptomic atlas of aged human microglia. *Nature Communications,* 9**,** 539.

ORGOGOZO, J. M., GILMAN, S., DARTIGUES, J. F., LAURENT, B., PUEL, M., KIRBY, L. C., JOUANNY, P., DUBOIS, B., EISNER, L., FLITMAN, S., MICHEL, B. F., BOADA, M., FRANK, A. & HOCK, C. 2003. Subacute meningoencephalitis in a subset of patients with AD after Abeta42 immunization. *Neurology,* 61**,** 46-54.

ORRE, M., KAMPHUIS, W., OSBORN, L. M., JANSEN, A. H. P., KOOIJMAN, L., BOSSERS, K. & HOL, E. M. 2014. Isolation of glia from Alzheimer's mice reveals inflammation and dysfunction. *Neurobiology of Aging,* 35**,** 2746-2760.

ORTONA, E., PIERDOMINICI, M., MASELLI, A., VERONI, C., ALOISI, F. & SHOENFELD, Y. 2016. Sex-based differences in autoimmune diseases. *Ann Ist Super Sanita,* 52**,** 205-12.

OVEISGHARAN, S., ARVANITAKIS, Z., YU, L., FARFEL, J., SCHNEIDER, J. A. & BENNETT, D. A. 2018. Sex differences in Alzheimer's disease and common neuropathologies of aging. *Acta Neuropathol,* 136**,** 887-900.

PALMQVIST, S., MATTSSON, N. & HANSSON, O. 2016. Cerebrospinal fluid analysis detects cerebral amyloid-β accumulation earlier than positron emission tomography. *Brain,* 139**,** 1226-36.

PALMQVIST, S., STOMRUD, E., CULLEN, N., JANELIDZE, S., MANUILOVA, E., JETHWA, A., BITTNER, T., EICHENLAUB, U., SURIDJAN, I., KOLLMORGEN, G., RIEPE, M., VON ARNIM, C. A. F., TUMANI, H., HAGER, K., HEIDENREICH, F., MATTSSON-CARLGREN, N., ZETTERBERG, H., BLENNOW, K. & HANSSON, O. 2023. An accurate fully automated panel of plasma biomarkers for Alzheimer's disease. *Alzheimers Dement,* 19**,** 1204-1215.

PALOMER, E., BUECHLER, J. & SALINAS, P. C. 2019. Wnt Signaling Deregulation in the Aging and Alzheimer's Brain. *Front Cell Neurosci,* 13**,** 227.

PAOLICELLI, R. C., SIERRA, A., STEVENS, B., TREMBLAY, M.-E., AGUZZI, A., AJAMI, B., AMIT, I., AUDINAT, E., BECHMANN, I., BENNETT, M., BENNETT, F., BESSIS, A., BIBER, K., BILBO, S., BLURTON-JONES, M., BODDEKE, E., BRITES, D., BRÔNE, B., BROWN, G. C., BUTOVSKY, O., CARSON, M. J., CASTELLANO, B., COLONNA, M., COWLEY, S. A., CUNNINGHAM, C., DAVALOS, D., DE JAGER, P. L., DE STROOPER, B., DENES, A., EGGEN, B. J. L., EYO, U., GALEA, E., GAREL, S., GINHOUX, F., GLASS, C. K., GOKCE, O., GOMEZ-NICOLA, D., GONZÁLEZ, B., GORDON, S., GRAEBER, M. B., GREENHALGH, A. D., GRESSENS, P., GRETER, M., GUTMANN, D. H., HAASS, C., HENEKA, M. T., HEPPNER, F. L., HONG, S., HUME, D. A., JUNG, S., KETTENMANN, H., KIPNIS, J., KOYAMA, R., LEMKE, G., LYNCH, M., MAJEWSKA, A., MALCANGIO, M., MALM, T., MANCUSO, R., MASUDA, T., MATTEOLI, M., MCCOLL, B. W., MIRON, V. E., MOLOFSKY, A. V., MONJE, M., MRACSKO, E., NADJAR, A., NEHER, J. J., NENISKYTE, U., NEUMANN, H., NODA, M., PENG, B., PERI, F., PERRY, V. H., POPOVICH, P. G., PRIDANS, C., PRILLER, J., PRINZ, M., RAGOZZINO, D., RANSOHOFF, R. M., SALTER, M. W., SCHAEFER, A., SCHAFER, D. P., SCHWARTZ, M., SIMONS, M., SMITH, C. J., STREIT, W. J., TAY, T. L., TSAI, L.-H., VERKHRATSKY, A., VON BERNHARDI, R., WAKE, H., WITTAMER, V., WOLF, S. A., WU, L.-J. & WYSS-CORAY, T. 2022. Microglia states and nomenclature: A field at its crossroads. *Neuron,* 110**,** 3458-3483.

PARAJULI, B., SONOBE, Y., KAWANOKUCHI, J., DOI, Y., NODA, M., TAKEUCHI, H., MIZUNO, T. & SUZUMURA, A. 2012. GM-CSF increases LPS-induced production of proinflammatory mediators via upregulation of TLR4 and CD14 in murine microglia. *J Neuroinflammation,* 9**,** 268.

PARK, S. Y., CHA, N., KIM, S., CHAE, S., LEE, W. J., JUNG, H. & BAE, H. 2024a. Blocking Microglial Proliferation by CSF-1R Inhibitor Does Not Alter the Neuroprotective Effects of Adoptive Regulatory T Cells in 3xTg Alzheimer's Disease Mice. *Curr Issues Mol Biol,* 46**,** 2871-2883.

PARK, S. Y., YANG, J., YANG, H., CHO, I., KIM, J. Y. & BAE, H. 2024b. Therapeutic Effects of Aβ-Specific Regulatory T Cells in Alzheimer's Disease: A Study in 5xFAD Mice. *Int J Mol Sci,* 25.

PAUMIER, A., BOISSEAU, S., JACQUIER-SARLIN, M., PERNET-GALLAY, K., BUISSON, A. & ALBRIEUX, M. 2021. Astrocyte–neuron interplay is critical for Alzheimer's disease pathogenesis and is rescued by TRPA1 channel blockade. *Brain,* 145**,** 388-405.

PEREZ-TUR, J., FROELICH, S., PRIHAR, G., CROOK, R., BAKER, M., DUFF, K., WRAGG, M., BUSFIELD, F., LENDON, C., CLARK, R. F. & ET AL. 1995. A

mutation in Alzheimer's disease destroying a splice acceptor site in the presenilin-1 gene. *Neuroreport,* 7**,** 297-301.
PERRIOT, S., CANALES, M., MATHIAS, A. & DU PASQUIER, R. 2021. Differentiation of functional astrocytes from human-induced pluripotent stem cells in chemically defined media. *STAR Protoc,* 2**,** 100902.
PICCIO, L., DEMING, Y., DEL-ÁGUILA, J. L., GHEZZI, L., HOLTZMAN, D. M., FAGAN, A. M., FENOGLIO, C., GALIMBERTI, D., BORRONI, B. & CRUCHAGA, C. 2016. Cerebrospinal fluid soluble TREM2 is higher in Alzheimer disease and associated with mutation status. *Acta Neuropathol,* 131**,** 925-33.
PIEHL, N., VAN OLST, L., RAMAKRISHNAN, A., TEREGULOVA, V., SIMONTON, B., ZHANG, Z., TAPP, E., CHANNAPPA, D., OH, H., LOSADA, P. M., RUTLEDGE, J., TRELLE, A. N., MORMINO, E. C., ELAHI, F., GALASKO, D. R., HENDERSON, V. W., WAGNER, A. D., WYSS-CORAY, T. & GATE, D. 2022. Cerebrospinal fluid immune dysregulation during healthy brain aging and cognitive impairment. *Cell,* 185**,** 5028-5039.e13.
PLANTONE, D., PARDINI, M., MANCO, C., RIGHI, D., ALÌ, P. A., ARNALDI, D., PELAGOTTI, V., MASSA, F., D'ALESSANDRO, M., BARGAGLI, E. & DE STEFANO, N. 2025. CSF IL-6, GDF-15, GFAP and NfL levels in early Alzheimer disease: a pilot study. *Ther Adv Neurol Disord,* 18**,** 17562864251314773.
POSILLICO, C. K., GARCIA-HERNANDEZ, R. E. & TRONSON, N. C. 2021. Sex differences and similarities in the neuroimmune response to central administration of poly I:C. *J Neuroinflammation,* 18**,** 193.
POTLURI, T., FINK, A. L., SYLVIA, K. E., DHAKAL, S., VERMILLION, M. S., VOM STEEG, L., DESHPANDE, S., NARASIMHAN, H. & KLEIN, S. L. 2019. Age-associated changes in the impact of sex steroids on influenza vaccine responses in males and females. *NPJ Vaccines,* 4**,** 29.
POTTER, H., WOODCOCK, J. H., BOYD, T. D., COUGHLAN, C. M., O'SHAUGHNESSY, J. R., BORGES, M. T., THAKER, A. A., RAJ, B. A., ADAMSZUK, K., SCOTT, D., ADAME, V., ANTON, P., CHIAL, H. J., GRAY, H., DANIELS, J., STOCKER, M. E. & SILLAU, S. H. 2021. Safety and efficacy of sargramostim (GM-CSF) in the treatment of Alzheimer's disease. *Alzheimers Dement (N Y),* 7**,** e12158.
QIN, X., WANG, Y. & PAUDEL, H. K. 2017. Inhibition of Early Growth Response 1 in the Hippocampus Alleviates Neuropathology and Improves Cognition in an Alzheimer Model with Plaques and Tangles. *Am J Pathol,* 187**,** 1828-1847.
RAHMAN, M. T., GHOSH, C., HOSSAIN, M., LINFIELD, D., REZAEE, F., JANIGRO, D., MARCHI, N. & VAN BOXEL-DEZAIRE, A. H. H. 2018. IFN-γ, IL-17A, or zonulin rapidly increase the permeability of the blood-brain and small intestinal epithelial barriers: Relevance for neuro-inflammatory diseases. *Biochem Biophys Res Commun,* 507**,** 274-279.
RANDOLPH, C., TIERNEY, M. C., MOHR, E. & CHASE, T. N. 1998. The Repeatable Battery for the Assessment of Neuropsychological Status (RBANS): preliminary clinical validity. *J Clin Exp Neuropsychol,* 20**,** 310-9.
RECASENS, M., ALMOLDA, B., PÉREZ-CLAUSELL, J., CAMPBELL, I. L., GONZÁLEZ, B. & CASTELLANO, B. 2021. Chronic exposure to IL-6 induces a desensitized phenotype of the microglia. *Journal of Neuroinflammation,* 18**,** 31.
RICHETIN, K., PETSOPHONSAKUL, P., ROYBON, L., GUIARD, B. P. & RAMPON, C. 2017. Differential alteration of hippocampal function and plasticity in

females and males of the APPxPS1 mouse model of Alzheimer's disease. *Neurobiology of Aging,* 57**,** 220-231.
RISSMAN, R. A., LANGFORD, O., RAMAN, R., DONOHUE, M. C., ABDEL-LATIF, S., MEYER, M. R., WENTE-ROTH, T., KIRMESS, K. M., NGOLAB, J., WINSTON, C. N., JIMENEZ-MAGGIORA, G., RAFII, M. S., SACHDEV, P., WEST, T., YARASHESKI, K. E., BRAUNSTEIN, J. B., IRIZARRY, M., JOHNSON, K. A., AISEN, P. S. & SPERLING, R. A. 2024. Plasma Aβ42/Aβ40 and phospho-tau217 concentration ratios increase the accuracy of amyloid PET classification in preclinical Alzheimer's disease. *Alzheimers Dement,* 20**,** 1214-1224.
ROGAEV, E. I., SHERRINGTON, R., ROGAEVA, E. A., LEVESQUE, G., IKEDA, M., LIANG, Y., CHI, H., LIN, C., HOLMAN, K., TSUDA, T. & ET AL. 1995. Familial Alzheimer's disease in kindreds with missense mutations in a gene on chromosome 1 related to the Alzheimer's disease type 3 gene. *Nature,* 376**,** 775-8.
ROGERS, J., LUBER-NAROD, J., STYREN, S. D. & CIVIN, W. H. 1988. Expression of immune system-associated antigens by cells of the human central nervous system: Relationship to the pathology of Alzheimer's disease. *Neurobiology of Aging,* 9**,** 339-349.
ROSENKRANZ, D., WEYER, S., TOLOSA, E., GAENSLEN, A., BERG, D., LEYHE, T., GASSER, T. & STOLTZE, L. 2007. Higher frequency of regulatory T cells in the elderly and increased suppressive activity in neurodegeneration. *J Neuroimmunol,* 188**,** 117-27.
ROSI, S., PERT, C. B., RUFF, M. R., MCGANN-GRAMLING, K. & WENK, G. L. 2005. Chemokine receptor 5 antagonist D-Ala-peptide T-amide reduces microglia and astrocyte activation within the hippocampus in a neuroinflammatory rat model of Alzheimer's disease. *Neuroscience,* 134**,** 671-6.
ROSSET, M. B., LUI, G., DANSOKHO, C., CHAIGNEAU, T. & DOROTHÉE, G. 2015. Vaccine-induced Aβ-specific CD8+ T cells do not trigger autoimmune neuroinflammation in a murine model of Alzheimer’s disease. *Journal of Neuroinflammation,* 12**,** 95.
ROSTAMI, J., FOTAKI, G., SIROIS, J., MZEZEWA, R., BERGSTRÖM, J., ESSAND, M., HEALY, L. & ERLANDSSON, A. 2020. Astrocytes have the capacity to act as antigen-presenting cells in the Parkinson’s disease brain. *Journal of Neuroinflammation,* 17**,** 119.
SADICK, J. S., O'DEA, M. R., HASEL, P., DYKSTRA, T., FAUSTIN, A. & LIDDELOW, S. A. 2022. Astrocytes and oligodendrocytes undergo subtype-specific transcriptional changes in Alzheimer's disease. *Neuron,* 110**,** 1788-1805.e10.
SAETZLER, V., RIET, T., SCHIENKE, A., HENSCHEL, P., FREITAG, K., HAAKE, A., HEPPNER, F. L., BUITRAGO-MOLINA, L. E., NOYAN, F., JAECKEL, E. & HARDTKE-WOLENSKI, M. 2023. Development of Beta-Amyloid-Specific CAR-Tregs for the Treatment of Alzheimer's Disease. *Cells,* 12.
SALA FRIGERIO, C., WOLFS, L., FATTORELLI, N., THRUPP, N., VOYTYUK, I., SCHMIDT, I., MANCUSO, R., CHEN, W. T., WOODBURY, M. E., SRIVASTAVA, G., MÖLLER, T., HUDRY, E., DAS, S., SAIDO, T., KARRAN, E., HYMAN, B., PERRY, V. H., FIERS, M. & DE STROOPER, B. 2019. The Major Risk Factors for

Alzheimer's Disease: Age, Sex, and Genes Modulate the Microglia Response to Aβ Plaques. *Cell Rep,* 27**,** 1293-1306.e6.
SALEH, R. N. M., HORNBERGER, M., RITCHIE, C. W. & MINIHANE, A. M. 2023. Hormone replacement therapy is associated with improved cognition and larger brain volumes in at-risk APOE4 women: results from the European Prevention of Alzheimer's Disease (EPAD) cohort. *Alzheimer's Research & Therapy,* 15**,** 10.
SALLOWAY, S., SPERLING, R., FOX, N. C., BLENNOW, K., KLUNK, W., RASKIND, M., SABBAGH, M., HONIG, L. S., PORSTEINSSON, A. P., FERRIS, S., REICHERT, M., KETTER, N., NEJADNIK, B., GUENZLER, V., MILOSLAVSKY, M., WANG, D., LU, Y., LULL, J., TUDOR, I. C., LIU, E., GRUNDMAN, M., YUEN, E., BLACK, R. & BRASHEAR, H. R. 2014. Two phase 3 trials of bapineuzumab in mild-to-moderate Alzheimer's disease. *N Engl J Med,* 370**,** 322-33.
SÁNCHEZ-JUAN, P., VALERIANO-LORENZO, E., RUIZ-GONZÁLEZ, A., PASTOR, A. B., RODRIGO LARA, H., LÓPEZ-GONZÁLEZ, F., ZEA-SEVILLA, M. A., VALENTÍ, M., FRADES, B., RUIZ, P., SAIZ, L., BURGUEÑO-GARCÍA, I., CALERO, M., DEL SER, T. & RÁBANO, A. 2024. Serum GFAP levels correlate with astrocyte reactivity, post-mortem brain atrophy and neurofibrillary tangles. *Brain,* 147**,** 1667-1679.
SANCHEZ-MICO, M. V., JIMENEZ, S., GOMEZ-ARBOLEDAS, A., MUÑOZ-CASTRO, C., ROMERO-MOLINA, C., NAVARRO, V., SANCHEZ-MEJIAS, E., NUÑEZ-DIAZ, C., SANCHEZ-VARO, R., GALEA, E., DAVILA, J. C., VIZUETE, M., GUTIERREZ, A. & VITORICA, J. 2021. Amyloid-β impairs the phagocytosis of dystrophic synapses by astrocytes in Alzheimer's disease. *Glia,* 69**,** 997-1011.
SANFILIPPO, C., CASTROGIOVANNI, P., IMBESI, R., MUSUMECI, G., VECCHIO, M., LI VOLTI, G., TIBULLO, D., BROGGI, G., CALTABIANO, R., ULIVIERI, M., KAZAKOVA, M., PARENTI, R., VICARIO, N., FAZIO, F. & DI ROSA, M. 2022. Sex-dependent neuro-deconvolution analysis of Alzheimer's disease brain transcriptomes according to CHI3L1 expression levels. *Journal of Neuroimmunology,* 373**,** 577977.
SANFILIPPO, C., MALAGUARNERA, L. & DI ROSA, M. 2016. Chitinase expression in Alzheimer's disease and non-demented brains regions. *J Neurol Sci,* 369**,** 242-249.
SANKARAN-WALTERS, S., MACAL, M., GRISHINA, I., NAGY, L., GOULART, L., COOLIDGE, K., LI, J., FENTON, A., WILLIAMS, T., MILLER, M. K., FLAMM, J., PRINDIVILLE, T., GEORGE, M. & DANDEKAR, S. 2013. Sex differences matter in the gut: effect on mucosal immune activation and inflammation. *Biol Sex Differ,* 4**,** 10.
SCHINDLER, S. E., BOLLINGER, J. G., OVOD, V., MAWUENYEGA, K. G., LI, Y., GORDON, B. A., HOLTZMAN, D. M., MORRIS, J. C., BENZINGER, T. L. S., XIONG, C., FAGAN, A. M. & BATEMAN, R. J. 2019. High-precision plasma β-amyloid 42/40 predicts current and future brain amyloidosis. *Neurology,* 93**,** e1647-e1659.
SCHINDLER, S. E., GRAY, J. D., GORDON, B. A., XIONG, C., BATRLA-UTERMANN, R., QUAN, M., WAHL, S., BENZINGER, T. L. S., HOLTZMAN, D. M., MORRIS, J. C. & FAGAN, A. M. 2018. Cerebrospinal fluid biomarkers measured by Elecsys assays compared to amyloid imaging. *Alzheimers Dement,* 14**,** 1460-1469.

SELKOE, D. J. 1991. The molecular pathology of Alzheimer's disease. *Neuron,* 6**,** 487-498.

SERIO, A., BILICAN, B., BARMADA, S. J., ANDO, D. M., ZHAO, C., SILLER, R., BURR, K., HAGHI, G., STORY, D., NISHIMURA, A. L., CARRASCO, M. A., PHATNANI, H. P., SHUM, C., WILMUT, I., MANIATIS, T., SHAW, C. E., FINKBEINER, S. & CHANDRAN, S. 2013. Astrocyte pathology and the absence of non-cell autonomy in an induced pluripotent stem cell model of TDP-43 proteinopathy. *Proceedings of the National Academy of Sciences,* 110**,** 4697-4702.

SERRANO-POZO, A., LI, H., LI, Z., MUÑOZ-CASTRO, C., JAISA-AAD, M., HEALEY, M. A., WELIKOVITCH, L. A., JAYAKUMAR, R., BRYANT, A. G., NOORI, A., CONNORS, T. R., HU, M., ZHAO, K., LIAO, F., LIN, G., PASTIKA, T., TAMM, J., ABDOURAHMAN, A., KWON, T., BENNETT, R. E., WOODBURY, M. E., WACHTER, A., TALANIAN, R. V., BIBER, K., KARRAN, E. H., HYMAN, B. T. & DAS, S. 2024. Astrocyte transcriptomic changes along the spatiotemporal progression of Alzheimer's disease. *Nature Neuroscience,* 27**,** 2384-2400.

SHENG, W., WU, Z., WEI, J., WANG, J., ZHANG, S., DING, Z., ZHONG, J., DENG, D., ZHONG, Z., YIN, Y., LI, Y. & WANG, Q. 2025. Astrocyte-derived CXCL10 exacerbates endothelial cells pyroptosis and blood–brain barrier disruption via CXCR3/cGAS/AIM2 pathway after intracerebral hemorrhage. *Cell Death Discovery,* 11**,** 373.

SHERRINGTON, R., ROGAEV, E. I., LIANG, Y., ROGAEVA, E. A., LEVESQUE, G., IKEDA, M., CHI, H., LIN, C., LI, G., HOLMAN, K., TSUDA, T., MAR, L., FONCIN, J. F., BRUNI, A. C., MONTESI, M. P., SORBI, S., RAINERO, I., PINESSI, L., NEE, L., CHUMAKOV, I., POLLEN, D., BROOKES, A., SANSEAU, P., POLINSKY, R. J., WASCO, W., DA SILVA, H. A., HAINES, J. L., PERKICAK-VANCE, M. A., TANZI, R. E., ROSES, A. D., FRASER, P. E., ROMMENS, J. M. & ST GEORGE-HYSLOP, P. H. 1995. Cloning of a gene bearing missense mutations in early-onset familial Alzheimer's disease. *Nature,* 375**,** 754-60.

SHI, Y., KIRWAN, P. & LIVESEY, F. J. 2012. Directed differentiation of human pluripotent stem cells to cerebral cortex neurons and neural networks. *Nature Protocols,* 7**,** 1836-1846.

SIMS, J. R., ZIMMER, J. A., EVANS, C. D., LU, M., ARDAYFIO, P., SPARKS, J., WESSELS, A. M., SHCHERBININ, S., WANG, H., MONKUL NERY, E. S., COLLINS, E. C., SOLOMON, P., SALLOWAY, S., APOSTOLOVA, L. G., HANSSON, O., RITCHIE, C., BROOKS, D. A., MINTUN, M. & SKOVRONSKY, D. M. 2023. Donanemab in Early Symptomatic Alzheimer Disease: The TRAILBLAZER-ALZ 2 Randomized Clinical Trial. *Jama,* 330**,** 512-527.

SMITH, A. M., DAVEY, K., TSARTSALIS, S., KHOZOIE, C., FANCY, N., TANG, S. S., LIAPTSI, E., WEINERT, M., MCGARRY, A., MUIRHEAD, R. C. J., GENTLEMAN, S., OWEN, D. R. & MATTHEWS, P. M. 2022. Diverse human astrocyte and microglial transcriptional responses to Alzheimer's pathology. *Acta Neuropathologica,* 143**,** 75-91.

SONG, Y. J., LI, S. R., LI, X. W., CHEN, X., WEI, Z. X., LIU, Q. S. & CHENG, Y. 2020. The Effect of Estrogen Replacement Therapy on Alzheimer's Disease and Parkinson's Disease in Postmenopausal Women: A Meta-Analysis. *Front Neurosci,* 14**,** 157.

SOUDY, M., BARS, S. L. & GLAAB, E. 2025. Sex-dependent molecular landscape of Alzheimer's disease revealed by large-scale single-cell transcriptomics. *Alzheimers Dement,* 21**,** e14476.
SOUYRIS, M., CENAC, C., AZAR, P., DAVIAUD, D., CANIVET, A., GRUNENWALD, S., PIENKOWSKI, C., CHAUMEIL, J., MEJÍA, J. E. & GUÉRY, J. C. 2018. TLR7 escapes X chromosome inactivation in immune cells. *Sci Immunol,* 3.
SQUIRE, L. R., STARK, C. E. & CLARK, R. E. 2004. The medial temporal lobe. *Annu Rev Neurosci,* 27**,** 279-306.
SRIRAM, K., BENKOVIC, S. A., HEBERT, M. A., MILLER, D. B. & O'CALLAGHAN, J. P. 2004. Induction of gp130-related cytokines and activation of JAK2/STAT3 pathway in astrocytes precedes up-regulation of glial fibrillary acidic protein in the 1-methyl-4-phenyl-1,2,3,6-tetrahydropyridine model of neurodegeneration: key signaling pathway for astrogliosis in vivo? *J Biol Chem,* 279**,** 19936-47.
ST GEORGE-HYSLOP, P. H., TANZI, R. E., POLINSKY, R. J., HAINES, J. L., NEE, L., WATKINS, P. C., MYERS, R. H., FELDMAN, R. G., POLLEN, D., DRACHMAN, D., GROWDON, J., BRUNI, A., FONCIN, J.-F., SALMON, D., FROMMELT, P., AMADUCCI, L., SORBI, S., PIACENTINI, S., STEWART, G. D., HOBBS, W. J., CONNEALLY, P. M. & GUSELLA, J. F. 1987. The Genetic Defect Causing Familial Alzheimer's Disease Maps on Chromosome 21. *Science,* 235**,** 885-890.
STARR, R., WILLSON, T. A., VINEY, E. M., MURRAY, L. J., RAYNER, J. R., JENKINS, B. J., GONDA, T. J., ALEXANDER, W. S., METCALF, D., NICOLA, N. A. & HILTON, D. J. 1997. A family of cytokine-inducible inhibitors of signalling. *Nature,* 387**,** 917-21.
STEPHEN, T. L., BRENINGSTALL, B., SURESH, S., MCGILL, C. J. & PIKE, C. J. 2022. APOE genotype and biological sex regulate astroglial interactions with amyloid plaques in Alzheimer's disease mice. *J Neuroinflammation,* 19**,** 286.
STEPHEN, T. L., CACCIOTTOLO, M., BALU, D., MORGAN, T. E., LADU, M. J., FINCH, C. E. & PIKE, C. J. 2019. APOE genotype and sex affect microglial interactions with plaques in Alzheimer's disease mice. *Acta Neuropathol Commun,* 7**,** 82.
STUBBE, M., VANDERHEYDE, N., GOLDMAN, M. & MARCHANT, A. 2006. Antigen-specific central memory CD4+ T lymphocytes produce multiple cytokines and proliferate in vivo in humans. *J Immunol,* 177**,** 8185-90.
STYM-POPPER, G., MATTA, K., CHAIGNEAU, T., RUPRA, R., DEMETRIOU, A., FOUQUET, S., DANSOKHO, C., TOLY-NDOUR, C. & DOROTHÉE, G. 2023. Regulatory T cells decrease C3-positive reactive astrocytes in Alzheimer-like pathology. *Journal of Neuroinflammation,* 20**,** 64.
SU, W., SARAVIA, J., RISCH, I., RANKIN, S., GUY, C., CHAPMAN, N. M., SHI, H., SUN, Y., KC, A., LI, W., HUANG, H., LIM, S. A., HU, H., WANG, Y., LIU, D., JIAO, Y., CHEN, P.-C., SOLIMAN, H., YAN, K.-K., ZHANG, J., VOGEL, P., LIU, X., SERRANO, G. E., BEACH, T. G., YU, J., PENG, J. & CHI, H. 2023. CXCR6 orchestrates brain CD8+ T cell residency and limits mouse Alzheimer's disease pathology. *Nature Immunology,* 24**,** 1735-1747.
TAGLIATTI, E., DESIATO, G., MANCINELLI, S., BIZZOTTO, M., GAGLIANI, M. C., FAGGIANI, E., HERNÁNDEZ-SOTO, R., CUGURRA, A., POLISENO, P., MIOTTO, M., ARGÜELLO, R. J., FILIPELLO, F., CORTESE, K., MORINI, R.,

LODATO, S. & MATTEOLI, M. 2024. Trem2 expression in microglia is required to maintain normal neuronal bioenergetics during development. *Immunity,* 57**,** 86-105.e9.

TAIPA, R., DAS NEVES, S. P., SOUSA, A. L., FERNANDES, J., PINTO, C., CORREIA, A. P., SANTOS, E., PINTO, P. S., CARNEIRO, P., COSTA, P., SANTOS, D., ALONSO, I., PALHA, J., MARQUES, F., CAVACO, S. & SOUSA, N. 2019. Proinflammatory and anti-inflammatory cytokines in the CSF of patients with Alzheimer's disease and their correlation with cognitive decline. *Neurobiol Aging,* 76**,** 125-132.

TAKAHASHI, K., TANABE, K., OHNUKI, M., NARITA, M., ICHISAKA, T., TOMODA, K. & YAMANAKA, S. 2007. Induction of pluripotent stem cells from adult human fibroblasts by defined factors. *Cell,* 131**,** 861-72.

TAKAHASHI, K. & YAMANAKA, S. 2006. Induction of pluripotent stem cells from mouse embryonic and adult fibroblast cultures by defined factors. *Cell,* 126**,** 663-76.

TCW, J., QIAN, L., PIPALIA, N. H., CHAO, M. J., LIANG, S. A., SHI, Y., JAIN, B. R., BERTELSEN, S. E., KAPOOR, M., MARCORA, E., SIKORA, E., ANDREWS, E. J., MARTINI, A. C., KARCH, C. M., HEAD, E., HOLTZMAN, D. M., ZHANG, B., WANG, M., MAXFIELD, F. R., POON, W. W. & GOATE, A. M. 2022. Cholesterol and matrisome pathways dysregulated in astrocytes and microglia. *Cell,* 185**,** 2213-2233.e25.

THOMSON, J. A., ITSKOVITZ-ELDOR, J., SHAPIRO, S. S., WAKNITZ, M. A., SWIERGIEL, J. J., MARSHALL, V. S. & JONES, J. M. 1998. Embryonic Stem Cell Lines Derived from Human Blastocysts. *Science,* 282**,** 1145-1147.

UBOGU, E. E., CALLAHAN, M. K., TUCKY, B. H. & RANSOHOFF, R. M. 2006. Determinants of CCL5-driven mononuclear cell migration across the blood-brain barrier. Implications for therapeutically modulating neuroinflammation. *J Neuroimmunol,* 179**,** 132-44.

ULLAND, T. K., SONG, W. M., HUANG, S. C.-C., ULRICH, J. D., SERGUSHICHEV, A., BEATTY, W. L., LOBODA, A. A., ZHOU, Y., CAIRNS, N. J., KAMBAL, A., LOGINICHEVA, E., GILFILLAN, S., CELLA, M., VIRGIN, H. W., UNANUE, E. R., WANG, Y., ARTYOMOV, M. N., HOLTZMAN, D. M. & COLONNA, M. 2017. TREM2 Maintains Microglial Metabolic Fitness in Alzheimer's Disease. *Cell,* 170**,** 649-663.e13.

ULRICH, J. D., ULLAND, T. K., MAHAN, T. E., NYSTRÖM, S., NILSSON, K. P., SONG, W. M., ZHOU, Y., REINARTZ, M., CHOI, S., JIANG, H., STEWART, F. R., ANDERSON, E., WANG, Y., COLONNA, M. & HOLTZMAN, D. M. 2018. ApoE facilitates the microglial response to amyloid plaque pathology. *J Exp Med,* 215**,** 1047-1058.

VAN DYCK, C. H., SWANSON, C. J., AISEN, P., BATEMAN, R. J., CHEN, C., GEE, M., KANEKIYO, M., LI, D., REYDERMAN, L., COHEN, S., FROELICH, L., KATAYAMA, S., SABBAGH, M., VELLAS, B., WATSON, D., DHADDA, S., IRIZARRY, M., KRAMER, L. D. & IWATSUBO, T. 2022. Lecanemab in Early Alzheimer's Disease. *New England Journal of Medicine,* 388**,** 9-21.

VAN DYCK, C. H., SWANSON, C. J., AISEN, P., BATEMAN, R. J., CHEN, C., GEE, M., KANEKIYO, M., LI, D., REYDERMAN, L., COHEN, S., FROELICH, L., KATAYAMA, S., SABBAGH, M., VELLAS, B., WATSON, D., DHADDA, S.,

IRIZARRY, M., KRAMER, L. D. & IWATSUBO, T. 2023. Lecanemab in Early Alzheimer's Disease. *N Engl J Med,* 388**,** 9-21.
VAN OLST, L., KAMERMANS, A., HALTERS, S., VAN DER POL, S. M. A., RODRIGUEZ, E., VERBERK, I. M. W., VERBERK, S. G. S., WESSELS, D. W. R., RODRIGUEZ-MOGEDA, C., VERHOEFF, J., WOUTERS, D., VAN DEN BOSSCHE, J., GARCIA-VALLEJO, J. J., LEMSTRA, A. W., WITTE, M. E., VAN DER FLIER, W. M., TEUNISSEN, C. E. & DE VRIES, H. E. 2024. Adaptive immune changes associate with clinical progression of Alzheimer's disease. *Molecular Neurodegeneration,* 19**,** 38.
VAN WAGONER, N. J., OH, J. W., REPOVIC, P. & BENVENISTE, E. N. 1999. Interleukin-6 (IL-6) production by astrocytes: autocrine regulation by IL-6 and the soluble IL-6 receptor. *J Neurosci,* 19**,** 5236-44.
VATINE, G. D., BARRILE, R., WORKMAN, M. J., SANCES, S., BARRIGA, B. K., RAHNAMA, M., BARTHAKUR, S., KASENDRA, M., LUCCHESI, C., KERNS, J., WEN, N., SPIVIA, W. R., CHEN, Z., VAN EYK, J. & SVENDSEN, C. N. 2019. Human iPSC-Derived Blood-Brain Barrier Chips Enable Disease Modeling and Personalized Medicine Applications. *Cell Stem Cell,* 24**,** 995-1005.e6.
VELDHOEN, M., HOCKING, R. J., ATKINS, C. J., LOCKSLEY, R. M. & STOCKINGER, B. 2006. TGFbeta in the context of an inflammatory cytokine milieu supports de novo differentiation of IL-17-producing T cells. *Immunity,* 24**,** 179-89.
VERMA, K., OGONEK, J., VARANASI, P. R., LUTHER, S., BÜNTING, I., THOMAY, K., BEHRENS, Y. L., MISCHAK-WEISSINGER, E. & HAMBACH, L. 2017. Human CD8+ CD57- TEMRA cells: Too young to be called "old". *PLoS One,* 12**,** e0177405.
VERMUNT, L., SIKKES, S. A. M., VAN DEN HOUT, A., HANDELS, R., BOS, I., VAN DER FLIER, W. M., KERN, S., OUSSET, P. J., MARUFF, P., SKOOG, I., VERHEY, F. R. J., FREUND-LEVI, Y., TSOLAKI, M., WALLIN Å, K., OLDE RIKKERT, M., SOININEN, H., SPIRU, L., ZETTERBERG, H., BLENNOW, K., SCHELTENS, P., MUNIZ-TERRERA, G. & VISSER, P. J. 2019. Duration of preclinical, prodromal, and dementia stages of Alzheimer's disease in relation to age, sex, and APOE genotype. *Alzheimers Dement,* 15**,** 888-898.
VILA-CASTELAR, C., AKINCI, M., PALPATZIS, E., AGUILAR-DOMINGUEZ, P., OPERTO, G., KOLLMORGEN, G., QUIJANO-RUBIO, C., BLENNOW, K., ZETTERBERG, H., FALCON, C., FAURIA, K., GISPERT, J. D., GRAU-RIVERA, O., SUÁREZ-CALVET, M., ARENAZA-URQUIJO, E. M., ANASTASI, F., BETETA, A., BRUGULAT-SERRAT, A., CACCIAGLIA, R., CUMPLIDO-MAYORAL, I., CAÑAS, A., DEL CAMPO, M., DEULOFEU, C., DOMINGUEZ, R., EMILIO, M., FERNÁNDEZ-ARCOS, A., FUENTES, S., GENIUS, P., GONZÁLEZ-ESCALANTE, A., HERNÁNDEZ, L., HERNÁNDEZ-VILLAMIZAR, F., HUGUET, J., LÓPEZ-MARTOS, D., LUGO, F., MARNE, P., MENCHÓN, T., MINGUILLON, C., ORTIZ, P., PELKMANS, W., POLO, A., PRADAS, S., RODRÍGUEZ-FERNÁNDEZ, B., SÁNCHEZ-BENAVIDES, G., SHEKARI, M., SOTERAS, A., STANKEVICIUTE, L., VILANOVA, M., VILOR-TEJEDOR, N. & FOR THE, A. S. 2025. Sex/gender effects of glial reactivity on preclinical Alzheimer's disease pathology. *Molecular Psychiatry,* 30**,** 1430-1439.

VOIRIN, A.-C., PEREK, N. & ROCHE, F. 2020. Inflammatory stress induced by a combination of cytokines (IL-6, IL-17, TNF-α) leads to a loss of integrity on bEnd.3 endothelial cells in vitro BBB model. *Brain Research,* 1730**,** 146647.
WAGNER, A., GARNER-SPITZER, E., JASINSKA, J., KOLLARITSCH, H., STIASNY, K., KUNDI, M. & WIEDERMANN, U. 2018. Age-related differences in humoral and cellular immune responses after primary immunisation: indications for stratified vaccination schedules. *Sci Rep,* 8**,** 9825.
WAN, W., CAO, L., LIU, L., ZHANG, C., KALIONIS, B., TAI, X., LI, Y. & XIA, S. 2015. Aβ(1-42) oligomer-induced leakage in an in vitro blood-brain barrier model is associated with up-regulation of RAGE and metalloproteinases, and down-regulation of tight junction scaffold proteins. *J Neurochem,* 134**,** 382-93.
WANG, C., XIONG, M., GRATUZE, M., BAO, X., SHI, Y., ANDHEY, P. S., MANIS, M., SCHROEDER, C., YIN, Z., MADORE, C., BUTOVSKY, O., ARTYOMOV, M., ULRICH, J. D. & HOLTZMAN, D. M. 2021a. Selective removal of astrocytic APOE4 strongly protects against tau-mediated neurodegeneration and decreases synaptic phagocytosis by microglia. *Neuron,* 109**,** 1657-1674.e7.
WANG, J., TANILA, H., PUOLIVÄLI, J., KADISH, I. & GROEN, T. V. 2003. Gender differences in the amount and deposition of amyloidβ in APPswe and PS1 double transgenic mice. *Neurobiology of Disease,* 14**,** 318-327.
WANG, L., ZHANG, Y., ZHAO, Y., MARSHALL, C., WU, T. & XIAO, M. 2019. Deep cervical lymph node ligation aggravates AD-like pathology of APP/PS1 mice. *Brain Pathol,* 29**,** 176-192.
WANG, X., CAMPBELL, B., BODOGAI, M., MCDEVITT, R. A., PATRIKEEV, A., GUSEV, F., RAGONNAUD, E., KUMARASWAMI, K., SHIRENOVA, S., VARDY, K., ALAMEH, M.-G., WEISSMAN, D., ISHIKAWA-ANKERHOLD, H., OKUN, E., ROGAEV, E. & BIRAGYN, A. 2024a. CD8+ T cells exacerbate AD-like symptoms in mouse model of amyloidosis. *Brain, Behavior, and Immunity,* 122**,** 444-455.
WANG, Y., EMRE, C., GYLLENHAMMAR-SCHILL, H., FJELLMAN, K., EYJOLFSDOTTIR, H., ERIKSDOTTER, M., SCHULTZBERG, M. & HJORTH, E. 2021b. Cerebrospinal Fluid Inflammatory Markers in Alzheimer's Disease: Influence of Comorbidities. *Current Alzheimer Research,* 18**,** 157-170.
WANG, Y., FU, A. K. Y. & IP, N. Y. 2022. Instructive roles of astrocytes in hippocampal synaptic plasticity: neuronal activity-dependent regulatory mechanisms. *Febs j,* 289**,** 2202-2218.
WANG, Y., JIANG, R., LI, M., WANG, Z., YANG, Y. & SUN, L. 2024b. Characteristics of T Cells in Single-Cell Datasets of Peripheral Blood and Cerebrospinal Fluid in Alzheimer's Disease Patients. *J Alzheimers Dis,* 99**,** S265-s280.
WANG, Y., ULLAND, T. K., ULRICH, J. D., SONG, W., TZAFERIS, J. A., HOLE, J. T., YUAN, P., MAHAN, T. E., SHI, Y., GILFILLAN, S., CELLA, M., GRUTZENDLER, J., DEMATTOS, R. B., CIRRITO, J. R., HOLTZMAN, D. M. & COLONNA, M. 2016. TREM2-mediated early microglial response limits diffusion and toxicity of amyloid plaques. *J Exp Med,* 213**,** 667-75.
WATANABE, K., UENO, M., KAMIYA, D., NISHIYAMA, A., MATSUMURA, M., WATAYA, T., TAKAHASHI, J. B., NISHIKAWA, S., NISHIKAWA, S.-I., MUGURUMA, K. & SASAI, Y. 2007. A ROCK inhibitor permits survival of dissociated human embryonic stem cells. *Nature Biotechnology,* 25**,** 681-686.

WEISGRABER, K. H., INNERARITY, T. L. & MAHLEY, R. W. 1982. Abnormal lipoprotein receptor-binding activity of the human E apoprotein due to cysteine-arginine interchange at a single site. *J Biol Chem,* 257**,** 2518-21.
WEISGRABER, K. H., RALL, S. C., JR. & MAHLEY, R. W. 1981. Human E apoprotein heterogeneity. Cysteine-arginine interchanges in the amino acid sequence of the apo-E isoforms. *J Biol Chem,* 256**,** 9077-83.
WILMUT, I., SCHNIEKE, A. E., MCWHIR, J., KIND, A. J. & CAMPBELL, K. H. S. 1997. Viable offspring derived from fetal and adult mammalian cells. *Nature,* 385**,** 810-813.
WISNIEWSKI, T., GHISO, J. & FRANGIONE, B. 1991. Peptides homologous to the amyloid protein of Alzheimer's disease containing a glutamine for glutamic acid substitution have accelerated amyloid fibril formation. *Biochem Biophys Res Commun,* 179**,** 1247-54.
WITTER, M. P. 2007. The perforant path: projections from the entorhinal cortex to the dentate gyrus. *In:* SCHARFMAN, H. E. (ed.) *Progress in Brain Research*. Elsevier.
WU, T., DEJANOVIC, B., GANDHAM, V. D., GOGINENI, A., EDMONDS, R., SCHAUER, S., SRINIVASAN, K., HUNTLEY, M. A., WANG, Y., WANG, T.-M., HEDEHUS, M., BARCK, K. H., STARK, M., NGU, H., FOREMAN, O., MEILANDT, W. J., ELSTROTT, J., CHANG, M. C., HANSEN, D. V., CARANO, R. A. D., SHENG, M. & HANSON, J. E. 2019. Complement C3 Is Activated in Human AD Brain and Is Required for Neurodegeneration in Mouse Models of Amyloidosis and Tauopathy. *Cell Reports,* 28**,** 2111-2123.e6.
WUNDERLICH, P., GLEBOV, K., KEMMERLING, N., TIEN, N. T., NEUMANN, H. & WALTER, J. 2013. Sequential proteolytic processing of the triggering receptor expressed on myeloid cells-2 (TREM2) protein by ectodomain shedding and γ-secretase-dependent intramembranous cleavage. *J Biol Chem,* 288**,** 33027-36.
XIA, M. Q., BACSKAI, B. J., KNOWLES, R. B., QIN, S. X. & HYMAN, B. T. 2000. Expression of the chemokine receptor CXCR3 on neurons and the elevated expression of its ligand IP-10 in reactive astrocytes: in vitro ERK1/2 activation and role in Alzheimer's disease. *J Neuroimmunol,* 108**,** 227-35.
XIA, M. Q., QIN, S. X., WU, L. J., MACKAY, C. R. & HYMAN, B. T. 1998. Immunohistochemical study of the beta-chemokine receptors CCR3 and CCR5 and their ligands in normal and Alzheimer's disease brains. *Am J Pathol,* 153**,** 31-7.
XU, J., XIAO, N. & XIA, J. 2010. Thrombospondin 1 accelerates synaptogenesis in hippocampal neurons through neuroligin 1. *Nat Neurosci,* 13**,** 22-4.
XU, Q., BERNARDO, A., WALKER, D., KANEGAWA, T., MAHLEY, R. W. & HUANG, Y. 2006. Profile and regulation of apolipoprotein E (ApoE) expression in the CNS in mice with targeting of green fluorescent protein gene to the ApoE locus. *J Neurosci,* 26**,** 4985-94.
XU, W. & LARBI, A. 2017. Markers of T Cell Senescence in Humans. *Int J Mol Sci,* 18.
YANG, H., BYUN, M. S., HA, N. Y., YANG, J., PARK, S. Y., PARK, J. E., YI, D., CHANG, Y. T., JUNG, W. S., KIM, J. Y., KIM, J., LEE, D. Y. & BAE, H. 2024. A preclinical and phase I clinical study of ex vivo-expanded amyloid beta-specific human

regulatory T cells in Alzheimer's disease. *Biomed Pharmacother,* 181**,** 117721.

YEAPURI, P., MACHHI, J., LU, Y., ABDELMOATY, M. M., KADRY, R., PATEL, M., BHATTARAI, S., LU, E., NAMMINGA, K. L., OLSON, K. E., FOSTER, E. G., MOSLEY, R. L. & GENDELMAN, H. E. 2023. Amyloid-β specific regulatory T cells attenuate Alzheimer's disease pathobiology in APP/PS1 mice. *Mol Neurodegener,* 18**,** 97.

YIN, F., YAO, J., SANCHETI, H., FENG, T., MELCANGI, R. C., MORGAN, T. E., FINCH, C. E., PIKE, C. J., MACK, W. J., CADENAS, E. & BRINTON, R. D. 2015. The perimenopausal aging transition in the female rat brain: decline in bioenergetic systems and synaptic plasticity. *Neurobiol Aging,* 36**,** 2282-2295.

YSHII, L., PASCIUTO, E., BIELEFELD, P., MASCALI, L., LEMAITRE, P., MARINO, M., DOOLEY, J., KOUSER, L., VERSCHOREN, S., LAGOU, V., KEMPS, H., GERVOIS, P., DE BOER, A., BURTON, O. T., WAHIS, J., VERHAERT, J., TAREEN, S. H. K., ROCA, C. P., SINGH, K., WHYTE, C. E., KERSTENS, A., CALLAERTS-VEGH, Z., POOVATHINGAL, S., PREZZEMOLO, T., WIERDA, K., DASHWOOD, A., XIE, J., VAN WONTERGHEM, E., CREEMERS, E., ALOULOU, M., GSELL, W., ABIEGA, O., MUNCK, S., VANDENBROUCKE, R. E., BRONCKAERS, A., LEMMENS, R., DE STROOPER, B., VAN DEN BOSCH, L., HIMMELREICH, U., FITZSIMONS, C. P., HOLT, M. G. & LISTON, A. 2022. Astrocyte-targeted gene delivery of interleukin 2 specifically increases brain-resident regulatory T cell numbers and protects against pathological neuroinflammation. *Nat Immunol,* 23**,** 878-891.

YU, J., HU, K., SMUGA-OTTO, K., TIAN, S., STEWART, R., SLUKVIN, I. I. & THOMSON, J. A. 2009. Human Induced Pluripotent Stem Cells Free of Vector and Transgene Sequences. *Science,* 324**,** 797-801.

YU, J., VODYANIK, M. A., SMUGA-OTTO, K., ANTOSIEWICZ-BOURGET, J., FRANE, J. L., TIAN, S., NIE, J., JONSDOTTIR, G. A., RUOTTI, V., STEWART, R., SLUKVIN, I. I. & THOMSON, J. A. 2007. Induced Pluripotent Stem Cell Lines Derived from Human Somatic Cells. *Science,* 318**,** 1917-1920.

YUAN, L., XIE, L., ZHANG, H., ZHANG, Y., WEI, Y., FENG, J., CUI, L., TIAN, R., FENG, J., YU, D. & LV, C. 2023. Low-dose IL-2 Treatment Rescues Cognitive Deficits by Repairing the Imbalance Between Treg and Th17 Cells at the Middle Alzheimer's Disease Stage. *J Neuroimmune Pharmacol,* 18**,** 674-689.

YUN, S. P., KAM, T. I., PANICKER, N., KIM, S., OH, Y., PARK, J. S., KWON, S. H., PARK, Y. J., KARUPPAGOUNDER, S. S., PARK, H., KIM, S., OH, N., KIM, N. A., LEE, S., BRAHMACHARI, S., MAO, X., LEE, J. H., KUMAR, M., AN, D., KANG, S. U., LEE, Y., LEE, K. C., NA, D. H., KIM, D., LEE, S. H., ROSCHKE, V. V., LIDDELOW, S. A., MARI, Z., BARRES, B. A., DAWSON, V. L., LEE, S., DAWSON, T. M. & KO, H. S. 2018. Block of A1 astrocyte conversion by microglia is neuroprotective in models of Parkinson's disease. *Nat Med,* 24**,** 931-938.

ZAISS, D. M. W., GAUSE, W. C., OSBORNE, L. C. & ARTIS, D. 2015. Emerging Functions of Amphiregulin in Orchestrating Immunity, Inflammation, and Tissue Repair. *Immunity,* 42**,** 216-226.

ZENG, J., LIU, J., QU, Q., ZHAO, X. & ZHANG, J. 2022. JKAP, Th1 cells, and Th17 cells are dysregulated and inter-correlated, among them JKAP and Th17 cells

relate to cognitive impairment progression in Alzheimer's disease patients. *Irish Journal of Medical Science (1971 -),* 191**,** 1855-1861.

ZHANG, H., CAO, F., ZHOU, Y., WU, B. & LI, C. 2025. Peripheral Immune Cells Contribute to the Pathogenesis of Alzheimer's Disease. *Mol Neurobiol,* 62**,** 264-270.

ZHANG, H., ZHANG, L., ZHOU, D., HE, X., WANG, D., PAN, H., ZHANG, X., MEI, Y., QIAN, Q., ZHENG, T., JONES, F. E. & SUN, B. 2017. Ablating ErbB4 in PV neurons attenuates synaptic and cognitive deficits in an animal model of Alzheimer's disease. *Neurobiol Dis,* 106**,** 171-180.

ZHANG, Y. & NIU, C. 2022. Relation of CDC42, Th1, Th2, and Th17 cells with cognitive function decline in Alzheimer's disease. *Ann Clin Transl Neurol,* 9**,** 1428-1436.

ZHAO, A., JIAO, Y., YE, G., KANG, W., TAN, L., LI, Y., DENG, Y. & LIU, J. 2022. Soluble TREM2 levels associate with conversion from mild cognitive impairment to Alzheimer's disease. *J Clin Invest,* 132.

ZHONG, L., CHEN, X. F., WANG, T., WANG, Z., LIAO, C., WANG, Z., HUANG, R., WANG, D., LI, X., WU, L., JIA, L., ZHENG, H., PAINTER, M., ATAGI, Y., LIU, C. C., ZHANG, Y. W., FRYER, J. D., XU, H. & BU, G. 2017. Soluble TREM2 induces inflammatory responses and enhances microglial survival. *J Exp Med,* 214**,** 597-607.

ZHONG, L., CHEN, X. F., ZHANG, Z. L., WANG, Z., SHI, X. Z., XU, K., ZHANG, Y. W., XU, H. & BU, G. 2015. DAP12 Stabilizes the C-terminal Fragment of the Triggering Receptor Expressed on Myeloid Cells-2 (TREM2) and Protects against LPS-induced Pro-inflammatory Response. *J Biol Chem,* 290**,** 15866-15877.

ZHONG, M. Z., PENG, T., DUARTE, M. L., WANG, M. & CAI, D. 2024. Updates on mouse models of Alzheimer's disease. *Molecular Neurodegeneration,* 19**,** 23.

ZHOU, S., LIU, C., WANG, J., YE, J., LIAN, Q., GAN, L., DENG, S., XU, T., GUO, Y., LI, W., ZHANG, Z., YANG, G. Y. & TANG, Y. 2024. CCL5 mediated astrocyte-T cell interaction disrupts blood-brain barrier in mice after hemorrhagic stroke. *J Cereb Blood Flow Metab,* 44**,** 367-383.

ZHOU, T., LI, Y., LI, X., ZENG, F., RAO, Y., HE, Y., WANG, Y., LIU, M., LI, D., XU, Z., ZHOU, X., DU, S., NIU, F., PENG, J., MEI, X., JI, S.-J., SHU, Y., LU, W., GUO, F., WU, T., YUAN, T.-F., MAO, Y. & PENG, B. 2022. Microglial debris is cleared by astrocytes via C4b-facilitated phagocytosis and degraded via RUBICON-dependent noncanonical autophagy in mice. *Nature Communications,* 13**,** 6233.